Development of a Physical Simulation of the Human Defecatory System for the Investigation of Continence Mechanisms

by

William Elliot Stokes

Submitted in accordance with the requirements for the degree of
Doctor of Philosophy

The University of Leeds
Institute of Design, Robotics and Optimisation
School of Mechanical Engineering

May 2018

The candidate confirms that the work submitted is his own, except where work which has formed part of jointly-authored publications has been included. The contribution of the candidate and the other authors to this work has been explicitly indicated below. The candidate confirms that appropriate credit has been given within the thesis where reference has been made to the work of others.

Components of the research presented in Chapters 2-5 have been published in the papers below:

i. *"A physical simulation to investigate the effect of anorectal angle on continence"* – Biomedical Engineering (BioMed), 2017 13th IASTED International Conference on Incontinence

   Authors: W. Stokes, D. Jayne, A. Alazmani, P. Culmer

ii. *"A biomechanical model of the human defecatory system to investigate mechanisms of continence"* – Proceedings of the Institution of Mechanical Engineers, Part H: Special Issue on Incontinence, Journal of Engineering in Medicine, 2018

   Authors: W. Stokes, D. Jayne, A. Alazmani, P. Culmer

Both of these published works present literature findings from Chapter 2, design criteria and fabrication methods from Chapter 3, methodologies and results from Chapter 4 (Section 4.1.2. '*Rheology of smectite clay suspensions in water*', Section 4.2.2. '*Sphincter complex*' and Section 4.3.2. '*Simulating defecation*') and finally experimental methodologies from Chapter 5 (Section 5.2. '*Experimental Investigation*' and results from Section 5.2. '*Results*'). I was responsible for the technical work carried out, the co-authors were responsible for reviewing the papers.

I would like to acknowledge the IMPRESS network, who have partially funded this work.

Acknowledgements

I would first like to acknowledge the support and guidance from my three supervisors: Pete Culmer, Ali Alazmani and David Jayne. Between them they have expertise and knowledge in a breadth of medical, robotic and engineering disciplines, with which this project has flourished. Thank you for your infectious enthusiasm, friendship and always pushing me to aim higher.

I was very fortunate to receive tuition and advice alongside my PhD from a host of clinical personal located in St James University Hospital and Leeds General Infirmary, through the conception of the IMPRESS network (of which Pete and Ali form the core team), to all of whom I am grateful. Extended thanks to Sarah King for her involvement as project manager within the network, for booking my trains, hotels and always being there to navigate the London tube in a hurry. Also thanks to Richard Day (Co-investigator of IMPRESS) at UCL, London, for saving me the unruly task of thawing, dissecting and testing his 'calamari rings' (porcine sphincter). Also here I'd like to thank the friendly team at TORAX® medical across the pond, for their light-heartedness, and letting me use their continence restoration systems within my simulation.

Being part of the Surgical Technologies group has been an academically and culturally insightful experience. Thanks to all past and present members, it has been an asset and a pleasure working with you.

Thank you to my family, and friends (who are now too many to mention), who have offered moral and emotional support over the years. Alongside many lengthy discussions down the pub on the ultimate solution for faecal incontinence…

Thank you to everyone who has shared office 3.32a with me, for your companionship, uncountable 'brews', puns and daily shenanigans. An extended gratitude to players of 'PhD Eindhoven', who accompanied me on the 5-a-side pitch for what was always the highlight of the working week.

Lastly I would like to thank my beautiful girlfriend, Zoe. Thank you for encouraging me to pursue my dreams while offering your unwavering love and support along the way.

Abstract

Faecal incontinence is a highly debilitating condition, prevalent across the population worldwide. Coupled with a large unmet need for clinically viable treatment options, a paucity of research into the biomechanics of continence inhibits the development of treatments which address multi-faceted challenges associated with the condition. Consequently, this thesis presents a method to fabricate, measure and control a physical simulation of the human defecatory system to investigate individual and combined effects of anorectal angle and sphincter pressure on continence. To illustrate the capabilities and clinical relevance of the work, the influence of a passive-assistive artificial anal sphincter (FENIX) is evaluated.

A model rectum and associated soft tissues, based on geometry from an anonymised computerised tomography dataset, was fabricated from silicone and showed behavioural realism in terms of their morphology to the biological system and *ex-vivo* tissue. Simulated stool matter with similar rheological properties to human faeces was developed. Instrumentation and control hardware were used to regulate injection of simulated stool into the system, define the anorectal angle and monitor stool flow rate, intra-rectal pressure, anal canal pressure and puborectalis force. Studies were conducted to examine the response of anorectal angles at 80°, 90° and 100° with simulated stool. Tests were then repeated with the inclusion of a FENIX device.

Stool leakage was reduced as the anorectal angle became more acute. Conversely, intra-rectal pressure increased. Overall inclusion of the FENIX reduced faecal leakage, while combined effects of the FENIX and an acute anorectal angle showed the greatest resistance to faecal leakage. These data demonstrate that the anorectal angle and sphincter pressure are fundamental in maintaining continence. Furthermore it demonstrates that use of the FENIX can increase resistance to faecal leakage and reduce anorectal angles required to maintain continence.

The physical simulation of the defecatory system is an insightful tool to better understand, in a quantitative manner, the effects of the anorectal angle and sphincter pressure on continence. This work is valuable in helping improve our understanding of the physical behaviour of the continence mechanism and facilitating improved technologies to treat severe faecal incontinence.

Contents

List of Figures

List of Tables

Chapter 1: Introduction

This chapter introduces faecal incontinence as a condition; its prevalence, effect on quality of life and the current conservative and interventional treatments available to manage its symptoms. With these challenges in mind, aims & objectives for the project are defined.

1.1. Background

Faecal Incontinence (FI) is the inability to carry out controlled defecation and leads to the involuntary passing of bowel content, including flatus, mucus and liquid and solid faeces. The overall prevalence of FI in adults is estimated between 11% [4] and 15% [5] and this increases with age, with approximately 42% of people living in retirement homes (or similar institutions) affected [6]. Stigma and social taboo are associated with FI, leading to its underreporting.

The rectum is a hollow muscular tube, typically 13cm in length when non-distended [7], composed of a continuous layer of longitudinal muscle that interlaces with the underlying circular muscle. The anal canal is a muscular tube 2.5-4cm in length [8]. At rest, it forms an angle of approximately 105° [9] with the axis of the rectum. During voluntary squeeze the angle becomes more acute, whereas during defecation, the angle becomes more obtuse, Figure 1.1.

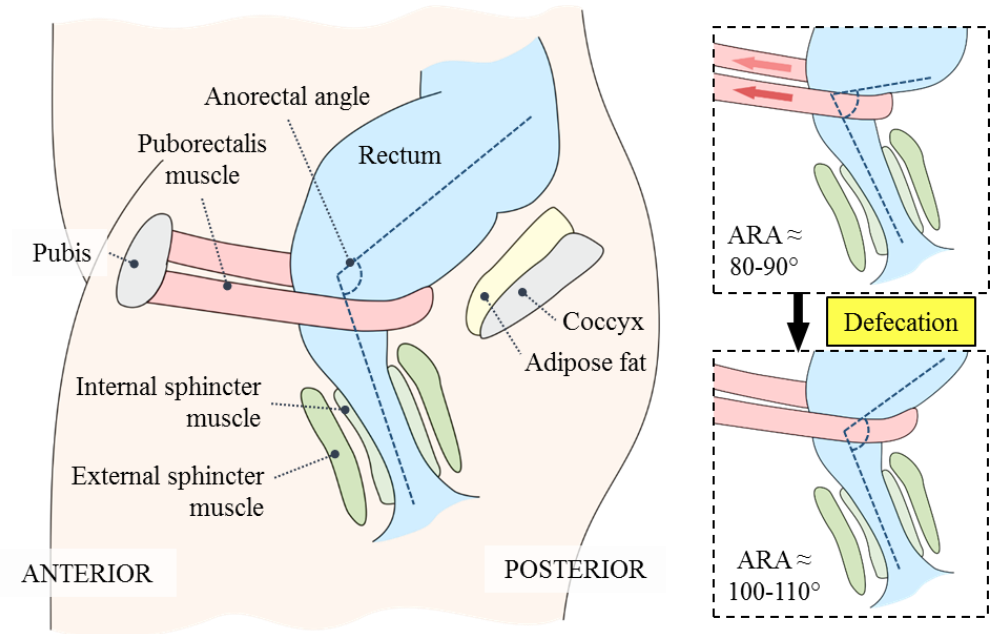

Figure 1.1 Schematic overview of physiological components of the defecatory system and role of the Puborectalis muscle in maintaining continence.

Continence relies on the coordinated function of the nervous system, gastrointestinal (GI) tract, and anal sphincter and pelvic floor musculature [10-14]. The sphincter complex (internal and external sphincters) applies pressure over the length of the anal canal creating occlusion, while the puborectalis (PR) and levator muscles produce occlusion in the upper anal canal. The PR also creates angulation between the anal canal and the rectum, termed the anorectal angle (ARA). The presence of an acute ARA has been considered important in maintaining continence [15, 16]. Dysfunction of only one of these components can result in severe FI, with common causes including diarrhoea, obstetric trauma, spinal cord injury and rectal prolapse [17]. Constipation, damaged muscle innervation and obstructed defecation (OD) can lead to low rectal compliances [18]. Frequent bowel movements and FI from damaged rectal sensation is common in patients with low rectal compliance [19]. FI is a condition with profound consequences for individuals, their family/friends, and the wider healthcare system [20].

Efforts to improve the technology to treat FI have taken inspiration from those applied for urinary incontinence. These techniques involve using an inflatable cuff to occlude the urethra [21, 22]. Efforts to use a similar approach to treat FI by occluding the sphincter [23, 24] have been plagued with complications including local ischaemia due to the large occlusive pressures necessary to maintain continence [13, 25-27]. Currently only a small number of surgical treatments are available for patients with severe FI and these focus on augmentation of the anal sphincter.

The paucity of commercially available, clinically viable systems to treat FI reflect the difficulty of designing to meet the multi-faceted challenges surrounding this complex condition. A key failure mode in existing systems occurs when device-tissue interaction causes tissue erosion, resulting in device migration or rejection [28, 29].

There is a clear clinical need to develop improved devices to treat FI, and recent research reveals promising opportunities to exploit ARA modulation. To further advance this work requires an in-depth biomechanical understanding of continence mechanisms and rectal disorders and models to capture their complex behaviour. This would allow detailed investigation into the complex device-tissue interactions which occur in the biological system and provide test environments to speed development prior to pre-clinical and human trials.

Whilst computational studies have been developed, a physical model provides opportunities to further understand the biomechanics of FI to help develop and optimise new systems for treatment. In particular, physical models can readily simulate the complex physical properties of faecal matter and the physical interactions between this and different tissues. Furthermore, they provide a convenient means to evaluate new treatment concepts. Accordingly, our research concerns the development of a physical model to investigate the effect of ARA and sphincter occlusion on continence for the future development and evaluation of novel FI technologies.

1.2. Project Aims & Objectives

1.1.1. Aims

This research aims to develop a physical model of the human defecation system to investigate the influence of biomechanical mechanisms associated with continence.

1.1.2. Objectives

1. Review relevant literature and consult clinicians to understand current clinical practice and define requirements of a physical simulation of the defecatory system
    a. Define FI, prevalence and its effect on QoL
    b. Review existing/emerging interventional treatments for FI
    c. Review existing (physical & computational) simulations of the defecatory system
    d. Identify and define influential biomechanics associated with continence and abnormalities which lead to FI
    e. Determine the clinical needs of the simulation
2. Review methods used to fabricate complex soft models to select or develop an appropriate method to fabricate tissue phantom models
    a. Identify a material which represents the properties of biological tissue and lends itself to the fabrication of complex geometries
    b. Develop a fabrication method to recreate complex geometries of biological tissues

3. Equip the simulation with control and instrumentation hardware and software required to regulate continence parameters and measure fundamental system metrics in a laboratory setting
4. Conduct a component-level- and global- simulation validation through cross-analysis with the human system
    a. Conduct ex-vivo tissue testing on biological tissues represented in the simulation, where properties were not previously recorded
    b. Conduct in-silico testing on biomimetic materials
    c. Match the properties of artificial materials and biological tissue
    d. Match the rheological properties of simulated stool material with human stool
5. Conduct an experimental investigation to determine the influence of continence parameters on severity of incontinence
    a. Apply an experimental matrix to observe the individual and combined effects of key biomechanical variables
    b. Identify correlations between biomechanical variables and severity of incontinence/other system parameters

1.3. Chapter Descriptions

Chapter 1 - Introduction

This chapter introduces faecal incontinence as a condition; its prevalence, effect on quality of life and the current conservative and interventional treatments available to manage its symptoms. With these challenges in mind, aims & objectives for the project are defined.

Chapter 2 – Literature Review

A review of literature around faecal incontinence; description of the condition, history, prevalence and treatments, is conducted. Important biomechanics of the system are identified and corresponding values are pulled from literature; anatomical dimensions, forces, pressures and material properties are reported where possible. Comparisons are made between studies where conflicting data is presented. Furthermore the review compares current and novel FI devices in terms of their design and efficacy. Computational and physical simulations of the faecal system are also

reviewed to understand the current status of scientific community research and identify important modelling aspects which have been used previously.

Chapter 3 – Technical Requirements, Design, Fabrication and Control of a Physical Simulation of the Human Defecatory System

This chapter presents technical requirements for the conceived research questions defined in Chapter 2. Technical requirements are used to develop a series of specifications and an associated conceptual approach to the project. Tables of biomechanics of the biological system are compiled from literature, required for accurate representation of the defecation system with a physical simulation. Design considerations, fabrication methods and choice of control hardware and software for the physical simulation are documented along with a detailed overview of the simulation.

Chapter 4 – Validation of the Physical Simulation

This chapter compares the physical simulation to the human system. Firstly, by considering the component parts (simulated stool, rectum model, anal canal/sphincter complex and pelvic floor) and comparing these to corresponding aspects of the human system; stool viscosity, pelvic floor descent, rectum morphology and anal canal distensibility are among the metrics used in the cross-comparison. The individual parts were then brought together to compare the simulation as a whole, through replication of a typical biological scenario, to the human system. Component-level validation, and validation of the simulation as a combined entity, strengthens its viability as a development tool for new technologies in the management of faecal incontinence.

Chapter 5 – Experimental Investigation into the Effects of Anorectal Angle and Sphincter Occlusion on Continence

This chapter presents an exploratory investigation using the physical simulation developed and validated in the previous chapters. A protocol using the physical simulation aims to first investigate the effects of rectal compliance and changing ARA on continence and second explores the clinical relevance of the work by evaluating the influence of two models of a passive-assistive artificial anal sphincter (FENIX and FENIX Plus). This work provides the fundamental testing of the simulation for grounds on which its capabilities and relevance were explored.

Chapter 6 – General Discussion, Conclusions and Future Work

The research presented in this thesis has shown the development, analysis and application of a physical simulation of the human defecatory system. The proposed simulation was designed for the investigation of the effects of ARA, sphincter occlusion and rectal compliance on IR pressure and faecal leakage, to inform the design of emerging technologies in the treatment of FI. Findings from the investigation identify correlations between the modelled continence mechanisms and degree of continence. This discussion considers key features of this research regarding the validity of the technique, how it compares to current simulations and how it may be applied to the development of clinically viable technologies. Reassessment of research objectives and identification of potential modifications concludes this chapter along with a proposal of future work.

Chapter 2: Literature Review

A review of literature around faecal incontinence; description of the condition, history, prevalence and treatments, is conducted. Important biomechanics of the system are identified and corresponding values are pulled from literature; anatomical dimensions, forces, pressures and material properties are reported where possible. Comparisons are made between studies where conflicting data is presented. Furthermore the review compares current and novel FI devices in terms of their design and efficacy. Computational and physical simulations of the faecal system are also reviewed to understand the current status of scientific community research and identify important modelling aspects which have been used previously.

2.1. Faecal Continence, Incontinence & Quality of Life

Faecal continence is the ability to voluntarily retain a bodily discharge. Continence is maintained by the anorectum (caudal end of the GI tract) which is also responsible for defecation. The continence mechanism is highly complex, it relies on the coordinated function of the central nervous system, GI tract and pelvic floor musculature. For normal defecation, three biomechanical operations coordinate:

1. Spontaneous rectal contraction that initiates during storage (autonomic function) [30-32]
2. Relaxation of the anal canal with an obtuse ARA (somatic function) [33, 34]
3. Straining (somatic function) [35, 36]

Failure in one of these operations can lead to incontinence, and the successful function of each depends on a complex interaction of a variety of nerves, muscles and supporting structures. Incontinence arises from anorectal disorders and the anatomical and physiological mechanisms must be clearly understood for successful treatment and restoration of continence. FI is a highly debilitating condition. Patients with more severe cases of FI experience substantial negative effects on lifestyle and QoL, through the restriction of social activity or interaction [20, 37]. This might be influenced by an event of soiling in public which is recognised as one of the most humiliating experiences a person can endure. Furthermore, patients who fail to respond to treatments are obliged to manage symptoms using time-consuming techniques, constant changing of pads, dietary modifications and constipation medications [38].

2.1.1. Causes

Due to the complexity of faecal continence, incontinence can rarely be attributed to a single factor and is often a result of multiple pathogenic mechanisms [39], brought about by a physical condition, with the most common causes being:

- Problems with the rectum [40]
- Problems with the sphincter muscles [40]
- Nerve damage [40]
- Other medical conditions

Problems with the rectum generally involve two conditions, constipation and diarrhoea. Constipation is the leading cause of FI, it causes faecal impaction in the rectum which in severe cases can stretch the muscles, weakening them. Watery stools then leak around the compacted faeces in an incontinence episode. This is called overflow incontinence and occurs in people of all ages but most commonly in those who are elderly. Diarrhoea can be more difficult for the rectum to hold than solid stools and therefore, people with recurring diarrhoea can develop FI. Conditions that can cause recurring diarrhoea commonly include irritable bowel syndrome (IBS) which can also lead to scarring and weakening of the rectum, further evoking incontinence.

Problems with the sphincter muscles can result in FI if they become weakened. Childbirth is a common cause of damage to the sphincter muscles, with further causes including other injuries, or damage during bowel or rectal surgery. During vaginal delivery, the sphincter muscles can become damaged from over-distention or through the use of forceps.

Damage to the nerves connecting the brain and the rectum can mean that the body is unaware of stools in the rectum, making it difficult to properly control the anal sphincters. Neurogenic bowel dysfunction arises when there is damage to the autonomic nervous system leading to impairment of either sensory or motor control, or both. Diagnosis of neurogenic bowel dysfunction may include constipation, incontinence and disordered defecation. The autonomic neural pathways which control the rectum, colon and anal canal are disrupted as a consequence of damage or disease to the central nervous system [41].

A number of conditions are associated with central nervous system damage and/or disease; these include spinal cord injury, multiple sclerosis, spinal bifida, cauda equina, cerebral palsy, stroke and Parkinson's disease. While these conditions cause other disabilities with the patient, bowel dysfunction is also a significant burden. It has been suggested in previous studies that approximately half of patients with spinal cord injury have moderate to severe neurogenic bowel dysfunction symptoms. It has also been reported that around 52% of patients with multiple sclerosis will develop bowel symptoms [42]. Furthermore, around 34% of young patients with spinal bifida experience FI.

2.1.2. Prevalence

A limited number of prevalence studies for FI have been carried out in the past [43]. Among patients <65 years, prevalence of FI has been estimated at 0.7% [44] in the United States and 0.9% [45] in the United Kingdom. More commonly prevalence studies are carried out for patients >60 years. These estimate a prevalence between 3.1% (United states) and 8.2% (New Zealand) although sample sizes tend to be small [46, 47] and individual studies are conducted in different demographic regions. However in all studies, a strong correlation between age and FI has been shown [48], with prevalence in the very elderly (>85 years) significantly higher.

The majority of published work suggest a higher prevalence of FI in females than males, for reasons related to childbirth [49]. However one study carried out by Gut [20] reported that 1.4% of the global population had severe FI, and while it showed that incontinence was more prevalent and severe in older people, there was no significant difference between genders. The paper draws results from a rigorous questionnaire and suggests that previous and clinical studies lack attention to the male population.

A more recent study by the National Institutes of Health [50] estimated that prevalence of FI in women living in the community world-wide lies at 6% in <40 year olds and increases to 15% in those who are older. Among men living in the community, FI is estimated at around 6-10%, with the rate increasing with age. The paper also addressed prevalence of FI in nursing homes, concluding that it varies widely depending on mental/physical ability and patient dependency, but overall prevalence was estimated at around 45% (ranging from 10-70%). A small number of studies comparing racial or ethnic groups did not find any differences.

It is apparent that data on prevalence and severity of FI in the overall population is too limited for accurate estimation of the actual statistic. However it can be learned that there is little difference in prevalence between men and women although prevalence is certainly prominent in our society, with the severity of symptoms increasing with age.

2.1.3. Treatment Ladder

Depending on the severity of FI, different managements are available. Conservative methods of symptom management are trialled in the initial stages of the treatment process and if unsuccessful, increasingly more invasive methods are employed. Figure 2.1 demonstrates the stages of interventions in bowel management. In some instances it may be necessary to bypass conservative methods, particularly in the case of central nervous system damage where mobility and dexterity impairment may limit the incontinence management strategy [41].

In the case of mild constipation, lifestyle and dietary/fluid modifications may restore normal function. For moderate classifications of FI, rectal interventions such as suppositories and enemas offer more intrusive treatment and for those whom conservative interventions are unsuccessful, irrigation techniques can resolve symptoms. Otherwise, progression up the treatment ladder leads to surgical interventions (such as sacral nerve stimulation) and lastly regular irrigations or antegrade colonic irrigation are reserved for patients with severely damaged sphincter muscles to manage symptoms long-term, while a stoma and colostomy bag would restore continence as a final resort.

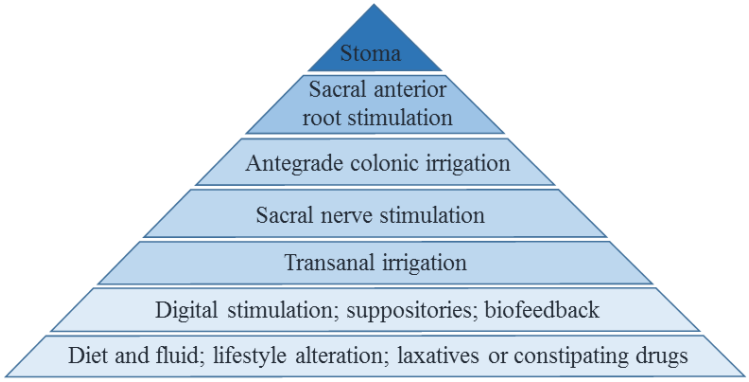

Figure 2.1 Proposed stepped approach to the treatment of bowel dysfunction; pale blue layers represent conservative methods, mid-tones represent minimally invasive methods and darker tones indicate incrementally more invasive methods [41].

2.2. Anatomy & Biomechanics

To investigate mechanisms associated with continence, first, the anatomy of fundamental parts of the human defecatory system should be understood, in healthy and abnormal states. Following which attention can be turned to modelling more complex physiology and biomechanics of the simulation platform. The physiological function of the fundamental components are addressed for a clearer understanding of the biomechanics of the defecation system and finally, biomechanical properties of these components are investigated and presented when possible.

2.2.1. Anatomy

Anatomical geometries play a central role in the development of a physical simulation of the human defecatory system. Biological tissues possess complex geometrical parameters tailored for particular functions as a part of the overall defecation system. Important components of the human defecation system are shown in Figure 2.2.

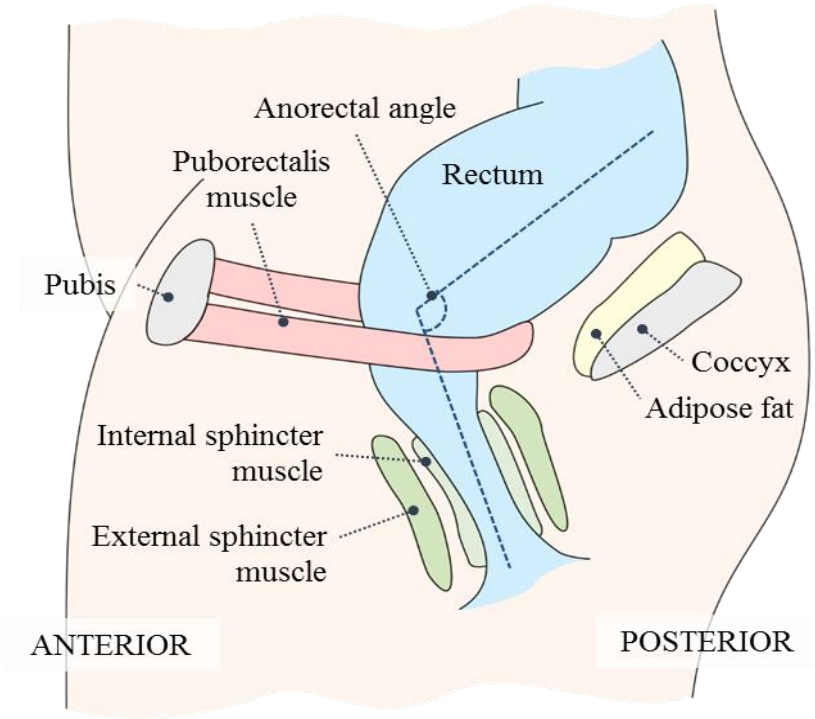

Figure 2.2 Schematic overview of key physiological components of the defecation system.

The rectum, PR muscle and internal and external anal sphincters are fundamental in the maintenance of continence. Studies which shed light on the geometries and positioning of anatomical components are reviewed in detail in this section.

2.2.1.1. Rectum

The rectum is a muscular tube, composed of continuous longitudinal muscle which interconnects with underlying circular muscle [52]. These muscle layers are responsible for the peristalsis action which moves faecal matter along the gut. Posteriorly, the rectum interfaces with the rectouterine pouch and posteriorly it sits next to a layer of omental adipose tissue. A schematic overview of the tissues which interface with the rectum are shown in Figure 2.3.

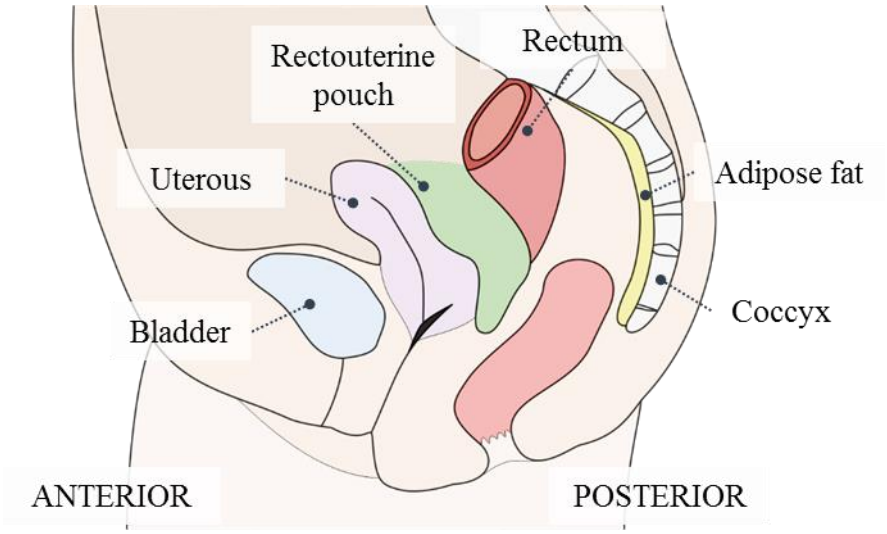

Figure 2.3 Schematic overview of the female pelvic cavity in the sagittal plane, indicating viscera within the cavity.

Anterior to the rectum sits the rectouterine pouch, serving as space into which the rectum can expand upon filling, and as such, movement of the anterior rectum is unconstrained. To the posterior, the rectum interfaces with the mesorectum which provides cushioning from the sacrum. The posterior rectum is constrained to the mesorectum which in turn is fixed to the sacrum and coccyx, preventing movement of the posterior rectal wall.

The rectum has various anatomical features for the controlled transit of faeces through it, as demonstrated in Figure 2.4.

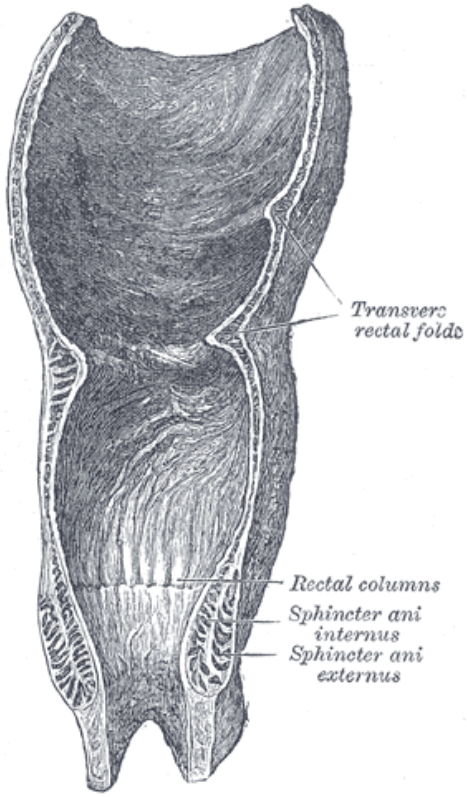

Figure 2.4 Coronal section of the rectum and anal canal, indicating the location of transverse rectal folds, rectal columns and internal and external anal sphincters [7].

Upper and lower rectums are separated by a horizontal fold. The upper rectum is derived from the embryological hind gut, generally contains faeces, and can distend toward the peritoneal cavity. The lower part, derived from the cloaca, is surrounded by condensed extra peritoneal connective tissue and is generally empty in normal subjects, except during defecation. Where the lower part of the rectum is contracted, its mucous membrane is contorted into a number of folds, longitudinal in direction. There are also permanent transverse folds, in the empty state of the rectum, these folds overlap each other [8].

Anatomical Dimensions

The rectum is typically 130 mm long [7] and 32 mm in diameter [53] [54]. A sensation of the presence of stool is usually experienced around 10 and 30 ml in the adult with a desire to defecate occurring at an average volume of 150ml, urgency between 150 and 300 ml [55] and maximum distension around 400 ml [56]. The rectum contains a number of transverse folds, usually three. One is situated near the start of the rectum on the right side, a second extends inward from the left side, opposite the middle of the sacrum and a third (the largest) projects backward from the forepart of the rectum

opposite the bladder. They are generally about 12 mm in width [57]. The geometry of the rectum is complex and highly variable between patients.

Diseased States

Faecal continence relies on a healthy, properly functioning rectum and associated tissues. Impairment to one of these tissues can lead to a host of problems including OD and FI. OD is a broad term of the pathophysiologic condition describing the inability to evacuate contents from the rectum. Common causes include descending perineum syndrome, rectoceles, pelvic floor dysfunction and anal stenosis [58].

During normal defecation, the rectum will contract, providing a low compliance tube through which faecal matter can easily transit. However in patients with FI, a lack of rectal sensation can inhibit this mechanism leading to a large rectal volumes and FI.

2.2.1.2. Adipose Tissue

The mesorectum is composed of adipose tissue (composed of adipocyctes) which connects the posterior rectum to the sacrum. It provides a soft interface between the two which acts to cushion the rectum, while constraining the rectum to the posterior, preventing anterior movement of the entire rectum when the PR muscle contracts to prevent the passing of faeces, also acting to enhance the ARA.

2.2.1.3. Pelvic Floor

The pelvic floor is a dome-shaped muscular sheet [59] mainly composed of striated muscle with midline permeations from the bladder, uterus and rectum, joined by connective tissue. The pelvic floor supports the abdominal viscera and plays an important role in maintaining continence between periods of evacuation of urine and stool.

Pelvic floor tone is widely considered fundamental for the function of normal bowel behaviour. Many patients with FI have weak pelvic floor tone and consequently experience large rectal descents during defecation. Pelvic floor dysfunction is often caused by obstetric trauma, sphincter injury or damage to innervation [60] and there is a strong correlation between it and age [48]. Pelvic floor dysfunction entails a variety of conditions including OD and FI [61]. Options for pelvic floor reconstructive procedures are few and have poor efficacy. However, the PR muscle is a major component of the pelvic floor and it has been identified that poor PR function is a

contributing factor to the difficulties experienced by patients with weak pelvic floors. The pelvic floor is composed of the levator ani muscle which is subdivided into four muscles (pubococcygeus, ileococcygeus, coccygeus and PR), and these are attached peripherally to the pubic body as shown in Figure 2.5.

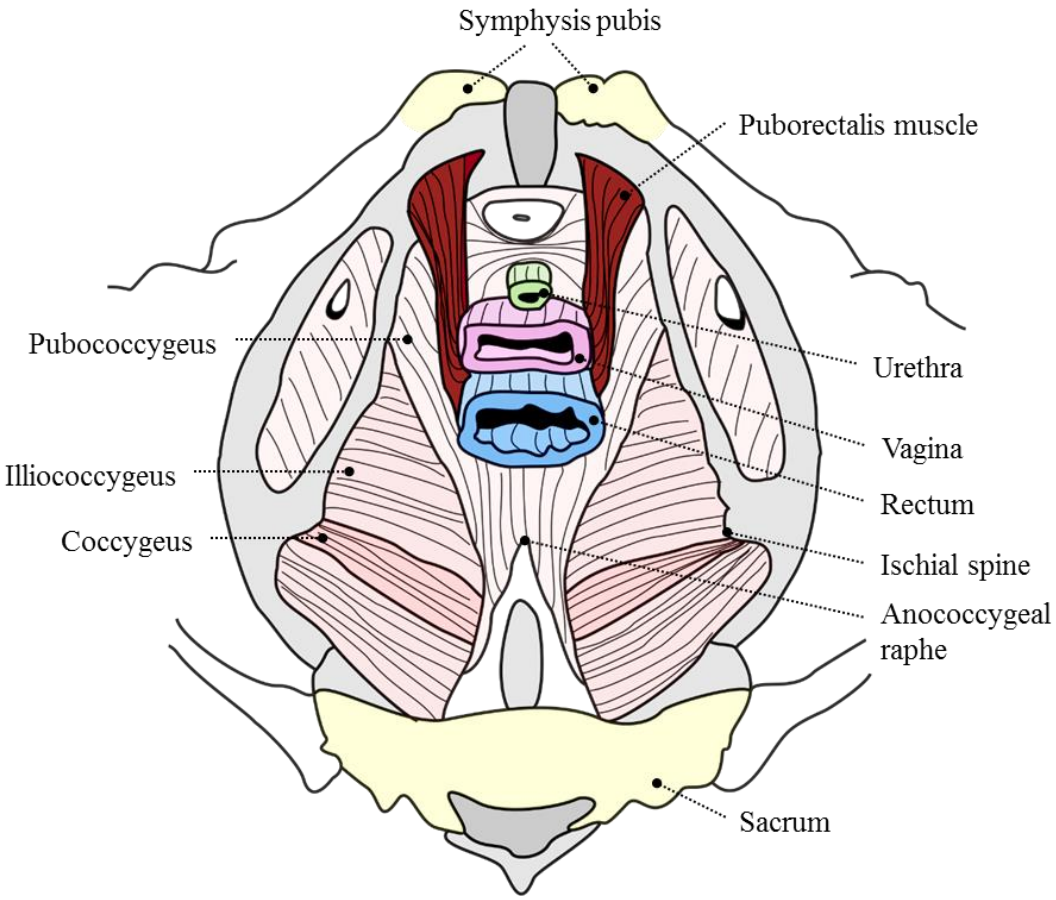

Figure 2.5 Pelvic view of the levator ani demonstrating its four main components: puborectalis, pubococcygeus, iliococcygeus and coccygeus muscles.

The pelvic floor is complex and consists of a variety of separate muscles, each with their own particular function, although together, they form a muscular sheet which provides support to the pelvic visceral organs. Perhaps the most influential muscle in the maintenance of continence, the levator ani consists of the PR muscle, which forms a sling extends from the symphysis pubis to wrap around the posterior rectum, responsible for modulation of the ARA.

It is not known whether the PR should be considered a component of the levator ani complex or of the external anal sphincter. The PR appears as a distinct entity from the majority of the levator ani and rather as a continuous part of the EAS [62]. However,

the PR and EAS are innervated by separate nerves, suggesting evolutionary differences between the two muscles [63].

2.2.1.4. Anal Sphincters and Puborectalis Muscle

The sphincter complex sits around the anal canal, it consists of two muscles; the internal anal sphincter (IAS) and external anal sphincter (EAS). These muscles apply pressure to the anal canal which cause occlusion, preventing the passing of bowel contents when it is not appropriate to do so. Both sphincters are separate and independent. The anus is normally closed by subconscious activity of the IAS although the barrier is reinforced during voluntary squeeze of the EAS. The other contributors to anal resting tone include the EAS, the anal mucosal folds and the PR muscle.

Internal Anal Sphincter

The IAS is a thickened extension of the circular smooth muscle layer surrounding the colon that contains discrete muscle bundles separated by large septa. It is primarily responsible for ensuring that the anal canal is closed at rest [64]. It has been estimated during studies that anal resting tone is generated by nerve-induced activity in the IAS at 45% of anal resting tone [65]. However anal resting pressure is not fixed at these values but varies during the day by circadian and ultradian rhythm variations dependant on sleep/wake cycles [62].

External Anal Sphincter

The external anal sphincter (EAS) is composed of superficial blends with the PR [8]. In men, this laminar pattern is preserved around the sphincter circumference. In women however, the anterior portion of the external sphincter is a single mass of muscle. External sphincter fibres are small, circumferentially oriented and separated by connective tissue [66].

Though resting sphincter tone is predominantly attributed to the IAS, studies under general anesthesia or after pudendal nerve block suggest the external anal sphincter generally accounts for 25-50% of resting anal tone [62]. When there is an urge to defecate and it is not appropriate to do so, the EAS contracts to augment anal tone, preserving continence. This response may be voluntary or it may be induced by

increased intra-abdominal (IA) pressure. Conversely, the EAS relaxes during defecation.

Puborectalis Muscle

The PR muscle (indicated in Figure 2.5) is a U-shaped sling and component of the levator ani muscle of the pelvic floor, it extends from the pubic bone, past the urogenital hiatus and around the anal canal with a primary function to maintain faecal continence. When it contracts, it tightens against the anorectum towards the anterior, accordingly enhancing the ARA. Some fibres of the PR muscle form another U-shaped sling which interface with the urethra, important in the preservation of urinary continence.

Anatomical Dimensions

The anatomy of the musculature surrounding the anal canal at different points along its length can be revealed using MRI and an endo-anal coil to obtain images in the transverse plane, Figure 2.6. Slice A) shows the lowest part of the EAS, the two halves of which are embedded within the ischioanal space, slice B) shows visible bundles of longitudinal muscle between the two folds of the EAS, the two anterior halves of the EAS are connected, in slice C) anterior EAS is visible and forms a circular profile, while the posterior EAS has a thickened protrusion in contact with the urogenital diaphragm. Finally, visible in slice D), fibres of the PR muscle extend anteriorly to the urogenital diaphragm [67].

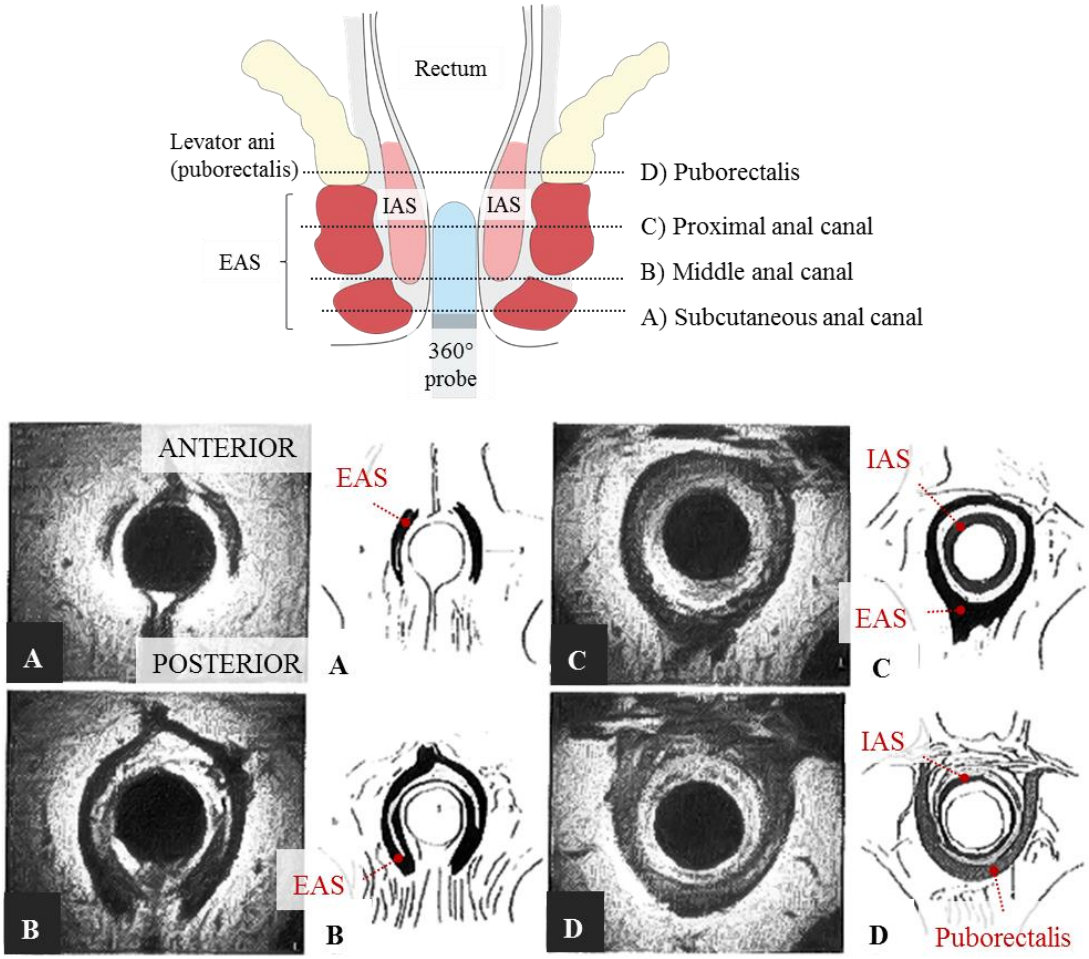

Figure 2.6 *Top*; schematic of the musculature surrounding the anal canal and *Bottom*; slices through the anal canal at the above locations, showing: A) Lowest part of the EAS; B) Slice slightly cranial to *A*; C) Slice slightly cranial to *B* and D) Slice slightly cranial to *C* [67].

Still images from the magnetic resonance (MRI) analysis demonstrate the anal sphincters, PR muscle and surrounding structures. Towards the distal end of the EAS, posteriorly it is connected to the anococcygeal body and towards the caudal end, anterior fibres connect to superficial perineal muscle of the urogenital diaphragm [67].

Using ultrasonography, the lengths (along the proximal-distal axis of the anal canal) of the IAS, EAS and PR [1] have been measured along with the circumferential thickness of the PR [2] and EAS [3]. Another study used computerised tomography (CT) defecography to measure the morphological parameters of the PR muscle, this revealed that the PR is 147.6 mm in length at rest, it contracts to 127 mm during squeeze and extends to 189.8 mm during defecation [68]. These findings combined with length dimensions are summarised in Table 2.1.

Table 2.1 Summary of reported anal sphincter and Puborectalis length and thickness measurements:

Muscle	Measurement	Anterior	Posterior	Patient details
EAS	Length (mm) [1]	22.0	32.0	Female
	Thickness (mm) [2]	4.8	4.8	Female (Sphincter damage)
IAS	Length (mm) [1]	20.7	30.2	Female
	Thickness (mm) [3]	1.2	1.8	Mixed gender

2.2.1.5. Anorectum and Anal Canal

Continence is maintained by the structural and functional integrity of the anorectal unit. As a consequence, abnormalities of the anorectal unit often lead to FI. The anorectum consists of the distal portion of the rectum and the anal canal. The anal canal is a muscular tube, with various features to identify the composition of bowel contents and prevent evacuation when not appropriate to do so, Figure 2.7.

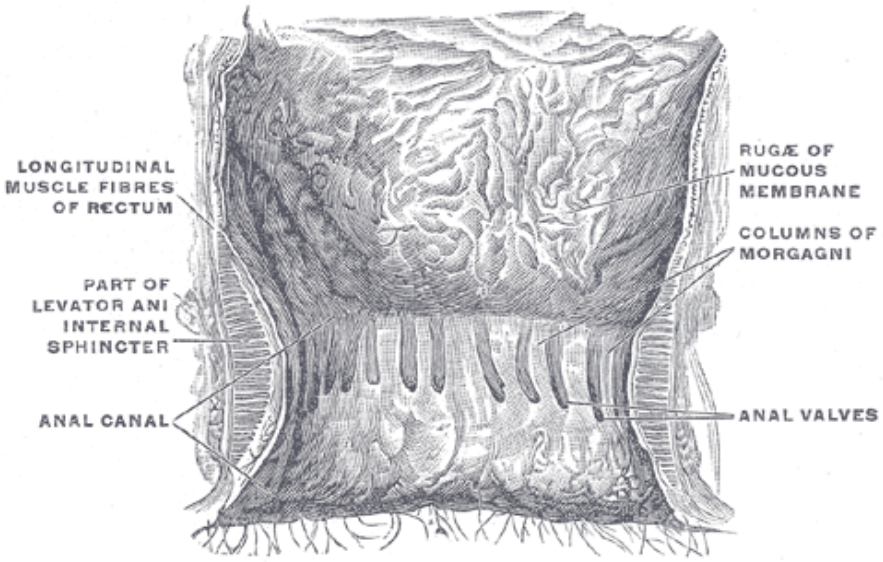

Figure 2.7 Anatomy of the anorectum and anal canal; showing the anal columns and anal valves, which help provide a tight seal to prevent the passing of bowel contents.

The anal canal is surrounded by the IAS, supported by the Levator ani and encircled at its base by the EAS. In an empty state, it presents the appearance of a slit in the sagittal plane [69]. Posterior to the anal canal is a mass of muscular and fibrous tissue named the anococcygeal body. Anteriorly in the male, the anococcygeal body is

separated from the urethra by connective tissue whereas in the female, it is separated from the vagina by a mass of muscular and fibrous tissue named the perineal body.

Anatomical Dimensions

The anal canal is a muscular tube, it forms an angle with the lower part of the rectum, named the ARA. The anal canal measures from 2.5 to 4 cm in length [8] and 3cm in diameter when distended [69], with a basal diameter of 19mm [70]. The axis of the rectum forms almost a right angle with thee axis of the rectum. It has been established that the anal canal is an antero-posterior slit in the resting state [69].

2.2.2. System Biomechanics

Physiological parameters of the defecation system include forces and pressures applied by system components on one another to regulate the passing of bowel content. Some of the important physiological interactions are detailed in this section, to aid the design of actuation mechanisms of components of the physical simulation.

2.2.2.1. Mucosal Folds

The anal mucosal folds, together with expansive anal vascular cushions creates a tight seal. These barriers are further enhanced by the PR muscle which provides a forward pull and reinforces the ARA. Anal endovascular cushions consist of blood-filled vascular tissue of the anal mucosa that completely fill the anal orifice following contraction of the IAS, they exert pressures of 9mmHg and contribute 10 to 20 % of resting anal pressure [71]. It has been suggested that bowel contents are sensed periodically by anorectal sampling [72]. This process is the relaxation of the IAS to allow the stool contents from the rectum to come into contact with specialized sensory organs in the upper anal canal. The likely role of anal sensation is to discriminate between flatus and faeces.

2.2.2.2. Anal Sphincters and Puborectalis Muscle

It has been shown that the IAS and EAS contribute toward the pressures in the anal canal although the role of the PR in pressure generation is poorly understood. It has been reported however that the PR is responsible for the closure of the cranial part of the anal canal [2, 73]. The anal canal ‘high pressure zone’ is 39+/-1mm in length and the IAS, EAS and PR have been clearly visualised along its length to investigate their contribution towards the pressure profile. The pressure profiles through the anal canal

at rest and during squeeze are shown in Figure 2.8. It has been suggested that the critical level of anorecto-puborectalis pressure below which incontinence occurs seems to be about 18 mm Hg [74].

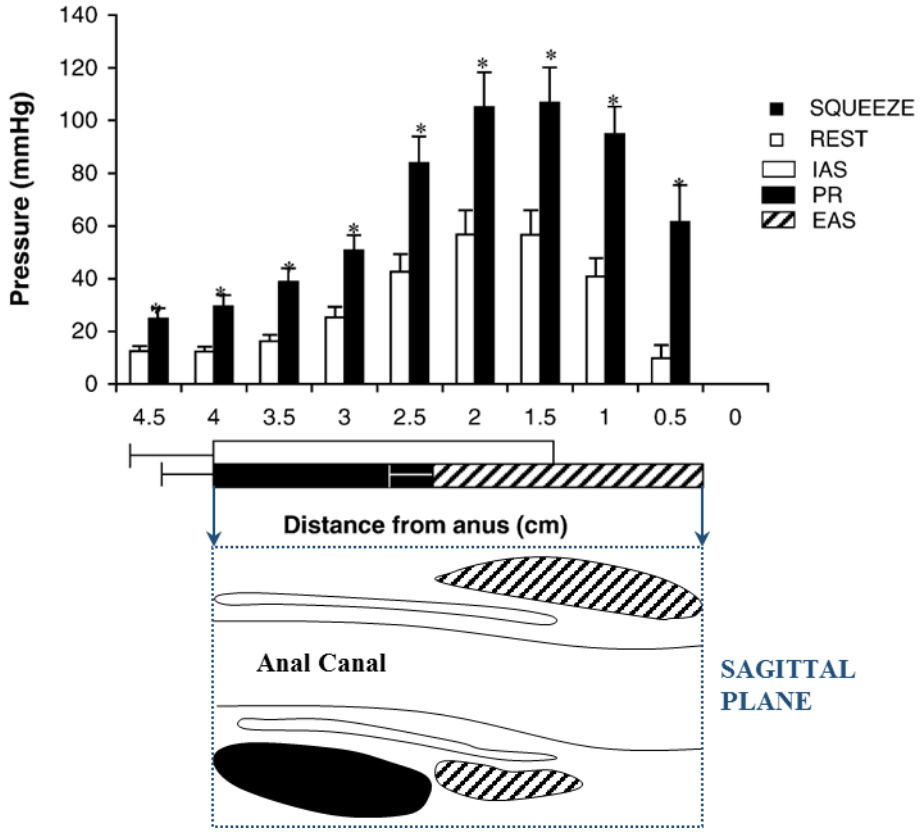

Figure 2.8 *Top*; anal canal pressure profile during the manometer pull through, all pressures during squeeze are far greater than at rest and the locations of the IAS, EAS and PR are shown. *Bottom*; trace of an ultrasound image showing the location of the muscles which correspond to different sections of the pressure profile [2].

As can be seen from this pressure profile, the IAS, EAS and PR muscles all contribute toward closure of the anal canal during rest. Upon squeezing, the PR muscle contributes to the pressure increase in the proximal part of the anal canal and the EAS to the distal anal canal. This suggests that the PR squeeze-related increase in anal canal pressure might be important in the maintenance of continence.

At rest, the PR muscle produces an angle between the anal canal and axis of the rectum, causing passive occlusion of the anorectum and resistance to bowel contents.

2.2.2.3. Anorectal Angle

The presence of an acute ARA has been considered important in maintaining continence [15, 16]. During voluntary ‘squeeze’ the PR muscle tightens against the

anorectal junction to enhance the ARA and increase resistance to faecal leakage and the ARA becomes more acute, whereas during defecation, the angle becomes more obtuse to allow easy passage to bowel contents.

Dynamic proctography is a radiographic procedure widely used in the evaluation of pelvic floor function. The ARA is one parameter usually quantified during this examination, used among other observations as an indicator of a factor leading to incontinence. Accuracy and reproducibility of the ARA measurement has been criticised in the past due to the high variability of the anal canal between patients and the obscurity of how it should be defined. Two methods commonly used to determine the ARA area demonstrated in Figure 2.9.

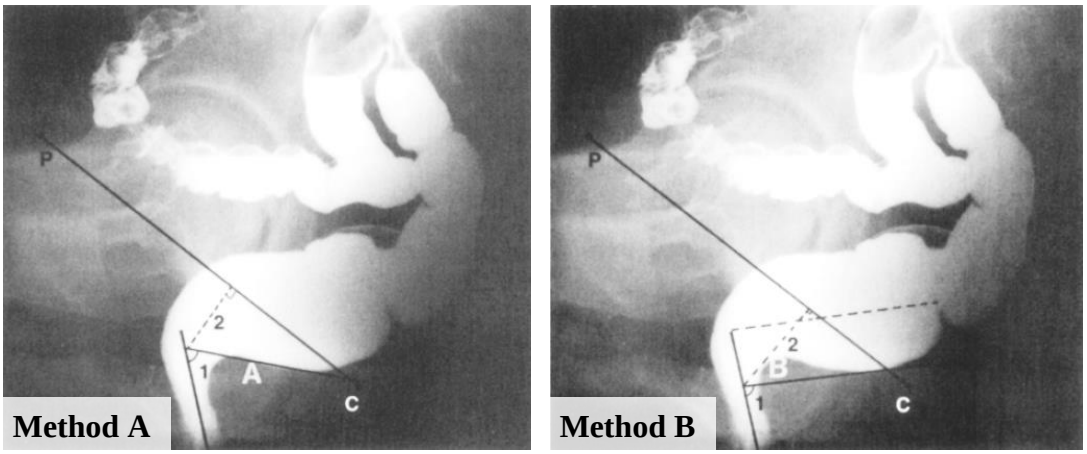

Figure 2.9 *Method A*; The posterior rectal wall (line A) is plotted based on the impression of the puborectalis muscle and the tangential of the posterior rectal wall. *Method B*; The posterior rectal wall (line B) is plotted parallel to the central longitudinal axis, 1 = ARA; 2 = perineal descent; P = pubic symphysis; C = coccyx [75].

The ARA is highly variable between patients and its definition is often disputed. Numerous studies have been compared in order to determine the most consistent values from a range of sources, particularly for incontinent and healthy subjects during states of rest and squeeze. The standard procedure, outlined in the journal of neurogastroenterology and motility [76], is to deliver a barium contrast to the rectum and with the patient seated, dynamic radiology is performed. Several literature studies make use of this imaging technique to observe the reproducibility of measuring the ARA. On study carried out by Mahieu et al. [77] imaged 56 normal healthy patients, of which 22 were men and 34 were women with a combined mean age of 47.5 years (range, 17-80 years), representing a demographic ARA value for healthy subjects. In

another study conducted by Felt-Bersma et al. [78], using the standard protocol, defecographic examinations were carried out on 92 patients (30 of which had symptoms of FI). The ARA was not seen to be influenced by gender or age.

ARA values have also been measured using the standard radiology protocol to observe differences between methods of ARA measurement (methods 'A' and 'B' described above). In a study conducted by Shorvon et al. [79], 47 healthy young volunteers underwent examination to determine the normal range. The study reported a broad range of ARA values being observed despite the volunteers being healthy, with a significantly more acute ARA values being observed using 'method A' over 'method B' at rest.

Furthermore, the standard procedure was also adhered to observe differences in ARA between continent (N=69) subjects and incontinent (N=82) patients in a study carried out by Piloni et al. [9]. It was demonstrated that incontinence resulted in a significantly more obtuse ARA during states of both 'rest' and 'squeeze'.

Novel methods to image the ARA have also been explored. In a study conducted by Barkel et al. [80], to determine the influence of different body positions on the ARA, a novel method of imaging the anorectum was developed in which a cylindrical balloon was placed in the anorectum and anal canal and filled with a fluid. A gamma camera was then used to image the angulation of the balloon during states of 'rest', 'squeeze' and 'defecation'. This revealed that 'sitting' produces the most obtuse ARA compare with 'lying' or 'standing', and therefore of the positions tested, provides the least resistance to the passing of faeces.

A summary of the values obtained from the studies discussed are presented in Table 2.2.

Table 2.2 Summary of ARA values obtained from separate studies, using a variety of protocols (balloon topography & dynamic radiology) and methods of ARA measurement:

Study	Participants	Test protocol	ARA definition	Other factors		Mean (°)	SD (°)	Range (°)
Barkel, D. C. et al. (1988)	13 healthy participants. Seven men, six women. Age 25 to 61 years (mean 35).	Balloon topography, balloon filled to assume rectum	Method A	Lying	**Rest**	102	18	-
					Squeeze	81	19	-
				Sitting	**Rest**	119	17	-
					Squeeze	87	15	-
				Standing	**Rest**	107	11	-
					Squeeze	88	6	-
Mahieu, P. et al. (1984)	56 healthy patients, 22 men, 34 women. Age 17 – 80 years (mean 47.5).	Standard dynamic radiology	Method A	-	**Rest**	92	-	-
					Squeeze	-	-	-
Felt-Bersma, R. J. F. et al. (1990)	30 mixed gender patients with faecal incontinence. Age unknown.	Standard dynamic radiology	Method A	-	**Rest**	104	17	
					Squeeze	-	-	-
			Method B	-	**Rest**	124	18	
					Squeeze	-	-	-
Shorvon, P. J. et al. (1989)	48 healthy subjects. 23 women mean age 21. 25 men mean age 26.	Standard dynamic radiology	Method A	Men	**Rest**	96	17	61
					Squeeze	80	16	71
				Women	**Rest**	95	16	64
					Squeeze	71	12	41
			Method B	Men	**Rest**	118	12	49
					Squeeze	113	17	70
Piloni, P. et al. (1999)	69 continent and 82 incontinent subjects. Approximately half men, half women. Age 56.5±10.22 and 59.3±9.7 years respectively.	Standard dynamic radiology	Method A	Continent	**Rest**	104.5	10.3	-
					Squeeze	84.5	14.2	-
				Incontinent	**Rest**	116.2	23.6	-
					Squeeze	95.1	20.1	-

Comparison of the results point to similarities but a high level of variation depending on the experimental method and definition of ARA. As has been recognised [76], the standard procedure for measuring ARA values is to use the definition from method A. The majority of studies practise this method and it will be taken as the preferred measurement in this thesis.

There is notable variation between studies, depending on the population, investigative procedure and method for measuring the ARA. While Felt-Bersma and Shorvon have both demonstrated a prominent variation depending of on the method for ARA measurement, other factors also play a cause; Barkel demonstrated that depending on whether the patient was sitting, lying or standing, there could be substantial difference in the values observed. The review aimed to investigate the variation in ARA during rest and squeeze pressures. During squeeze, the pelvic floor muscles contract enhancing the angulation of the anorectum as seen across all studies, evident by a decrease in the ARA upon squeezing. FI appears to have a prominent impact on the values of ARA recoded, evident in an increase at rest for healthy subjects from 92° (Mahieu) and 95.5° (Shorvon) to 104° (Felt-Bersma) and 116.2° (Piloni). Demonstrating an increasing in the resting ARA of around 10-15° due to FI. ARAs observed during voluntary squeeze appear to be affected in a similar way, with healthy subjects producing an ARA during squeeze of 87° (Barkel) and 75.5° (Shorvon) compared with 95.1° observed for FI patients by Piloni et al. This suggests that the FI patients included in the study still have pelvic floor tone which can enhance the angulation of the anorectum, though perhaps not sufficiently to maintain continence. Little variation is observed between genders at rest although Shorven et al observed a more acute ARA in women during squeeze, however it is generally thought that gender and age are not factors which strongly effect the ARA [78].

Despite similarities in overall trends observed across the studies between healthy and FI subjects, there are still differences between reported values. This could be due to various reasons such as a small sample size, or the observer's discretion. For the purpose of this thesis, values from Shorvon and Piloni are taken for healthy and FI subjects, due to their large sample sizes compared with the other studies.

2.2.2.4. Rectal Compliance

Rectal compliance is an aspect of anorectal function. The volume of fluid inside the rectum is incrementally increased and values of volume and corresponding rectal pressure are taken at certain physiological events; when the subject first experiences rectal sensation, upon the feeling of urge and the maximum tolerable volume. The measurement of rectal compliance is generally performed with a latex balloon filled with water. There are varied opinions in literature on the most accurate procedure, depending on the size and elasticity of the balloon [81-83]. However the values

reported in this review are from a study which uses a routine rectal compliance measurement with a compliant latex balloon in healthy subjects and patients referred for anorectal function evaluation [18] (discussed below).

A person's inability to detect faecal matter within the rectum negatively impacts on their ability to retain bowel contents, evident from observation of the volume at first sensation with an increase from 73 ml in healthy subjects to 94 ml in FI patients, also correlating in a slight increase in rectal pressure between the two subject groups. The variation in rectal pressures between the two groups becomes more pronounced as the rectal volume increases, upon sensing 'urge', in healthy subjects mean rectal pressures are observed of 29 mmHg whereas in FI patients mean pressures are observed of 34 mm Hg. This increase in pressure could mean that an FI patient has less time to find an appropriate place to evacuate their bowels compared with a healthy subject, while the ability for an FI patient to overcome rectal pressure and retain the contents of their bowel is probably much worse. In patients with rectoceles, but without FI, much larger maximum tolerable rectal volumes are observed, evident in an increase in volume from a mean of 230 ml in healthy subjects to 251 ml in patients with rectoceles. Interestingly this volume increase is observed without a corresponding increase in pressure, with a mean of 29 mmHg recorded in both cases. This suggests that the addition of a rectocele essentially reduces the elasticity of the rectum, requiring a larger volume to achieve equivalent pressures.

2.2.3. Mechanical Properties

Where possible, the mechanical properties of important components of the human defecatory system are identified from literature, to inform the material selection for biological tissue phantoms.

2.2.3.1. Rectum

Several studies have addressed the tensile properties of porcine and human rectal tissue. One study conducted by Rubod et al. [84] produced test specimens from 5 fresh female cadavers, uniaxial tensile data was obtained through cyclic loading the specimens at a constant strain rate of 20mm/s at an ambient temperature of 20°C. 8 samples were taken from each specimen, both in the longitudinal and transverse orientations and at the posterior and anterior portions to capture the global properties

of the tissue organ. The test area of each sample measured 15mm in length and 4mm in width.

Another study conducted by Christensen et al. [85] compared the tensile properties of human and porcine rectum tissue. During the study, approximately 300mm of porcine bowel tissue was obtained immediately after slaughter, extending from the anus to sigmoid colon. Similar sized human bowel tissue samples were also obtained from a commercial tissue donation centre from 5 males (mean age 70.8 years) and 6 females (mean age 64.2 years). All samples were stored at -20°C prior to mechanical testing. Four samples measuring 50mm in length and 10mm in width were taken from each rectum sample in total, two orientated in the transverse direction to muscle fibres and two longitudinal. Prior to tensile testing, samples were pre-conditioned using ten cycles of 20% strain. Each sample was then loaded to failure at a constant strain rate of 0.5mm/s. The study concluded that human tissue was generally stronger, stiffer, and less compliant than porcine tissue.

Finally in a study conducted by Qiao et al. [86], tensile specimens were taken from the porcine rectum wall in the transverse, longitudinal and 45° inclined orientations. The testing area of the specimens measured 1mm in length and 1mm in width. Prior to testing, 5 preconditioning cycles were carried out up to a strain of 40% before specimens were loaded to failure at a constant rate of 6mm/min.

The stress-strain profiles obtained from these studies are compared in Figure 2.10.

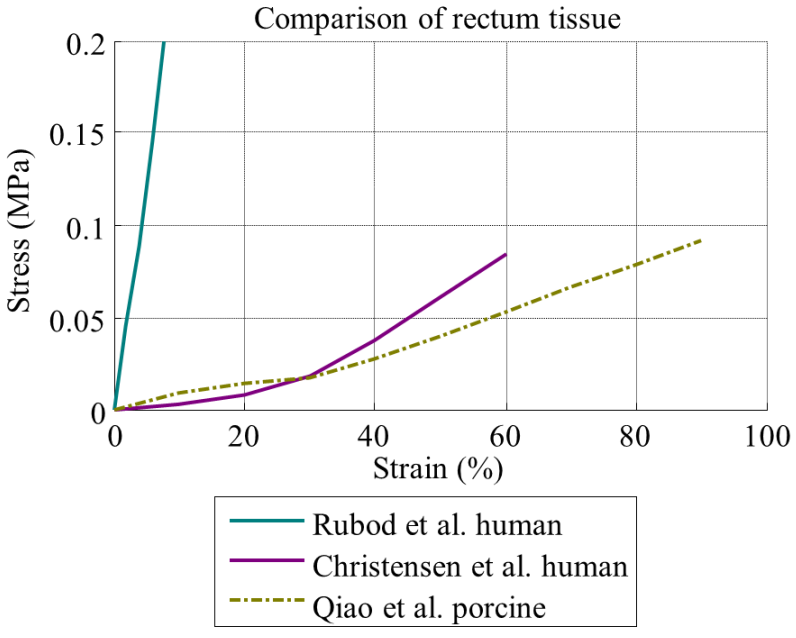

Figure 2.10 Comparison of rectum tensile data from separate studies.

While the loading profiles observed by Christenesen and Qiao are comparable, the loading profile observed by Rubod shows a much steeper gradient, demonstrating a greater material stiffness. Although omitted from Figure 2.10 for clarity, in the investigation conducted by Rubod, rectal tissue ruptured at a mean of around 25% strain, much lower than the rupture strains observed by Christensen (60%) and Qiao (90%). This is probably due to a faster loading rate used by Rubod (20mm/s) compared to tests conducted by Christensen (0.5mm/s) and Qiao (0.1mm/s). Due to the viscoelasticity of tissue, its loading profile is characterised by hysteresis, as visible in greater material stiffness observed for larger displacements, and this also attributes greater stiffness to the tissue when loaded at increased strain rates. The rectum model used in the physical simulation is expected to undergo similar strain rates to those employed by Christensen and Qiao. Given that the tests by Christensen et al. were conducted on human rectal tissue and the sample area was larger (therefore spanning muscle fibres and connective tissues), results from this particular study will be used within this thesis.

2.2.3.2. Adipose Tissue

Very few studies have been carried out on the tensile properties of adipose fatty tissue. The study described presents findings from a fairly large range of data, and will be considered a reliable representation of the tissues mechanical behaviour.

In a study carried out by Alkhouli et al. [87], adipose tissue was obtained from 44 patients of mixed gender undergoing surgery. Samples were taken which varied from 8-17mm in length, 3-6.5mm in width and 1.5-3.5mm in thickness. They were then attached to paddles with a superglue gel and immersed in saline solution in preparation for tensile loading at a rate of 0.3mm/min. Results from the study are shown in Figure 2.11.

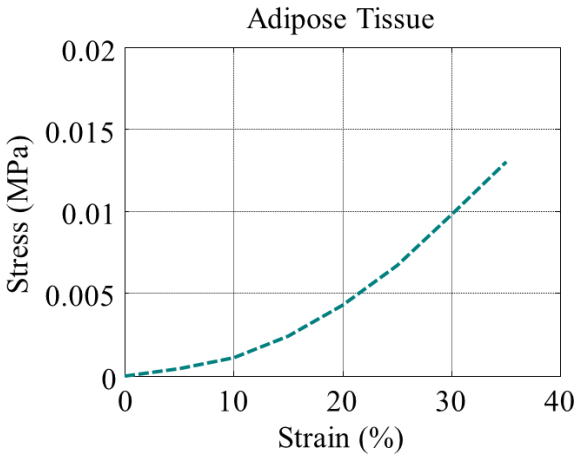

Figure 2.11 Tensile properties of adipose tissue [87].

2.3. Interventional Treatments for Faecal Incontinence

Typically, the treatment process for FI is divided into categories based on severity of the symptoms and degree of success from previous treatment attempts.

2.3.1. Irrigation

Transanal irrigation (TAI) of the rectum and colon became established in the UK as an important player of the treatment schedule for many patients with bowel symptoms. It was initially introduced as a treatment for patients with neurological illnesses which caused bowel dysfunction although it has increasingly become considered for use in patients with functional disorders. TAI assists the evacuation of faeces from the bowel by introducing water via the anus. Regular use of TAI can help re-establish controlled bowel function which enables users to develop a consistent bowel routine.

TAI can be used to manage long-term FI and/or constipation. It is generally used where other treatments have failed and consequently, is often reserved for those with more severe/neurogenic bowel dysfunction. Neurogenic bowel dysfunction is often diagnosed from birth as an underlying burden of a larger scale neurological disorder and therefore should be managed with the patient from an early age. The Peristeen TAI system was introduced in Our Lady's Hospital (Dublin, 2011) where the colorectal department evaluated it to determine patient satisfaction. Of the 89 children evaluated, 75% still use Peristeen, 19% do not and a further 6% are scheduled for re-training. Reasons for discontinuation include returning to another irrigation system and surgical intervention [88].

2.3.2. Antegrade Continence Enema

The antegrade continence enema (ACE) procedure was first introduced as a technique to control faecal leakage in children [89]. An appendix is used to access the caecum creating a catheterisable channel though which antegrade enemas could be given. Technical modifications have meant that it is no longer necessary to reverse the appendix and introduction of laparoscopic technique has simplified it further. The ACE procedure has had consistent success in paediatric practice and its indication has been extended to include adults with FI [90]. Patients who are resistive to biofeedback or conventional surgery have had an underlying rectal evacuation disorder as a result of both sensory and motor disturbances within the anorectal complex. The ACE procedure aims at improving symptoms of disturbed evacuation and can also improve FI by regular colonic emptying.

There is currently limited data on the experience of the ACE procedure in adults [91]. Short term results have shown that it has been successful in 40-60% of patients. However, although longer term results have be acceptable [92], they have not been without complications, the biggest being compliance of patients. The most common side effect of the procedure is leakage of material from the stoma. However, with good patient education, results are much more satisfactory and the ACE has offered patients considerable improvement of symptoms and QoL [93].

2.3.3. Anal Plugs

Anal plugs have been used to reduce the loss of stool. The anal plug was first introduced in 1986 and was adapted from a stoma plug [94]. Coloplast has since modified the design of the device with the Peristeen® Anal Plug. It consists of a cup-shaped foam plug with a gauze string for removal. The plug expands upon insertion to fit the contour of the lower rectum, effectively plugging the anus and preventing faecal leakage. Users are able to wear the device for up to 12 hours. Previous studies have shown that although it may be useful in the containment of faecal leakage, it is poorly tolerated in many patients [95-97]. These studies concluded that the plug was not suitable for permanent use, mainly due to discomfort. But it offers good protection against incontinence episodes.

2.3.4. Anterior Sphincteroplasty

Anterior sphincteroplasty is a surgical procedure in which scar tissue in the anterior anal sphincter is divided before the muscle is repaired by overlapping the healthy tissue. Statistical analysis of the procedure has been carried out in a previous study; of 120 (median age of 58) patients who underwent the procedure, 23% encountered a postoperative complication, 21% of which experienced wound infection and the majority required further surgery to treat their complication. Follow-up results (median time interval of 111 months) revealed that of the patients operated on, 60% experienced a moderate to excellent outcome and 40% experienced a poor outcome, 18% of which underwent additional surgery [98].

2.3.5. Graciloplasty

Stimulated graciloplasty involves creating a new anal sphincter using transposed Gracilis muscle. Electrodes are implanted in the transposed muscle and connected to an electric pulse generator implanted in the abdominal wall. A continuous current from the pulse generator alters the character of the Gracilis muscle fibres, causing them to contract to provide continence, or relax during defecation. A systematic review of 37 studies of the graciloplasty procedure found that between 42% and 85% of patients became continent. Complications with the procedure arose however, in keeping with its poor safety record. The most common complication was wound infection. In a case series which included 121 patients, serious infection which needed hospitalisation was reported in 15%. In one study of 48 patients, 48% had technical problems with the pulse generator leading to hospitalisation. In a comparative study of 48 patients, 69% had evacuation difficulties or pain following graciloplasty, requiring hospitalisation. In a case series of 123 patients, 2% had deep vein thrombosis and one died following a pulmonary embolism 3 weeks after surgery [99].

2.3.6. Parks Post-Anal Repair

A number of operations were developed in the 20th century to provide a treatment solution to patients whose anal sphincter was intact, but damaged or weak. One alternative strategy is the post-anal repair operation for idiopathic FI, designed to correct an overly obtuse ARA [11] by reducing the angulation [100, 101]. Devised in 1975 the procedure used sutures to restore the ARA. Despite a good success being observed in some patients, other procedures failed due to the limited properties of

materials available, inadequate modification to the ARA and poor patient cooperation with post-operative care [11].

2.3.7. Sacral Nerve Stimulation

In patients with a weak but structurally intact sphincter, it may be possible to alter sphincter and bowel behaviour using the surrounding nerves and muscles. Sacral nerve stimulation (SNS) involves applying an electric current to one of the sacral nerves via an electrode placed through the corresponding sacral foramen. Commonly, the procedure is tested in each patient over a 2- to 3-week period, with a temporary percutaneous peripheral nerve electrode attached to an external stimulator. If significant benefit is achieved, then the permanent implantable pulse generator can be implanted. The procedure benefits over half of patients reviewed. In patients that received the permanent implant, 41-75% experienced complete continence and 75-100% of patients experienced a 50% decrease in number of incontinence episodes [102]. Of the patients that received permanent implants, 2% became infected, 5% experienced lead migration and 4% experienced pain [102].

2.3.8. Faecal Incontinence Devices

AAS devices based on a circular cuff design, as used to treat urinary incontinence [21, 22], have been applied to the treatment of FI in animals and humans. In early reports they were shown to produce intestinal ischaemia at operating pressures which maintain continence [24]. Due to a non-compliant implant-tissue interface, Artificial Anal Sphincter (AAS) devices can cause crenation of the anal canal tissue, leading to high localised pressure zones and tissue damage. The physiological structure of the bowel differs greatly from the urethra, and as a result it is less tolerant to ischaemia than the urethra [103]. Early developments of the AAS showed poor conformity with the bowel, this heterogeneous application of pressure has the potential to create localized high-pressure zones which may damage the bowel if it crenates into these areas [54, 103].

Large sphincter pressures from AAS devices can lead to tissue necrosis and abnormally large rectal volumes. In many cases with the implantation of an AAS, it is not uncommon for patients with prior history of FI to become constipated [104]. While it is widely accepted that the anal sphincters play a fundamental role in the maintenance of continence, their contribution in coordination with other continence

mechanisms are poorly understood. Studies have shown that the EAS is only 'active' during sensations of 'urge' or during 'squeeze', despite this, current AAS devices apply pressure to the anal canal at all times between periods of expulsion [105].

Despite its importance in maintaining continence, few FI devices aim to assist the modulation of the ARA. Although studies have shown that the ARA is effective in obstructing the passage of faeces, there is little understanding on its contribution to continence [106]. Currently only a small number of surgical treatments are available for patients with severe FI and these focus on augmentation of the anal sphincter.

2.3.8.1. Passive Artificial Anal Sphincter

The FENIX® Continence Restoration System is a relatively new commercially available passive-assistive medical device to treat FI. It consists of a ring of magnetic beads which sit around the anal canal. The beads pop open during defecation, enabling the device to expand radially to reduce anal canal occlusion and resistance to passing faeces. It assists the sphincter muscles, keeping them closed at rest. Early studies on a few patients suggest that this device functions as intended but clinical data is limited and more studies are needed [107]. Benefits of the device are that it is passive and internal and does not require manual operation by the patient. However the system was first implanted in 2008 and long term clinical data is non-existent. It is unclear how the device might perform over a longer period of time, particularly in younger patients. Several devices have failed due to device migration by erosion through the rectum and infection of surrounding tissue.

2.3.8.2. Active Artificial Anal Sphincter

Numerous studies have been carried out into the development of AASs. Inflatable AAS designs [105, 108, 109] consist of 3 components; an inflatable cuff, fluid reservoir and a pump. The inflatable cuff is positioned around the anal canal, and its internal pressure is regulated by a pump, aiming to mimic pressures generated from the natural function of the sphincter muscles. When fluid is displaced from the cuff, it relaxes the pressure applied to the anal canal and defecation occurs. The balloon reservoir is positioned subcutaneously such that it has a sigmoid pressure-volume relationship and provides the hydraulic pressure to drive the system, while a constant maximum pressure is maintained in the system irrespective of inflation volume. The control pump provides the energy to transfer fluid between the sphincter component

and balloon reservoir. Other non-inflatable AAS devices have also been developed, making use of novel actuation methods [110], with a reduced number of components in an attempt to and increase the longevity of the device. An overview of a variety of AAS systems reported in literature are visible in Figure 2.12.

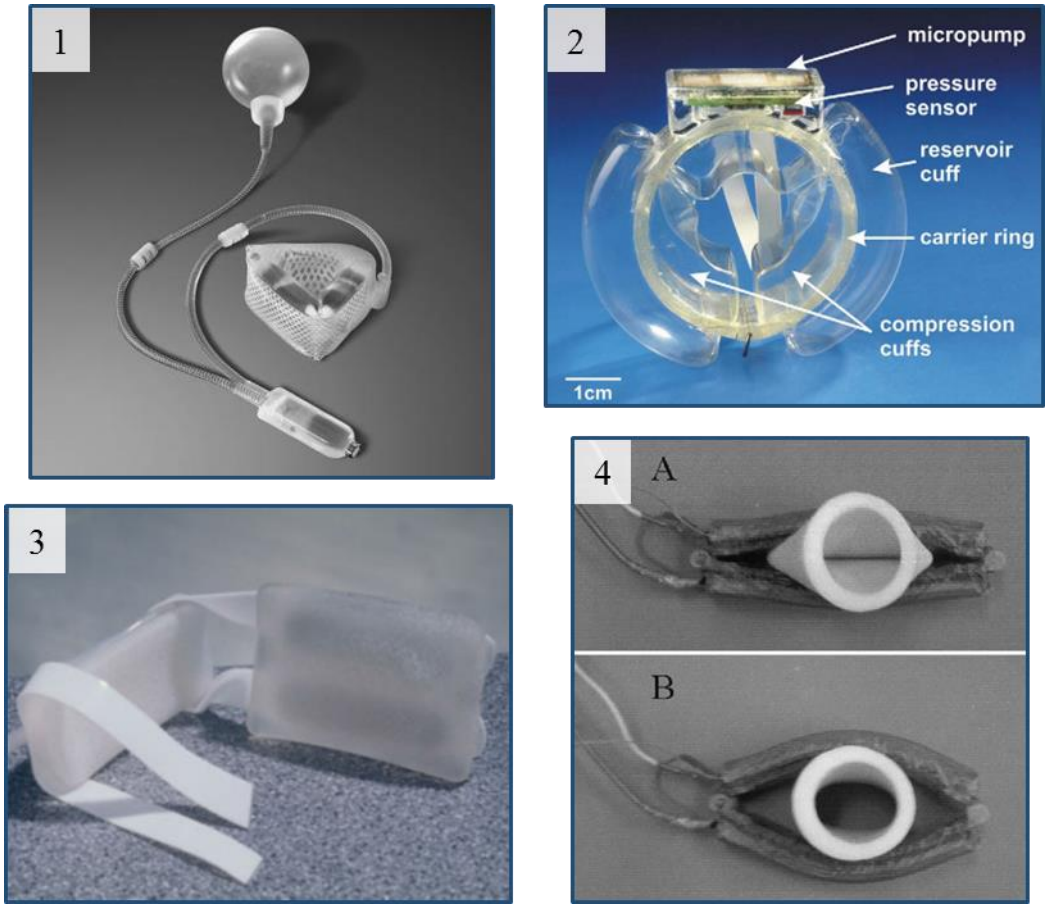

Figure 2.12 Images of AAS devices displaying; 1) Acticon Neosphincter[105]; 2) German Artificial Sphincter System[108]; 3) Novel Prosthetic Anal Sphincter [109] and 4) SMA Artificial Anal Sphincter [110] (in 'A': non-actuated closed state and 'B': actuated open state).

Acticon Neosphincter

Originally the American Medical Systems urinary sphincter was adapted for use as an artificial bowel sphincter. Inspired by this, the Acticon Neosphincter AAS has now been developed [105]. This AAS has three components: an inflatable cuff (the sphincter), a pressure regulating balloon and a control pump [111]. The device actively prevents incontinence and can be implanted in patients with no anal sphincter control. However it requires a complex surgical procedure and many devices failed due to infection and by causing erosion to the anal sphincter. Furthermore the system

includes external components and requires manual operation by the patient. Studies have shown success rates (for people with a functioning device) of 65%, at a mean follow up of 26.5 months [112].

German Artificial Sphincter System

Operation of the German artificial sphincter system is controlled by fluid which is pumped into the inflatable cuff using a micro piezo-electric pump, capable of applying a pressure of 120mmHg. Due to the use of an electric pump, the device eliminates a physical human input. This reduces operation time and effort required for defecation [113]. Due to the inclusion of fluid transfer mechanisms and electric components, this device is more complex and has an increased risk of failure and increased manufacture costs.

Novel Prosthetic Anal Sphincter

The prosthetic anal sphincter [114] consists of a fluid filled cuff element that is placed around the bowel at the level of the anorectal junction, to augment the action of the anal sphincters. This differs from other AAS designs by using a novel cuff design to reduce restriction of colonic blood flow [115]. The fluid filled cuff (sphincter component) consists of an inflatable linear expander and a soft gel-filled pillow, when the expander is inflated, it flattens the bowel against the pillow to cause angulation (Figure 2.12) in addition to circumferential stenosis.

SMA Artificial Anal Sphincter

An SMA AAS concept has been developed [116]. The device consists of two SMA's attached to flexible heaters which promote actuation. Both are secured to hinges located at either end, allowing the artificial sphincter to clamp the anal canal when unactuated and form a circular profile when heated, releasing the anal canal and allowing bowel evacuation. The heaters are activated wirelessly using a transcutaneous energy transmission system [117, 118] (eliminating the need for percutaneous connections) and heat the SMA's to 55° (their phase transformation completion temperature). Silicone pads surround the SMA's and heaters to reduce pressure applied to the anal canal and help prevent tissue damage.

Transcutaneous Power Delivery System Artificial Anal Sphincter [119]

This AAS system uses a transcutaneous power delivery system to transfer energy by means of electromagnetic induction between two coils placed face-to-face on either side of the abdomen. The transcutaneous power delivery system AAS makes use of a reservoir, front cuff, sensor cuff and micro-pump. There are two sensors to detect the pressure of the anal canal. One measures pressure of the front cuff (clamping the rectum) and the other measures pressure of the rectum. This allows the system to vary internal pressure of the artificial sphincter and consequently, the state of continence. Advantages of this system are that it monitors pressure within the anal canal to adjust cuff pressure to that required and notifies the user when to start and stop defecation.

2.3.9. Pelvic Floor Mesh Support

The use of meshes in the application of female pelvic floor reconstructive surgery has given rise to numerous complications, usually leading to surgical revisions or removals [120]. Pelvic floor meshes generally fail due to the material not being flexible and compliant. The TOPAS system consists of a minimally invasive self-fixating mesh sling which is implanted and bonds to the pelvic floor providing reinforcement. This system aims to enhance the ARA and reduce incontinence episodes in women with moderate FI symptoms. A study which included 29 women implanted with the TOPAS system revealed that the number of incontinence episodes per week decreased from 6.9 prior to the treatment to 3.5 at 24 months follow-up. The most common adverse effects of the treatment were urinary incontinence in 6 cases, worsening FI in 2 cases and constipation in 2 cases. No device related erosions or extrusions were reported [121].

2.4. Physiological Organ Simulators

While organ simulations and bio-reactors have been developed for a greater understanding of the biomechanics of the human system, very few models aim to replicate the defecatory system and mechanisms associated with continence. However a small number of physiological models of the pelvic floor and components of the pelvic cavity have been developed and these are detailed in this review.

2.4.1. Computational Models of the Pelvic Floor

Finite element models of the pelvic floor have been developed in attempts to understand its function in the urinary and faecal continence mechanisms. One model has been developed to investigate the effect of stool consistency on continence [122]. While another looks at the effect of damaged ligaments on stress urinary incontinence [123]. Computational models have also been developed to characterise the global behaviour of the pelvic floor muscles [124-128]. However, there are large quantitative differences between the models and parameters used.

2.4.1.1. Pelvic Organs and Pelvic Floor Musculature

One study conducted by Brandão et al. [129] develops a numerical simulation which models the voluntary contraction of the pelvic floor muscles to evaluate the resulting displacements of the muscles along with pelvic organs. Structures were segmented from MRI images taken of a young female volunteer before material properties were attributed from a variety of constitutive models. Using a FE method, displacements produced in the model, Figure 2.13, were compared to those measured from MRI images.

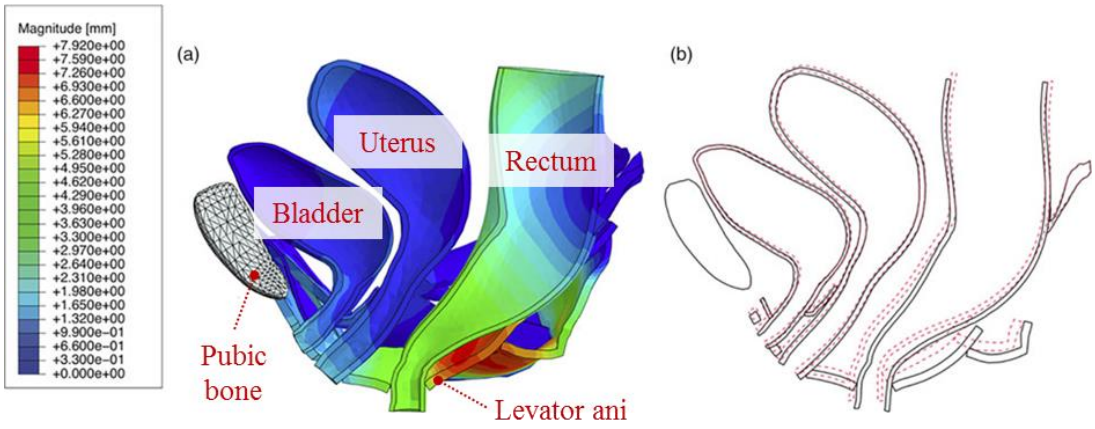

Figure 2.13 Morphology of the pelvic organs and musculature showing a) magnitude values from FEA nodal displacements of the pelvic organs and pelvic floor muscles and b) schematic of variation in pelvic organ position from rest (*solid, black*) to their contraction (*dashed, red*) [129].

There were conflicting levels of agreement between the computational study and human measurements, movement of the pelvic floor musculature in the anterior direction was comparable between the two, evident from 5.2 mm observed in the numerical model compared with 5 mm in the human system. However there was

substantial difference in the magnitude of movement observed in the vertical direction, with a movement of 6.6 mm observed in the simulation and 2.5 mm in the human system. The study hypothesises that this is due to a difference in intra-abdominal pressure which is assumed a baseline value throughout the study.

2.4.1.2. Stool Consistency

A computational model was developed to investigate the effect of stool consistency on faecal leakage [130]. A FE model was developed which included influential structures in maintaining continence (rectum, vagina, uterus, bladder, levator ani and sphincter muscles), material properties were applied using constitutive models and a closing pressure of 88 mmHg was applied to the IAS to simulate anal resting tone. During tests IR pressure was incrementally increased under two different stool consistencies (solid and a semi-solid). As the intra-abdominal pressure increased the resting anorectal pressure could no longer retain stool in the rectum and leakage occurred. Results from the study showed that the minimum intra-abdominal pressure that resulted in leakage of stool regardless of consistency, was 73 mmHg. However, compared to solid stool, semi-solid stool resulted in a larger volume of stool leakage under similar biomechanical conditions. This work demonstrates that in addition to impaired EAS function, stool consistency plays a direct role in the volume of stool leakage with FI.

2.4.2. Physical Models of the Pelvic Floor

Alternative strategies to sphincter augmentation have also been explored. Notably, in *vitro* studies have shown that increasing the ARA reduces the occlusion pressure required to hold back solids and semi-solids [106, 115]. Similarly, another study reported increased retention of semisolid material when increasing ARA in an ex vivo porcine rectum, but no effect for water [106]. The question of whether the ARA or sphincter occlusion pressure is a greater contributor to continence remains unanswered, despite previous studies comparing the two [79, 131]. It is evident that modulating ARA is a key feature in maintaining continence and provides a complementary strategy to sphincter augmentation. There are currently no clinically available devices that exploit these features.

2.4.2.1. Anal Sphincter Tone

Physical models of the anal sphincter muscle have been developed with the intension for improved haptic-based simulation tools for learning and training digital rectal examinations. In total, three sphincter models were developed [132], Figure 2.14, using different actuation techniques to investigate their ability to reproduce sphincter pressures observed in clinic.

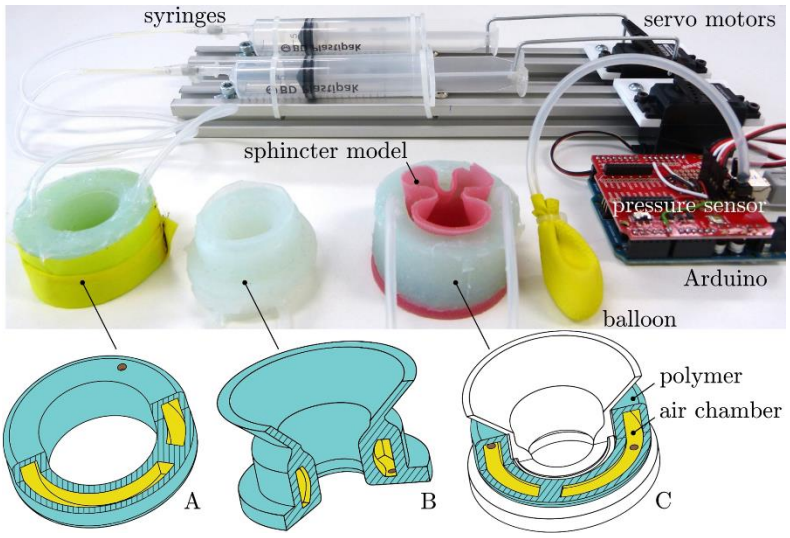

Figure 2.14 Pneumatic and cable driven anal sphincters, showing *top*; the pneumatic mechanisms (A, B and C), a thin layer of inextensible fabric (in *yellow*) encapsulates the actuators to prevent ballooning [132].

The designs consist of silicone sphincter model which is pneumatically actuated, another which is a pneumatic assembly encompassed by another pneumatic actuator and lastly, a cable driven model. Anorectal manometry was conducted on the sphincter models to empirically assess their performance, in addition to examinations conducted by nurse practitioners and colorectal surgeons.

This study concluded that both actuation mechanisms were able to reproduce enough pressure on an examining finger along with a range of healthy and abnormal cases.

2.4.2.2. Rectum Phantom

In a qualitative study, a rectum was modelled using a silicone phantom based on CT scans of a male patient. A mould was made from which silicone rectum phantoms were cast using different grades of silicone (based on shore values) including different quantities of additives. Five surgical residents and one surgical consultant were asked to evaluate the rectum models. The rectum deemed to ‘feel’ the most realistic, in terms

of compressive strength and elasticity, was manufactured from silicone Ecoflex 00-30 with a slacker softening agent [133].

2.4.3. Physical Models of Arteries

Physical models of human organs have been developed in the past. They are particularly advantageous over computational methods when simulating complex biomechanical parameters, for example to observe wave propagation in arteries. Development a comprehensive model to observe this phenomenon presents a difficult challenge due to the viscoelasticity of arterial walls, together with their intricate geometries and transport of pulsatile flow of blood.

2.4.3.1. Physical Modelling of Human Arteries

A similar method to fabricate human arterial models has been employed by studies in the past; of the circle of Willis for testing blood flow characteristics [134] and of the human cerebral artery the influence of medical devices [135]. This method starts with a numerical model of the arterial structure to model, segmented from CT data, which is simplified to remove noise and small side-branches. The numerical model is then fabricated from wax using fused deposition rapid prototyping. The vasculature wax structure is dipped into elastomeric material to represent the arterial wall (silicone and polyurethane elastomers have been used) and then left to cure to create a membrane around the wax core. Finally, the composite wax-elastomer structure is placed in a hollow transparent casing and embedded with a silicone gel to represent the surrounding human tissue. Finally, the wax core is removed by selective dissolution using acetone as a solvent to complete the phantom model, Figure 2.15. [135]

Figure 2.15 Physical model of the human cerebral artery fabricated from polyurethane and silicone elastomers. [135]

Transparent materials are selected for each component for ease of visualising the structure, and the flow of fluid through it. Transparency also allows photoelastic analysis to be conducted on the model to observe the distribution of stress in the arterial walls, when subject to a flow regime through the system [135].

2.4.3.2. Simulating Pulsatile Blood Flow

A physical test simulation has been developed to observe characteristics of pulsatile blood flow during passage through a prosthetic porcine aorta [136]. A commercially available prosthetic porcine aorta valve was incorporated into a recirculating test simulation. Control hardware was implemented through use of a pulsatile flow system (Superdupr, Vivitro Systems Incorporated, Victoria, BC, Canada) to modulate the flow characteristics of a blood analogue around the simulator. The pulsatile flow system consisted of a waveform generator and a piston-in-cylinder pump head driven by a low inertia electric motor. Waveforms characteristic of physiological pulsatile flows through the aorta were generated and used as inputs to control the pump. PIV imaging, consisting of a video camera, laser-sheet lighting and addition of polycrystalline powder (as s seed particle for flow visualisation), was used to observe the flow velocity of blood exiting the aortic valve. Using these flow generation and imaging techniques the flow regime through the aortic valve were successfully observed in a 2-dimensioanl plane

2.5. Summary

Despite disagreement between prevalence studies on FI, it is clear that a large proportion of the population are bearers of the condition. Those who suffer from FI experience a range in the severity of symptoms; while conservative treatments are successful for some, there is a large unmet need in the treatment for patients with severe incontinence which is greatly more debilitating with a larger negative impact on QoL. While surgical interventions have been trialled, they often show poor efficacy and are not fit for of worldwide adoption. Current efforts have focussed around the AAS device, with many adaptions and iterations failing to address the complexities of the challenge at hand. Consequently, there is a need to investigate the function of other continence mechanisms which could be manipulated by future FI technologies. During this literature review, the roles of the pelvic floor, rectum, sphincter complex and PR muscle have been analysed in detail. It is evident that to preserve continence

requires coordination of numerous ‘components’ of the defecation system. To develop a device to assist the healthy function of a system, requires an understanding of the biomechanics of the native environment in which it will operate.

The vast majority of FI devices rely on animal studies and clinical trials for development since the resources are not available for rigorous evaluation in laboratory environments. Through observation of an FI device within a physical simulation, the efficacy can be empirically assessed while the potential for the simulation to analyse FI devices can also be addressed. Additionally, the inclusion of an FI device which complements the natural occlusion pressure of the sphincter muscles on the anal canal facilitates observation of the effect of augmenting sphincter occlusion on the simulation, in conjunction with other continence mechanisms.

A handful of physical and computational models of the faecal system have been developed in the past. Many of which look only at certain aspects of the faecal system, while negating others, and many models focus on the innervation to the pelvic floor or ligament forces. From this review, a distinct paucity in the modelling (computational and physical) of FI and continence mechanisms has been identified. Existing work is dominated by the use of computational models to simulate aspects of the pelvic floor system. FE models of the pelvic floor have been developed in attempts to understand its function in urinary and faecal continence mechanisms. One model has been developed to investigate the effect of stool consistency on continence [122], while another looks at the effect of damaged ligaments on stress urinary incontinence [123]. Computational models have also been developed to characterise the global behaviour of the pelvic floor muscles [124, 137-140]. However, there are large quantitative differences between the models and parameters used [141].

While computational models allow iterative improvement to the model and longevity, and system properties to be simulated accurately with ease, they show deficits in realism when simulating complex interactions between multiple ‘components’. On the other hand, physical modelling of tissues is challenging, in regards of both geometrical and mechanical properties. Despite fabrication challenges, a physical simulation provides opportunities for a deeper understanding of the biomechanics involved during faecal continence, and can aid and accelerate the evaluation of numerous treatment concepts during early development stages.

A detailed review of literature has provided values for geometric and kinematic parameters of the system, summarised in Table 2.3.

Table 2.3 Biomechanical parameters and variables required for simulation modelling, obtained from the literature review:

Simulation component	**Parameters**	**Conditions**	**Values**
Stool	Apparent viscosity @1Hz	Homogeneous (high moisture); Heterogeneous	52.8 Pa.s [142]
	Volume	-	100 ml [143]
	Flow rate	-	9.26 ml/s [143]
Rectum	Length	Empty	130 mm [7]
	Diameter	Empty, male	32 mm [53]
	IR Pressures	Strain	71±33 mmHg [144]
	Anorectal angle	Rest; Strain	84.5°;104.5° [9]
	Elastic modulus (0-35%)	'Active'	0.060 MPa [85]
PR muscle	Length	Rest; Squeeze; Strain	147.6 mm; 127 mm; 189.8 mm [68]
	Width	-	18 mm [2]
EAS	Anterior length	Rest, male	34.2±1.8 mm [1]
	Posterior length	Rest, male	36.6±1.8 mm [1]
	Elastic modulus (0-35%)	'Passive'	0.996 MPa (Presented in Chapter 4)
Anal canal	Pressure	Rest; Squeeze	73±23 mmHg ; 290±155 mmHg [144]
	Distensibility index	Rest (healthy); Rest (FI)	1.5 (0.3-10.4, N=40) ; 3.9 (0.7-12.1, N=34) [145]
Omental adipose tissue	Elastic modulus (0-35%)	-	0.038 MPa [87]

Despite the identification of these parameters, the complete biomechanics of faecal continence are still not properly understood. While studies have been carried out on rectal volume tolerability and corresponding IR pressures [18], the material properties of rectum tissue vary greatly with age [146, 147] and clinical abnormalities. Furthermore, since the rectum is a muscle, its properties are vastly different between states of rest and squeeze. The influence of rectum properties of the normal function of the defecation system is poorly understood. In addition, although sphincter occlusion pressure has been considered the major attributor for continence [79, 131] in the past, numerous studies also report that the PR muscle (through its modulation of the ARA) could be of greater significance than previously believed [2, 73, 106]. As of yet, there is poor understanding on the actual contribution of each of these mechanisms towards continence during different biological 'states' (including the variation of stool consistency), both individually and combined.

A number of clinicians (two colorectal surgeons and a consultant radiologist) were consulted to help understand the biomechanics of continence, and recognise pitfalls in knowledge surrounding FI. The clinical personal were briefed prior to the meetings that there was need for improved technologies for the treatment of severe FI, as identified among patients, clinicians (Appendix II) and in published literature (above). During the meetings, a number of challenges in the area of improvement to knowledge surrounding continence mechanisms and technologies for the treatment of FI were brought to light. Combined with the literature review, four research questions in particular where derived:

"What is the influence of:

1. Sphincter occlusion
2. Anorectal angulation
3. Rectal compliance
4. A commercially available FI device

   …on the faecal system and continence?"

Research questions are established as prerequisites in the development of any surgical robotic application, by defining the goals and specifications of a project. This thesis presents the steps taken to answer these questions by providing a greater understanding on the effect of rectal compliance on the faecal system, and the ability for continence mechanisms (sphincter occlusion and ARA) to retain a range of rectal

contents. It is with this motive, that a physical simulation of the faecal system is developed.

Chapter 3: Technical Requirements, Design, Fabrication and Control of a Physical Simulation of the Human Defecatory System

This chapter presents technical requirements for the conceived research questions defined in Chapter 2. Technical requirements are used to develop a series of specifications and an associated conceptual approach to the project. Tables of biomechanics of the biological system are compiled from literature, required for accurate representation of the defecation system with a physical simulation. Design considerations, fabrication methods and choice of control hardware and software for the physical simulation are documented along with a detailed overview of the simulation.

3.1. Research Questions

A set of research questions were conceived in Chapter 2 which this project looks to address. These were carefully defined from an in-depth review of literature, listening to patient demands at IMPRESS Network events, and discussion with clinical personnel on the deficits in currently available treatments, and their needs in the pursuit of effective treatments for FI.

Four research questions emerged from this; “What is the influence of 1) sphincter occlusion; 2) anorectal angulation; 3) rectal compliance and 4) a commercially available FI device on the faecal system and continence?”

The physical simulation will be developed to focus on these key themes by considering the technical requirements and associated specifications linked with each.

3.2. Simulation Requirements

Research questions are taken into consideration individually and translated into a set of technical requirements for the physical simulation. They are then reviewed together to define global simulation requirements, for an understanding of its characteristics and to assess external devices on the system.

1. What is the influence of sphincter occlusion on the faecal system and continence?

   For an understanding of the effect of sphincter pressure on continence, a geometrical representation of the sphincter complex is required, which is positioned according to the human anatomy, in a physical simulation of the human

faecal system. The elastic modulus of the sphincter complex component should be similar to the biological equivalent, to ensure representative pressures are applied to the anal canal and that the distensibility of the simulated anal canal is consistent with clinical data. In addition, the component should replicate the closure mechanism of the natural system.

2. What is the influence of the ARA on the faecal system and continence?

   An anatomical representation of the anorectum is required, which represents the natural system with an obtuse ARA, similar to during defecation. The ARA of the representation should be configurable, such that the anorectal junction can positioned posteriorly or anteriorly to produce different angulations, in a range for typical 'continent' and 'defecation' values in healthy patients. A means to visually or autonomously monitor the ARA needs to be implemented for its measurement before and during tests along with a method to quantify the influence of the ARA on faecal leakage.

3. What is the influence of rectal compliance on the faecal system and continence?

   Rectum models with a range of rectal compliances should be included within the simulation. Through investigation with the rectal compliances and implementation of an experimental matrix which incrementally varies important system variables one at a time, the influence of rectal compliance on the faecal system and continence can be observed. Properties of the rectum model should aim to represent the distensibility of the human rectum, through data obtained in literature, and a range of rectal compliances should be selected based on this.

4. What is the influence of a commercially available FI device on the faecal system and continence?

   By observing the effect of an FI device which complements the natural occlusion pressure of the sphincter muscles on the anal canal, the efficacy of such a device can be empirically assessed, along with its influence in conjunction with other continence mechanisms.

The first three modelling aspects are brought together to form the simulation. Then their individual and combined effects are observed on the system, together with a commercially available FI device.

3.3. Conceptual Approach to a Physical Simulation

There are a number of different components that need to be included in the physical simulation of the defecatory system, and each component with a potential to be configured in numerous ways i.e. to represent different genders, age groups, or 'healthy' or 'incontinent' states. A detailed review of literature has provided values for geometric and kinematic parameters of the system and these are used in addition to the technical requirements, in assisting design decisions during the conception of the simulation.

3.3.1. Soft Components

Soft representations of biological components, shown in Figure 3.1, that are paramount in the maintenance of continence are housed in a rigid frame to form the basis of the simulation. At the heart of the simulation is a phantom model of the human rectum combined with the anal canal, the rectum is based on the anatomy of a nulliparous subject in an empty 'resting' state. Since the anal canal is closed at rest, its diameter is instead modelled based on a maximum diameter as experienced during evacuation, measured during distensibility studies. The anal canal forms an angle with the rectum which assumes a healthy value during 'strain', it is then augmented to form a more acute angle. The rectum model is fixed superiorly where it would connect to the colon in the biological system, and inferiorly to the 'anal verge'. A configurable rigid frame is used to provide support and fixation to soft components.

The levator ani has been identified as an important component of the pelvic floor in the maintenance of continence. Subsequently the PR muscle forms part of the levator ani and is considered responsible for interacting with rectum and modulating the

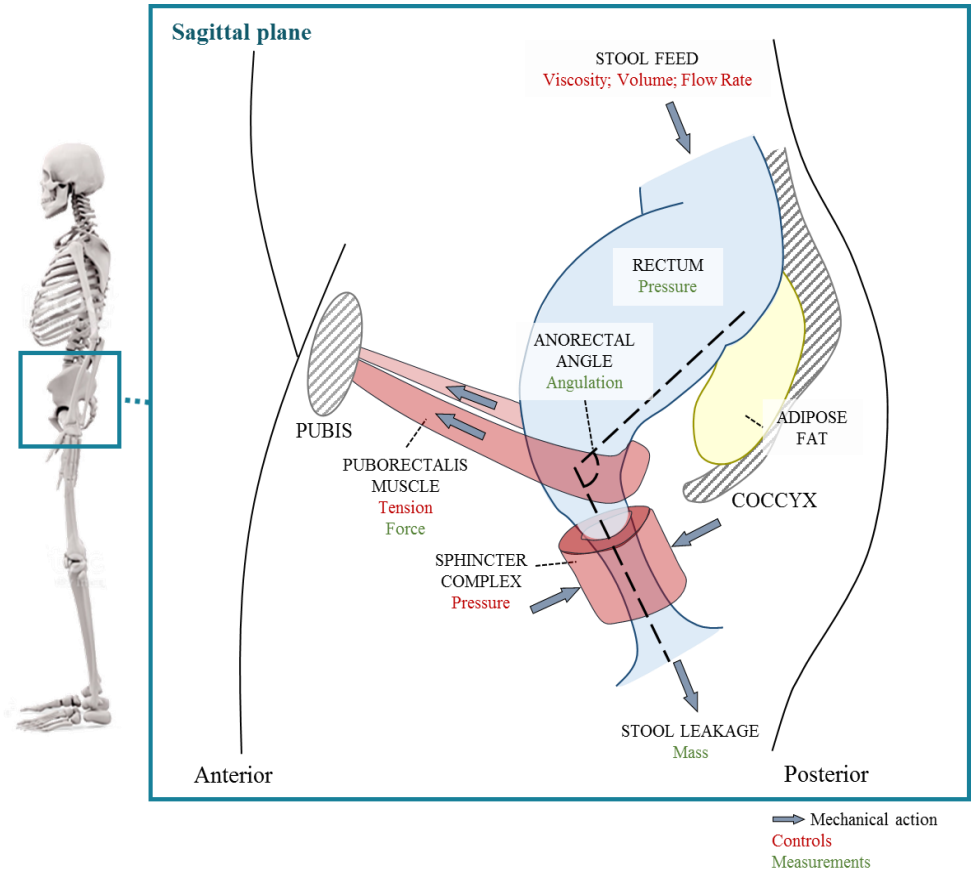

Figure 3.1 Schematic overview of the biomechanical mechanisms of the physical simulation of the faecal system, 'controls' are shown in *red* and 'measurements' are shown in *green*.

ARA. In the physical simulation, a model of the PR muscle acts on the base of the rectum to apply a force and augment the ARA. A model of the sphincter complex is positioned around the anal canal and applies 'passive' resistance to the passage of faeces, by recreating the natural closing mechanisms of the anal canal, as within in a healthy 'resting' system.

The inclusion of a FI device enhances anal canal pressures to values observed in a healthy system during 'squeeze', and these effects on the intra-rectal (IR) pressure and faecal leakage from the system can be monitored, along with the influence of the PR muscle component, rectal compliance and stool consistency.

3.3.2. Simulated Stool

Simulated stool material forms a flow regime through the rectum. A homogeneous medium models diarrhoea as a worst case scenario, whereas use of a heterogeneous medium would be used to represent a 'normal' movement of stool though the bowel. Biomechanics of the rectum are recreated to ensure the flow regime through the

system is consistent with the natural system, this means close simulation of mechanical properties, methods of constraint and interaction with surrounding soft tissues. Posteriorly, the rectum interfaces with simulated adipose tissue whereas anteriorly, it will be free to expand without constraint. The volume and flow rate of the stool introduced to the system is controlled, together with rectal biomechanics, to recreate a flow regime characteristic of homogeneous stool through the biological the system. Stool transit through the system is a direct indication of continence. The pressure inside the rectum is observed along with leakage of stool from the anal canal, allowing factors affecting the pressure and transit rate of stool through the system to be quantified.

3.3.3. System Control

Control hardware is used to enable regulated delivery of stool analogue to the system and the position of the anorectum by loosening and tightening the PR muscle phantom, shown in Table 3.1.

Measurement hardware is implemented, to monitor the force applied to the rectum by the PR muscle component, and measure the mass of faecal leakage from the anal canal. Visualisation of the rectum and anal canal models is used in the manual measurement of the ARA in preparation for testing.

Table 3.1 Details of controls and measurements for components of the physical simulation:

Simulation Component	Controls	Measurements
Stool simulant	Stool viscosity; Homogeneous/heterogeneous	-
Stool transit	Flow rate; Volume	Mass leakage
Rectum	Mechanical properties; Anorectal angle	IR pressure; ARA
PR muscle & anal canal	Mechanical properties; PR tension	PR force
EAS	Mechanical properties; Sphincter pressure	Sphincter distension

3.4. Specifications of a Physical Simulation of the Human Defecatory System

Table 3.2 includes the major design specifications that were derived from the requirements. Requirements are defined for each modelling aspect of the simulation based on the research questions in Section 3.1. Specifications for the simulation are then derived from these requirements.

Table 3.2 Technical requirements and corresponding specifications of the system:

Model aspect	Requirement	Specifications
Rectum	Represent biological rectal geometry	Length: 130 mm [7]; Diameter: 32 mm [53]; Include anatomical features (rectal folds)
	Replicate rectum interfaces	Inclusion of omental adipose tissue with biological tensile properties (E=0.038 MPa [87]), positioned between proximal rectum and sacrum
	Replicate starting pressure (priming method)	Rectum modelled in non-distended state; rectum filled with stool simulant but not distended before tests
	Represent anorectal geometry with an obtuse ARA	Possess a 'resting' ARA of 104.5° [9]
	Mimic rectum properties (E)	Elastic modulus of 0.06 MPa [85]
	Configurable	Anorectal junction should move in posterior and anterior directions
	Represent rectum properties in its 'active' state	Be stiff enough to produce IR pressures observed during defecation
	Recreate biological attachments	Constrained at proximal (connection to colon) and distal (connection to epidermis)
Sphincter complex	Represent sphincter complex geometry and positioning	Sit around anal canal; anterior length: 34±1.8 mm; posterior length: 36±1.8 mm; thickness: 3mm; OD at least 16mm [1]
	Represent mechanical properties	Elastic modulus of 0.996 MPa (presented in Chapter 4)
	Simulate closure mechanism	Produce mucosal folds in the anal canal
	Produce 'FI' distensibility index in anal canal	Produce a radial DI of 1.5 [145]
Pelvic floor	Represent contact area with rectum	22mm at posterior/along sides of anorectum
	Mimic augmentation of rectum	Range of motion of 10.3 mm [68]; produce forces in axis between anorectum and pubic bone
	Simulate 'continent' and 'defecation' ARA values	Able to produce a range of ARA's from 84.5° to 104.5° [9]
	Mimic material properties (E)	Elastic modulus of 0.996 MPa (presented in Chapter 4)
	Positions anorectum	Ability to maintain different positions during tests
Stool	Produce a biological flow regime (stool viscosity/stool flow rate)	Apparent viscosity @1HZ: 52.8 Pa.s [142]; Flow rate: 9.26 ml/s [148]
	Represent a range of stools indicated on the Bristol stool form scale	Formation of homogeneous and heterogeneous stools; while encompassing a range of viscosities
Instrumentation	Measure ARA	Visualisation of the anorectum for measurement of the ARA
	Measure IR pressure	Ability to measure pressure in the rectum, using an appropriate pressure transducer
	Measure faecal leakage	Measure mass of stool leakage from the system during controlled delivery at the inlet to the rectum, for 'continent' and 'defecation' values
	Measure force	Measurement of the forces applied by the pelvic floor, to the rectum
FI device	Produce 'healthy' DI in anal canal	Produce a radial DI of 3.9 [87] along the anal canal

The subsequent sections describe the design and fabrication processes of the simulation. Each requirement is considered individually, and an approach is developed which allows each specification to be met by the particular modelling aspect. Where there is a lack of clarity in fully defining the parameters for a modelling aspect, an approach is implemented based on an interpretation of the biological component.

3.5. A Physical Simulation of the Human Defecatory System

This section provides a full description of the physical simulation of the human defecatory system, and is divided into two sections based on key components; soft tissue models and connective and supporting structures.

Biomechanical representations of the soft tissue components of the physical simulation are achieved using a casting process, in which the geometry and mechanical properties of each component are approximated. As presented in Section 3.3.1. , the simulation includes sphincter complex, pelvic floor, rectum, anal canal and adipose fat components to capture characteristics of the human defecatory system. The pelvic floor is formed by the levator ani muscle, coccygeus muscles and the covering fascia. It provides support to the pelvic viscera and is an important component of the simulation. The PR fibres of the levator ani muscles blend with the deep part of the EAS, Figure 3.12. These fibres form a sling which is attached in front to the pubic bones and passes around the junction of the rectum and the anal canal, pulling the two forward at an acute angle. The sphincter complex and PR muscle work in coordination with one another, and both muscles will be included in the simulation, although as separate discrete components.

3.5.1. Material Selection

Biological tissues are composed of structural proteins (collagen and elastin) and cells. The concentration and structural arrangement of constituents such as these strongly influence the mechanical behaviour of biological tissue [149]. They exhibit viscoelasticity as is evident through inherent hysteresis effects, which reveal an in-elastic response. It is thought that the dissipative effect of viscous energy is partially due to the motion of proteins within the viscous ground substance of the extracellular matrix [150].

Biological tissues structures form complex geometries and possess material properties of anisotropic behaviour and viscoelasticity. With further non-linearity's observed in these properties with age [146, 147]. Furthermore there are large anatomical variations between ethnicities [151] and gender. Consequently, the simulation aims to represent 'typical' geometries, characteristic of the western male population <60 years of age, while acknowledging modelling deficits.

A large majority of biomedical materials and implants are stiff structures, designed to work in conjunction with bony tissue. However, for the case of interaction with the soft tissue of the pelvic cavity, more flexible, compliant materials are required. There is a dearth of research into soft tissue implants, although current studies have developed soft materials for a range of applications including arterial prosthesis, pericardial and hernia patches, tracheal conduits and oesophageal tubes [152]. Silicone and hydrogel are two materials recognised as having good tissue-mimicking properties [153] combined with the ability to be used with moulds to form complex geometries.

Silicone is a commercially available chemically synthesised polymer which can exhibit a wide range of mechanical properties, which are commonly identified by their shore hardness value (once cured). It is usually supplied in two parts (catalyst and cross linker) as a fluid which are then mixed in equal proportions to initiate curing, lending itself well to casting techniques for the formation of batch-produced components with complex geometries. Low shore hardness silicones have been used in previous studies as tissue phantoms [154, 155], as they exhibit similar elastic behaviour under low strains [156]. Furthermore, additives can be introduced to the material upon mixing to tailor its properties, such as mineral oil to reduce surface friction [155]. However these can often produce a tacky surface and may require encapsulation before the phantoms are usable. Silicones do not contain water and therefore are not affected by problems of evaporation or bacteria growth. Its wide range of mechanical properties and long-term stability [157] provide additional advantages over other polymer based materials [153].

Another common tissue phantom material is PVA hydrogel [158, 159]. Hydrogels are water-swollen cross-linked polymer networks which often exhibit tissue characteristics, such as tissue-like elasticity and mechanical strength. The appearance and feel of PVA hydrogel are similar to those of human arterial tissue [160]; the

mechanical properties of PVA arterial vessels developed in a previous study [161] are similar to those of porcine aortas. PVA can be used not only for bio-artificial materials but also for phantom materials used for medical research. Forecasting soft tissue deformation by analysing interventional treatments, and performing minimally invasive surgery simulations, may greatly improve the proposed treatment as well as the accuracy of surgical procedures [162]. Simulation experiments require the use of tissue-simulating objects that mimic the properties of human or animal tissues. These phantom materials should have similar deformation rates of elasticity as compared with the target tissue, as well as exhibit long term structural stability (when stored in water), high water content and optical transparency. Using an appropriate ratio of PVA and water, a gel can be formed that possesses such tissue-mimicking properties [163].

Silicone is recognised as an excellent material for rapid manufacture of prototypes and functional parts, and has been used along with casting techniques in phantom tissue studies in the past [133]. Although PVA hydrogels possess properties which more closely match soft tissues, silicone is better suited to repeatable testing and has superior elastic properties, determined by its range of attainable elastic moduli (0.2-25.8 kPa [164, 165]) compared with PVA hydrogel (10-100 kPa [166]). Consequently, silicone is selected as the material to fabricate tissue phantoms in this thesis.

3.5.1.1. Uniaxial Tensile Testing

While the tensile properties of human rectum and adipose tissues were available in literature [84, 85, 87], the mechanical properties of the sphincter muscle were not. Therefore tests were conducted in a first instance on porcine IAS and EAS to obtain loading data which can be used to characterise their tensile properties. This is combined with values from literature to form a complete set of tensile data, to inform the validation of materials selected for the simulation components. Following on from tissue testing, various grades of silicone were tested using a similar test method, to directly compare their tensile properties to biological tissue.

IAS and EAS

To measure the mechanical properties of the IAS & EAS, a tensile testing method was employed similar to a method used in a previous study to characterise the tensile

properties of human rectal tissue [85]. Porcine sphincter tissue (Fresh Tissue Supplies, East Sussex, UK) were dissected to isolate the intact IAS and EAS muscle from surrounding tissue. 'Dumbbell' shape test samples were cut from the isolated IAS and EAS muscles using a dumbbell die cutter, in orientations perpendicular and parallel to the direction of the muscle fibres. In total 40 specimens were tested to failure. As many repeats as possible were taken from the muscles, with each endeavouring to replicate the orientation and thickness of the other samples. Due to the geometry of the muscles, it was more challenging to gain repeatability with perpendicular samples and therefore fewer repeats for these were obtained. The test samples were then mounted into a uniaxial tensile test machine (Zwick Z2.5/TN zwicki-line) and submerged in a water bath heated to body temperature (37 °C). They were then loaded at a rate of 30 mm/s until rupture. Force and deflection of the samples were recorded during tests, which was normalised by calculating engineering stress and strain for each sample.

Any samples which showed an elongation ±2SD than the mean were omitted from post-analysis. With 14 of the specimens tested, the water bath could not be brought up to body temperature, therefore the data for these specimens were gathered at room temperature (21°C). These have been plotted but were omitted from the forthcoming analysis.

There is notable variation between the samples tested for each muscle and orientation. This is a common attribute of tissue tests, an explanation for these inconsistencies could be due to the number of muscle fibres contained within each specimen and their orientation. Since the individual location and orientation of specimens were controlled by eye from areas of similar thickness and predominant fibre orientation. Furthermore the low friction interface between hydrated tissue and tester grips caused slight slippage with some samples which could cause greater strains being measured than were observed in reality. Both muscles demonstrate a greater stiffness in the transverse orientation (perpendicular to the muscle fibres), suggesting that the endomysium connective tissue provides a greater stiffness than the muscle fibres themselves. However since both the IAS and EAS expand radially during defecation, requiring extension in the longitudinal direction, only longitudinal data is used during the post-analysis. Following omission of any anomalies, the mean stress is plotted versus strain for the IAS and EAS muscles in the longitudinal orientation, Figure 3.2.

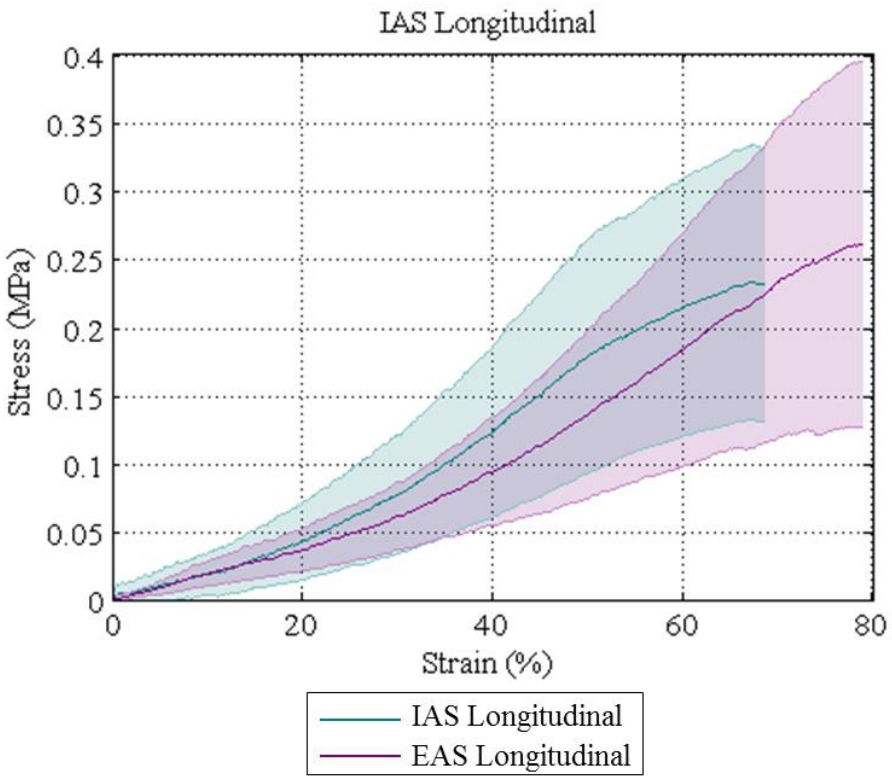

Figure 3.2 Mean (N=10) stress vs strain values for IAS and EAS longitudinal muscle with ±1 STD shaded region.

The stress-strain profiles show consistent loading characteristics in both muscles. Stress increases exponentially with strain at first due to the viscoelasticity of the tissue. This continues until the sample begins to rupture, at which point the curve plateaus as the ability for the muscle fibres to store elastic energy diminishes, until the sample eventually fails.

Silicone

Uniaxial tensile tests were also carried out on silicone specimens to observe their loading response. This allows a grade of silicone to be selected to model the biological tissue components which exhibit similar linear properties. During testing, the ASTM D412-A protocol (for testing elastic materials) was followed to produce consistent results. Three grades of silicone were selected for testing which have been used for the fabrication of tissue phantoms in the past [133]. Silicones were used which had shore harness values of 00-20, 00-30 and 00-50, selected from the Ecoflex range (Smooth-On^{TM}, Minnesota). To fabricate specimens with dimensions as defined in the protocol, a mould was built from 2D laser-cut sections of acrylic, this ensured each cast specimens was identical. The samples were then mounted in the grips of a uniaxial tensile test machine (Mecmesin, Imperial 1000) and loaded at a rate of 500mm/min up to a displacement of 200mm, the load was then removed at 500mm/min and the loading regime repeated 5 times for each specimen. An example of the response of the loading curves obtained during testing is shown in Figure 3.3.

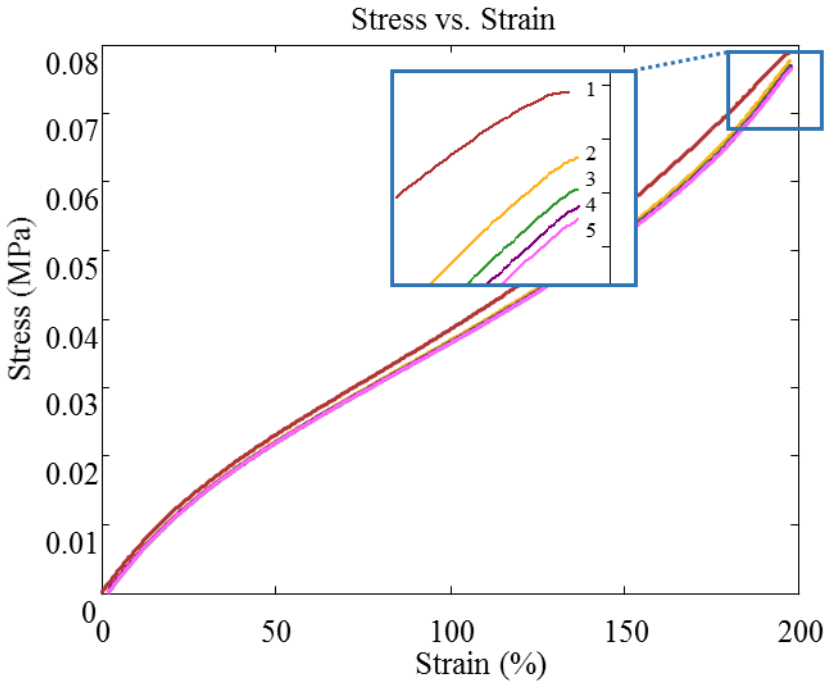

Figure 3.3 Cyclic stress-strain response from 5 repeats of silicone shore 00-30, demonstrating the decrease in stiffness for progressive cycles.

Five cycles were carried out for each specimen, the elastic modulus of the specimen decreases slightly with progressive cycles. The step change in elastic modulus is most significant from cycle 1 to cycle 2, with the step decrease getting smaller for

progressive cycles, Figure 3.3. This demonstrates that silicone is suited to applications in which it is stressed repeatedly, as maintains its elastic properties over repeated use. The mean of the responses from the final cycle, following preconditioning, were compared (Figure 3.4).

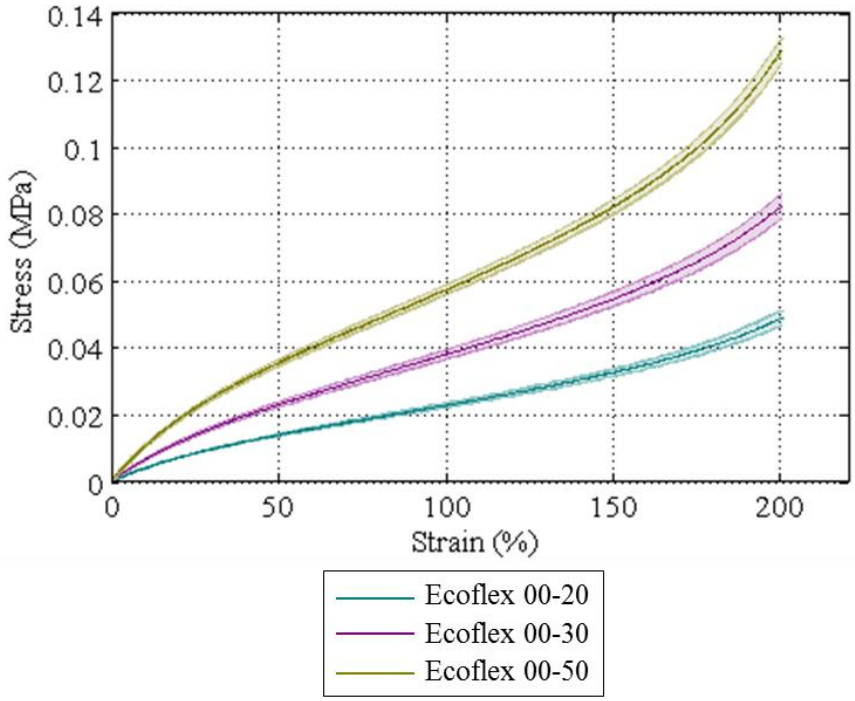

Figure 3.4 Comparison of the loading responses of silicones with various shore 00-grades.

3.5.1.2. Matching Silicone and Biological Tissue Properties

There are several types of viscoelastic models in which elastic and viscous parameters are linearly combined. There are advantages and shortcomings of these models in relation to phenomena such as creep, relaxation and hysteresis. Stress exhibited by an elastic component (σ_E) can be expressed as a product of elastic modulus (E) and strain (ε):

$$\sigma_E = E.\varepsilon$$

Whereas stress created by a viscous element (σ_η) depends on the derivative of strain and viscosity (η):

$$\sigma_\eta = \eta.\frac{d\varepsilon}{dt}$$

The Kelvin-Voigt model is composed of an idealised spring (with elasticity) and a damper (with viscosity) in parallel and represents a material which is subject to

reversible viscoelastic strain. The benefit of which is that it produces realistic model parameters for constant stress.

The Maxwell model is represented by a spring and damper placed in series. A limitation of Maxwell model is that it produces an unrealistic creep prediction when a constant load is applied. Therefore, when constant load is applied in the simulation, the Kelvin-Voigt model is better suited to represent the viscoelastic response than the Maxwell model. However the Kelvin-Voigt is only suited to low strains due to its limited degrees of freedom.

Linear modulus has been used to characterise biological tissues in the past [167]. In consideration of the complexity of capturing the behaviour of a viscoelastic material with an elastomer, in the first instance of this simulation a linear relationship is used to capture the properties of biological tissue at a particular strain value. A corresponding grade of silicone is then selected which exhibits a similar elastic modulus at this value.

For the research presented in this thesis, tensile data is obtained for porcine IAS and EAS through tensile testing, while data for human rectum and adipose tissues were taken from literature. Tensile testing is also conducted on various grades of silicone to obtain their stress-strain responses. Using a method which has been used previously for determining linear modulus of highly non-linear materials [168], linear fits are applied to the loading profiles of both the biological tissues and grades of silicone, to calculate a mean elastic modulus over a portion of the loading curve. The elastic moduli metrics of the tissues were then compared to those for the different grades of silicone, in order to match each tissue to a grade of silicone which most closely represents its tensile properties.

Elastomeric materials possess highly non-linear elastic properties whereas biological tissues possess viscoelasticity, this presents a challenge in matching their tensile properties. The physical simulation aims to replicate the behaviour of the biological system as closely as possible, requiring accurate representation of the tensile behaviour of biological tissues. For example, for the simulation to behave correctly, a rectum phantom model should apply the same elastic contraction force to its contents, as the biological rectum during defecation. Aspects of the loading profiles for silicone and biological tissues were compared to provide a means to match their properties, for which various metrics were considered:

a) Maximum stress at maximum distension (Figure 3.5a)

b) Elastic moduli at the maximum distension for tissue (Figure 3.5b)

c) Mean elastic modulus over a portion of the loading curve (Figure 3.5c)

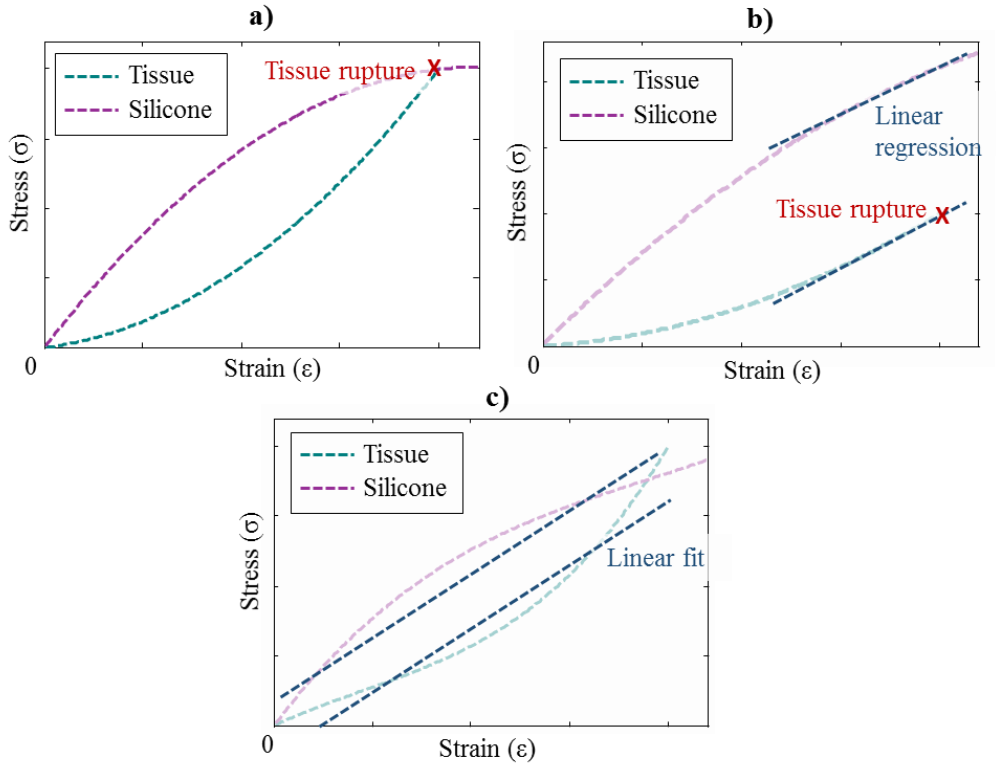

Figure 3.5 Schematic demonstration of a method to match the loading profile of silicone to biological tissue by; *a)* matching the stress at the rupture strain for tissue; *b)* matching the elastic modulus at the rupture strain for tissue; and *c)* matching the mean elastic moduli over a portion of the loading curve.

Matching stress at maximum distension (method *a)*), would result in a silicone which possessed a greater stiffness at rest than its biological counterpart. Given the different loading profiles of tissue and silicone, this would not be a suitable method since the rectum phantom is required to simulate the properties of active muscle. With this in mind method *b)* exaggerates the issue, although the properties for the phantom and tissue would be equivalent at maximum distension, the initial properties will contain greater discrepancies. Method *c)* produces an approximation of the properties of biological tissue over the range of its operational strain. The silicones elastic modulus at 0 % strain will be more comparable to the elastic modulus of tissue at its maximum strain (for the chosen range), than with the other options, and therefore this method was chosen for the analysis.

Linear Analysis

The mean loading curves of the biological tissues were compared with stress-strain data from the various grades of silicone tested, Figure 3.6.

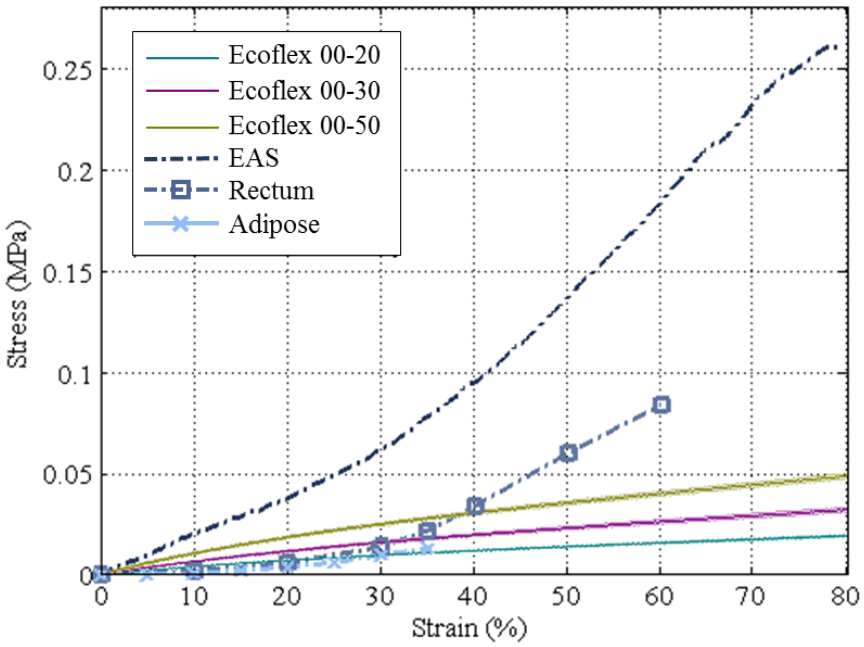

Figure 3.6 Comparison of the loading responses from various shore 00-grade silicones with tissue tensile data (EAS, Rectum and Adipose).

A linear fit is computed using a custom built algorithm in Matlab (Mathworks) which implements the 'polyfit' function to approximate the elastic modulus over a portion of these stress-strain curves. The coefficient of determination (R^2) compares how closely a mathematical function relates to the plotted data. The expression for R^2 is defined using equation 1, an R^2 value of greater than 0.99 denotes that the respective portion of a loading curve is linear [167].

$$R^2 = \left(\frac{1}{n}\sum \frac{(x_i - \bar{x})(y_i - \bar{y})}{\sigma_x \sigma_y}\right)^2$$

Where n = the number of data points, x_i = the x value for analysis, $\bar{x}$ = the mean x value, y_i = the y value for analysis, $\bar{y}$ = the mean y value, σ_x = the standard deviation of x, σ_y = the standard deviation of y

The linear fit is applied to stress-strain curves for the biological tissues represented in the physical simulation. The mean elastic modulus is approximated across a strain range of 0-35%. Over this range, it is apparent that adipose and rectum tissue were fairly well matched to silicone 00-20 and 00-30 respectively, although a stiffer silicone is required to simulate the properties of the EAS, as shown in Figure 3.7.

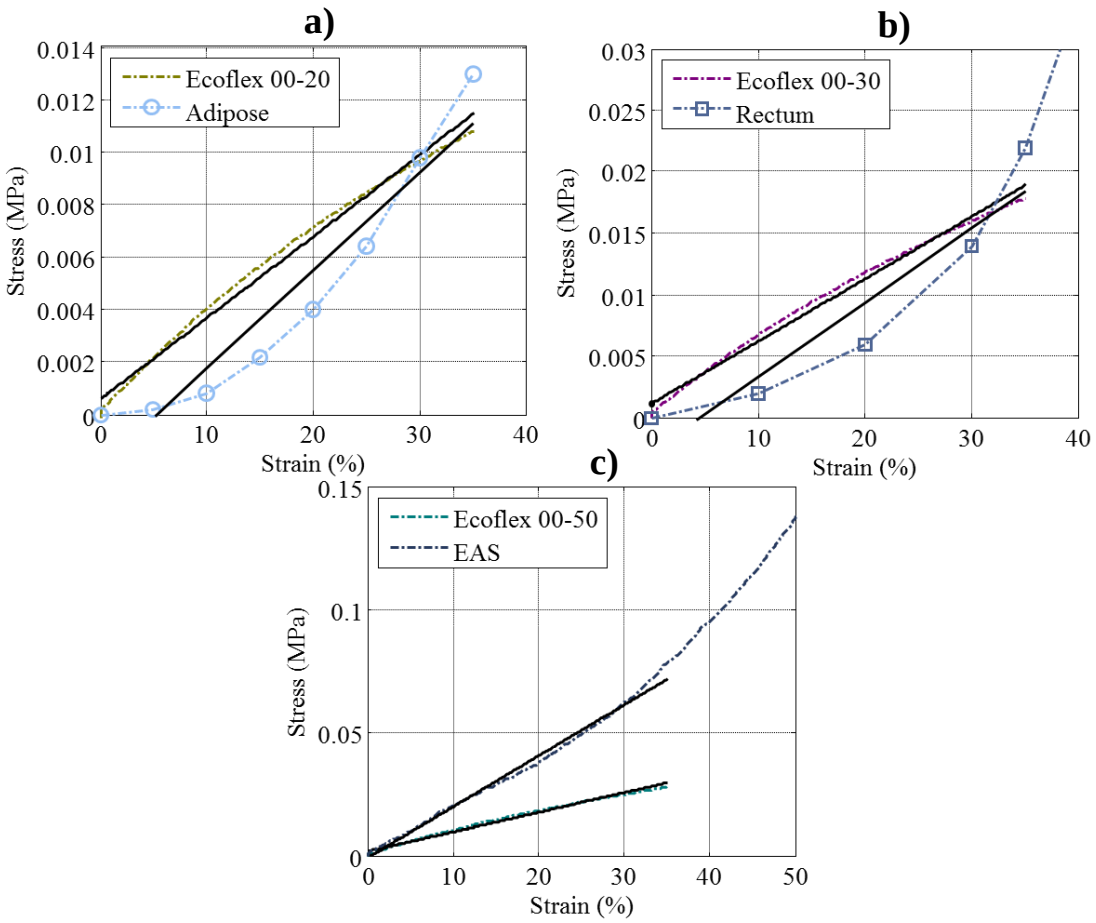

Figure 3.7 Comparison of linear fits (*solid, black*) for tissue constituents and corresponding silicone grades for a) adipose, b) rectum and c) EAS.

Table 3.3 summarises the elastic modulus and R^2 values calculated the biological tissues and Table 3.4 summarises the values for silicone.

Table 3.3 Linear fit gradient of tissue loading responses over a 0-35% strain range:

Tissue constituent	Elastic Modulus (MPa)	R^2
Adipose	0.038	0.956
Rectum	0.060	0.946
EAS	0.210	0.996

Table 3.4 Silicones and the corresponding Elastic Modulus approximated from 0-35% strain:

Silicone Shore Value	Elastic Modulus (MPa)	R^2
00-20	0.031	0.994
00-30	0.051	0.995
00-50	0.080	0.0994

A large variation in stiffness and strains to failure were exhibited by the different tissues modelled by the physical simulation. Silicone demonstrates similar linear fits over the specified strain range, with all values for $R^2 > 0.99$. Whereas the biological tissues appear to possess less linearity over their initial loading response, with both Adipose and Rectum tissue displaying values for $R^2 < 0.99$. This suggests that while the average elastic modulus is comparable between tissue and silicone, the characteristics of the loading response is not.

Based on the approximated elastic moduli, the tissue properties were matched to silicone over a small strain range, demonstrated in Figure 3.7. From this analysis, Table 3.5 indicates components of the simulation and their corresponding silicone grades, none of the silicones tested during this analysis show a stiffness great enough to model the EAS.

Table 3.5 Biological tissues and corresponding grades of silicone:

Tissue constituent	Silicone grade (Ecoflex series)
Adipose	00-20
Rectum/IAS	00-30
EAS	>00-50

3.5.2. Rectum and Anal Canal

The rectum and anal canal are modelled as a single continuous component, its modelling considerations and implementation are detailed below.

Faecal continence relies on a healthy, properly functioning rectum and associated tissues. During normal defecation, the rectum will contract, providing a low compliance tube through which faecal matter can transit. However in patients with FI, a lack of rectal sensation can inhibit this mechanism leading to large rectal volumes and FI. Consequently in natural circumstances, the rectum can exhibit a range of material properties. As a result, rectum models will be fabricated with a range of compliances to investigate its influence on the system.

The rectum has a highly complex anatomy, Figure 3.8.

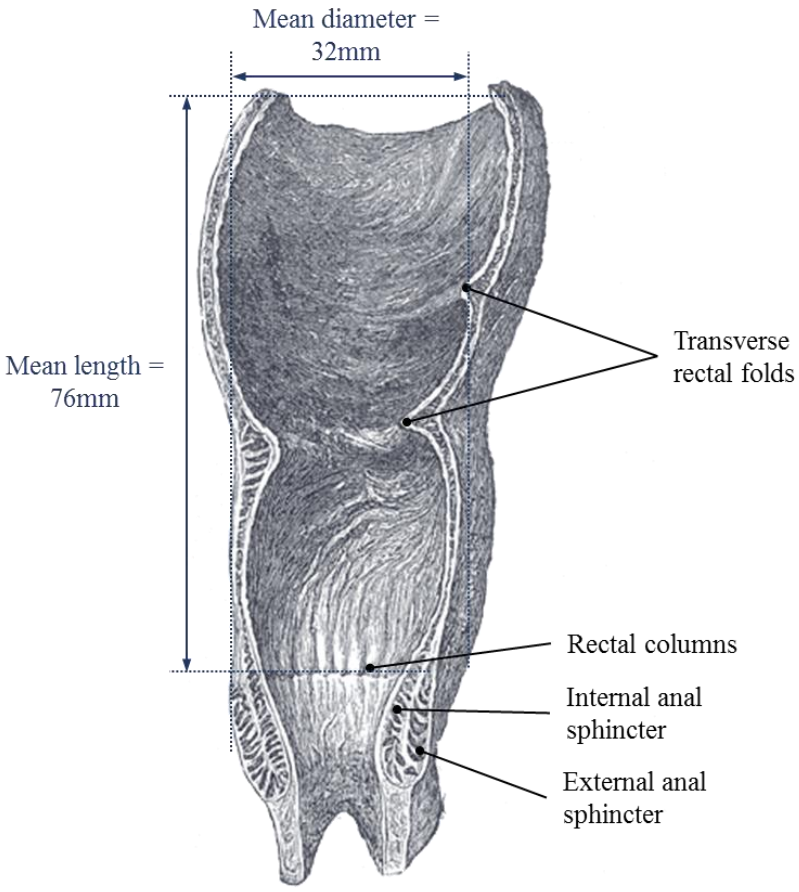

Figure 3.8 Illustration of the rectum indicating its geometrical and anatomical features [53].

To represent the behaviour of the rectum in the simulation, its biomechanics and geometry must be carefully modelled. For manufacture of a rectum with anatomical features, a die mould is used with a vacuum casting process. Die moulds are generally complex and their production can be costly in terms of both time and money. To rapidly manufacture a mould for the fabrication of the rectum model, the mould is made by 3D printing. Despite the limitations of material properties which can be

achieved with 3D printed parts, its fast lead times and low costs make it well suited to a mould intended for small batch production.

3.5.2.1. Physiological Overview

The rectum is a continuation of the sigmoid colon; it passes downward following the curve of the sacrum and coccyx before piercing the pelvic floor and forming the anal canal. The lower part of the rectum is dilated to form the rectal ampulla. The peritoneum covers the surfaces of the first third of the rectum and the anterior surface of the middle third, leaving the lower third uncovered. The mucous membrane of the rectum and inner circular muscle layers form semi-circular permanent folds called transverse folds of the rectum, as demonstrated in Figure 3.8. There are usually three of these folds. Posteriorly, the rectum is in contact with the adipose tissue lining the sacrum and coccyx. The rectum will be modelled as an anatomical tube, continuous with the anal canal, fixed at the terminal rectum and distal anal canal. It will be supported by replicate adipose tissue adjacent to the sacrum and constrained at the anorectal junction by the PR muscle, and the anal canal by the sphincter complex muscles.

3.5.2.2. Model Overview

Flanges provide fixation points, as demonstrated by Figure 3.9, which allow the model to be constrained in the same way as the rectum in the body. Due to their similar tissue properties, the rectum, anal canal and IAS will be modelled as a single continuous component.

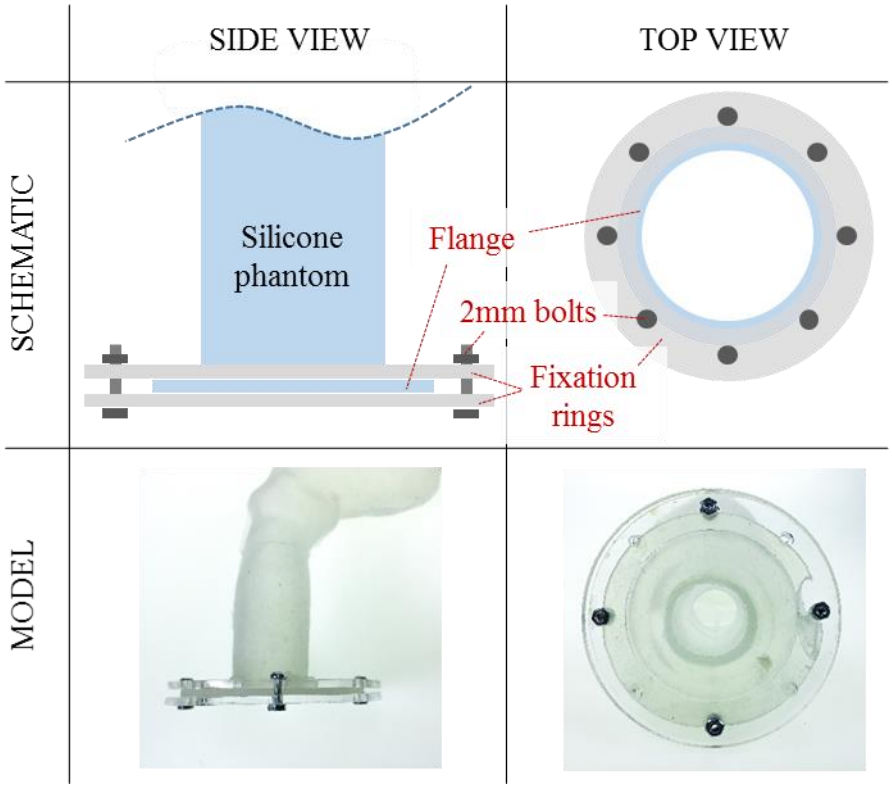

Figure 3.9 Schematic representations and corresponding images demonstrating flanges used to fix the tissue phantoms within a rigid housing.

While the modelled rectum represents associated anatomical features, an anal canal section has been approximated. Due to the nature of the anal canal, it is always closed in its resting state and therefore it is challenging to define its dimensional anatomy from CT scans. The anal canal section was therefore assumed to be cylindrical, and an arbitrary diameter was selected for the initial test mould.

Several anatomical CAD models were considered to form the basis of a rectum phantom, Figure 3.10.

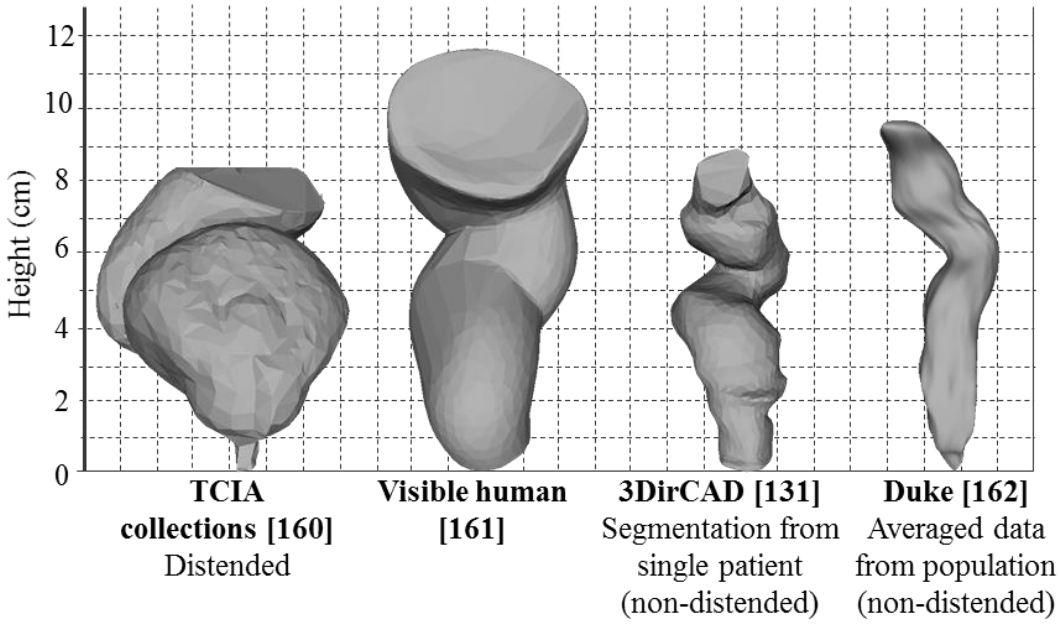

Figure 3.10 Side-by-side comparison of numeric rectum model geometries from separate sources, overlaid on a cm × cm grid.

Each model included geometrical features of the rectum, but were based on different 'states' (empty, filled and distended), and segmented using different techniques, therefore they possess different dimensions and volumes. For the simulation, a rectum in its natural 'resting' state is required.

The TCIA collections profile [169] is segmented from CT data of a distended rectum, while this demonstrates all the anatomical features of the rectum the rectal walls have been greatly elongated. The Visible Human rectum [170] is based on data taken from a male human cadaver which has been sliced into 1mm sections, photographed and digitised to produce a numerical dataset. While the 'state' of the rectum is uncertain prior to digitisation, its features are less pronounced than other models used in the comparison and the rectal volume appears greater. This could be because the rectum was in a 'filled' sate during the analysis, or variations in the segmentation method compared to using CT/MRI scan data. The 3DirCAD profile [133] is segmented CT data from a 44 year old male patient with focal nodular hyperplasia of the liver, but no condition relating to FI. This model showed pronounced features and close agreement with other published works [7, 54] on the size and volume of the human rectum. Finally, the Duke rectum [171] was segmented from population-averaged data of the human rectum in an empty state. While this model closely resembles rectal dimensions, its features also appear smoothed, making it less suited for used in the simulation since these features are paramount in the maintenance of continence. Based

on this comparison and with the advice of clinical personnel, the 3DirCAD rectum was selected for used in the simulation.

A model for the rectum to be used in the simulation was made using SolidWorks (Dassault Systèmes, Vélizy-Villacoublay, France). This was constructed using a 3D model of the human rectum was segmented by 3DirCAD [171] from simulated CT data. This model was imported into SolidWorks and various features added to allow the manufactured model to be integrated into the test simulation setup, Figure 3.11.

Figure 3.11 SolidWorks render of the 3DirCAD rectum model cast using the die mould, detailing its features.

Flanges are located at the distal and caudal end of the rectum phantom to allow fixation to the rigid simulation housing. A balloon catheter port allows the insertion of a balloon catheter into the rectum to facilitate pressure measurements during testing, a cable tie tightened around the silicone catheter port seals the entrance and secures the catheter in place.

3.5.3. Pelvic Floor Components

Influential aspects of the pelvic floor are modelled in the simulation, these are identified in the following sections along with details of fabrication.

3.5.3.1. Physiological Overview

The pelvic floor is formed by sheet like '*levator ani'* musculature, '*coccygeus'* musculature and the covering fascia. It provides support to the pelvic viscera and is an important component of the simulation. The PR fibres of the levator ani blend with the deep part of the EAS, Figure 3.12.

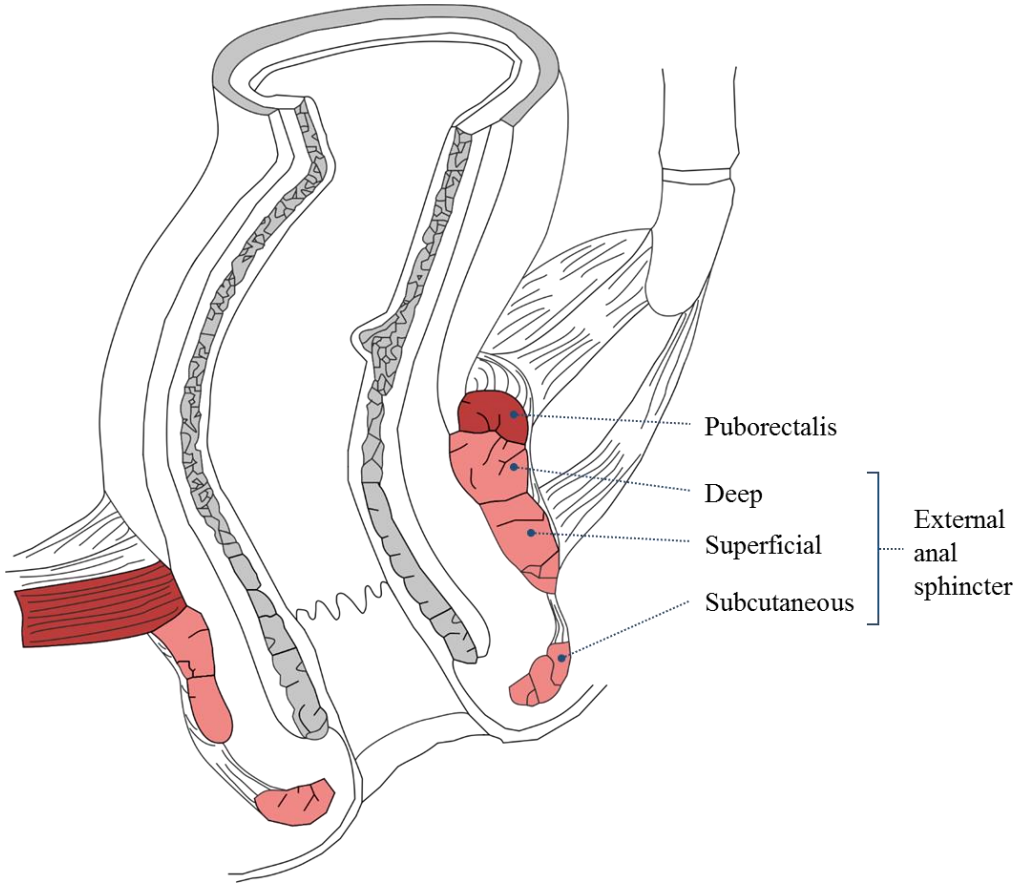

Figure 3.12 Schematic representation of the rectum and anal canal, demonstrating the arrangement of muscle fibres of the PR and various parts of the EAS.

The PR fibres form a sling which is attached in front to the pubic bones and passes around the junction of the rectum and the anal canal, pulling the two forward at an acute angle. The sphincter complex and PR muscle work in coordination with one another, and both muscles are included in the simulation, although as separate entities.

3.5.3.2. Model Overview

The anal canal and sphincter complex are modelled as a passive assembly, consisting of an inner silicone tube (the anal canal) and an outer constraint layer used to represent the combined occlusive action of the sphincter complex. The anal canal was modelled in a distended state (as during 'defecation') which is then constrained by the passive

sphincter element to produce an occlusion, with features representing mucosal folds. The dimensions of these features were obtained from anatomical studies [1, 2] and the 3D-IRCADb database [172] discussed above. A 1mm × 3mm retaining groove was added to the outer wall of the sphincter to locate a FI device and prevent the device moving longitudinally along the canal during use.

An important aspect of the PR to be recreated within the simulation is its contact area with the rectum, this was approximated from anatomical studies [2, 68] and defined as 18mm in width, Figure 3.13. The length of the PR varies during its operation, Figure 3.14, and in the simulation this is modulated through an actuation mechanism (described in Section 3.7.1.).

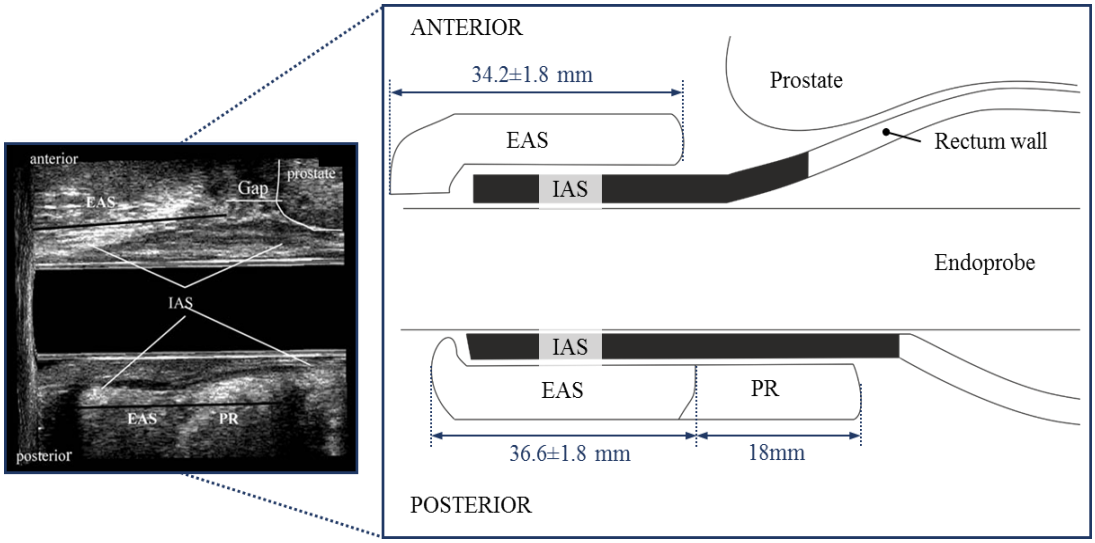

Figure 3.13 *Left;* ultrasound image of an endo probe in the anal canal and *Right;* schematic representation of the anal canal showing lengths of the surrounding musculature.

Figure 3.14 Seated CT defecography; images of puborectalis plane *A)* At rest, the puborectalis is lower case "u"-shaped *B)* During squeeze, the puborectalis shortens and becomes "v"-shaped; the centripetal force of the puborectalis shuts the genital hiatus and anus tightly *C)* During defecation, the puborectalis lengthens and becomes capital "U"-shaped; the centrifugal force of the levator ani opens the genital hiatus and anus.

3.5.4. Connective and Supportive Structures

A range of elements were made to hold and support the functional parts of the defecation models (rectum, anal canal, PR sling & sphincter complex), housed in an adult male pelvis model (Male Pelvis Skeleton, 3B Scientific, Hamburg, Germany) which provided visual anatomical reference points during simulation analysis, Figure 3.15.

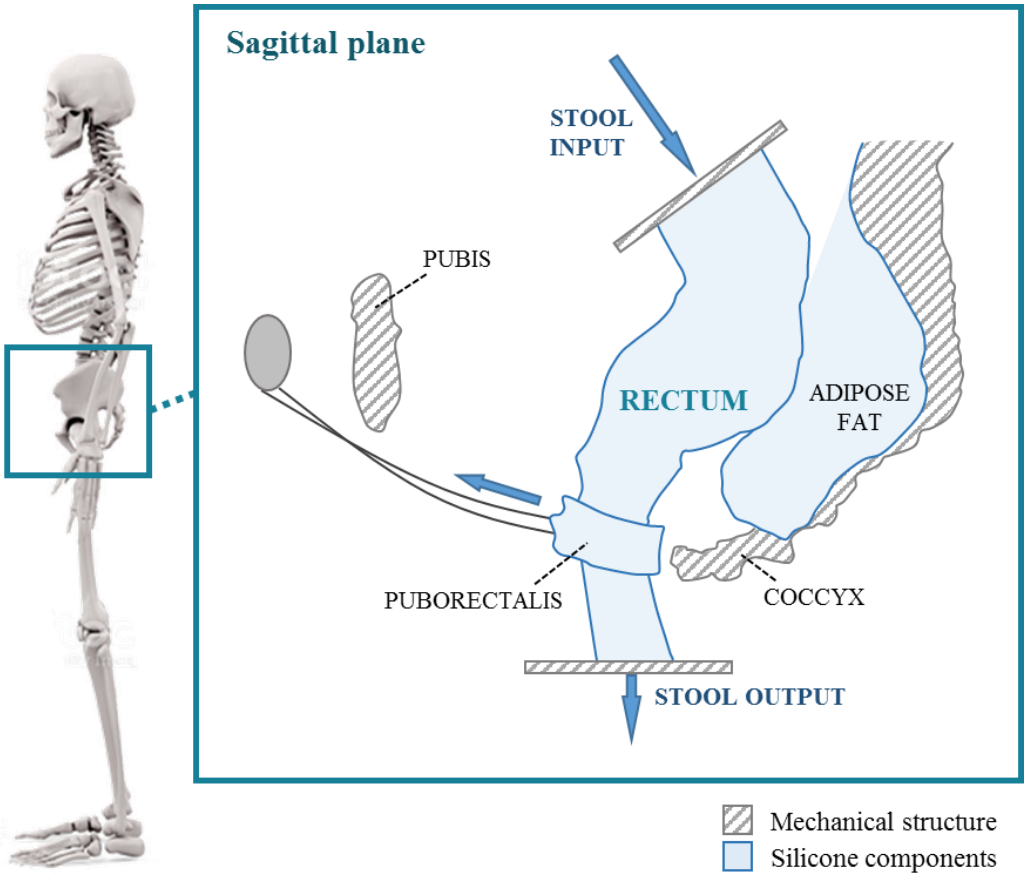

Figure 3.15 Schematic overview of the connective and supportive structures and soft tissue phantoms as part of the physical simulation assembly.

The bony pelvis provides a strong, stable connection between the trunk and the lower extremities. Its main functions are to transmit body weight from the vertebral column to the femurs, and to contain, support and protect the pelvic viscera, including the rectum. The pelvis provides attachment points for muscles of the pelvic floor which constrain the movement of the sphincter complex and provide support to the rectum.

Adipose fat was modelled using silicone which approximates the mechanical properties of adipose tissue in healthy adults [87], and it is attached to the sacrum to provide a soft interface between the posterior rectum and bony pelvis. The most distal

part of the anal canal and proximal end of the rectum are fixed relative to the pelvis using the soft silicone flanges, custom acrylic mounts and a customisable aluminium framework (Rexroth, Bosch), configured in a way that the rectum assumes a resting anatomical position.

The location of the rectum is determined by the position of the posterior anorectal junction relative to the apex of the sacrum, since this is a measurement which can be easily defined from clinical data. In the simulation, the anorectal junction is located 42 mm anteriorly to the apex of the sacrum, and 5 mm inferiorly, Figure 3.16. The PR control spool was positioned in place of the pubic bone (which in the biological system, anchors the PR muscle). As such, the spool was located 90 mm anteriorly to the anorectal junction and 40mm superiorly, Figure 3.16. This enabled the PR phantom model to be moved along the axis between the anorectal junction and pubic bone as it does in the biological system. To make this modification, the pubic bone was removed from the simulation in place of the stepper motor and spool assembly. The upper sacrum is constrained in the vertical axis and the distal anal canal flange is constrained in the horizontal axis.

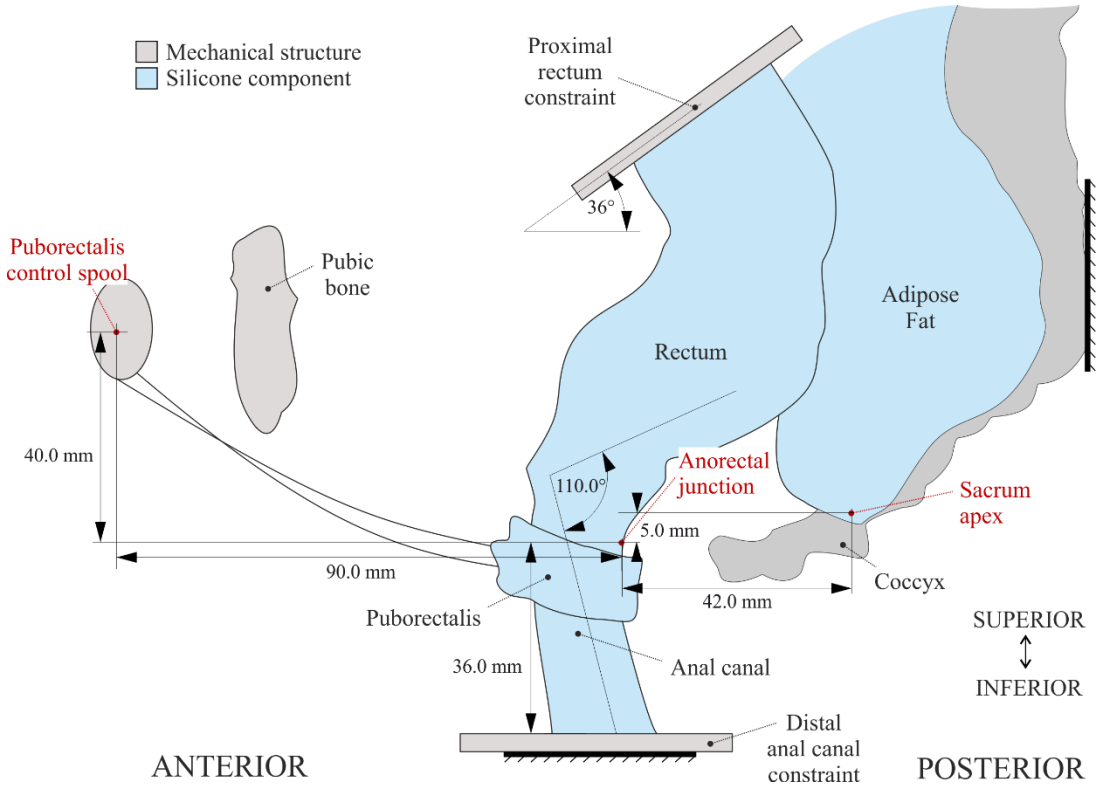

Figure 3.16 Scale dimension drawing of the simulation components in the sagittal plane, indicating the positions of the Puborectalis control spool and sacral base relative to the anorectal junction.

3.5.5. Simulated Stool

The composition of faecal matter can vary greatly between different people, and among different faecal samples from the same person. This variation is attributed to a person's diet, age, health, lifestyle, climate and geographical region [173]. And as such, it is common for human faeces to contain a wide range of moisture contents with large variability in homogeneity. The Bristol Stool form scale depicts the various forms of stool Figure 3.17.

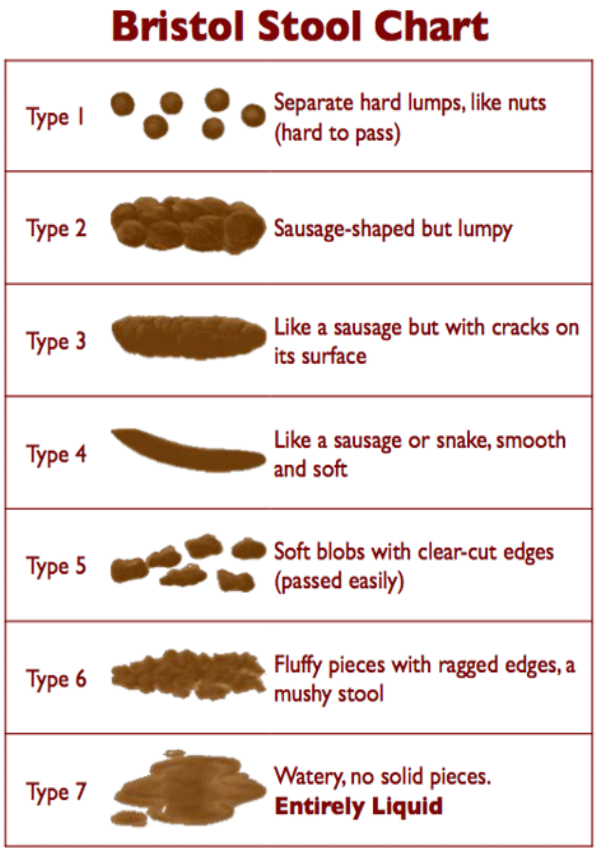

Figure 3.17 Overview of the different types of faeces which constitute the Bristol stool form scale.

While FI can occur in patients with all these forms of stool, a high moisture stool can increase severity. Type 7 in included in tests conducted with the physical simulation.

3.6. Fabrication

A range of techniques are used in the fabrication of components of the physical simulation, to meet their individual demands. These are discussed in detail in the following sections; '*Soft Tissues*' and '*Connective and Supportive Structures*'.

3.6.1. Soft Tissues

The procedures used to fabricate all silicone-based simulation components are described as follows:

1. Prepare the custom mould by cleaning with an acetone wash, and once dried, apply a mould release agent (Smooth-On, Universal® Mould Release)
2. Assemble the custom mould
3. Pour silicone catalyst and crosslinker parts into a dry mixing container in proportions specified on product information provided by the manufacturer
4. Load the mixing container into a planetary mixer and degassing machine (THINKY, ARA-250, Intertronics, Kidlington), mix for 30 seconds at 2000 rpm then degass for 120 seconds at 2200 rpm
5. Pour the premixed, degassed silicone into the prepared mould, allowing the silicone to flow naturally into any crevices
6. Leave to cure for the cure time specified in the product information
7. Demould and remove excess material with a sharp blade

3.6.1.1. Rectum and Anal Canal

A custom mould was required to fabricate the rectum as a hollow silicone shell. Firstly, the 3D geometry, Figure 3.18, was imported into a CAD package (SolidWorks™, Dassault Systèmes), and modified to add flanges for mechanical fixation and interfacing with adjoining components. A 3D mould, Figure 3.18, was then constructed using the modified rectum geometry. The mould consisted of two halves with an insert. Fixation points allowed the rectum insert to be correctly aligned within the mould cavity such that a uniform wall thickness was achieved. Lastly, a material reservoir and inlet ducts were added to the mould to enable fabrication by vacuum casting.

Due to the high variability of the biological anal canal, the mould features an adaptable anal canal section, allowing multiple anal canal geometries to be replicated using the same mould. The anal canal cavity sections are separate from the main body of the mould allowing them to be interchangeable with different profiles, Figure 3.18. The mould is manufactured by 3D printing, meaning that different anal canal geometries can be manufactured and incorporated in little time. The manufactured mould is shown in Figure 3.19.

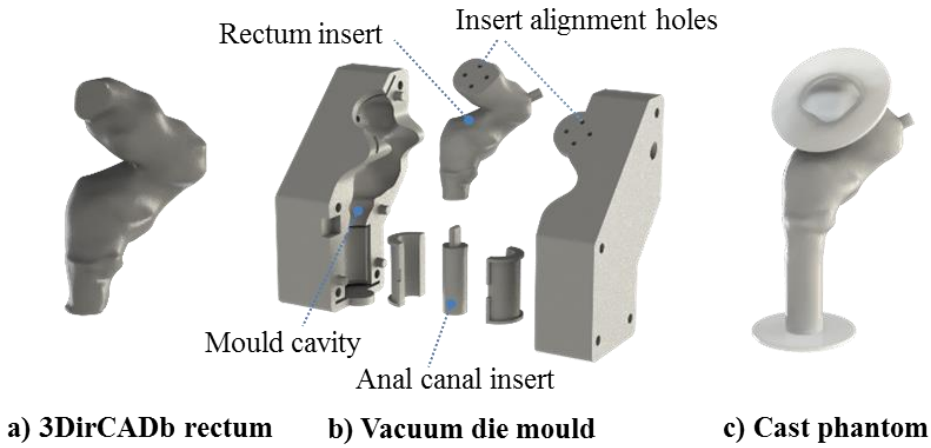

Figure 3.18 Fabrication process for the rectum phantom model detailing a) the segmented geometry b) exploded view of the 3D printed vacuum injection mould and c) cast phantom rectum Phantom.

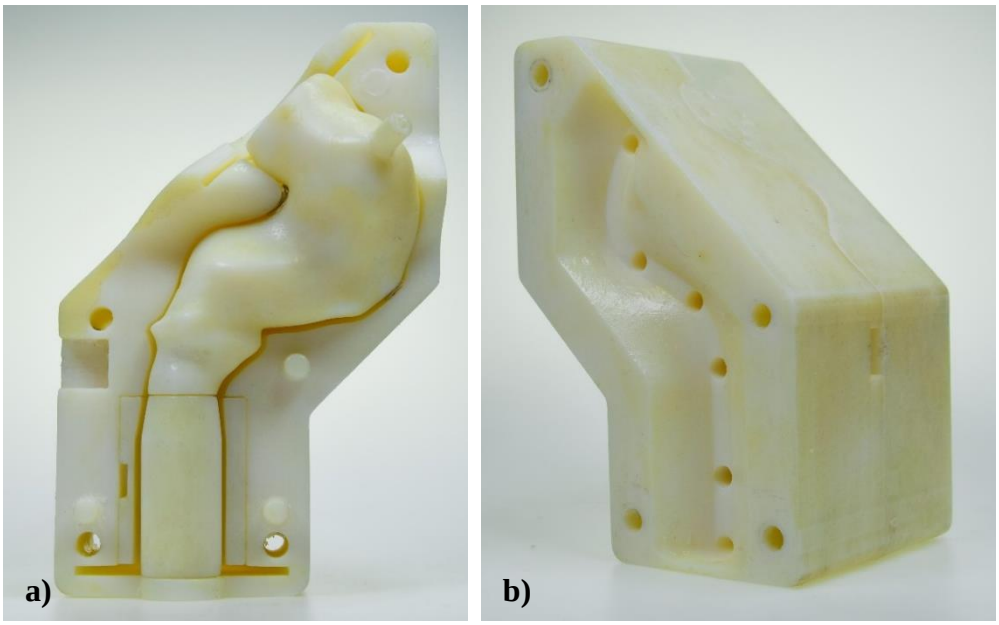

Figure 3.19 a) internal view of the mould, showing the mould cavity and core component; b) isometric view of the manufactured mould, showing the silicone reservoir and sprue.

With pre-mixed, de-gassed silicone in the material reservoir the mould was positioned in a vacuum chamber for 4 hours. When a vacuum is applied, air in the mould cavity is displaced with silicone where it cures, and the rectum model is de-cast (Figure 3.18).

Initial fabrication produced a part which contained air pockets, due to the viscosity of the silicone, all the air in the mould cavity was displaced. The casting method was

modified to include a step in which both sides of the mould were primed with degassed silicone, before assembling the mould. This produced a part which was fully degassed, Figure 3.20.

Figure 3.20 Image of the fabricated silicone rectum with casting runners removed.

3.6.1.2. Sphincter Complex

The sphincter complex phantom was fabricated using a mould compiled of layers of 2D acrylic profiles, manufactured by laser cutting. A high shore hardness grade silicone core, Figure 3.21, was fabricated separately (using a similar technique to the sphincter). This forms a complex, thin geometry which would otherwise be challenging to fabricate with acrylic. The acrylic profiles and core components are assembled to form the mould. Mould release agent (Smooth-On, Universal mould release spray) is applied to the inner surfaces of the mould to prevent silicone from adhering. Pre-mixed, degassed silicone is then poured into the mould cavity and left to cure at atmospheric pressure.

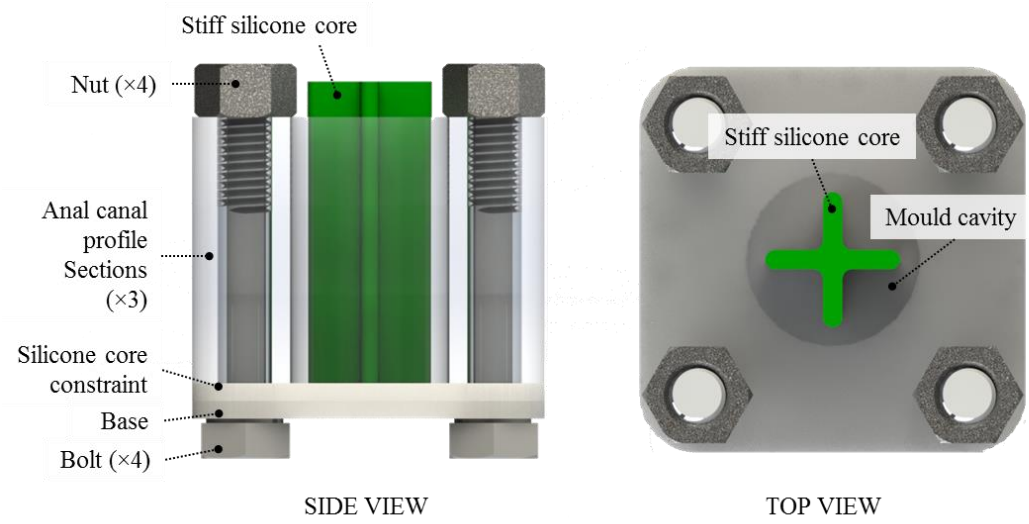

Figure 3.21 SolidWorks render of the sphincter mould, indicating its features and components.

The mould allows a sphincter phantom to be fabricated (Figure 3.22) with features that allow it to occlude the anal canal by mimicking the natural closure mechanism of the biological system, by producing mucosal folds in the anal canal wall. It also has a recess which keeps a FI device in position during testing.

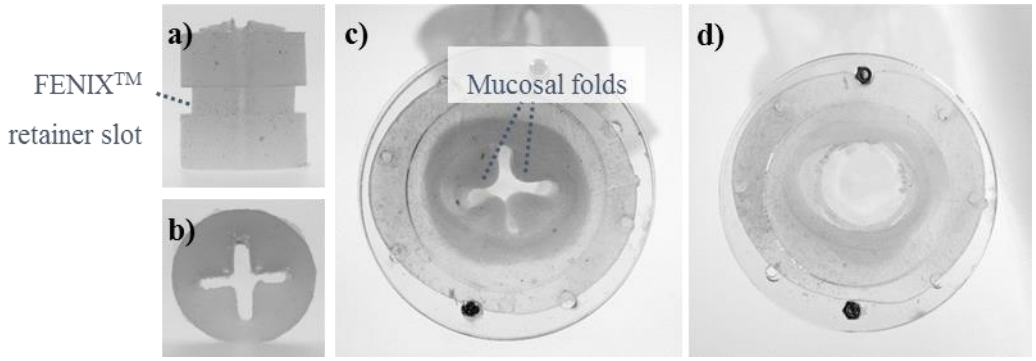

Figure 3.22 The model silicone sphincter showing a) side view; b) top view; c) simulated mucosal folds along the anal canal and d) the anal canal with the sphincter distended.

3.6.1.3. PR Muscle

Similar to the sphincter complex, the PR muscle phantom was fabricated using a soft silicone elastomer, providing a soft interface between PR and rectum, and backed by a fine inextensible mesh (fiberglass mesh) to allow precise positional adjustments without elongation of the phantom. A mould was manufactured using laser cut sheets of 2D acrylic to form a 3D mould, Figure 3.23. The mould consists of three sections (base constraint, PR profile and top constraint). The middle section features the profile

of the PR phantom, along with a silicone inlet (pictured) and air outlet (not pictured) slots. A layer of fibre-glass mesh is positioned and clamped between the middle and top acrylic layers, by tightening bolts which hold the mould sections together during fabrication. Pre-mixed, degassed silicone is then poured into the mould cavity and the phantom is left to cure at atmospheric pressure. Once cured the part is de-cast, excess mesh is removed and Nylon wire is threaded through each end, Figure 3.23, leading to a spool which is actuated to adjust the position of the phantom.

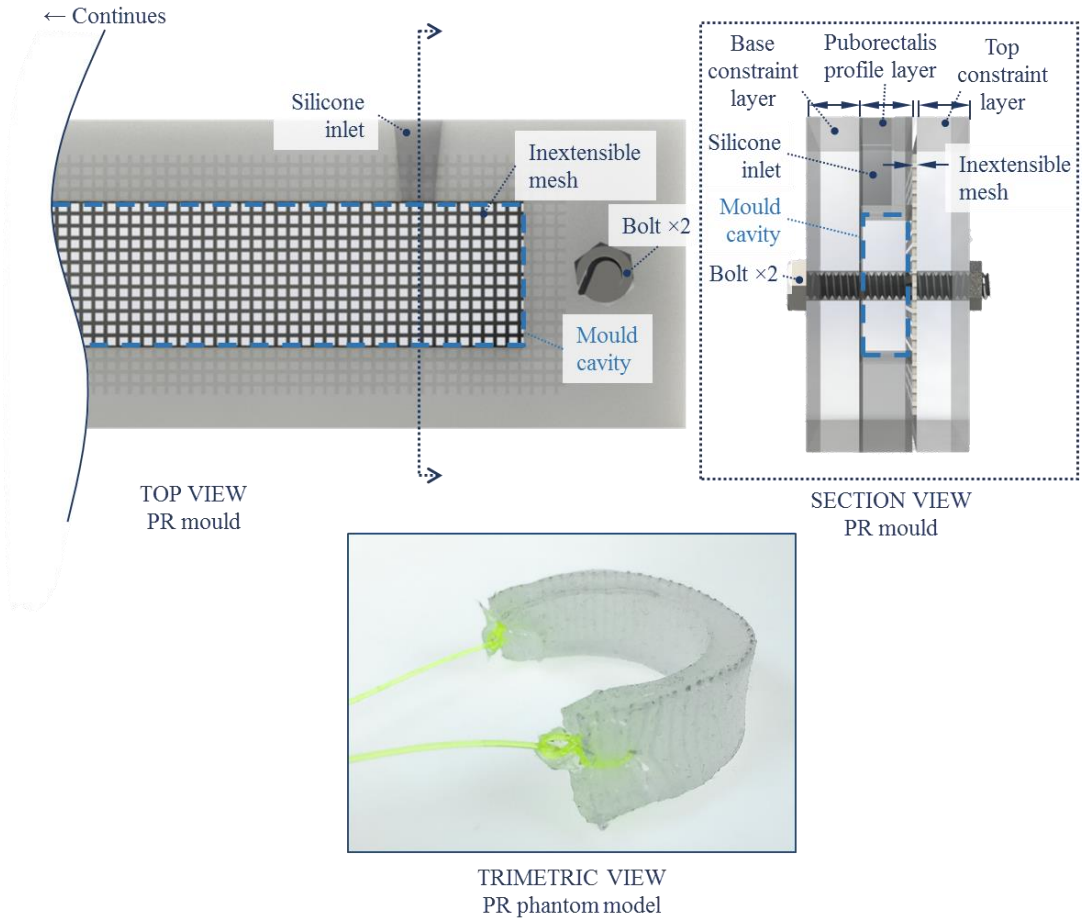

Figure 3.23 *Top*; SolidWorks renders of the mould used to fabricate the PR muscle phantom and *bottom*; image of the fabricated part, trimmed down and fitted with nylon wire.

3.6.1.4. Connective and Supportive Structures

Adipose tissue was fabricated using the same method as for the PR muscle, except there was no addition of a mesh constituent. A mould with a uniform rectangular cavity was bolted together and premixed silicone was poured into a silicone inlet where it flowed freely and filled the mould cavity. Once cured the part was de-cast. The tissue phantom was fixed to the sacrum using a silicone adhesive (SilPoxy^{TM},

Smooth-on), where excess hanging over the sides of the sacrum was removed. Finally, the surface of the adipose phantom was encapsulated using a silicone encapsulator (Super Baldiez^{TM}, Mouldlife) to produce a low friction surface which interfaces with the rectum phantom.

A Rexroth frame was constructed which was large enough to house all the soft tissue phantoms along with control and sensing instrumentation. The anatomical pelvis was bolted to the frame, and sections of Rexroth were positioned and connected to provide fixation for the soft tissue phantoms while allowing adjustments to their position in 3D space. This accommodated for changes in the geometries of phantom models and configurational modifications. Custom fixtures were cut from 2D sheets of acrylic, to secure the proximal and distal flanges of the rectum phantom to the rigid frame.

3.6.1.5. Simulated Stool

Simulated stool was prepared using a smectite clay (VEEGUM^{TM} R) suspension in water as used for a stool analogue in a previous study [148]. It was mixed in a ratio such that its moisture content was 91% to produce a consistency of 42.2 (as determined in Chapter 4, Section 4.1.2.3.), comparable to the consistency of high moisture content faeces, reported as 39.33 [142]. The mixture was homogenised using a hand held blender for 2 minutes and until no clumps of clay were apparent. To prevent dehydration of the suspension, it was covered when it wasn't in use, and it was always made on the day of testing. The suspension was regularly mixed to ensure that its molecular structure was in a consistent state of breakdown/repair.

3.7. Control and Data Acquisition

The physical simulation was instrumented with a range of hardware detailed in Table 3.6. Sensing hardware was used to sample the PR muscle force, IR pressures and faecal mass leakage. A global overview of the instrumentation and electronic subsystems of the physical simulation is presented in Figure 3.24.

Table 3.6 Details of simulation control hardware:

Testing variable	Hardware	Manufacturer and model
Anorectal angle	Stepper motor	RS Pro, 535-0366
Mass flow rate	Linear stage	PSAA-60 W
Test indicator	LED	-

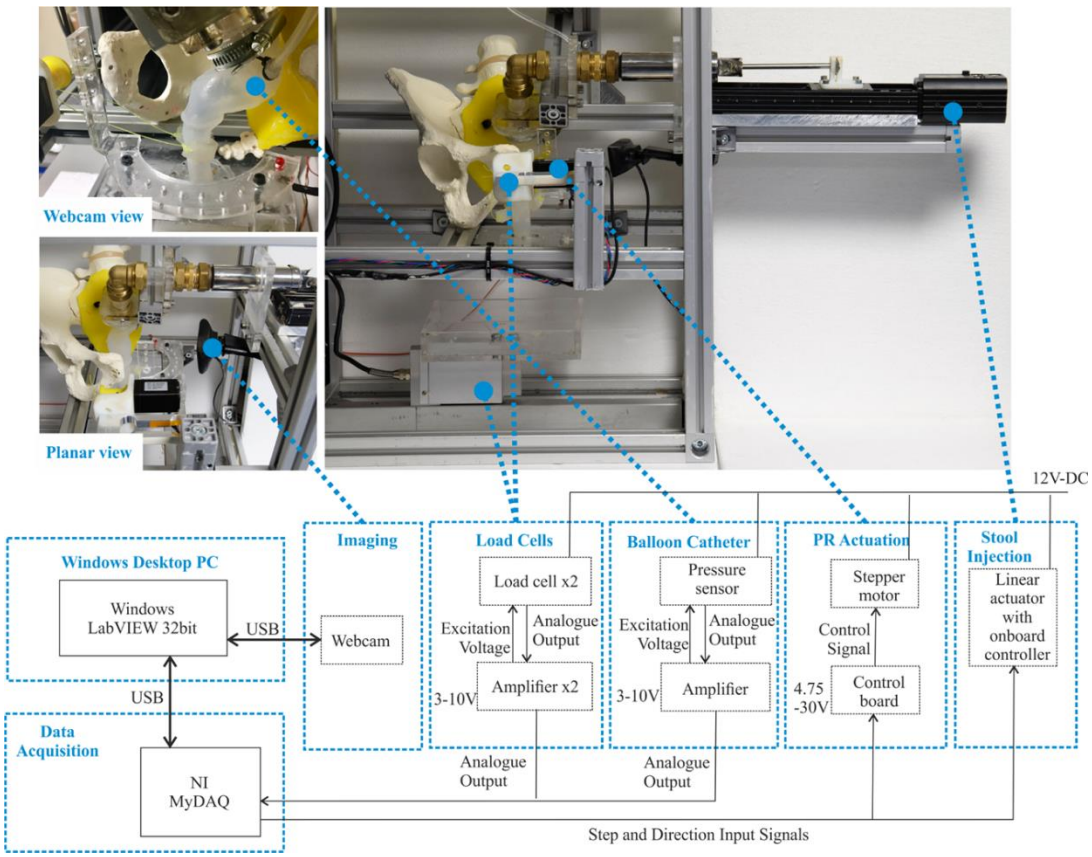

Figure 3.24 Overview of the instrumentation and corresponding electronic subsystems of the physical simulation assembly.

3.7.1. Control hardware

Augmentation of the ARA was driven using a stepper motor and spool assembly, controlled by a host PC. A complete wiring diagram for the control of the stepper motor is presented in Figure 3.26. Figure 3.25 shows a schematic of the simulation with all the control hardware detailed.

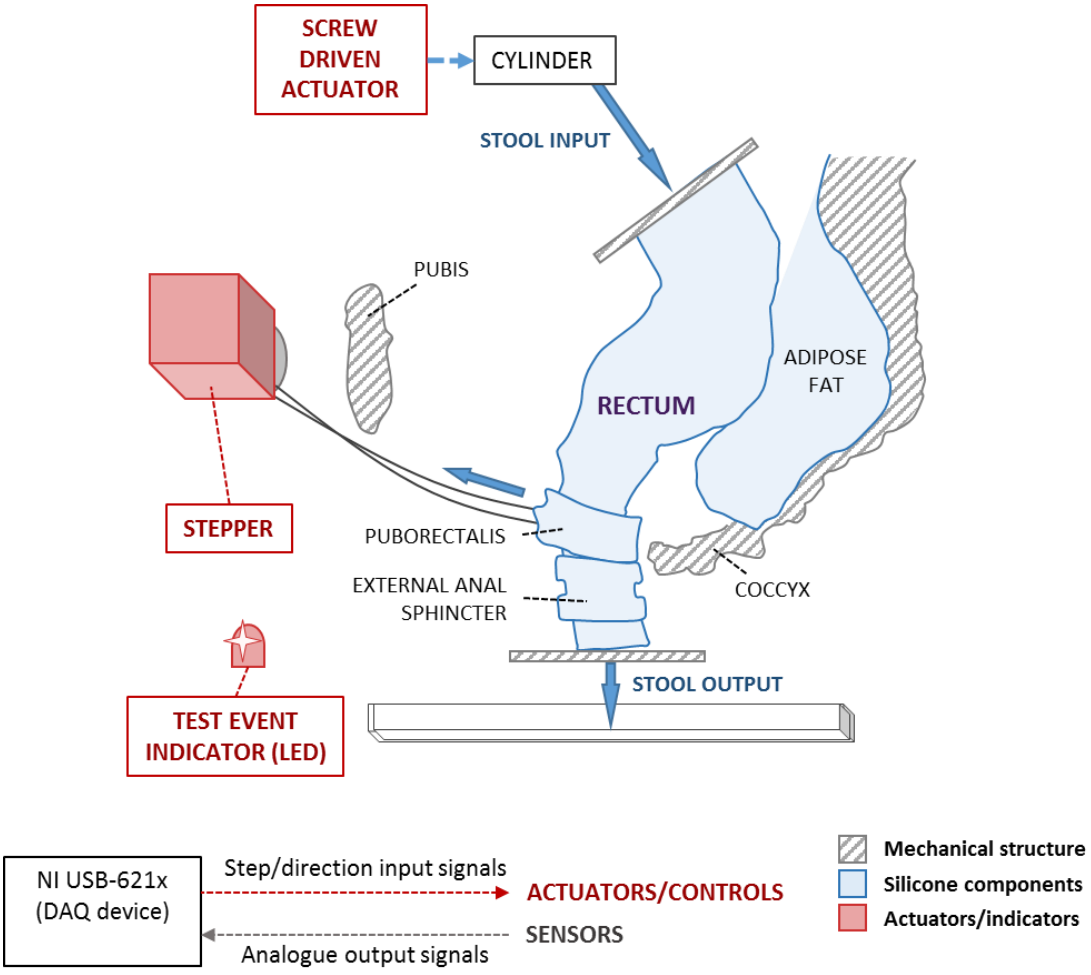

Figure 3.25 Schematic representation of the control hardware assembled within the physical simulation.

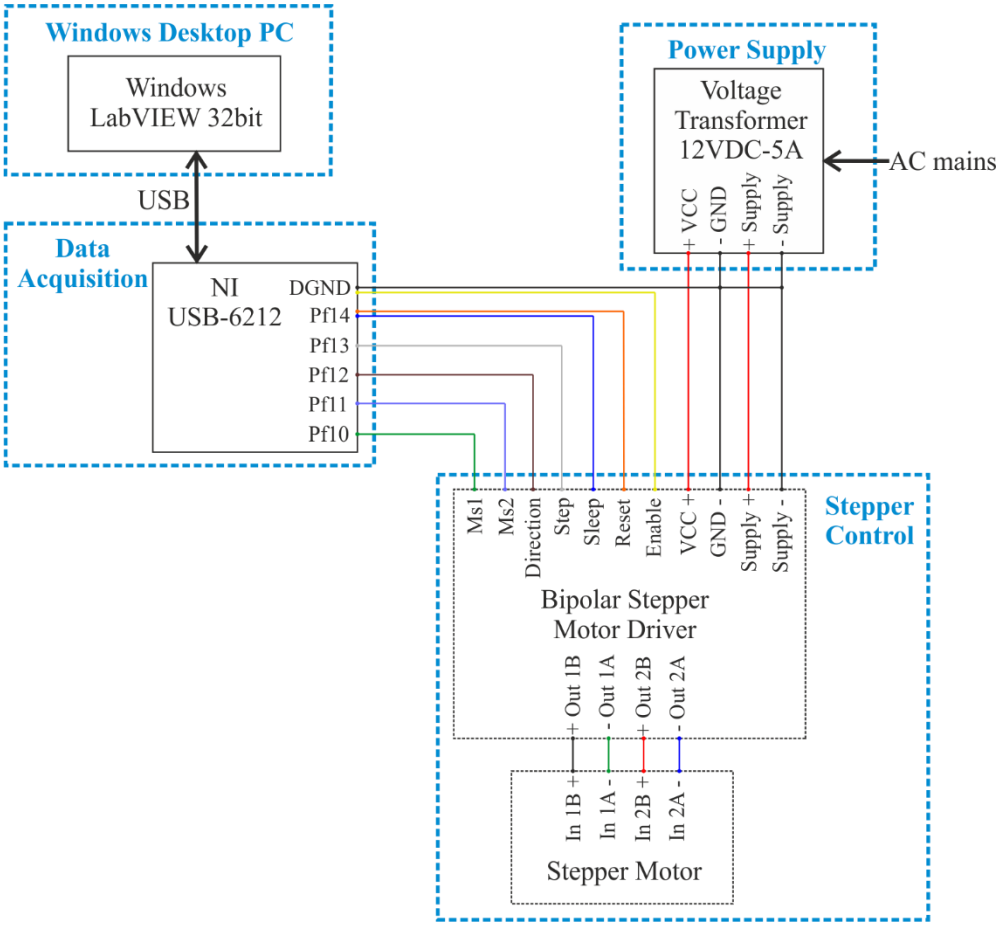

Figure 3.26 Wiring diagram of thee terminal connections between the bipolar stepper motor driver and DAQ device to control PR modulation.

The PR muscle is connected to the spool through an inextensible nylon cord and tightened against the anorectum through rotation of the spool, causing augmentation of the ARA. Stool simulant was introduced to the system by controlled injection using a lead-screw linear actuator which drove a syringe containing the stool simulant. Stool leakage from the anal canal is retained in a collection tray.

3.7.2. Sensing hardware

Sensing hardware was implemented to measure the PR muscle force, IR pressures and faecal mass passed from the system, these data were recorded at a sample rate of 100HZ to monitor the variables over time, as stool simulant was injected into the system. Table 3.7 details the sensing hardware implemented in the simulation, and

Figure 3.27 shows a schematic representation of the system highlighting the positions of sensing hardware.

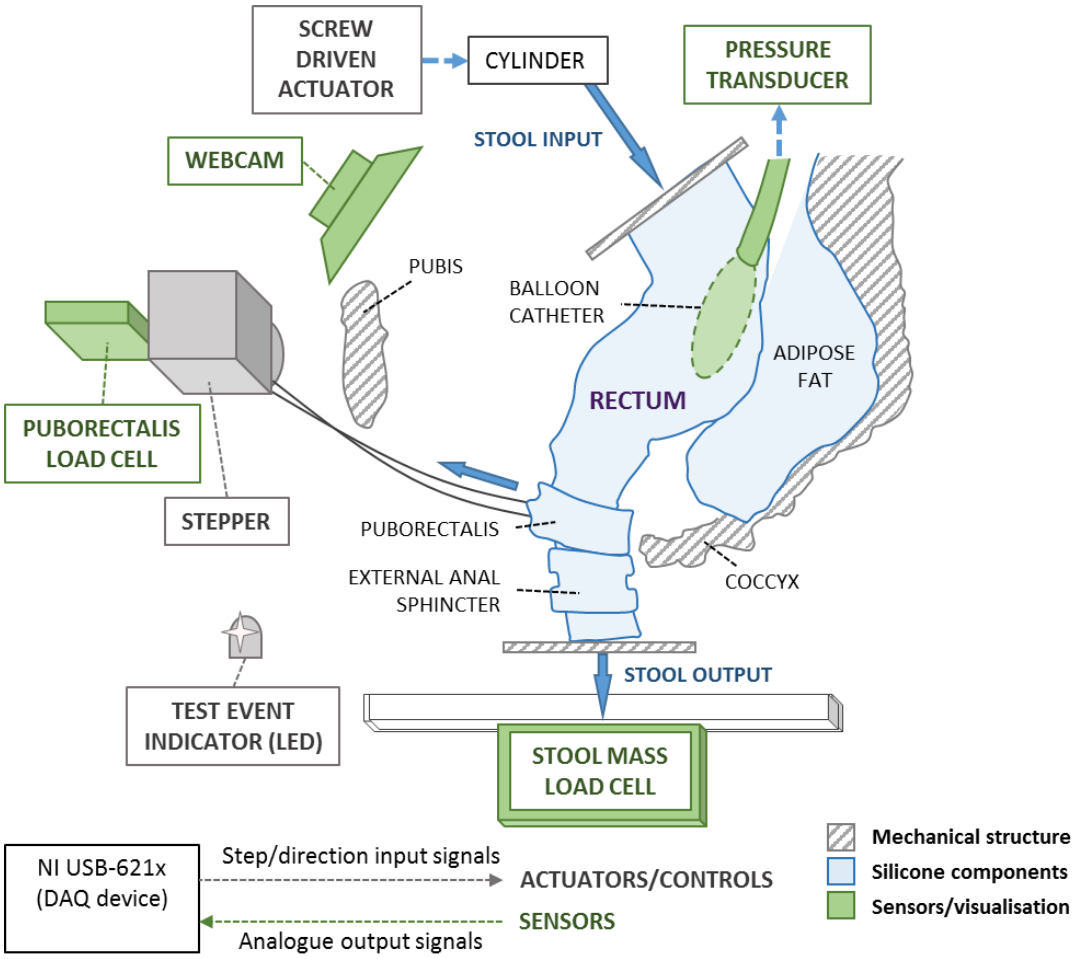

Figure 3.27 Schematic representation of the sensing hardware assembled within the physical simulation.

Table 3.7 Sensing hardware implemented within the physical simulation assembly:

Testing variable	Hardware	Manufacturer and model
Intra-rectal pressure	Balloon catheter	Medi Plus, 2309
	Pressure transducer	Utah Medical, Deltran® 6199
PR muscle force	Load cell	RS, 1004
Mass leakage	Load cell	RDP, RLS005kg
Visualisation	Webcam	Logitech, HD Pro C920

A balloon catheter (Medi Plus, 2309) was located within the rectum which fed to a pressure transducer (Utah Medical, Deltran® 6199), capable of measuring pressures in the range -50 to 300 mmHg. The transducer signal was amplified using an amplifier

(RDP, DR7DC) which allowed more accurate determination of the dynamic rectal pressures within the simulation. While the transducer is accurate to ±2 %, the configuration of the balloon catheter within the rectum means that readings might be less accurate. As rectal volume varies, it is likely that the catheter tip would move slightly in the vertical axis, resulting in varying proportions of the pressure observed being the static head. To compensate for this error, pressure readings will be considered accurate to ±5 % the measured value. A complete wiring diagram between transducer, amplifier, transformer and DAQ device terminals to acquire the pressure data is shown in Figure 3.28.

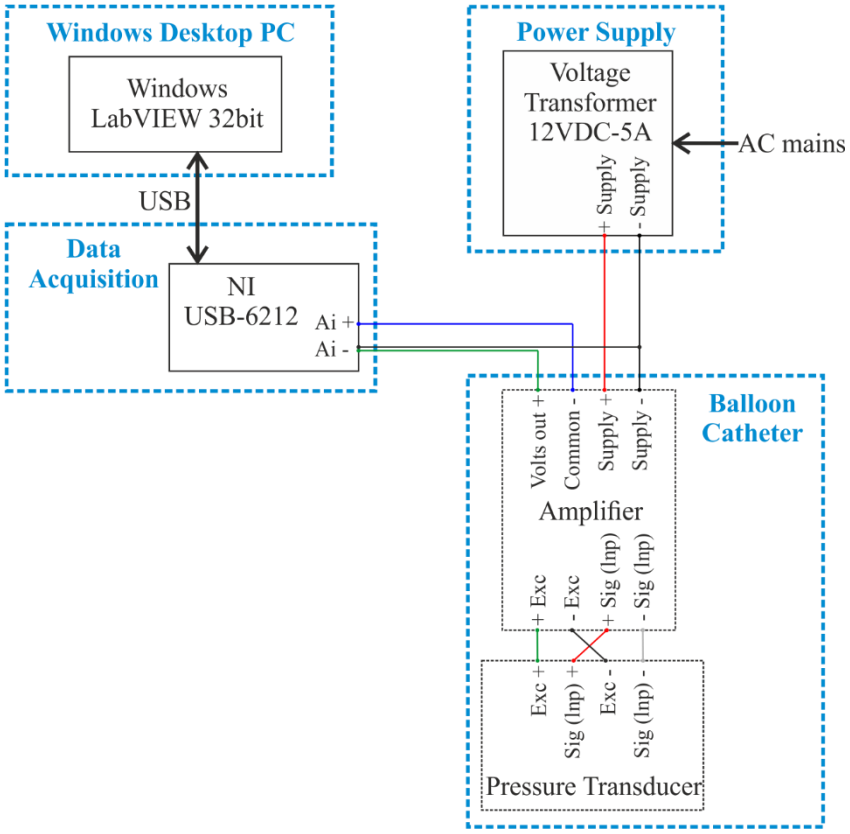

Figure 3.28 Wiring diagram of the terminal connections between the pressure transducer and DAQ device to measure intra-rectal pressure.

Two load cells are included in the simulation. The stepper motor used to regulate the position of the PR muscle was mounted to one load cell (Sensor Techniques, 1004) allowing the forces acting on the anorectum by the PR to be measured. Stool leakage retained by a collection tray was mounted to a second load cell (RDP, RLS005kg) such that mass, and mass flow rate, could be measured. While the load cell is accurate to ±0.007 % the applied load, discrepancies between actual and measured values arise

due to the configuration of the load cells and connected components. The stool load cell is orientated to measure force applied vertically, in the same axis as the force applied by the weight of faeces in the collection tray. The error for this measurement therefore will be considered accurate to the manufacturers quoted value. For measurement of PR force, the load cell is orientated to measure force applied in the horizontal axis. However the wire connecting the load cell to the PR phantom deviates slightly from being normal to the load cell due to the phenomena of pelvic floor descent. This means that the force observed will be a component of varying amounts the actual value. Consequently the values obtained for PR force will also be considered accurate to ±5 %. The wiring diagrams to obtain measurements from both of these load cells is demonstrated in Figure 3.29.

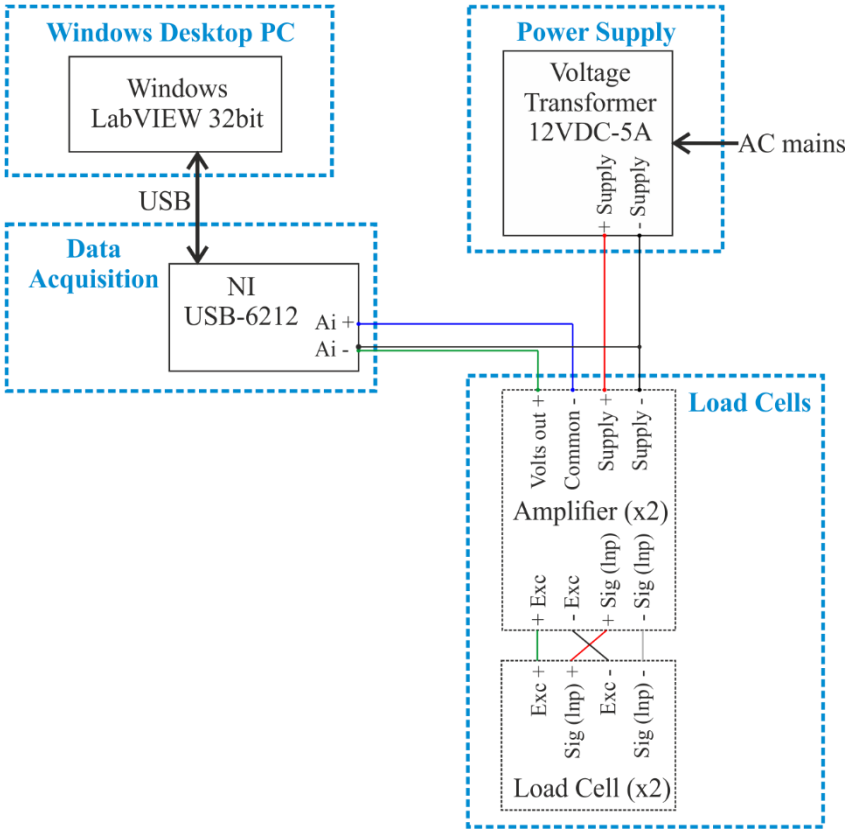

Figure 3.29 Wiring diagram of the terminal connections between the load cells and DAQ device to measure Puborectalis force and stool mass leakage.

A high definition universal serial bus webcam (C920 HD Pro, Logitech) was mounted on the model's supportive framework to provide a sagittal plane video-stream of the rectum at 30 Hz throughout each experiment. The video stream was used to monitor

and iteratively modulate the ARA as demonstrated by the loop control shown in Figure 3.30, and was recorded for post-hoc analysis.

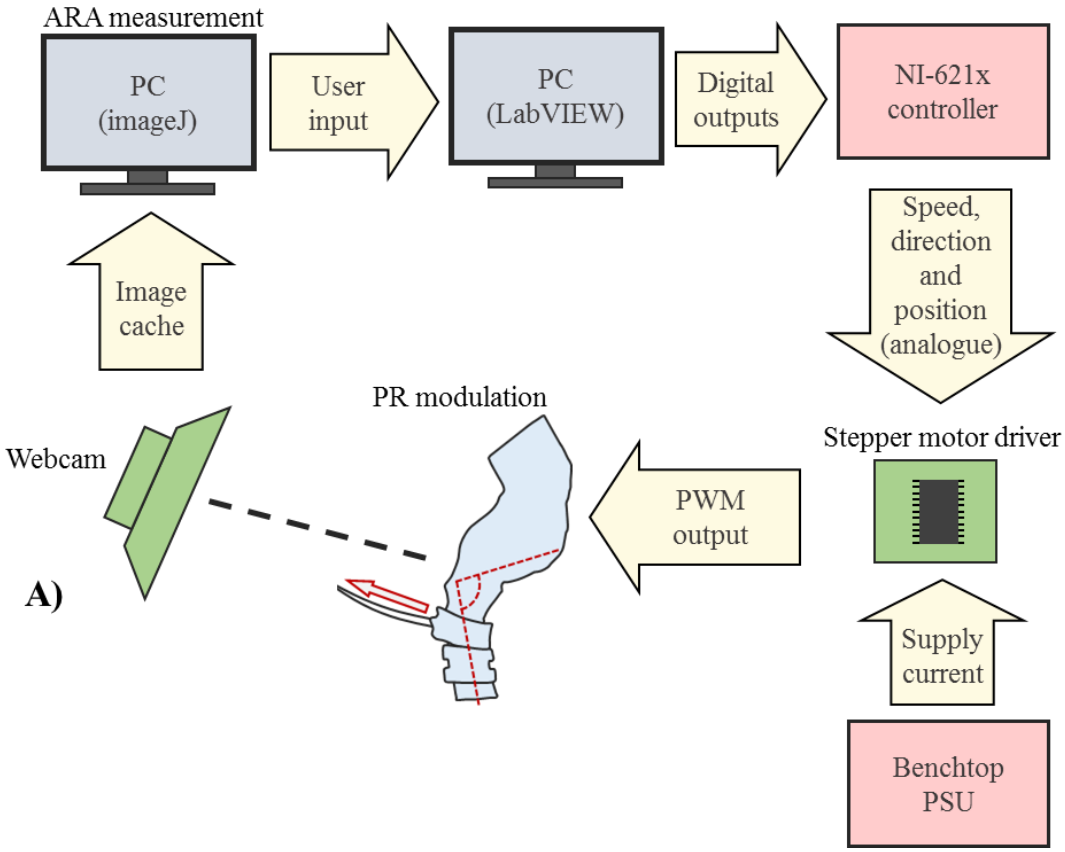

Figure 3.30 Flow chart demonstrating the loop control implemented for ARA augmentation, the loop begins at 'A)'.

The loop control presented in Figure 3.30 was used in the configuration of the ARA prior to testing. The ARAs included in the variable matrix for testing were configured individually while the positions required of the stepper motor to achieve each ARA was noted, this ensured that the PR muscle could be relaxed and returned to exactly the same position between tests. A short study was performed to verify the repeatability of measuring the ARA by visual analysis given the inevitability of human error. The ARA was configured to 90° and a snapshot was obtained using the serial bus webcam. Both axes (anal canal & rectum) which form the basis of the ARA measurement were then constructed by hand onto the image 10 times, independently of one another. On each image, the angle between the axes was then measured, Figure 3.31.

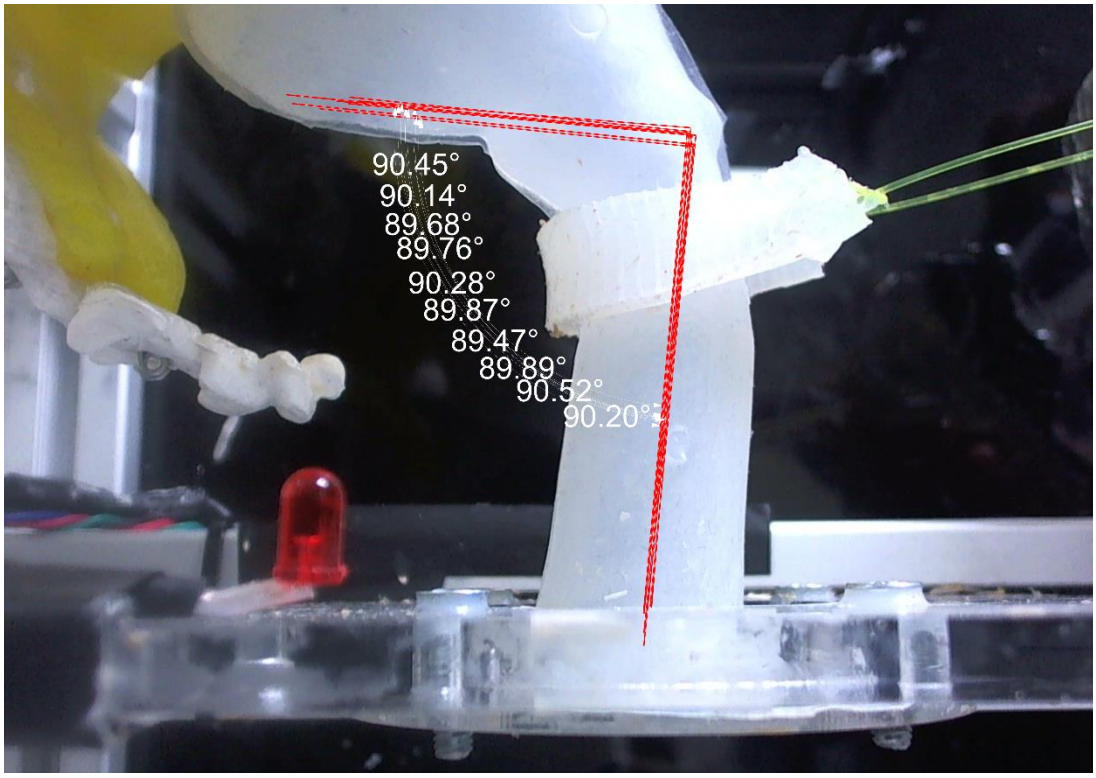

Figure 3.31 Ten repeat dimensions taken to test the repeatability of anorectal angle measurements.

Observation of the spread between ARA measurements provide an insight into the repeatability of this method to configure the PR position. The measurements ranged from 89.47° and 90.52° with a mean of 90.03° (standard deviation ±0.328°). This suggests that despite the arbitrary definition of the ARA, it can be measured reliably by visual analysis to within ±1° of the actual value.

Sensing hardware was tested to produce calibration curves. For the load cells, known masses were incrementally added up to a maximum and then removed incrementally, while the voltage outputs were recorded. Upper and lower limit values of the simulation are estimated for faecal mass passed (0 to 110 g) and for IR pressure (0 to 60 mmhg). The range of mass' and pressures tested during the calibration phase encompass this range. In order to calibrate the pressure transducer, a balloon catheter was connected to the pressure monitoring line and positioned at the base of a water-tight container while a head of water was incrementally increased to a maximum and then incrementally removed, while the voltage output was recorded. The hardware showed no hysteresis, and high linearity was observed (R^2>0.99), Figure 3.32. Coefficients from the calibration analysis, Table 3.8, were inputted to the LabVIEW

control platform so that real-time values of the test variables could be displayed during testing.

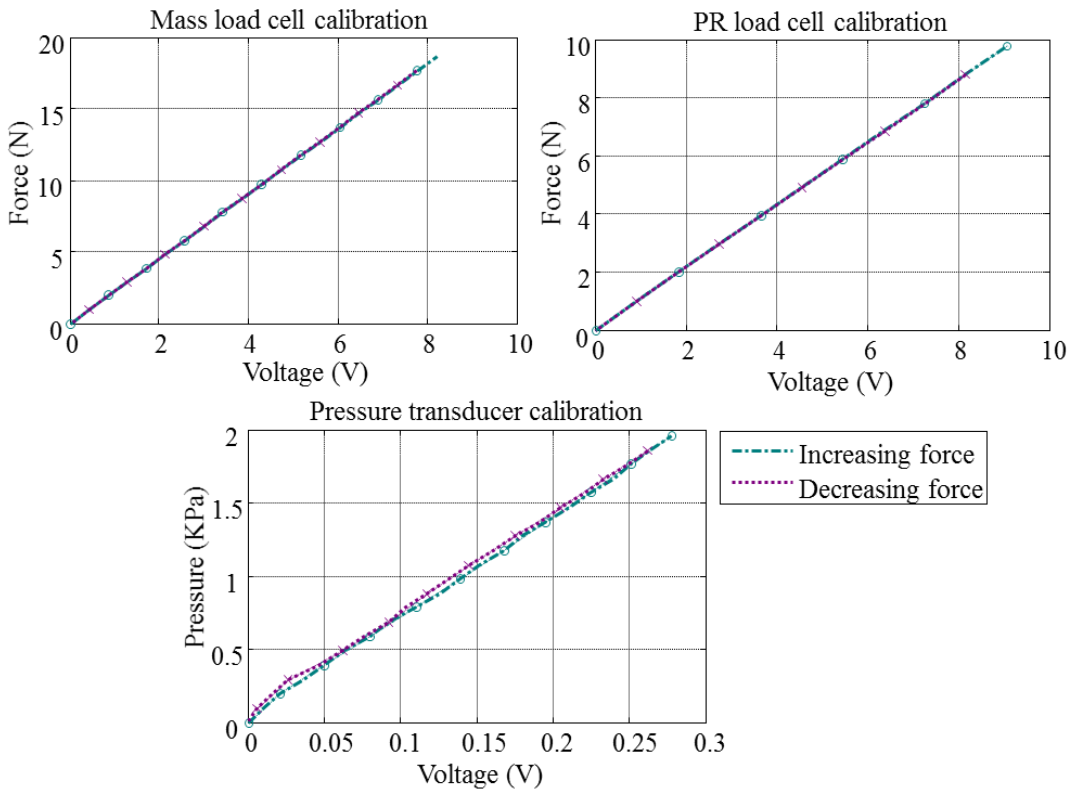

Figure 3.32 Calibration curves for simulation sensing hardware: mass load cell, PR load cell and pressure transducer.

Table 3.8 Calibration constants for sensing instrumentation:

	Pressure transducer	**Load cell 1 (PR)**	**Load cell 2 (Leakage)**
Coefficient	0.019	0.929	4.337

3.7.3. Control Software

This section describes the development of software for the data acquisition, control and data logging for the physical simulation. LabVIEW^{TM} (National Instruments) was used as a programming platform. The software architecture was selected and implemented to allow simple configuration of testing protocols. The user interface of the program is divided into two parts, a 'configuration' tab and a 'display' tab. The 'configuration' tab allows the user to define channels to write and read on the DAQ device for each piece of hardware, input custom calibration data and manually set the speed of the PR control stepper motor. The 'display' tab, Figure 3.33, shows plots of faecal mass passed, PR muscle force and IR pressure in real-time during testing. It also allows the position of the stepper motor and position and speed of the linear stage to be adjusted during testing, a file name to be defined and the initiation/termination of data recording. A flow chart for the operation of the *vi* is shown in Figure 3.33.

An overview of the faecal simulation is demonstrated in Figure 3.34, which details the tissue phantoms, control and instrumentation hardware along with the combined electronic subsystems.

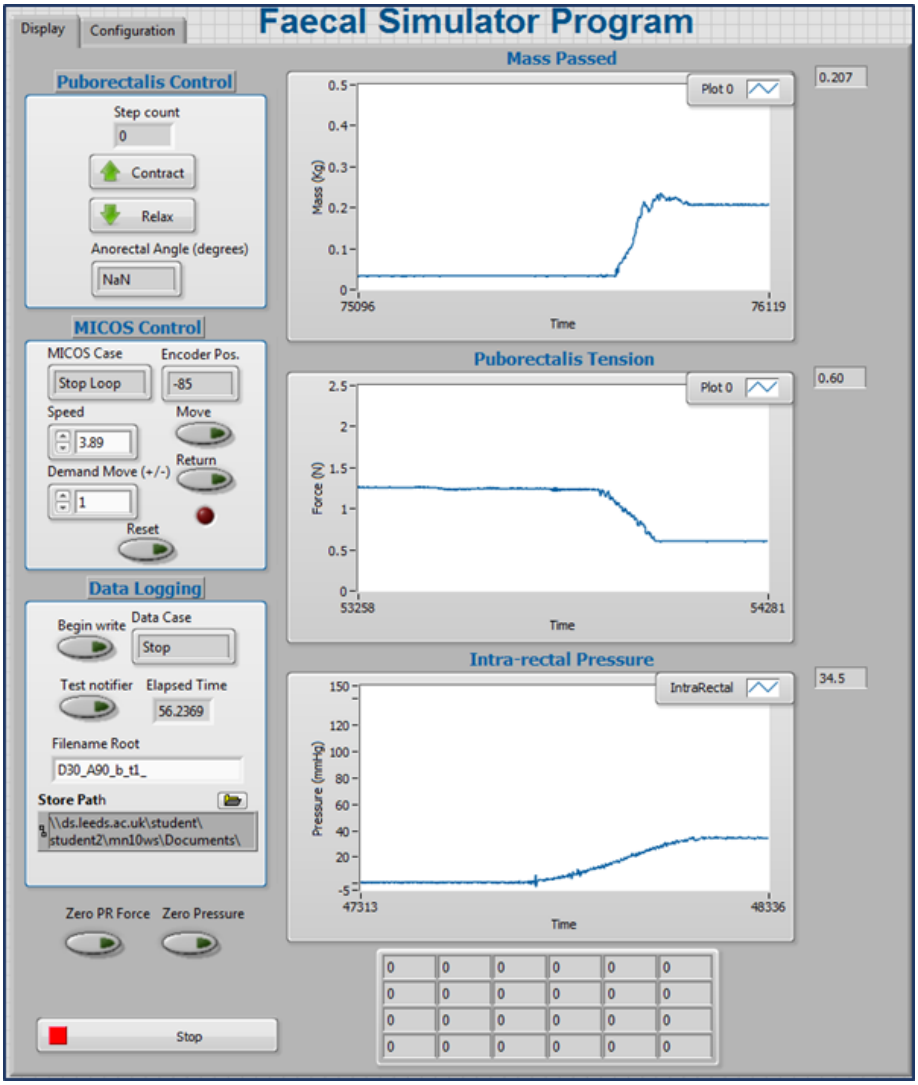

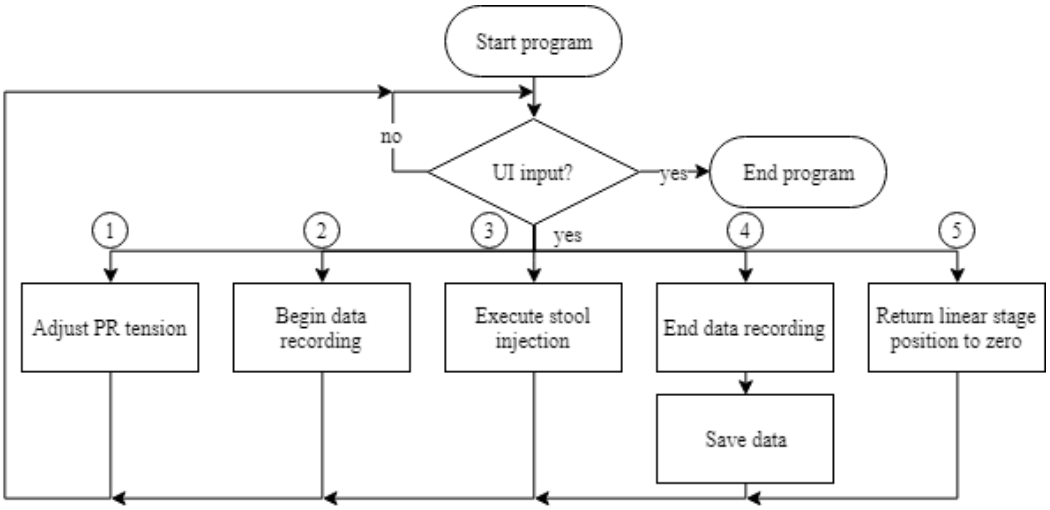

Figure 3.33 *Top;* LabVIEW program UI: 'Display' tab *Bottom;* Flow chart schematic of the software for user operation during a testing sequence.

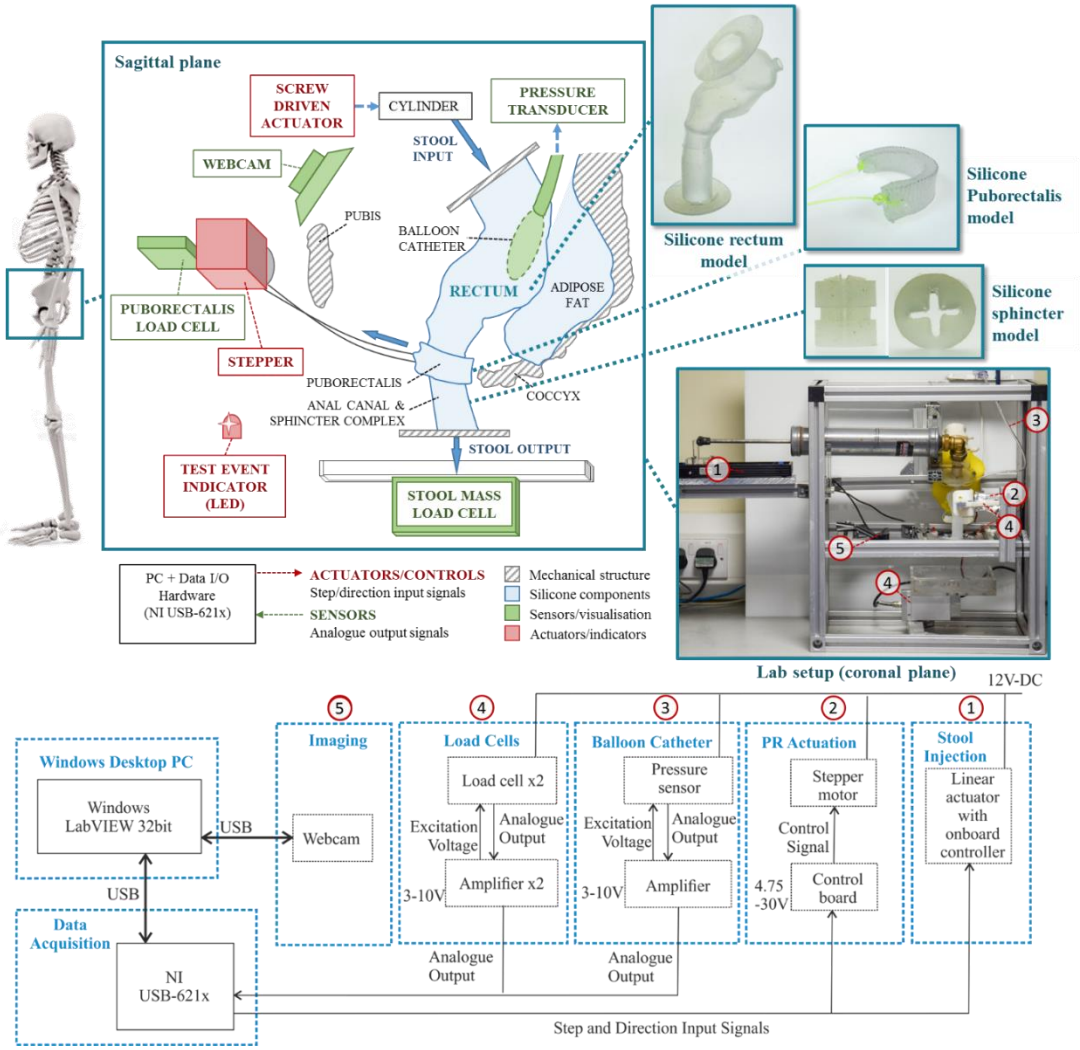

Figure 3.34 Schematic overview of the control and sensing hardware and silicone phantom model constituents of the physical simulation assembly together with the underlying electronic subsystems.

3.8. Summary

The full biological continence mechanism is complex and consists of the coordinated function of the nervous systems, GI tract, and anal sphincter and pelvic floor musculature. Our current model focusses on investigating the effects of varying ARA and sphincter pressure, and accordingly we have simplified the system to facilitate fabrication and detailed analysis of these functions.

In the development of a physical simulation of the faecal system, an approach was implemented which fabricated ‘soft’ representations of key parts of the anatomy, consisting of the rectum, PR muscle, sphincter complex and adipose tissue. These were developed from biomechanics of the human faecal system to be modelled, and manufactured using silicone fabrication techniques. Soft silicone representations were

combined with computerised control and instrumentation; implemented to control system variables to objectively monitor and regulate physiologically relevant parameters (derived from the simulation specifications). A stool simulant was implemented within the physical simulation to recreate the natural flow regimes observed in the biological system.

Tensile data was obtained from literature for rectum and adipose tissues and tests were conducted on porcine IAS and EAS to obtain force-displacement data, which together with data from literature, meant the loading profiles were obtained of all tissues represented in the simulator. Tensile data was also obtained for 3 grades of silicone, and a method to match a portion of their loading curve with the represented biological tissues identified Ecoflex 00-20 as matching the properties of Adipose tissue and Ecoflex 00-30 as matching the properties of Rectum and IAS tissues. Consequently, these silicones were used to fabricate their retrospective tissues, with the exception of the rectum in which 3 lower compliance grades were selected to represent an 'active' state, characteristic of the biological rectum during defecation.

The rectum, adipose fat and PR muscle components are simulated by cast, 1:1 scale, silicone models, anatomically positioned within a housing linking these elements to control and instrumentation, as shown in Figure 3.34. The system is driven through a stool injection mechanism while the ARA is regulated through an active PR muscle. By varying the pressure exerted by the PR muscle on the rectum, the ARA can be controlled and its effects on faecal leakage are observed during the influx of simulated stool. The anal canal is represented within the rectum geometry with passive occlusion from an anal sphincter cuff. The anal sphincter occludes the anal canal by instating mucosal folds in the wall of the rectum phantom. This allows for expansion without elastic deformation of the rectal wall, to critically observe effects of sphincter pressure on the system.

Chapter 4: Validation of the Physical Simulation

This chapter compares the physical simulation to the human system. Firstly, by considering the component parts (simulated stool, rectum model, anal canal/sphincter complex and pelvic floor) and comparing these to corresponding aspects of the human system; stool viscosity, pelvic floor descent, rectum morphology and anal canal distensibility are among the metrics used in the cross-comparison. The individual parts were then brought together to compare the simulation as a whole, through replication of a typical biological scenario, to the human system. Component-level validation, and validation of the simulation as a combined entity, strengthens its viability as a development tool for new technologies in the management of faecal incontinence.

4.1. Stool Simulant

Tests to determine the physical properties of faeces have shown that they vary considerably in viscosity, hardness and consistency [142]. A pharmaceutical grade smectite clay (VEEGUM R, Magnesium Aluminium Silicate NF Type IA, Vanderbilt Company) is used as simulated stool during nuclear proctographic studies, as it shows similar rheological properties (consistency) to human faeces. For this reason it has also been used as a stool analogue for research in the past [148]. It consists of dry particles which are multiple layers of individual platelets which form a homogenous solution with water. The extent to which the particles are delaminated into individual platelets depend on the degree of hydration. Proportions of clay and water and degree of hydration can be adjusted to obtain similar physical properties of density and viscosity comparable to those reported for soft faeces [142].

4.1.1. Simulation Stool Flow Characteristics

In the determination of shear rates which should be investigated for the characterisation of the stool analogue, the maximum shear rates through the simulation are estimated by modelling the laminar flow of a Newtonian fluid through a pipe, Figure 4.1.

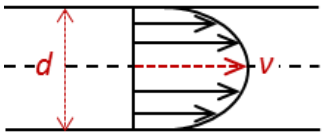

$$shear\ rate, \dot{y} = \frac{8v}{d} \qquad linear\ velocity, v = \frac{Q}{\pi\left(\frac{d}{2}\right)^2}$$

Where Q = volumetric flow rate, d = diameter

Figure 4.1 Calculation of shear rate by modelling the flow of a Newtonian fluid through a pipe.

To calculate the maximum estimated shear rate experienced by the stool simulant flowing through the simulation, a maximum volumetric flow of 9.26 ml s^{-1} is used together with the narrowest diameter of the rectum model, located at the anorectal junction (23 mm). This produces a maximum shear rate of 15.5 s^{-1}.

4.1.2. Rheology of Smectite Clay Suspensions in Water

The formulation of the stool simulant was determined through experimental analysis of its rheological properties. Dynamic viscosity curves of simulated stool are compared to fresh human faeces, following which power law indexes are calculated from the viscosity curves to compare shear thinning properties between the two. Finally, a stool suspension is selected based on its consistency through direct comparison with human faecal consistencies.

4.1.2.1. Dynamic Viscosity Curves

A range of samples were made by adding measured amounts of magnesium silicate powder to distilled water to produce suspensions with 91 %, 92 % and 93 % moisture contents. Moisture contents were initially chosen based on corresponding contents of runnier fresh human faeces [142], then 3 were selected to cover a range of consistencies up to the operational limits of the rheometer, as determined by trialling different solutions. Samples were dispersed using a chemical homogeniser for 2 minutes. Following homogenisation, samples were transferred immediately to the vessel of a rheometer (Bohlin Gemini II, Malvern Panalytical) to obtain shear rate-dynamic viscosity flow curves using a vane tool (V 25), for varying clay suspension moisture contents. During tests, samples were immersed in a water bath at a temperature of 25°C. Samples were pre-sheared for 10 s at a rate of 20 s^{-1} to

breakdown the molecular structure of the colloid suspension, as per the test protocol used to test human faeces [142], before being left to rest for 5 minutes. This ensures that temperature and concentration of colloid particles are uniform within the samples and establishes a consistent state of molecular breakdown/rebuild at the point of shearing. Finally the samples were subject to a logarithmic ramp of shear rates between 1×10^{-5} s^{-1} and 1000 s^{-1}, encompassing the approximate range of shear rates experienced within the simulation (maximum shear rate: 15.5 s^{-1}). The pre-shear, rest and ramp cycle was repeated 5 times.

The shear rate-dynamic viscosity flow curves obtained from the test are presented in Figure 4.2.

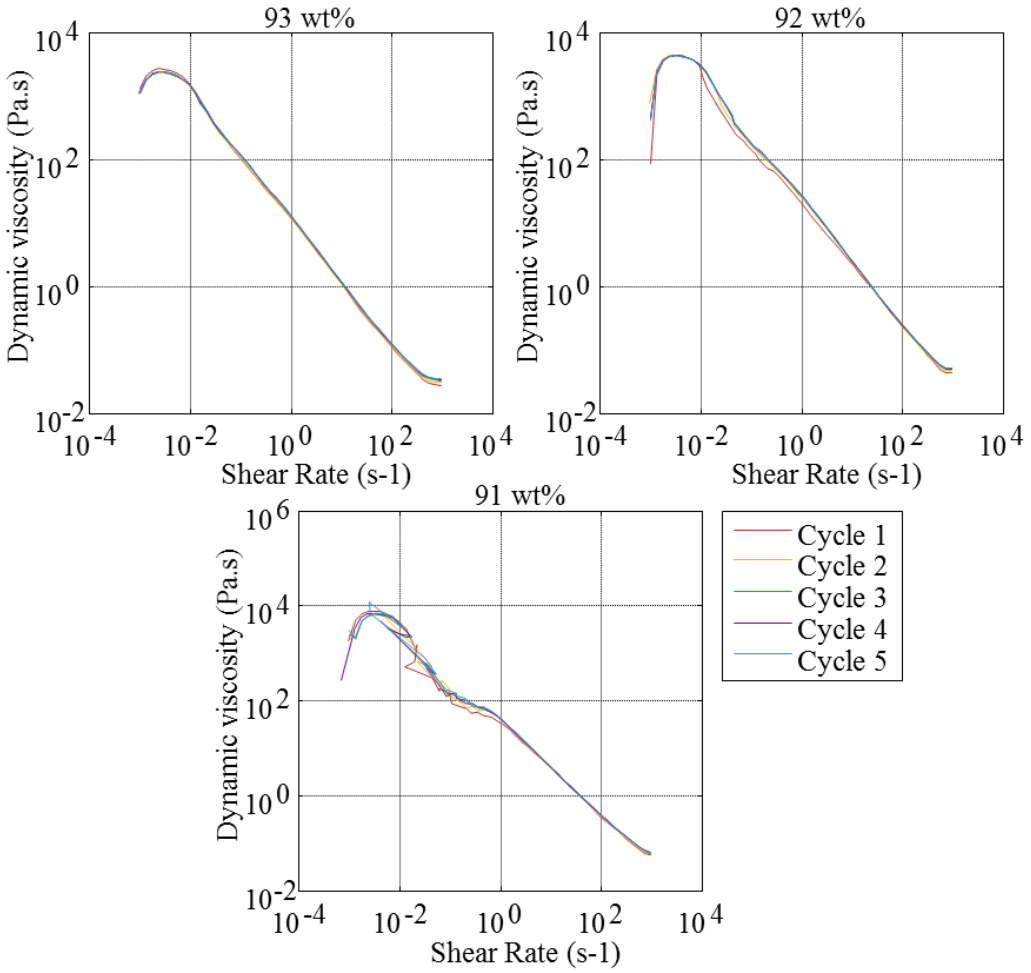

Figure 4.2 Raw dynamic viscosity profiles obtained for various moisture content VEEGUM R suspensions, each plot shows 5 cycles.

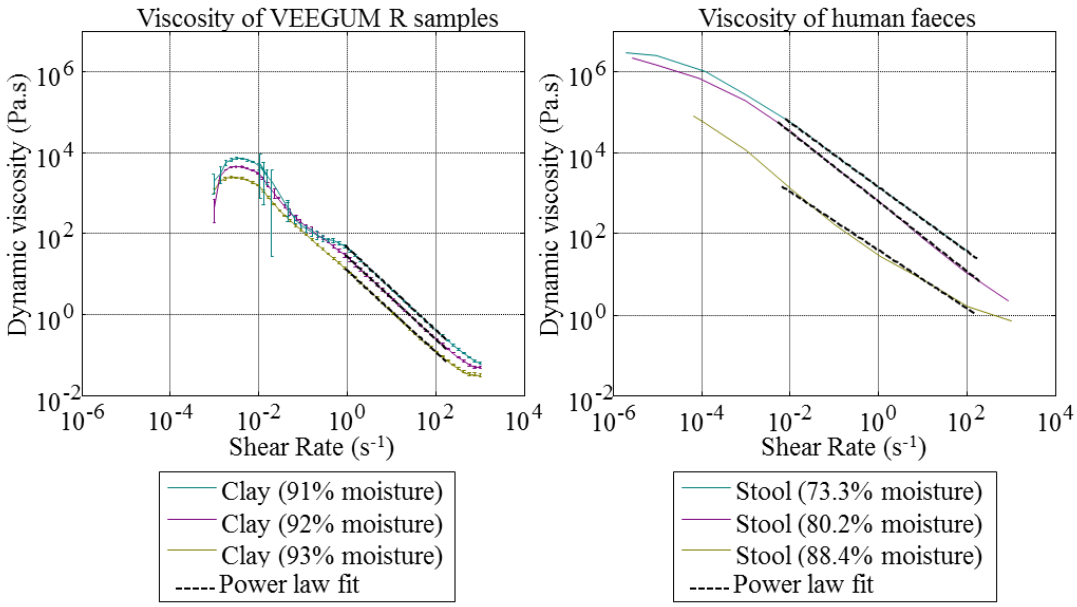

Figure 4.3 Dynamic viscosity profiles and power law fits of *left;* VEEGUM R suspensions in water showing mean (N=5) and *right;* typical human faecal samples with a range of moisture contents.

As can be seen, little variation is observed between cycles, indicating that the properties of suspensions do not vary over the course of the test. From the cyclic data, mean dynamic viscosities were calculated, displayed in Figure 4.3. It was noted that while testing the 91 % moisture suspension in particular, a large amount of noise is visible in the viscosity profile for shear rates under 1 s^{-1}, due to limitations of the rheometer.

4.1.2.2. Power Law Indexes

Using the mean plots of shear rate-dynamic viscosity, the power law index (PLI) is calculated using a standardised method [174] and compared to PLI's for dynamic viscosity profiles of a range of moisture contents human faeces, Figure 4.3. The power law region of a flow curve describes the shear thinning behaviour of fluids. This region shows linearity with a constant gradient on the log-log plot of dynamic viscosity vs shear rate. A power law fluid (or the Ostwald de Waele relationship), is a Newtonian fluid for which the shear stress, τ, is given by:

$$\tau = k\dot{\gamma}^n$$

$$Where\ k = consistency,\ \dot{\gamma} = shear\ rate$$

Which can be re-written to define an apparent viscosity, η:

$$\eta = k\dot{\gamma}^{n-1}$$

Consistency is defined as the dynamic viscosity of the solution at a shear rate of 1 s^{-1}.

PLIs were calculated for shear rates ranging from 1 s^{-1} to 100 s^{-1}, as all flow curves showed linearity between these limits. Values of PLI (η) and consistency (k) are displayed in Table 4.1 along with the R^2 value of the power law fit.

Table 4.1 PLI's calculated for various moisture content VEEGUM R suspensions and human stools:

Solution	Repeats (N)	PLI (η)	Consistency (k)	R^2 value
Clay (91% moisture)	5	1.01	42.2	0.999
Clay (92% moisture)	5	1.01	25.2	0.999
Clay (93% moisture)	5	1.01	11.9	0.999
Stool (73.3% moisture)	1	0.80	1410	0.999
Stool (80.2% moisture	1	0.86	617	0.999
Stool (88.4% moisture	1	0.72	39.3	0.997

A strong power law relationship (R>0.99) is seen for all flow curves displayed in Figure 4.3. The PLIs calculated for all suspensions were comparable, with little

variation between the different moisture contents tested. All PLIs for the suspensions were less shear thinning than a range of stools used in a previous study on human faeces; ranging from 0.72 at a 88.4% moisture content to 0.86 at an 80.2% moisture content [142], whereas the suspensions possess a PLI of 1.01. A range of moisture content stool samples were chosen from a previous study to include in the analysis, and since every stool is different, no repeats were obtained for each sample. However, human stools showed a relation between moisture content and consistency, ranging from 1410 Pa.s at a 73.3% moisture content to 39.3 Pa.s at an 88.4% moisture content [142]. Values observed for PLI of different moisture content stools were variable and with now apparent trend, probably due to a lack of repeat tests. Due to operating limitations of the rheometer, thicker consistency suspensions could not be tested, despite the need for thicker consistencies to represent lower moisture content faeces.

The observation that smectite clay suspensions possess smaller PLIs (demonstrating less shear-thinning behaviour) than human stool, suggests that the flow curves would cross over at low shear rates (< 0.1 s^{-1}). At the point of crossing, the fluids would possess the same apparent viscosity; indicating similar flow characteristics at this shear rate. It was estimated that the flow regime through the rectum model would produce a maximum shear rate of 15.5 s^{-1}. While the suspensions tested have greater shear thinning properties than the stool samples, lower moisture content suspensions can increase apparent viscosity. This would bring the flow characteristics of simulated stool more in line with human stool for a given shear rate. Since a maximum shear rate of 15.5 s^{-1} was estimated for stool flow within the simulation, the majority of flow would be subject to a shear rate smaller than this. Therefore the apparent viscosity of simulated and human stool are compared at a shear rate of 1 s^{-1} (also termed the 'consistency' of a fluid).

4.1.2.3. Determination of Stool Formulation

The consistencies of clay suspensions were plotted against moisture content, Figure 4.4. Interpolation of this relationship allows the moisture content to be estimated given a desired stool consistency, required of the simulation. This analysis produced an interpolated power law which showed close relationship to the viscosity-moisture content profile (R^2>0.99).

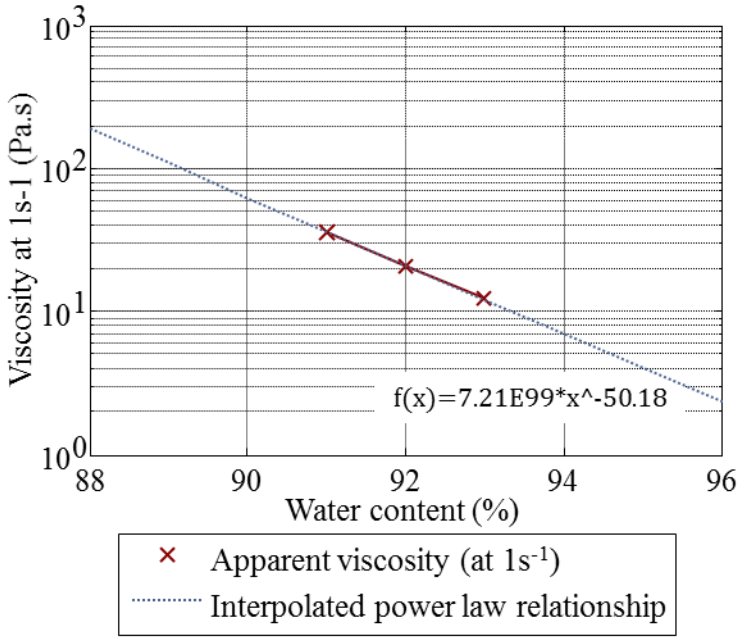

Figure 4.4 Interpolated power law of the relationship between apparent viscosity and water content for various moisture content VEEGUM R suspensions.

The measured moisture contents of human faeces range from 58.5% to 88.7% by mass, with consistencies ranging between 52.8 and 3306.3 Pa.s [142]. Using the power law relationship defined in Figure 4.4, the clay formulation was selected at 90.5% moisture content. This formulation produced a consistency of 47.1 Pa.s which is similar to high moisture-content semisolid faecal samples, yet fluid enough to pass through the simulation without damage to soft components. Also when mixed in this ratio, the simulated stool did not leak from the simulation at resting pressures. While this is not representative of the viscosity of a mean moisture content stool, it presents a 'worst case' with which to rigorously test the continence mechanisms in the physical simulation.

4.2. Tissue Phantoms

Direct comparison between individual soft tissue components and corresponding components of the human system is challenging as part of the full simulation. Therefore an isolated validation was performed on individual components highlighted in Figure 4.5 (rectum, sphincter complex and pelvic floor), to increase their face validity.

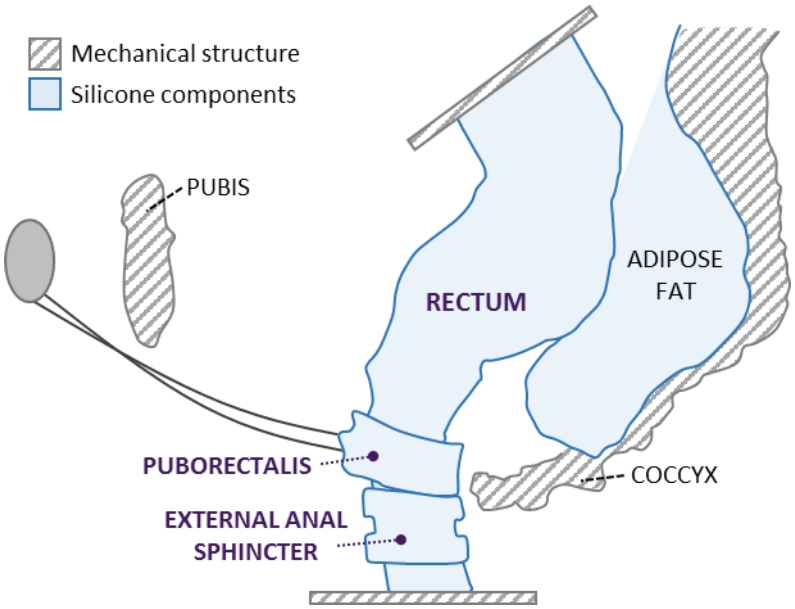

Figure 4.5 Soft silicone components are highlighted for which validation checks are carried out, before performing a typical test scenario on the components combined.

A majority of the modelling criteria for the components have been informed with data from literature. Each fabricated component was compared back to this data during the validation process. Tests were conducted on the rectum model to define a pressure-distension profile; a common assessment carried out in previous studies to determine the compliance of rectal tissue. Distensibility tests were carried out on the anal canal/sphincter assembly to obtain pressure-diameter data at various points along its length and calculate an index for cross-comparison with the human system, using the same protocol as used on human subjects in the past. Finally, the range of angulation achieved by modulating the position of the PR was observed and compared to a range of clinically observed values. Following individual validation, the components were brought together to compare aspects of the simulation as a whole to the biological system, while subject to parameters characteristic of ‘healthy’ defecation.

4.2.1. Rectum

Based on the analysis in Chapter 3 (Section 3.5.1.2.) preliminary stool injection tests were conducted with a rectum fabricated from Ecoflex 00-30, to investigate the effect of ARA on continence. However tests carried out with any substantial resistance to leakage (obtuse ARA's) caused gross distension of the rectum without the passing of faeces, due to inadequate elastic forces in the rectal wall. In Chapter 3, tests to analyse tensile properties of the rectum tissue, were performed in a 'passive'/resting state, whereas in the biological system during defecation it is 'active'. To counter this, three stiffer grades of silicone were chosen to represent the rectum in an 'active' state, characteristic of a rectum during defecation in a healthy subject, these included Dragon Skin 10A, 20A and 30A. The operational strains experienced by the rectum in the simulation lie well within the strains which these silicones undergo before failure (which are all in excess of 364 %). Furthermore, the elastic moduli of these silicones range from 0.15 MPa for Dragon Skin 10A to 0.59 MPa for Dragon Skin 30A, which encompass a range an order of magnitude stiffer than the Ecoflex-series silicones tested in Chapter 3 (Section 3.5.1.2.). A stiffer grade of silicone acts to simulate the properties of contracted muscle. During defecation, intrinsic contraction of the rectum plays an important role in reducing resistance to passing. It also allows the transit of higher viscosity stools in the simulation, which are similar to fresh human faeces. This allows the effects of a greater range of ARA's and sphincter occlusion pressures to be tested, since the elastic contraction of the rectum has the ability to overcome greater resistance to leakage.

In order to simulate rectal interfaces, a phantom model of adipose tissue was fabricated using Ecoflex 00-20, as identified in Section 3.5.1.2. to be positioned between the rectum and sacrum. A silicone deadener additive (Slacker^{TM}, Smooth-On^{TM}, Minnesota) was added to the silicone during fabrication in quantities defined on the product information for a 'very tacky' cast component. This modifies the rebound properties of the component in a way which behaves more like human tissue. The component was then brushed with a silicone encapsulator (Super Baldiex^{TM}, Mouldlife, Bury Saint Edmunds) to produce a low-friction finish. Table 4.2 displays materials used to fabricate the rectum and adipose components.

Table 4.2 Indicated tissue phantoms and corresponding materials:

Pelvic constituent	Model material
Rectum	Dragon Skin 10A, 20A & 30A [6]
Adipose fat	1:1 wt% Ecoflex 00-20:Slacker^{TM} [6]

4.2.1.1. Pressure-Distension Profile

Tests were conducted to observe the pressure-distension profile of the rectum, to compare with the biological system. A rectum fabricated from Dragon Skin 20A was used during the analysis and stool was formed with VEEGUM R using a 90.5% moisture content solution, prepared using the same method as in section 4.1.2. The simulation pressure transducer (to measure IR pressures) was set to zero under atmospheric pressure. The outlet to the rectum was fully occluded before introducing 50 ml of stool simulant at a rate of 2 ml/s at the inlet, while the change in IR pressure (with reference to atmospheric) was observed. A total of 10 repeats were conducted. Figure 4.6 demonstrates the measured mean ±1 STD of the IR pressure change during the distension.

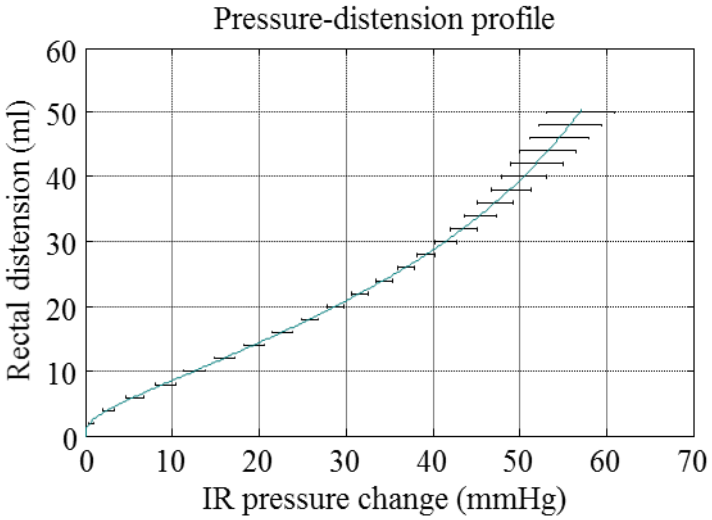

Figure 4.6 Variation of rectal pressure with time during a controlled influx of stool to the rectum, solid line shows mean (N=10) with 1STD error bars.

Studies have been carried out to assess the 'push' pressure in the rectum during defecation with balloon expulsion tests, using a high resolution manometry catheter. It has been reported that urged is sensed with a rectal volume of 167 ml [18] and at this distension, the IR pressure is 29 (21-36) mmHg. Another study [175] on healthy males revealed that the peak IR pressure during 'push' was 72.3±9.4 mmHg (N=64).

This suggests that a change in pressure of 41.3 mmHg is experienced between sensing urge and the maximum pressure experienced during ‘push’. From Figure 4.6, an IR pressure of 41.3mmHg in the physical simulation corresponds to a rectal distension of 29.9 ml. Taking into account the non-distended volume of the rectum, this correlates to a total rectal volume of 86.6 ml. Whereas greater rectal volumes were observed in the human system upon defecation, the pressures generated with the simulation were comparable with literature findings during defecation. Inclusion of a more compliant rectum with the simulation would allow the effect of greater rectal volumes to be investigated with the system.

4.2.2. Sphincter Complex

As determined in Chapter 3 (Section 3.5.1.2.), Ecoflex 00-20 was selected to model the IAS. Consequently this was used for fabrication of the sphincter phantom and the following section describes the steps taken to characterise it.

4.2.2.1. Anal Canal Distensibility

An important modelling consideration is that the pressure profile along the anal canal of the physical simulation and biological system are comparable. The physical simulation aims to model the resting pressures of FI patients, to form a ‘baseline’ configuration. An AAS device is then fitted with the intention of elevating pressures to be closer to the resting state of a healthy patient, demonstrated schematically in Figure 4.7.

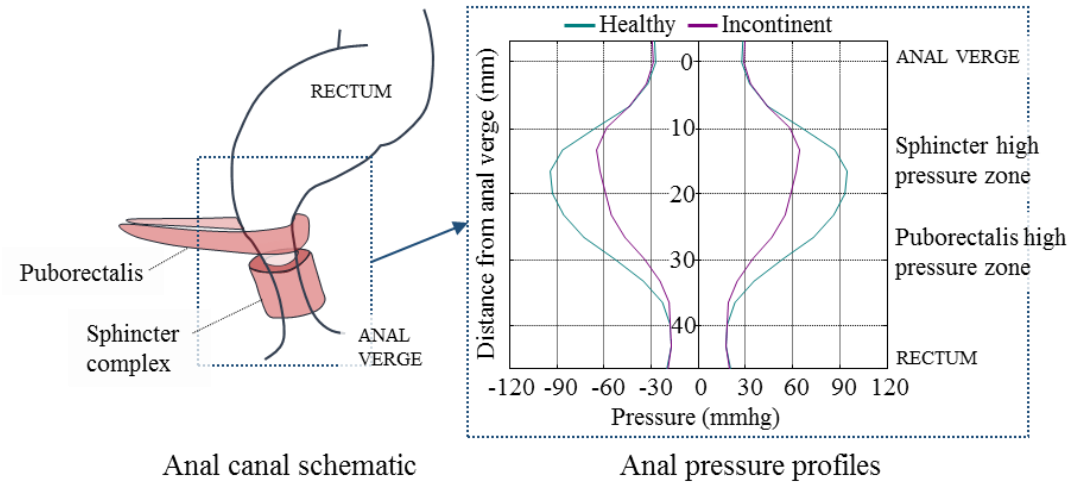

Figure 4.7 Typical ‘healthy’ and ‘incontinent’ anal canal pressure profiles at rest.

Since FI patients have poor EAS function, the sphincter phantom used a grade of silicone which represented the properties of the IAS. The IAS is composed of smooth

muscle and has similar properties to the rectum, which as determined in Section 3.5.1.2. is most closely matched to Ecoflex 00-30.

A series of tests were carried out using the EndoFLIP® to assess the distensibility of the anal canal, and contribution of a passive-assistive commercially available device with two stiffnesses (Consisting of the 'FENIX' and a stiffer model of the same design; the 'FENIX Plus') on sphincter pressures throughout the anal canal. The EndoFLIP system consists of a balloon catheter and pressure transducer/catheter volume control unit. The balloon catheter is constructed of a straight, stiff core with 16 impedance sensors along its length, contained in an inflatable non-compliant bag. The impedance sensors measure the diameter of the bag at various positions along its length to within ±1 mm and bag volume is modulated to within ±1 ml the desired value. The PR muscle forces were configured to produce ARAs of 80° and 100°. The simulation was orientated in the left lateral position and the EndoFLIP probe was inserted into place. Before using the system, air was removed from the probe and the baseline intra-bag pressure was set to zero. PR force, anal canal diameters and the mean anal canal pressure were recorded throughout.

The following protocol was followed for each test with the faecal simulator and EndoFLIP:

1. *Initialise System and position the EndoFLIP®.* Mineral oil is used to lubricate the probe which is then manoeuvred until its sensors occupy the `high pressure zone of the anal canal.
2. *Configure ARA position and sphincter.* Adjust PR tension until desired ARA achieved, FENIX/FENIX Plus is fitted if required.
3. *Run test.* Bag is inflated incrementally.
4. *End test.* Bag is deflated.

During tests, the EndoFLIP bag is inflated incrementally from 15 to 50 ml in intervals of 5 ml, at each increment inflation is paused to allow values to settle, before pressures and diameters were recorded. The EndoFLIP was positioned and secured at the start of testing and remained in place for the duration of tests. Anal canal diameters were recorded at 5 mm intervals, the distance between impedance sensors along the probe. The CSA measurements and pressures were sampled at 10 Hz and were stored in the data acquisition system. Measured outputs were mean anal canal pressure, anal canal diameters and PR muscle force. Tests for ARA effects were carried out, these were repeated 5 times for ARA values of 100° and 3 times for ARA values of 80°.

All tests were performed at room temperature (25°C). Images of the rectum were analysed using ImageJ™ (National Institutes of Health) to measure the augmented ARA, varying PR force iteratively until it was correct within 0.5°. Each test was

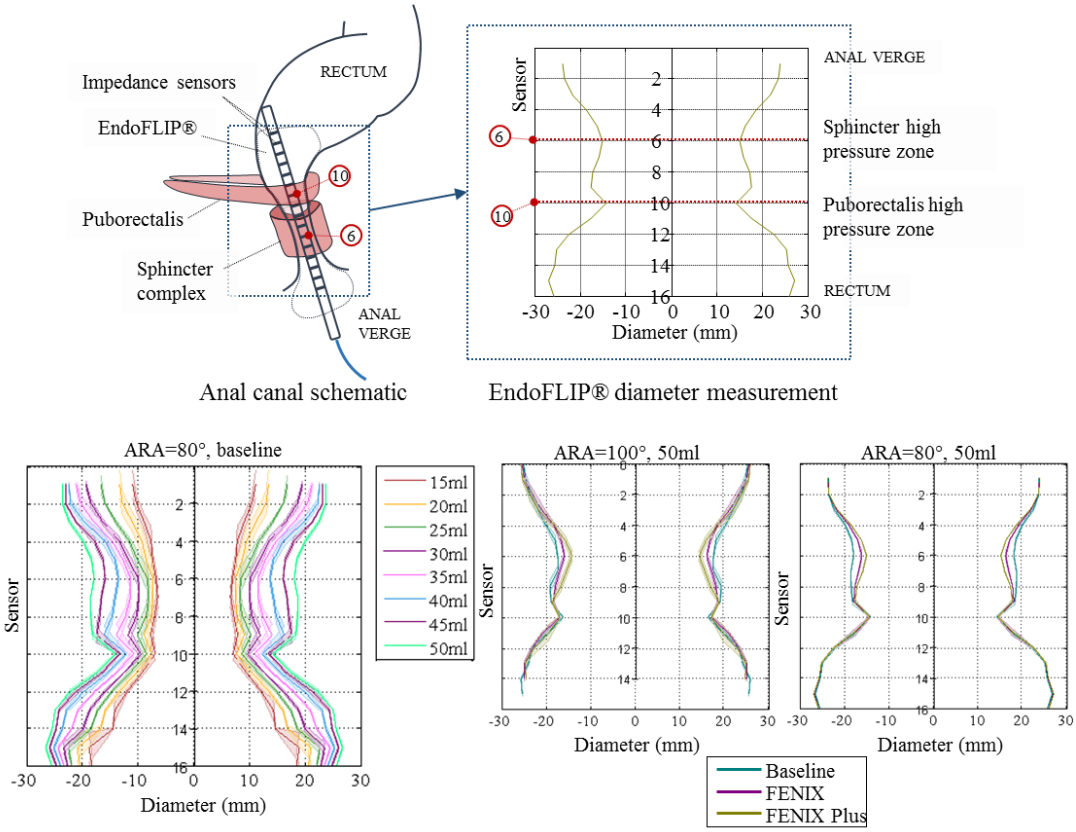

Figure 4.8 *Top*; schematic donating sensor locations of the EndoFLIP *Bottom left*; Anal canal diameters for the bag volumes recorded (N=3) *Bottom right*; Baseline, FENIX and FENIX Plus anal canal diameters recorded and ARA's of 80° (N=3) and 100° (N=5), mean diameters are shown in solid with 1 STD as shaded region.

recorded using a high definition universal serial bus webcam (C920 HD Pro, Logitech). Tests for sphincter effects were carried out for baseline values using a silicone sphincter model, and with the addition of a FENIX/FENIX Plus device. Figure 4.8 displays an experimental schematic (top), along with the data obtained during the analysis (bottom).

The full test protocols were successfully completed. Figure 4.9 shows images of each experimental configuration for stool injection testing (obtained from the webcam), the variation in ARA obtained by tensioning the model PR muscle. Figure 4.9 shows experimental stages for anal manometry testing with the FENIX, while balloon volumes were regulated with the EndoFLIP.

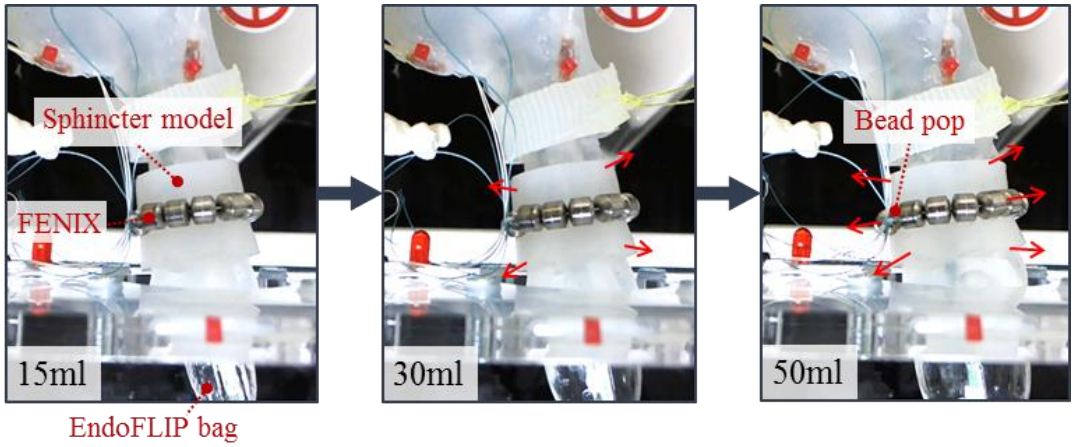

Figure 4.9 View of the anal canal during manometry testing with the FENIX device fitted, for a range of manometer-bag volumes tested.

The anal canal diameters and mean anal canal pressures were recorded. Figure 4.8 shows plots of anal canal diameters with changing bag volumes. Distension of the anal canal is most pronounced at the proximal and distal ends of the anal canal. Figure 4.8 demonstrates effects of ARA and FENIX on anal canal distension. Sensor 10 reveals the effect of the ARA on anorectal occlusion, approximately 50mm from the anal verge, with a reduced rectal diameter of 16.22 mm at an ARA of 100° to 14.13 mm at an ARA of 80°. Inclusion of the FENIX and FENIX Plus devices have also shown to reduce anal canal distension.

Sensor 6 was identified as being located at the centre of the high pressure zone in the anal canal, as demonstrated in Figure 4.8. At this location, calculated CSAs were plotted versus mean anal canal pressure (distensibility), displayed in Figure 4.10.

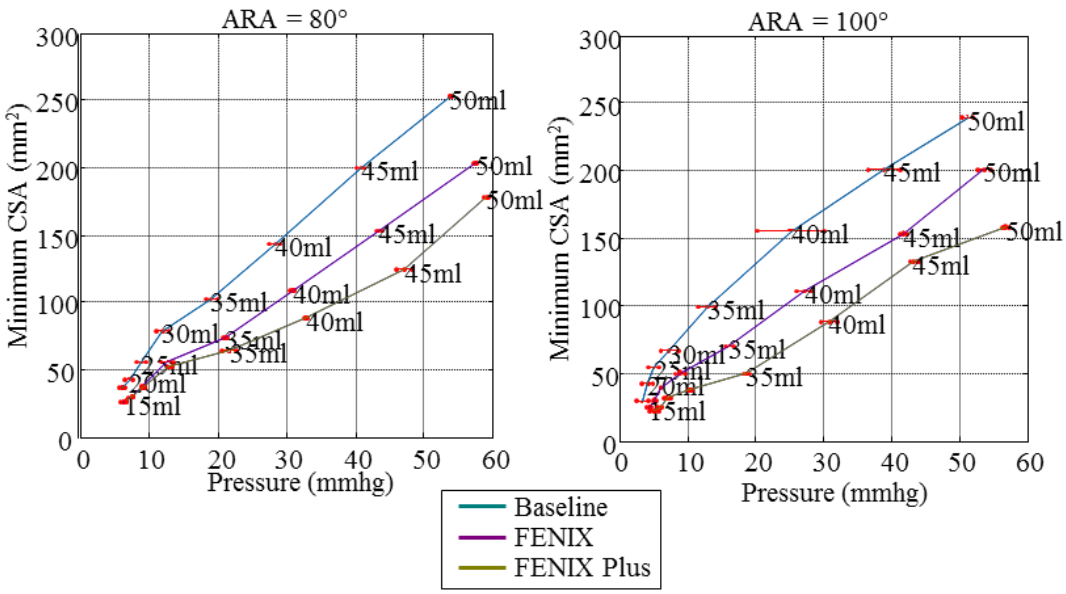

Figure 4.10 Anal canal CSA (at sensor 6) versus balloon pressures with different sphincter configurations for ARA = 80° (*left*) and ARA = 100° (*right*). Each plot shows mean (N=10) with 1 STD error bars.

The pressure in the bag in both tests increased as the anal canal diameter increased with growing distension volume. These data show a clear decrease in distensibility with use of the FENIX. For an ARA of 100°, at an inflation volume of 50 ml, CSA's of 240.0 mm^2 for baseline, 200.6 mm^2 with the FENIX and 158.4 mm^2 with the FENIX Plus were measured. For an ARA of 80°, at an inflation volume of 50 ml, CSA's of 252.6 mm^2 for baseline, 203.6 mm^2 with the FENIX and 178.3 mm^2 with the FENIX Plus were measured.

Distensibility Index

Based on previous studies on the esophagogastric junction, the distensibility index (DI) is a relevant parameter in clinical practice for defining distensibility. Using the same method as used in a previous studies [145, 176] DI is calculated as the median CSA at the narrowest point divided by the corresponding bag pressure, at 50 ml inflation volume. DIs are calculated for the physical simulation, and compared with values from literature, Figure 4.11.

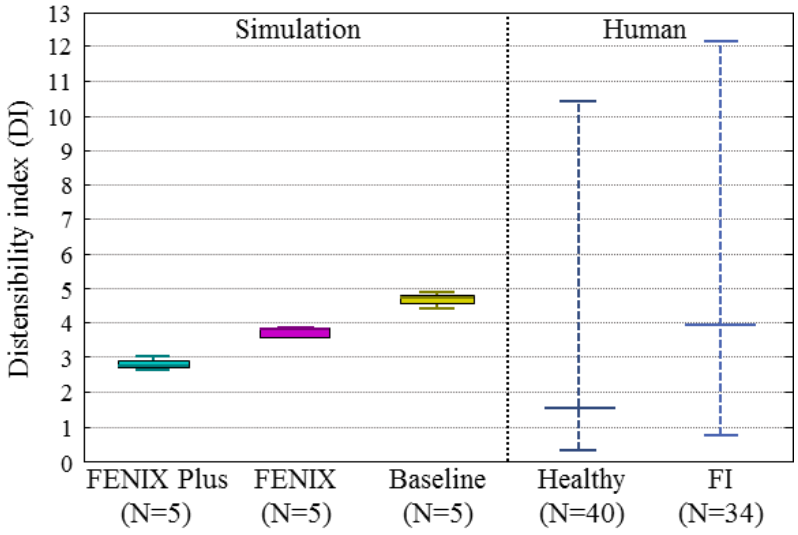

Figure 4.11 Calculated DIs for the physical simulation and biological system at rest, each plot shows the median (in solid) and range (whiskers).

When the ARA has minimum effect (ARA=100°), the rate of increase in the narrowest section of the anal canal relative to the rate of increase in bag pressure was 4.74 at baseline compared to 3.88 with the FENIX and 2.72 with the FENIX Plus. Higher DIs were associated with higher severities of FI. Previous assessments with the EndoFLIP [145] have reported the DI at rest as 3.9 (0.7-12.1, N=34) for FI patients, and 1.5 (0.3-10.4, N=40) for healthy patients.

The DI decreases with increased sphincter occlusion pressure (i.e. with inclusion of the FENIX and FENIX Plus). Therefore by addition of these devices, the anal canal DI can be modulated to become more in line with values observed for healthy patients. The simulated DI without an AAS device fitted is comparable to the DI for FI patients, suggesting that a similar pressure is required for expansion of the anal canal in both the human system and physical simulation. The FENIX and FENIX Plus offer an improvement to the DI of the anal canal, in-line with the biological values for healthy subjects when used with our model.

4.2.3. Pelvic Floor

The position of the fabricated PR model was regulated using a stepper motor which also allows ARA's to be maintained at a constant value during tests. By modulating the force this component applies to the rectum, a range of ARA's can be produced, Figure 4.12, which encompass those required for normal function as defined in the specifications in Chapter 3.

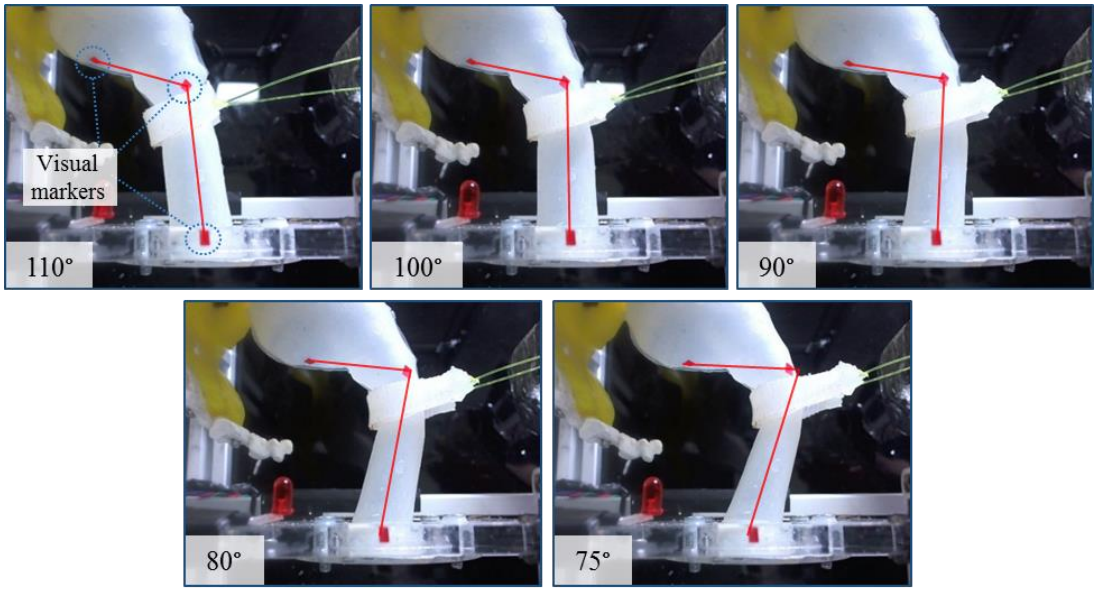

Figure 4.12 Webcam view of the ARA within the physical simulation, indicating the range of ARA's which can be configured.

The ARA's were measured by constructing the axes of the centre of the anal canal and inferior-posterior wall of the rectum (as per the method in Section 3.7.2.). Where they intersect, these axes form the ARA. A software package, ImageJ^{TM}, is used to manually construct these axes and measure the value for the ARA. Visual markers help in identifying anatomical landmarks used as reference in the potting of axes, positioned at 1) inferiorly and at the centre of the anal canal; 2) anorectal junction and 3) inferiorly on the posterior wall of the rectum. Inaccuracies arise due to a degree of dependency of the measurement on human judgment. Although as determined in Chapter 3 (Section 3.7.2.), using this method the ARA can be measured reliably to ±1° of the intended value.

By modulating the position of the PR component, ARA's were achieved between 75° and 110°. As identified in Chapter 2, ARAs observed in healthy patients at rest were 104.5°, and during squeeze these become more acute to 84.5° [9] to prevent the passing of faeces during urgency. The simulation has demonstrated its capability of reproducing a range of ARA's which encompass these biological limits. Furthermore, by observing the position of the stepper used to augment the PR muscle, it is noted that the PR muscle phantom moves 12mm between positions required to produce ARAs of 110° (simulating 'rest') and 80° (simulating 'squeeze'). This is comparable to values obtained from literature which show that the PR muscle augments 10.3 mm between positions at rest and squeeze [68].

4.3. The Physical Simulation

Following a component level validation, individual parts were brought together for comparison of the physical simulation as a whole to the human system. Images were taken of the simulation in the sagittal plane and compared alongside images from proctographic studies. In both systems, the pelvic floor descent is measured as a parameter to quantify similarities between their functionality. In addition, a short study is conducted to test a typical defecation scenario, from which metrics from the simulation were compared to the biological system, these include the total mass leakage and IR pressure change. Finally, rectal morphology was observed during the study, revealing the effect of IR pressures on expansion and rotation of the rectum.

4.3.1. Comparison with Proctographic Images

Proctographic images were taken in the sagittal plane during healthy biological 'states' [177], and compared to the physical simulation in corresponding configurations, Figure 4.13.

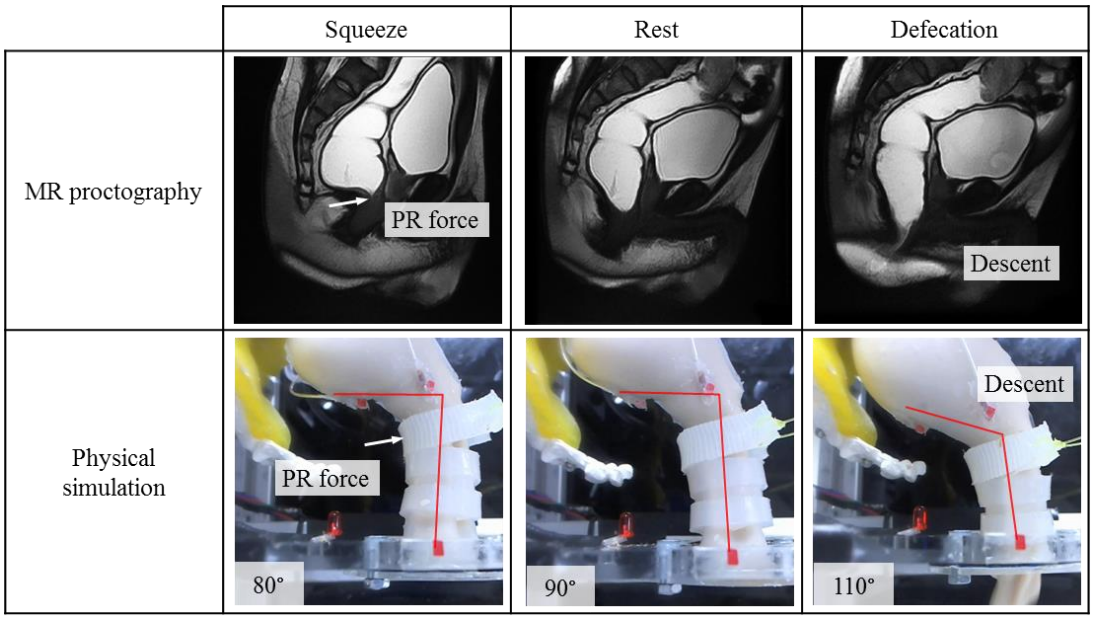

Figure 4.13 Comparison of MR proctographic scans of the biological system with the physical simulation during 3 different states; squeeze, rest & defecation.

During squeeze, the ARA is acute due to the indentation of the PR muscle on the posterior rectal wall, and at rest, this indentation is still present although less pronounced. During defecation, there is mild pelvic floor descent with relaxation of the PR, and consequently, the ARA becomes wider, so that the rectum and anal canal become aligned in an almost straight line followed by evacuation. These features were

visible in both systems, Figure 4.13, the physical simulation can be configured to represent each biological state: squeeze, rest & defecation.

4.3.1.1. Pelvic Floor Descent

During simulated defecation, the PR muscle descends with the onset of a transit of faeces through the rectum, as it straightens. In literature, this descent is defined by the perpendicular from the pubococcygeus line, down to the anteroposterior dimension of the hiatus. Analysis was conducted using the physical simulation to measure the pelvic floor descent. A rectum was selected which was fabricated from Dragon Skin 20A, and a stool simulant was formed using a 90.5 % moisture content solution of VEEGUM R and water. The rectum was filled with stool simulant. Two snapshots of the simulation were recorded for the analysis. A snapshot for 'rest' was achieved while the force applied by the PR muscle produced an ARA of 90°. Defecation was achieved by configuring the ARA to 100°, and injecting 100 ml of stool simulant into the rectum at a rate of 9.26 ml/s, the snapshot was recorded at the maximum observed distension of the rectum. ImageJ was used to process images of both states, and measure the pelvic floor descent from the transition between 'rest' and 'defecation', Figure 4.14.

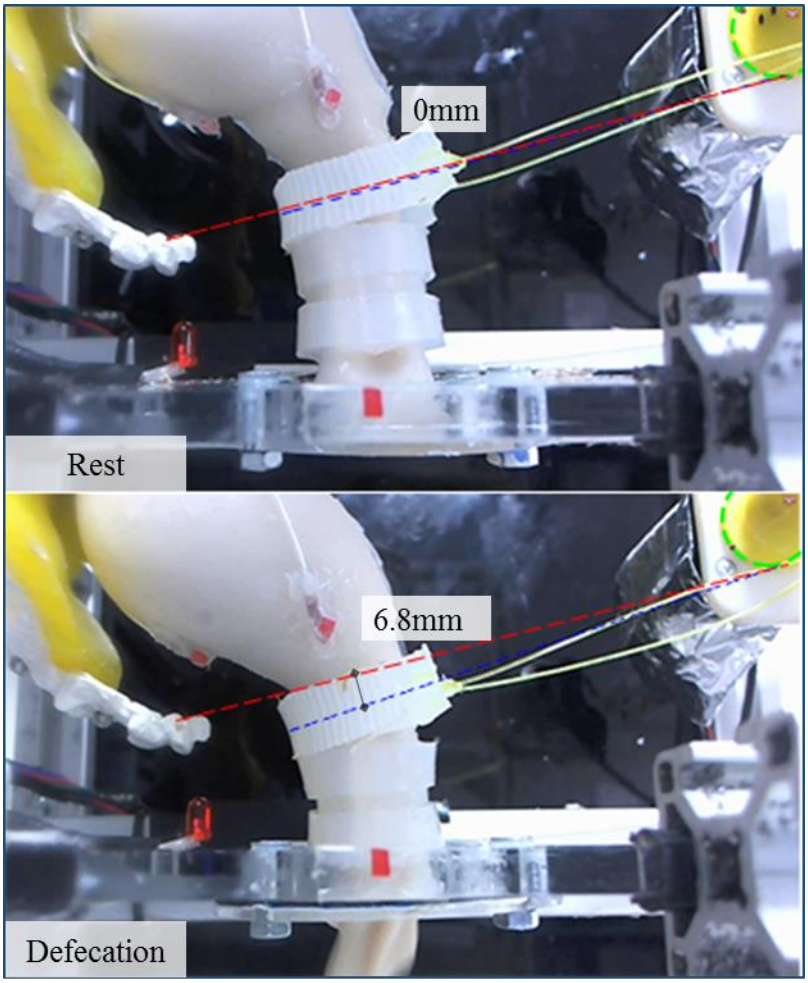

Figure 4.14 Comparison of the physical simulation in two states; rest and defecation/pelvic floor descent. Dashed lines denote the coccyx (green), pubococcygeus line (red) and anteroposterior dimension of the hiatus (blue).

In normal healthy subjects it is reported that the pelvic floor descends by 19mm between states of rest and defecation [178], in the physical simulation this was measured as 6.8mm. The pelvic floor descent in the simulation is less severe than observed in the human system, an explanation for this could be due to passive properties of the tissue phantoms. In the human system, the PR muscle relaxes in coordination with defecation, allowing the rectum to straighten and provide a passage of least resistance to the transit of faeces. In the physical simulation on the other hand, the PR muscle cannot relax, and continues to passively constrain the posterior rectum during an influx of stool to the rectum. However this is not an issue, since the simulation is used to evaluate the effect of the anteroposterior dimension of the hiatus on continence.

4.3.2. Simulating Defecation

A test scenario was implemented using the physical simulation to represent defecation, to characterise the relation between stool transit and IR pressure in the simulation. In addition, observation of rectal morphology during the test revealed the effect of stool influx (increasing IR pressure) on expansion and rotation of the rectum.

4.3.2.1. Mass Passed and IR Pressure Characteristics

For the study, a rectum was selected which was fabricated from Dragon Skin 20A, representing a compliance similar to the rectum in an 'active' state. The ARA was configured to 100°; characteristic of a healthy subject during defecation. During the test, 100 ml of stool simulant, formed using a 90.5 wt% moisture content solution of VEEGUM R and water, was introduced to the rectum at a rate of 9.26 ml/s, while the IR pressure change and mass leakage were observed, Figure 4.15.

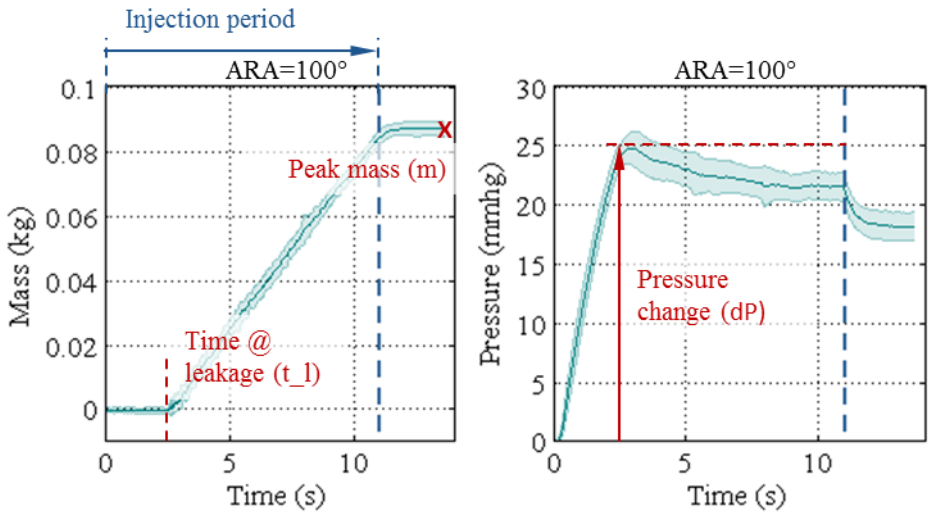

Figure 4.15 Variation of stool leakage and intra-rectal pressure with time during injection of stool into the simulation at a controlled rate, also indicating the definitions of metrics used for simulation characterisation: time @ leakage, peak mass and pressure change.

Metrics were calculated from the plots of mass leakage and IR pressure, versus time. These include the time at leakage, total mass passed and overall pressure change over the duration of the test, as demonstrated in Figure 4.15. Table 4.3 presents values for these metrics.

Table 4.3 Mean values ± 1SD (n=10) for stool injection tests, reporting peak mass, pressure change and time at leakage:

m (g)	dP (mmHg)	t_l (s)
86.6±2.2	25.1±1.3	2.79±0.27

As stool simulant is introduced to the rectum, the volume increases as the elastic potential of the rectum walls increases. When contraction of the rectum leads to IR pressures which are sufficient to overcome holdback pressures incurred by PR muscle forces, leakage from the anal canal occurs. As pressures reach an equilibrium, stool flows steadily from the anal canal. When the influx of stool into the rectum ceases, leakage continues at a reduced rate until the holdback pressure is sufficient to contain any remaining faeces in the rectum. The pressure change during this test was 25.1 mmHg, and this is in line with the change in rectal pressure between rest and defecation reported in literature (41.3 mmHg [18, 175]).

4.3.2.2. Rectum Morphology

A number of snapshots were taken using the webcam between initiation of stool injection, and the onset of stool leakage, at intervals of 1s. Outline traces of the rectum were then constructed for each image using Photoshop™ (CC, 2017) by maximising the image contrast then applying a *stroke*, the same construction method was applied for each image for consistency. Each trace was then overlaid on the initial image (t=0s) to display the morphology of the rectum in the sagittal plane throughout the test, Figure 4.16.

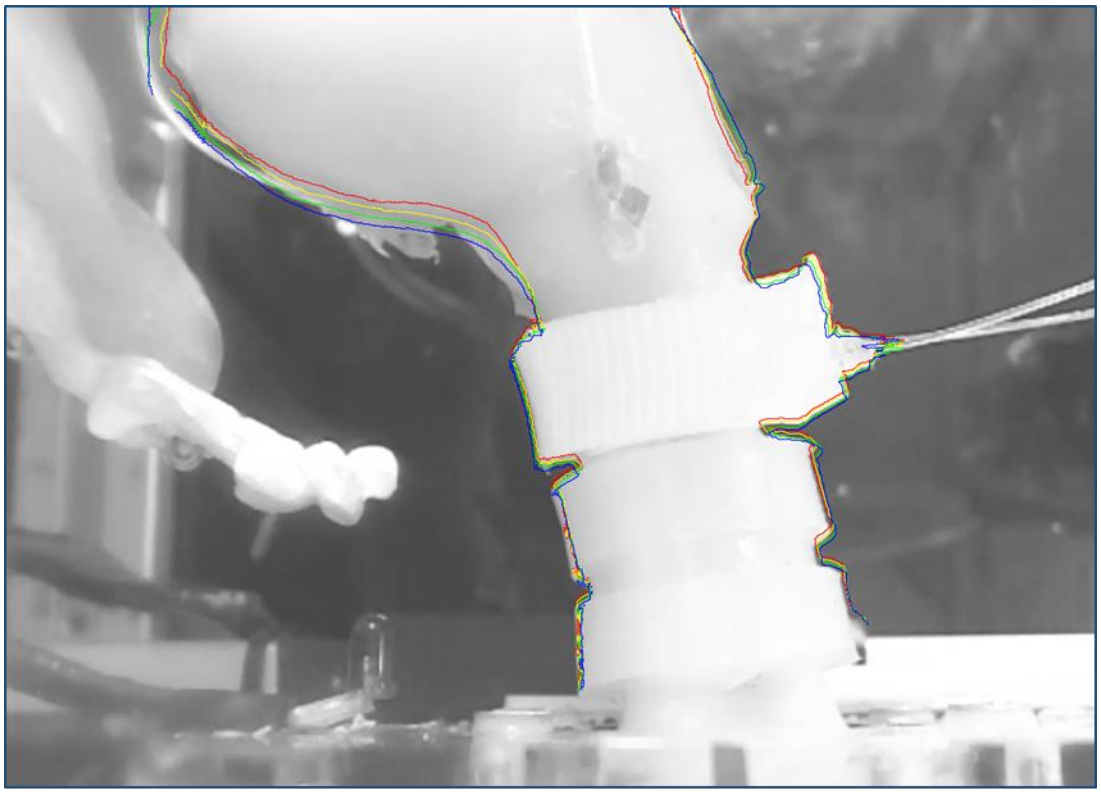

Figure 4.16 Traces of the rectum at various time increments since the onset of stool injection, with an ARA = 100°.

During the distension of the rectum, its morphology shows similarities when compared to the MR Proctographic scans in Figure 4.13. As stool is injected, expansion is visible and most pronounced in the posterior rectum, while the PR muscle descends to allow straightening of the anorectum. Movement of the proximal rectum to the posterior, coupled with the anorectum remaining close to stationary, shows that the rectum rotates slightly but visibly as stool is injected, this phenomenon has been observed in the human system and is described by the double-flap-valve mechanism [15]. This mechanism is a natural occurrence to resist leakage in which

the ARA becomes more acute upon rectum filling while forming a flap across the anal canal to block the passage of faeces.

4.4. Summary

Rheological properties of various-moisture-content smectite clay (VEEGUM R) suspensions were compared to fresh human faeces. A 91% moisture content suspension had a consistency of 42.2, which is comparable to the consistency of high moisture content faeces, reported as 39.33 [142]. Using this consistency with the simulation would represent a 'worst case' with regards to maintaining continence. Due to operational limitations of the rheometer used for rheology, thicker consistency suspensions could not be tested. However construction of an interpolated power law meant the dynamic viscosity of suspensions which weren't analysed, could be approximated, allowing use of thicker stool of known consistency to be used with the simulation. Furthermore, formulation of heterogeneous stool by addition of a fibre-reinforcement can form stools with a thicker consistency, to represent different types of stool identified on the Bristol stool form scale [148].

A stool injection test was conducted to construct a pressure-distension profile of the rectum, to provide an insight into the IR pressure experienced by the simulation for different rectal volumes. From this, the pressures generated at rectal volumes which were usually associated with a sense of urge were identified. In the human system, the rectum distends to 167 ml before urgency is experienced, corresponding to a change in IR pressure of 41.3 mmHg [18, 175], compared with pressures at rest. In the physical simulation, IR pressure increased by 41.3 mmHg with the injection of 86.6 ml of stool simulant. While this is lower than the volumes observed from clinical data, inclusion of a more compliant rectum with the simulation and adjustments to PR force and sphincter occlusion will allow the effect of greater rectal volumes to be investigated.

Data on the distensibility of the anal canal with and without the addition of a FENIX/FENIX Plus device was successfully obtained using an EndoFLIP device. Consequently, the DI for the anal canal was calculated as 4.74 for baseline values, and 2.72 with the FENIX Plus device. Previous assessments using the EndoFLIP reported values at rest of 3.9 for FI patients and 1.5 for healthy patients [145]. The values measured in the physical simulation were in line with those observed in the human

system. Despite values being more pronounced in the biological system, the baseline DI of the simulation was similar to FI patients. Addition of the FENIX Plus device increased the DI although it did not achieve the DIs observed in healthy subjects, suggesting that there would be some faecal leakage in patients using the device when experiencing normal IR pressures associate with urgency.

The functionality of the PR component of the pelvic floor was assessed, by demonstration it could achieve a full range of motion as defined in the technical requirements in Chapter 3. Indicating ARAs were configurable between 75° and 110°, encompassing the values associated with healthy subjects during rest (104.5°) and during squeeze (84.5°) [9].

The simulation as a whole was also compared to the biological system. Images taken in the sagittal plane of the physical simulation, assuming configurations to represent various biological states of 'rest', 'squeeze' and 'defecation', were compared to corresponding MR proctographic images. The physical simulation showed similarities to the human system regarding the ARAs observed during these states, while pelvic floor descended with the onset of defecation in both systems. Between states of 'rest' and 'defecation', the movement of the PR muscle was measured at 6.8mm in the physical simulation, while radio-proctographic studies have measured pelvic floor descents of 19mm in healthy subjects [178]. Pelvic floor descent is more pronounced in the human system than in the physical simulation, probably due to the passive properties of the simulation phantoms used to simulate active components of the biological system. Consequently the PR muscle cannot relax, and continues to passively constrain the posterior rectum, preventing it from straightening and producing downward movement of the sphincter complex and PR muscle.

A scenario was conducted using the physical simulation to recreate biological defecation. During the study, values of faecal leakage and IR pressure were recorded. These were used to calculate metrics, including total faecal leakage and IR pressure change during the tests. The change in IR pressure during the test was calculated as 25.1 mmHg, whereas during manometry studies in literature, values for IR pressure have been observed as 41.3 mmHg [18, 175]. Although the IR pressure change reported in literature is greater, these values were comparable. Outline traces of the rectum were constructed on selected images of the rectum, taken over the duration of stool injection, to observe rectal morphology throughout the distension. These

revealed that expansion is most pronounced towards the posterior rectal wall. It also showed that the anorectum remains relatively stationary while the proximal rectum appeared to move anteriorly, this could be described by phenomenon observed in the human system of a double-flap valve to prevent the passing of faeces [15].

The sections in this chapter have demonstrated that aspects of the physical simulation respond in a similar manner to the human system when subject to parameters representing biological scenarios. It has been demonstrated that the simulation components possess similar material properties to their biological counterparts. Furthermore, tests have shown that the forces and pressures used to augment the tissue phantoms, by magnitudes observed in the biological system, were in line with published values in literature based on human studies. In addition to the assessment of its components, the simulation as a whole has demonstrated its ability to be configurable, for the representation of a variety of relevant biological states. And a study to recreate a typical biological scenario reveals the ability of the simulation to acquire data on the response of important system variables while running pre-selected input parameters.

Chapter 5: Experimental Investigation into the Effects of Anorectal Angle and Sphincter Occlusion on Continence

This chapter presents an exploratory investigation using the physical simulation developed and validated in the previous chapters. A protocol using the physical simulation aims to first investigate the effects of rectal compliance and changing ARA on continence and second explores the clinical relevance of the work by evaluating the influence of two models of a passive-assistive artificial anal sphincter (FENIX and FENIX Plus). This work provides the fundamental testing of the simulation for grounds on which its capabilities and relevance were explored.

5.1. Introduction

The paucity of commercially available, clinically viable systems to treat FI reflects the difficulty of designing medical technologies to meet the multifaceted challenges surrounding this complex condition. A key failure mode in many attempts at new technology has been when device–tissue interaction causes tissue erosion, resulting in device migration or rejection [28, 29]. Alternative strategies to sphincter augmentation have also been explored. A comprehensive review on the importance of continence mechanisms was presented in Chapter 2. Notable in *vitro* studies have shown that increasing ARA reduces the occlusion pressure required to hold back solids and semi-solids [106, 115]. Similarly, another study reported increased retention of semisolid material when decreasing ARA in an ex vivo porcine rectum, but no effect for water [79]. The question of whether the ARA or sphincter occlusion pressure is a greater contributor to continence remains unanswered, despite previous comparative studies [79, 131]. However, it is evident that modulating the ARA is a key feature in maintaining continence, and that this provides a complementary strategy to sphincter augmentation.

It is clearly of clinical relevance to investigate mechanisms around ARA modulation which future FI technologies could exploit. The constituent models of the physical simulation of the human defecatory system were described together with the combined computational measurement and control in Chapter 3. Using the physical simulation, an in-depth investigation on the biomechanics of the associated physiological continence mechanisms and the effect of rectal disorders was carried

out. An experimental method was conceived to answer the research questions defined at the beginning of this project, outlined below.

"What is the influence of:

1. Sphincter occlusion
2. Anorectal angulation
3. Rectal compliance
4. Commercially available FI device

…on the faecal system and continence?"

These questions are answered through the application of an experimental matrix to observe the influence of the variables on continence, and the identification of correlations between them and important system parameters. The experimental method produced elevated rectal pressures in the model to investigate the individual and combined effects of ARA and sphincter occlusion on the system for a range of rectal compliances. Observation of the mass of stool leakage from the system together with the pressures generated in the rectum model allow quantification of the influence of continence mechanisms, and comparison with clinical and published data.

5.2. Experimental Methods

An experimental investigation was carried out to observe the effects of simulation variables, including the ARA, rectum compliance and sphincter augmentation (using a FENIX^{TM} and FENIX Plus^{TM} device), on continence using the physical simulation.

5.2.1. Controlled Variables and Measured Outputs

An experimental matrix was defined in which the controlled experimental variables were ARA (80°, 90° and 100°), rectum compliance (using materials: DragonSkin 10A, 20A and 30A) and sphincter state (baseline, with FENIX/FENIX Plus fitted). In turn, each variable was incrementally changed while the others remained fixed to produce a comprehensive array of different configurations to be tested, displayed in Table 5.1.

Table 5.1 Experimental matrix employed during the experimental investigation; indicating baseline ("b"), FENIX ("F") and FENIX Plus ("F+") sphincter occlusion configurations, tested for various anorectal angle and rectal compliance arrangements:

		Rectal compliance (Shore A grade)		
		10	20	30
Anorectal Angle (°)	100	b, F, F+	b, F, F+	b, F, F+
	90	b	b	b
	80	b, F, F+	b, F, F+	b, F, F+

A series of tests were then conducted during which a fixed volume of stool (100 ml) was injected into the proximal rectum at a uniform controlled rate (9.26 ml^{-1}). During each test permutation, one of the variables was changed systematically to evaluate its effect on the system, averaged across 10 repeats. The FI devices were only fitted for the extremes of the ARA values tested (80° and 100°), to simplify the test matrix and observe their combined effect with ARA.

5.2.2. System Configuration

Prior to any laboratory testing using the simulation, steps were taken to configure the system to ensure consistent test conditions across tests carried out on different days.

Instrumentation and control systems were integrated into the model to quantitatively measure key aspects of the model and to provide repeatable automation of the defecation process, as discussed in Chapter 3 (shown schematically in Figure 3.34). A central PC was used to coordinate the measurement and control components using a commercially available data interface (NI USB-6212; National Instruments Ltd., Austin, Texas, USA) in conjunction with a custom control program on the LabVIEW platform (National Instruments).

5.2.2.1. Control Program

Throughout the tests, a custom control program on the LabVIEW platform (National Instruments) is used to define the operating configuration of the defecation model to initiate experiments and to record subsequent data streams with reference to a hardware-timed clock, Figure 5.1.

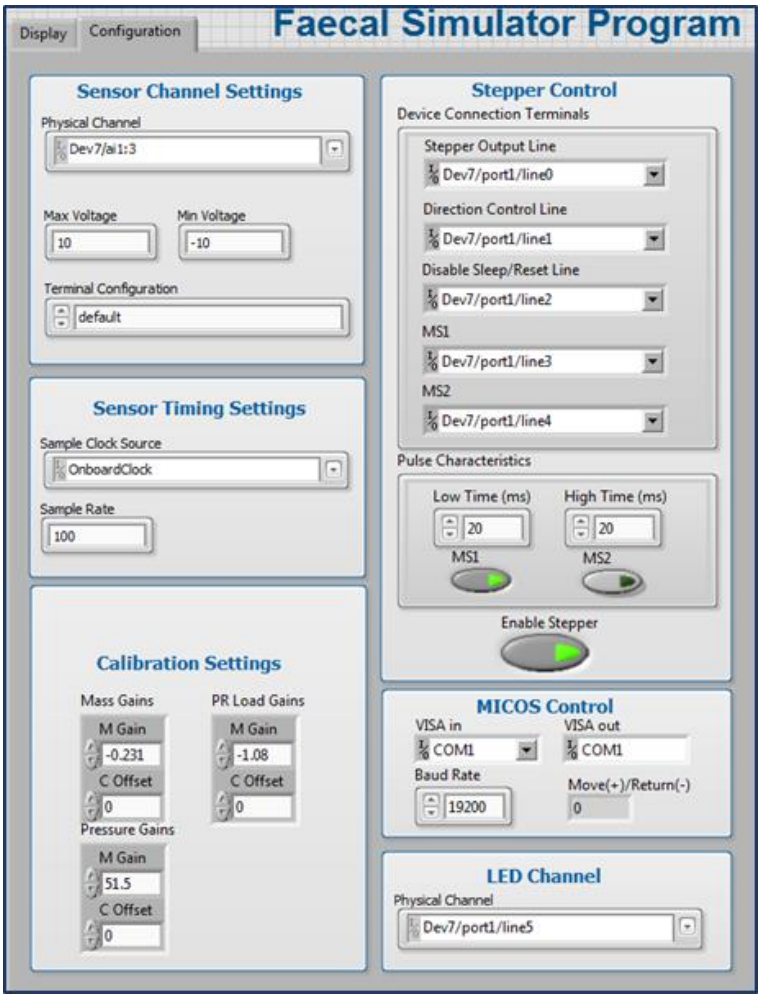

Figure 5.1 '*Configuration*' tab of the custom control program used to configure hardware of the physical simulation in preparation for testing.

The program is configured by inputting stool mass, PR load and IR pressure load cell calibration gains (defined during calibration in Chapter 3). The connected USB NI DAQ device is selected along with sensor input channels (stool mass load cell, PR load cell and IR pressure transducer) and hardware output channels (linear stage, stepper motor and LED). The stepper motor step increment could also be configured; during stool injection tests it was set to half-steps, with each increment producing a displacement of 0.9°.

The program measured and recorded IR pressure, PR force and stool mass leakage and a Boolean signal at 100Hz. The Boolean signal indicated operation of the linear stage (and hence stool injection), which facilitated the identification of data recorded during stool delivery to the system.

Video-stream data was acquired from the webcam at 30Hz using the corresponding manufacturer's software (Logitech Webcam Software), and this was saved with a time-stamp so video data could be matched to corresponding simulation data in post analysis. An LED was visible in the frame, which illuminated while the linear stage Boolean indicator was written to the data stream. Allowing synchronisation between video and measured variables.

5.2.2.2. Rectum

The compliance of rectum phantoms was regulated through the use of various pre-fabricated phantoms. Each phantom had identical geometries, and were fabricated using three different grades of silicone (Dragon Skin 10A, 20A and 30A). Prior to each test, a rectum with the desired compliance was loaded in the simulation and a balloon catheter (2309; Mediplus, High Wycombe, UK) was fed through the catheter port before being secured with a cable tie. Using a syringe, the balloon catheter was instilled with 5 ml water ensuring any air bubbles are displaced. The rectum was then primed with stool simulant. A rigid external housing with the same geometry as the rectum was placed around it, and stool injected until leakage from the anal canal occurred and all air was displaced, finally the housing was carefully removed. This was performed before each test to ensure a consistent initial rectal volume.

5.2.2.3. Stool Simulant

Stool simulant was prepared using the same technique as during rheology tests, presented in Chapter 4. Throughout this investigation the clay formulation was

selected at 90.5% water content, producing an apparent viscosity of 47.065 Pa.s; similar to high moisture-content semisolid faecal samples [142]. Stool leakage from the anal canal is collected in a tray mounted to a second load cell (RLS005kg; RDP). The tray was emptied before each test to ensure there was no risk of overflow.

5.2.2.4. Anorectal Angle

The different ARA permutations tested are shown in Figure 5.2.

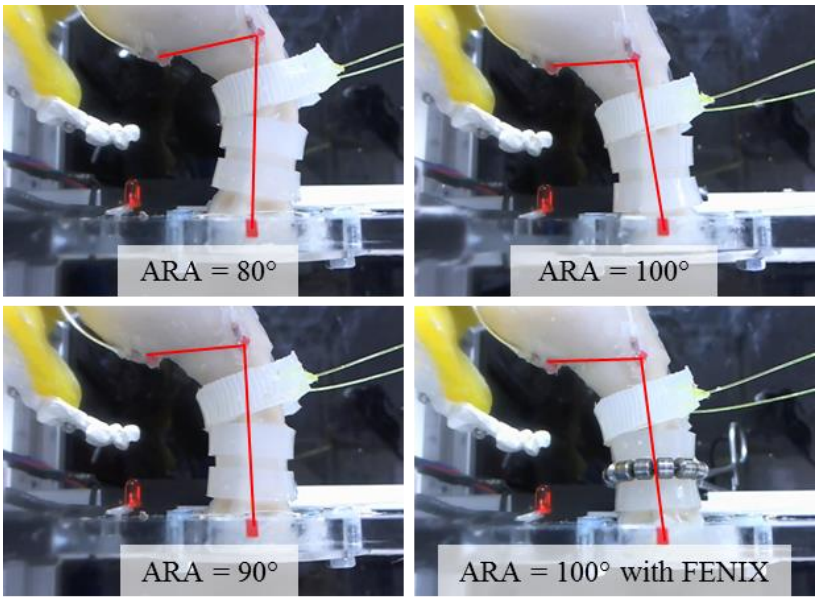

Figure 5.2 Webcam view of the model rectum for the range of ARA values used during the experimental investigation, and demonstration of the FENIX device fitted around the anal canal.

The desired ARA was configured by positioning the PR model, by manual adjustment through the control program and stepper motor and spool assembly. Analysis was then performed on the webcam (C920 HD Pro; Logitech, Lausanne, Switzerland) image of the rectum using ImageJ™ (National Institutes of Health) to measure the augmented ARA, determined by joining the visual markers as demonstrated in Figure 5.2. This process was iterated until an ARA was obtained within a tolerance of 0.5° to the desired value. Subsequent repeats at this ARA used the same PR configuration to help ensure consistency.

5.2.2.5. FI Device

The FENIX and FENIX Plus were fitted and configured as specified in the clinical guidance provided with the devices. A supplied sizing tool was used to measure the sphincter circumference and thus determine the appropriate length of the device. It

was then applied around the recess in the sphincter complex, shown in Figure 5.2. The same length was used for both devices.

5.2.3. Test Protocol

All experiments were performed at room temperature (20°C). During tests, 100ml of stool simulate was delivered to the proximal rectum at a constant flow of 9.26 ml/s, a typical flow rate for stool being passed during defecation [143], via the control program introduced in Chapter 3 (Section 3.3.3.). The protocol below was adhered to for each experiment, also demonstrated schematically in Figure 5.3.

1. *Assemble simulation components*
    a. Mount a rectum phantom with the desired material compliance into the simulation, securing it using custom fittings
    b. Feed a balloon catheter through the rectum catheter port and secure it in place with a cable tie, then instil 5ml of water to the catheter and ensure all air bubbles are removed
    c. Mix stool simulant with the specified water content and homogenise
    d. Lubricate soft-on-soft surfaces with mineral oil
2. *Initialise system*
    a. Ensure PR is fully relaxed and set PR force to zero
    b. Initiate data/webcam recording
    c. Prime the rectum: encase the rectum with a rigid external housing (with the geometry of the non-distended rectum) and inject stool simulant until leakage from the anal canal occurs and all air pockets are displaced, remove the housing
3. *Configure ARA position and sphincter*
    a. Adjust the PR position using the control program until the desired ARA is achieved. Set-up the sphincter configuration by fitting a FENIX or FENIX Plus device if required and lubricate with mineral oil
4. *Configure variables*
    a. Reset IR pressure and faecal mass passed to zero
5. *Run test*
    a. Inject a metered volume of stool simulate into the rectum at a pre-defined flow rate
6. *Save data & end test*

a. Wait until steady state (stool mass leakage) is achieved then relax the PR, stop data/webcam recording and save acquired data

For each test permutation within the variable matrix, a single test is conducted with the rigid housing secured around the rectum, essentially simulating an entirely non-compliant rectum. This data point is included on plots during analysis.

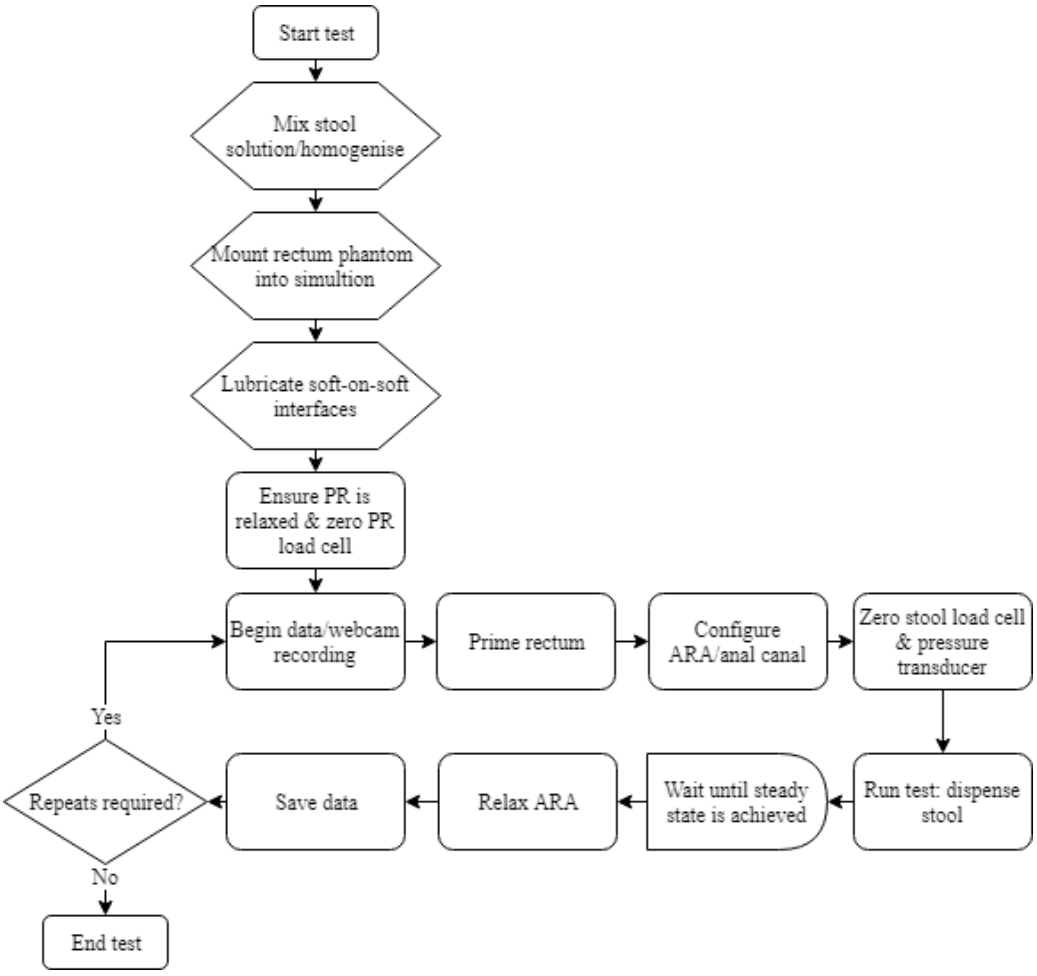

Figure 5.3 Hardware flowchart demonstrating the stool injection test protocol employed during the experimental investigation.

Measured outputs from each test include:

- Stool mass passed
- PR muscle force
- IR pressure

Following stool injection, these outputs are saved by the control program. Ten test repeats are carried out for each test permutation.

5.2.4. Data Analysis and Post-Processing

During tests, data files were acquired by the control program containing arrays for PR force, IR pressure, mass leakage, time and Boolean indication of linear stage operation. Arrays of PR force, IR pressure and mass leakage were plotted versus time from which metrics were calculated of the total mass passed, IR pressure change and time at faecal leakage. Metrics were presented to observe the effect of sphincter configuration, on separate plots for each test permutation (same ARA configuration and rectal compliance). The data files were saved with a timestamp so they could be matched to webcam footage recorded during the tests. If any unusual values appeared while plotting the measured outputs, webcam footage was reviewed to help find a cause for the discrepancy. An example of the unprocessed mass response data for one particular test permutation is demonstrated in Figure 5.4.

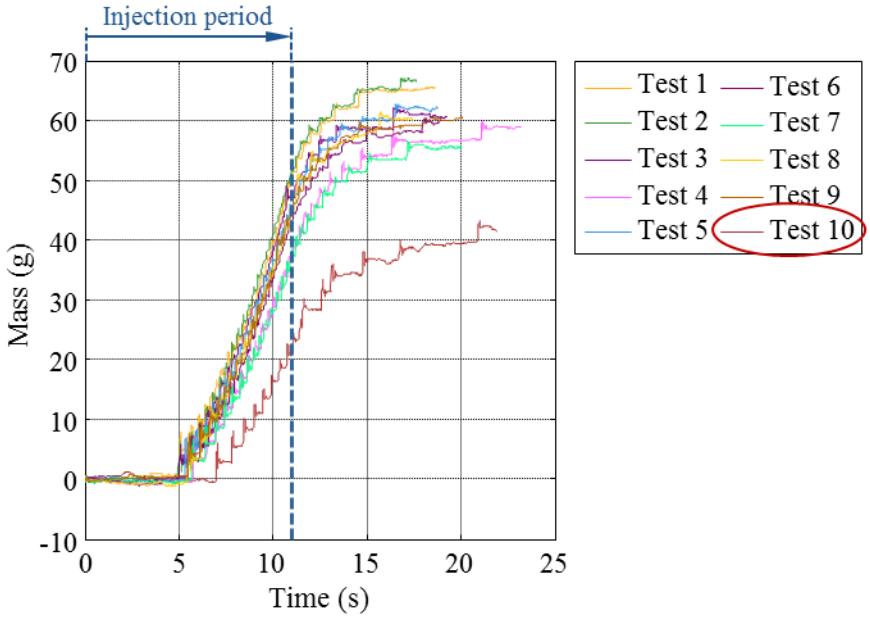

Figure 5.4 Unprocessed mass responses observed for repeats over a single test permutation, demonstrating the identification of anomalous data.

From observation of the unprocessed mass responses, it appears that test 10 is outside the normal range of values observed for this particular configuration. Reviewing webcam footage of this test revealed an air pocket which was trapped in the rectum and expelled during stool injection, resulting in a reduction in stool leakage for this test repeat. Consequently, data from this test was excluding from post-processing. This analysis was repeated for every variable measured during each test permutation.

With anomalies removed, algorithms were implemented in Matlab (Mathworks) to import the remaining data files, extract value arrays and create plots of each variable versus time, included in the Appendix (IV). A 10-point moving average is applied to the raw data arrays using the *smooth* function in Matlab to remove excessive noise. The mean and standard deviation (STD) from the ten repeats (minus anomalies) is then computed and plotted against time. Figure 5.5 shows typical data obtained from the system of faecal mass passed and IR pressure during simulated defecation, in this case without the presence of sphincter augmentation. Plots for the full experimental dataset is provided in the Appendix (III).

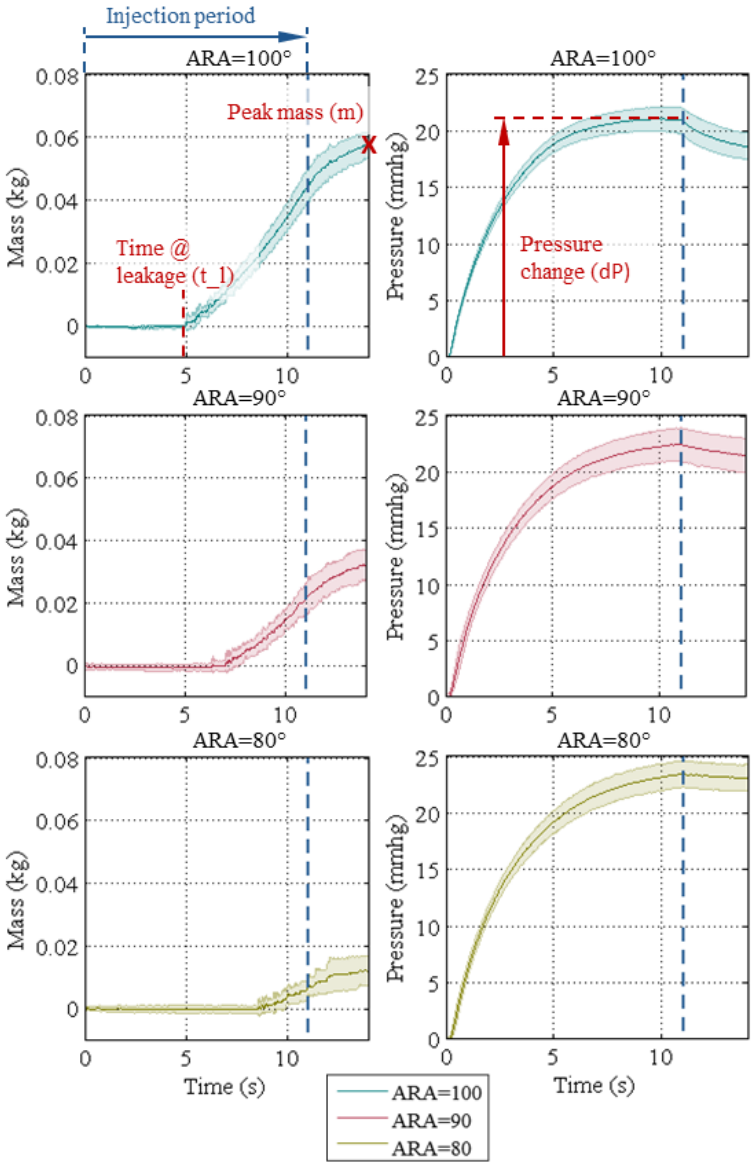

Figure 5.5 *Left*; Faecal mass passed and *Right*; IR pressure versus time for different ARA configurations. Each plot shows mean (N=10) in solid with 1 STD as shaded region.

The plots show the mean in solid with shaded error regions, which indicate values that fall within ± 1STD from the mean at any given time. From the variable responses, metrics of peak mass (m), pressure change (dP) and time at leakage (t_l) were calculated, as demonstrated in Figure 5.5. A definitive set of the calculated metrics is documented in Table 4.3, with significance between sphincter configurations denoted in Table 5.3.

5.3. Results

The metrics shown in Figure 5.6 reveal how the effects of rectal compliance and sphincter augmentation (through the FENIX device) couple with changing ARA. Table 5.2 summarises these metrics, with significance values between sphincter configurations indicated in Table 5.3.

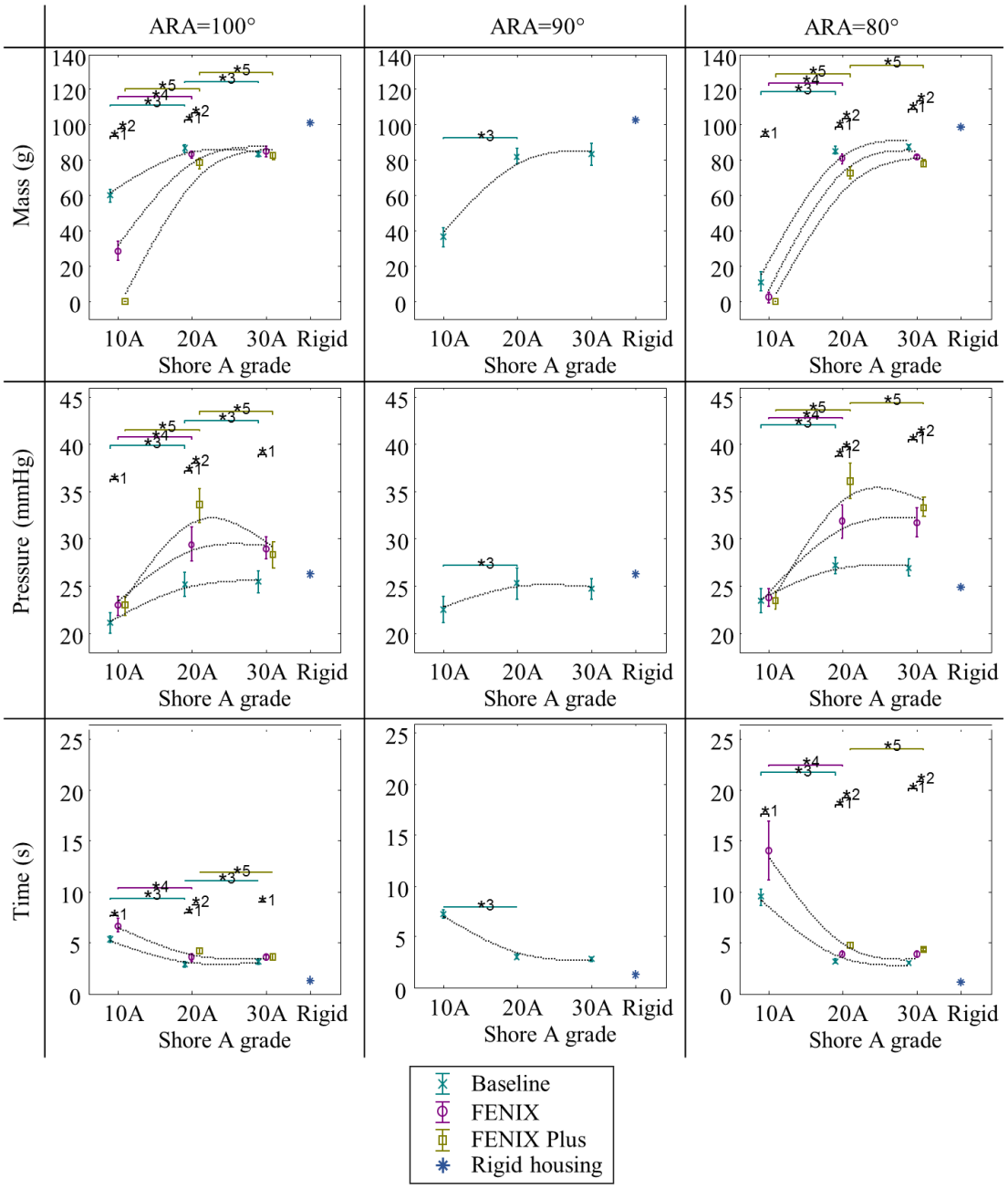

Figure 5.6 Effects of rectal compliance on faecal mass passed (top), IR pressure change (*middle*) and leakage time (*bottom*). Each plot shows mean (N=10) with 1STD error bars. Statistical significance ($p<0.05$) is shown between baseline/FENIX configurations of sphincter state (*1), FENIX/FENIX Plus configurations of sphincter state (*2), compliance with no device fitted (*3), compliance with the FENIX (*4) and compliance with the FENIX Plus (*5).

Table 5.2 Mean vales ± 1SE (n=10) for stool injection test metrics reporting peak mass, pressure change and time at leakage for ARAs of 80°, 90° and 100°:

ARA	Compliance	Sphincter configuration	m (g)	dP (mmHg)	t_l (s)
100°	10A	Baseline	59.7±3.6	21.0±1.1	5.25±0.29
		FENIX	28.5±5.6	22.9±1.0	6.67±0.70
		FENIX Plus	N/A	22.9±1.0	N/A
	20A	Baseline	86.6±2.2	25.1±1.3	2.79±0.27
		FENIX	83.2±2.2	29.4±1.8	3.50±0.36
		FENIX Plus	78.1±3.1	33.5±1.8	4.14±0.27
	30A	Baseline	83.4±2.0	25.4±1.2	3.14±0.24
		FENIX	84.7±2.6	28.9±1.2	3.53±0.22
		FENIX Plus	82.4±2.1	28.3±1.4	3.55±0.24
	Rigid	Baseline	100.8	26.2	1.24
90°	10A	Baseline	36.3±5.4	22.5±1.4	7.19±0.46
	20A		82.1±4.4	25.2±1.6	3.04±0.23
	30A		83.2±6.3	24.7±1.1	2.83±0.22
	Rigid		102.4	26.2	1.23
80°	10A **(n=9)**	Baseline	10.9±5.2	23.4±1.2	9.49±0.79
		FENIX	1.8±2.9	23.7±1.0	13.96±2.9 **(n=8)**
		FENIX Plus	N/A	23.4±1.0	N/A
	20A	Baseline	85.5±2.0	27.1±0.9	3.17±0.23
		FENIX	80.6±2.8	31.8±1.8	3.91±0.20
		FENIX Plus	72.3±3.4	36.1±1.9	4.76±0.31
	30A	Baseline	87.4±1.3	26.9±0.8	3.05±0.09
		FENIX	81.5±1.4	31.7±1.6	3.87±0.26
		FENIX Plus	77.9±1.9	33.3±1.0	4.24±0.16
	Rigid	Baseline	98.8	24.8	1.15

Table 5.3 Significance values, for metrics from stool injection tests between sphincter configurations (in columns I and J):

ARA	Compliance	I	J	m (g)	dP (mmHg)	t_l (s)
100°	10A	Baseline	FENIX	$p < 0.01$	$p < 0.01$	$p < 0.01$
			FENIX Plus	$p < 0.01$	$p < 0.01$	NA
		FENIX		$p < 0.01$	$p > 0.05$	NA
	20A	Baseline	FENIX	$p < 0.05$	$p < 0.01$	$p < 0.01$
			FENIX Plus	$p < 0.01$	$p < 0.01$	$p < 0.01$
		FENIX		$p < 0.01$	$p < 0.01$	$p < 0.01$
	30A	Baseline	FENIX	$p > 0.05$	$p < 0.01$	$p < 0.01$
			FENIX Plus	$p > 0.05$	$p < 0.01$	$p < 0.01$
		FENIX		$p > 0.05$	$p > 0.05$	$p < 0.01$
80°	10A **(n=9)**	Baseline	FENIX	$p < 0.01$	$p > 0.05$	$p < 0.01$
			FENIX Plus	$p < 0.01$	$p > 0.05$	NA
		FENIX		$p > 0.05$	$p > 0.05$	NA
	20A	Baseline	FENIX	$p < 0.01$	$p < 0.01$	$p < 0.01$
			FENIX Plus	$p < 0.01$	$p < 0.01$	$p < 0.01$
		FENIX		$p < 0.01$	$p < 0.01$	$p < 0.01$
	30A	Baseline	FENIX	$p < 0.01$	$p < 0.01$	$p < 0.01$
			FENIX Plus	$p < 0.01$	$p < 0.01$	$p < 0.01$
		FENIX		$p < 0.01$	$p < 0.05$	$p > 0.05$

Graphs of total mass passed, IR pressure change and time at faecal leakage are plotted for each ARA tested, presenting the mean ± 1STD (an exhaustive list of which is also given in Table 4.3). Rectal compliance form categories along the y-axis, while data on sphincter configurations are plotted in each single column (with an offset for clarity). Trend-lines are constucted using the *smoothingspline* function in Matlab, using a *smoothingparameter (p)* of 0.02. This constructs a spline across variable means between rectal compliances (for each sphincter configuration) using a mathematical function based on the value *p*; defined between 0 and 1, $p = 0$ produces a least-squares straight-line fit to the data while $p = 1$ produces a cubic spline interpolant. Statistical significance ($p<0.05$) is indicated between sphincter state (coloured bars) and rectal compliance (black bars). Numbered asterisk make distinguishing the error bars easier. An exhaustive and more detailed overview of statistical significance between sphincter states is given in Table 5.3. Finally, each plot includes a data point collected with a rigid housing secured around the rectum, without sphincter occlusion.

5.3.1. Mass Passed

Effect of sphincter occlusion on faecal leakage is most pronounced and significant ($p<0.05$) when the rectum has high compliance (10A) and the ARA is obtuse. As shown by a reduction of total faecal mass passed from 59.7 g with a baseline sphincter configuration to 28.5 g with the FENIX, with good statistical significance ($p<0.001$), and a further reduction to no mass being passed is observed with the FENIX Plus. Effect of sphincter occlusion on faecal leakage is least pronounced and insignificant ($p>0.05$) for a low compliance (30A) rectum and when the ARA is accute. Sphincter occlusion has a significant effect on faecal leakage with obtuse ARAs for the range of compliancies tested, and also for obtuse ARAs between compliances of 10A and 20A although it is insignificant with the lowest rectal compliance. While the rectal compliance as a large and across all ARAs, significant, effect on faecal leakage between 10A and 20A, its effect is much reduced between 20A and 30A, where significance is only denoted between baseline and FENIX Plus sphincter configurations for obtuse ARAs and FENIX Plus configurations for acute ARAs.

There is a visible correlation between ARA and faecal mass passed for high compliance rectums, shown by a reduction in faecal mass passed from 59.7 g at 100°

down to 36.3 g at 90° and 10.9 g at 80°. However there is no correlation between ARA and faecal leakage with low rectal compliance.

Use of a rigid housing (non-compliant rectum) produces the greatest mass leakage across all plots. With a rectal compliance of 30A and an obtuse ARA, the faecal leakage was recorded as 83.4 g, compared to 89.9 g with the non-compliant recctum.

In general, increasing sphincter occlusion, enhancing the ARA and increasing rectal compliance reduce mass of stool leakage from the rectum.

5.3.2. Intra-Rectal Pressure

Effect of sphincter occlusion on IR pressure change is least pronounced and least significant for high rectal compliances (10A) and acute ARA's, with no significant difference ($p>0.05$) observed between IR pressures recorded for the various sphincter states. Effect of the FENIX compared with baseline sphincter occlusion on IR pressure change is small but significant for high rectal compliance (10A) and obtuse ARA's. Effect of the FENIX compared with baseline sphincter occlusion on IR pressure change is most pronounced and significant for lower rectal compliances (20A & 30A). Similarly effects of the FENIX Plus compared with occlusion from the FENIX were most pronounced with lower rectal compliances, although it is less prominent with the lowest rectal compliance compared with mid-rectal compliance for both ARA's, and even insignificant ($p>0.05$) with the lowest rectal compliance and an obtuse ARA. Effect of sphincter occlusion is most notable between rectal compliances of 10A and 20A when comparing trends with the FENIX Plus device fitted, with similar notable differences seen for both ARAs tested using the device, this effect is less pronounced with the FENIX fitted and only a small variation between these compliances is seen with no device fitted.

There is a small but noticable correlation between ARA and IR pressure change for high rectal compliances, evident from an increase from 21.0 mmHg at 100°, to 22.5 mmHg at 90° and 23.4 mmHg at 80°. There is no trend apparent for ARA and IR pressure change for low rectal compliance, with each compliance producing roughly the same pressure difference for each test.

Without sphincter occlusion, a non-compliant rectum produces an IR pressure change of 26.2 mmHg which is similar to the value recorded for the lowest rectal compliance (30A) tested (25.4 mmHg). However the IR pressures are greater than the IR pressure

change produced with a non-compliant rectum with an acute ARA, for all sphincter states.

In general increasing sphincter occlusion, enhancing the ARA and increasing rectal compliance increase IR pressure changes genreated in the rectum.

5.3.3. Time at Faecal Leakage

The effect of sphincter occlusion on time at faecal leakage is most pronounced and significant for high rectal compliance (10A) and acute ARA's. The effect of the FENIX compared with baseline sphincter configuration on time at faecal leakage is less pronounced for a rectal compliance of 20A compare with 10A, but still highly significant ($p<0.001$) for both ARA's. Effect of the FENIX compared with baseline sphincter configuration on time at faecal leakage is significant for all rectal compliancies tested for both ARAs (80° and 100°). The effect of sphincter occlusion on time at faecal leakage is least pronounced and least significant for low rectal compliances (30A), particularly for obtuse ARA's. The FENIX Plus is particularly effective on time at faecal leakage for high rectal compliance, since the trend tends to infinity. While the FENIX Plus is still effective at increasing time until leakage for lower compliance rectums its effect is less pronounced, with no significance apparent between FENIX Plus and FENIX sphincter states with a low compliance rectum and obtuse ARAs. The trends between rectal compliance and time at faecal leakage with all ARAs and sphincter states show a steep reduction in time to leakage between high to mid rectal compliancies (10A to 20A), but little to no trend between mid to low rectal compliancies. Particularly evident when using the FENIX with an acute ARA, showing reduction in time from 13.96 s for a rectal compliance of 10A to 3.91 s with a compliance of 20A, with high significance ($p<0.001$), however no reduction is seen using a rectal compliance of 20A and 30A. With the FENIX fitted, an uncharacteristically large standard deviation is produced for time at faecal leakage measured for an acute ARA and high rectal compliance of 2.9 s.

Similar to the trends observed between sphincter occlusion and time at faecal leakage, enhancing the ARA has a noticable effect at increasing time to leakage for high rectal compliances. Evident in an increase from 5.25 s at an ARA of 100° to 7.19 s at 90° and 13.96 s at 80°. While there's still a positive trend between ARA and time for a mid-compliant rectum, it is far less pronounced and no correlation is apparent for low rectal compliance.

Time to faecal leakage is greatly reduced across all ARAs tested by use of a non-compliant rectum. For an obtuse ARA and no sphincter occlusion, a reduction is seen from 3.14 s with a low compliance rectum (30A), down to 1.24 s with the rigid housing fitted.

In general increasing sphincter occlusion, enhancing the ARA and increasing rectal compliance increases time until faecal matter is passed from the rectum.

5.4. Discussion

Upon reflection of the research questions asked in the introduction to this work, this experimental investigation has shed light on the influences of sphincter occlusion, anorectal angulation and rectal compliance on the faecal system and continence, together with a FI device. In general, increasing sphincter occlusion and enhancing the ARA have led to a reduction in stool mass passed, increase in IR pressure and increase in time until faecal leakage. With these observations becoming more pronounced using high rectal compliances.

In the simulation, augmentation of the sphincter complex using the FENIX and FENIX Plus devices exhibits a similar effect to making the ARA more acute. Additional pressure applied to the anal canal by the device causes a restriction to flow and thus greater retention of faecal matter in the rectum, with consequent increases in IR pressures. The FENIX was particularly effective compared to a baseline sphincter configuration when used with more compliant rectum models (10A), where a significant difference ($p<0.01$) was observed in peak masses passed from 0.0597 to 28.5 g and generated IR pressures of 21.0 and 22.9 mmHg respectively. Similarly the FENIX Plus was effective compared with the FENIX use with a high rectal compliance, as no leakage was measured for regardless of the ARA. However, the effect of sphincter occlusion diminishes as variations were observed for less compliant rectum models (20A, 30A) although effects were still significant ($p<0.05$). This demonstrates that while sphincter augmentation can be effective at reducing faecal leakage it does not have universal application.

The effects from the PR modulating the ARA is notable. Upon varying the ARA, a prominent difference in leakage was observed between an ARA of 80° and 100°, increasing from 10.9 to 59.7 g. This demonstrates that as the ARA becomes more acute, a greater amount of stool is contained within the rectum during a controlled

influx of stool. It would also appear that if a threshold ARA is exceeded, the amount of leakage is drastically reduced, whereas at more obtuse ARA values, small changes in angle have little effect on leakage. This signifies that more acute ARAs produce an elevation in the apparent hold back pressure, and that if this is sufficient in relation to induced IR pressures, faecal leakage will be reduced. Fluctuation of the mass flow rate is apparent for all ARA values tested, with the phase of the fluctuation appearing larger at more acute ARA values and lower flow rates. These were formed as the semisolid exits the system in fluid globules, characteristic of viscous fluids with low surface tension under shear.

The results obtained from this experimental investigation reveal the complex dynamics of the defecation process and the interplay between the mechanisms involved. A particular benefit of this model is the ability to control and time the processes used, revealing the temporal characteristics of defecation. Once simulated stool starts to be introduced into the system (t=0s) there is a notable time lag before leakage of feacal matter which tends to occur after approximately two seconds have passed. This delay is due to rectal filling whilst holdback pressures were great enough to overcome pressures produced by elastic energy stored in the rectal walls. Consequently this delay varies as a function of rectal compliance, with longer delays observed from more compliant rectum models (which overcome the holdback pressure more slowly as they fill with stool simulant). This has a clinical analogue in those patients with low rectal muscle tone (and so high compliance) who find it difficult to generate sufficient driving pressure to defecate. Interestingly, in tests carried out simulating a non-compliant rectum (with the rigid housing attached), the time at faecal leakage does not tend to zero. This is due to an incomplete fit around the rectum due obstruction from parts of the simulation, and a slight gap between the anal canal from which faecal matter is leaked, and tray in which it's collected.

To defecate effectively requires a less acute ARA (i.e. straightening the rectum-canal configuration) and achieving a reduction in occlusive pressure at the sphincter, as observed during proctographic studies [79]. These traits were reflected in this investigation, particularly evident in tests using a low compliance rectum (30A) to simulate rectal contraction, and an obtuse ARA (100°) for which case there is no statistical significance ($p>0.05$) for faecal mass passed at baseline (83.4 g), with FENIX (84.7 g) and with the FENIX Plus (82.4 g).

Squatting is an effective position for defecation since it straightens the recto-anal passage, in turn reducing the pressures generated by the rectum and abdominal muscles to overcome the holdback pressures required for evacuation. Studies have shown that the ARA is 126° when squatting [179], requiring a pressure increase of 38.2 mmHg to evacuate, whereas the ARA becomes more acute while sitting (100°) which requires a greater pressure change of 47.8 mmHg to evacuate. This correlation between ARA and pressure change is widely reflected among all rectal compliances tested in the simulation. Shown prominently with a high compliance rectum (10A) and baseline sphincter occlusion; with an ARA reflecting healthy subjects in a sitting position (100°) the pressure change was 25.4 mmHg, and with a more acute ARA (80°) the pressure change saw a significant rise to 26.9 mmHg.

This investigation demonstrates that to effectively reduce faecal leakage, both anorectal angulation and occlusion pressure at the sphincter should be enhanced. Furthermore, it shows that to retain semisolid material in the rectum, it is not necessary to completely occlude the sphincter. Angulation of the rectum alone provides sufficient resistance to reduce stool leakage. Mean biological ARA values for healthy, nulliparous patients were measured at 104.5±10.3° at rest and 84.5±14.2° during squeeze [9]. These values were in agreement with the ARA's observed for the reduction in leakage in this investigation. This highlights the potential to develop new technologies for FI which do not rely solely on occlusion of the anal canal to maintain continence but also include modulation of ARA. Too much of either mechanism would result in OD. A combined and modulated strategy would allow a reduction in occlusive pressures and thereby help to mitigate against the issues of soft tissue erosion and device migration that have previously plagued implantable technology for FI.

5.5. Conclusion

The stool injection investigation with the physical simulation has given an insight into the biomechanics of the human faecal system and the combined effects of the ARA and sphincter occlusion on continence. As stool simulant is fed into the rectum, the volume expands as elastic potential energy is stored in the rectal walls. When the contraction of the rectum leads to IR pressures which were sufficient to overcome holdback pressures incurred by PR muscle forces, leakage from the anal canal occurs. As pressures reach an equilibrium, stool flows steadily from the anal canal. When the

influx of stool into the rectum ceases, leakage continues at a reduced rate until the holdback pressure is sufficient to contain any remaining faeces in the rectum.

This analysis has shown that in the simulation, both augmenting sphincter function and decreasing the ARA lead to increased resistance to the passing of faecal matter, helping to maintain continence. The provides rationale that modulation of the ARA could help relieve symptoms of chronic leakage associated with more severe cases of FI, complementing occlusion of the anal canal by existing technology like the FENIX.

Chapter 6: Discussion, Conclusions and Future Work

The research presented in this thesis has shown the development, analysis and application of a physical simulation of the human defecatory system. The proposed simulation was designed for the investigation of the effects of ARA, sphincter occlusion and rectal compliance on IR pressure and faecal leakage, to inform the design of emerging technologies in the treatment of FI. Findings from the investigation identify correlations between the modelled continence mechanisms and degree of continence. This discussion considers key features of this research regarding the validity of the technique, how it compares to current simulations and how it may be applied to the development of clinically viable technologies. Reassessment of research objectives and identification of potential modifications concludes this chapter along with a proposal of future work.

6.1. General Discussion

It is clear that a physical simulation which accurately models biological continence mechanisms could have a significant impact on the development of existing and emerging technologies for the treatment of FI, achieved through an improved understanding of the associated biomechanics and the opportunity to analyse technology in the laboratory, prior to animal experiments.

The work presented in this thesis has made significant contributions to the field with the publication of two papers [180, 181]. Notable contributions include:

1. A method for fabricating repeatable/reusable anatomical tissue phantoms of the pelvic floor anatomy
2. Empirical data on the biomechanics of faecal incontinence
3. A test environment for the evaluation of existing/new technologies for the treatment of faecal incontinence

Knowledge Base: During the conception of the simulation, an extensive review of literature revealed a handful of computational studies which provided an understanding of certain biomechanics of the pelvic floor [124], although fundamental mechanisms of continence had not been addressed such as the ARA and sphincter occlusion. This was probably due to the complexities of necessary modelling parameters. Due to the inherent complexity and variability in biological environments, the efficacy of FI devices can only be shown empirically, regardless of whether the

concept appeared promising. Despite this, to the best of my knowledge, there were no other studies reported in literature on the use of physical simulations to understand mechanisms associated with continence, or for the testing of FI devices. In contrast with a computational model, use of a physical model allowed complex interactions to be replicated with relative modelling ease, and established a basis around which biomechanical properties and physiological refinements could be made. The simulation presented in this thesis met these goals, by using a wealth of data from literature to recreate fundamental tissue components of the human defecatory system. Together with the tissue phantoms, instrumentation and control algorithms were used to form a controllable and adaptable test platform which effectively assessed the influence of continence mechanisms on forces and pressures within the system.

Model Overview: The full biological continence mechanism is complex and consists of the coordinated function of the nervous systems, GI tract, and anal sphincter and pelvic floor musculature. The current simulation presented in this thesis has focussed on investigating the effects of varying ARA, sphincter pressure and rectal compliance. Accordingly the system was simplified to facilitate fabrication and detailed analysis of these functions. The rectum/anal canal, IAS, PR muscle and adipose fat components were simulated by cast, 1:1 scale silicone models. An anatomical rectum model forms the basis of the simulation, continuous with an approximated-dimension anal canal. An inextensible-mesh-lined silicone pad forms the PR muscle, which interfaces with the rectum to modulate the ARA. A sphincter phantom replicated the natural anatomical features of the human sphincter by forming mucosal folds in the anal canal, allowing expansion of the anal canal for defecation without elastic deformation of the anal canal wall, catering for critical observation of the effects of sphincter occlusion pressure on the system. By constructing the simulation with a modular design, individual components could be refined or replaced should they become damaged, or the simulation required re-configuration or physiological modifications. This is advantageous since the effect of single component variability can be observed on the system, particularly necessary in the case of investigating rectal compliance; a pivotal variable on continence in humans, dependant on rectal ‘state’ and population attributes.

Tissue Phantom Fabrication Challenges: Fabrication of soft tissue surrogate models will always pose challenges, due to the anisotropic nature of biological tissue

properties. The materials used to fabricate the simulation phantoms were governed by the requirement that they needed to be reusable for test repeatability. While hydrogels have been shown to possess viscoelasticity similar to tissue [160, 161], they degrade following fabrication. Silicone was a good phantom material candidate since it exhibits excellent elastic properties without plastic deformation, while its elastic moduli can also be tailored by using different 'grades' and amounts of additives. Furthermore it is mixed as a liquid, lending it well to the fabrication of intricate parts via a vacuum casting technique. In the determination of suitable materials for tissue phantoms, tensile data was obtained from literature on rectum and adipose tissues, while uniaxial tensile tests were conducted on porcine IAS and EAS. This meant that together with literature, the loading profiles of all tissues represented in the simulator were acquired. Using a similar protocol as used on porcine sphincter, tensile data was also gathered for 3 grades of silicone. A method to match the properties of silicone and biological tissues presented in Chapter 4 was successfully implemented using linear analysis to compare the gradient of a portion of the loading curves. Subsequently the materials from this analysis were applied. Although with the exception of the rectum in which 3 lower compliance grades were selected to model an 'active' state (characteristic of the biological rectum during defecation), since it wasn't possible to determine the tensile properties of 'active' rectal wall using ex-vivo analysis. The shortcomings of matching biological and synthetic materials in this way is that the materials behave differently at each point along the loading curve due to inherent differences in their structure and bulk properties. Subject to a given force, tissue undergoes a greater deflection with low strains and conversely silicone will undergo a greater deflection with larger strains. To combat this, a small strain range based on the operational strains of the simulation phantoms increases the accuracy of the silicones behaviour when operating within that range.

Stool Analogue Formulation Challenges: Stool was formulated using smectite clay (VEEGUM R) suspensions in water, in harmony with a previous study using stool analogue [148]. Using measured rheological data, an interpolated plot of apparent viscosities (at 1 Hz) allowed approximation of the properties of smectite clay suspensions with thicker consistencies than could be tested, this identified a 90.5% moisture content solution as having similar rheological properties to high moisture content faecal samples [142]. Using this consistency with the simulation would represent a 'worst case' scenario in maintaining continence. However configuration

of ARA and sphincter occlusion required to retain stools of this runny consistency may block the passage to thicker stools completely. Including stool consistency within the experimental variable matrix would provide an insight into its effect on the system.

Limitations of Modelling Techniques: Due to the high variability and complexity of biological systems, the physical simulation has some limitations. Upon reflection of the valuable insights into the biological defecatory system gained during this work, through viewing radio proctography, cadaver dissections and meeting with clinical personnel; several improvements to the system were recognised. The non-linear, anisotropic behaviour typically found in human soft tissue have been approximated with an isotropic silicone model. Furthermore, complex surface interactions which occur between the between the rectum, pelvic floor, bladder and other surrounding tissues have been neglected. The anal canal closure mechanism is complex due to its interaction with adjoining tissue bodies, of particular relevance here is that contraction of the PR effects forces which act to occlude the anal canal, in conjunction with the EAS, due to connectivity of neighbouring tissues. These features were only partially approximated in the current model. The current simulation uses passive models and the active musculature in the rectum and sphincter have been neglected. While muscle contraction hasn't been included with the rectum and sphincter, muscle fatigue has been neglected with the PR muscle. During tests, the position of the PR phantom remains constant throughout the duration of the tests. The biological striated muscle which forms the Puborectalis is not capable of holding a position for a prolonged amount of time. Furthermore, the abdominal pressure has not been included within the simulation due this added modelling complexities this would ensue. To model abdominal pressure, soft phantoms and instrumentation would need to be embedded in a fluid to apply pressure across all the model surfaces. This would require additional mounts and systems to retain the fluid while preventing contact with electronic components.

The implications of all of these limitations regarding the removal of pressures and forces within the system, and discrepancies between the forces modelled and those generated in the biological system, mean that the simulation does not behave or respond in the same manor. While useful trends in biomechanical parameters have been observed, the values presented in this thesis should be viewed accordingly.

Fidelity of Simulation Components: Data on the distensibility of the anal canal using a dilation balloon (EndoFLIP) revealed the rate of increase in the narrowest section of the anal canal relative to the rate of increase in balloon pressure (DI) was 4.74. The DI became smaller with the FENIX (3.88) and smaller still with the FENIX Plus (2.72). Higher DIs were associated with higher severities of FI. Previous assessments with the EndoFLIP [145] have reported the DI at rest as 3.9 for FI patients, and 1.5 for healthy patients. The simulated DI without an AAS device fitted is comparable to the DI for FI patients, suggesting that a similar pressure is required for expansion of the anal canal in both the human system and physical simulation. The FENIX and FENIX Plus offer an improvement to the DI of the anal canal, more in-line with the biological values for healthy subjects when used with the simulation. This suggests that the devices were effective at producing occlusion sufficient to prevent leakage during 'resting' states. This empirical analysis of FI devices is valuable for their evaluation in early development stages through demonstration of their influence on simulation behaviour compared with biological mechanisms. This analysis revealed that a passive device would not be sufficient in maintaining continence altogether, and highlights the need for an active device which could modulate pressure exerted on the anal canal, better representing the biological sphincter. Through being adaptive, a device could prevent leakage under high anal pressures and reduce the occlusion pressure during periods of rest, along with stress applied to delicate soft tissues.

Fidelity of the Simulation: Recreation of biological defecation using the simulation indicated the mean change in IR pressure was 25.1 mmHg (between test initialisation and peak pressure during defecation). Published manometry studies showed values for IR pressure changes as 41.3 mmHg [18, 175] between 'rest' and 'defecation', which is similar to the values observed with the simulation, demonstrating similar behavioural traits. Outline traces of the rectum were constructed on selected images of the rectum, taken over the duration of defecation scenario, to observe rectal morphology throughout the distension. This revealed that the anorectum remains relatively stationary while the proximal rectum appeared to move anteriorly, as could be described by phenomenon observed in the human system of a double-flap valve to prevent the passing of faeces [15]. This observation was a surprise since it had been overlooked as one of the influential continence mechanisms. However this demonstrated that with the correct component-level modelling considerations the

simulation behaved in a similar manner to the human system, further validating it as a tool for the development of clinically viable FI devices. Furthermore, during the defecation scenario pelvic floor descent was measured, revealing a descent of 6.8 mm between states of 'rest' and 'defecation'. Equivalently in the human system, the descent is observed as 19 mm [178]. Pelvic floor descent in the simulation is less severe than observed in the human system, which could be explained by passive properties of the tissue phantoms. In the human system, the PR muscle relaxes in coordination with defecation, allowing the rectum to straighten and provide a passage of least resistance to the transit of faeces. In the physical simulation on the other hand, the PR muscle cannot relax, and continues to passively constrain the posterior rectum during an influx of stool to the rectum. Analysis of this parameter highlights the prerequisite for the inclusion of active tissue phantoms within the simulation, to form closer resemblance with the human system.

Investigative Findings: The simulation provides visibility to the notion that continence mechanisms act to reinforce one another [106]. As such, it is not viable to target a single mechanisms for the treatment of FI, which may partially explain the poor efficacy of current treatment methods. This investigation has demonstrated that to effectively reduce faecal leakage, both anorectal angulation and occlusion pressure at the sphincter should be enhanced. Furthermore, it shows that to retain semisolid material in the rectum, it is not necessary to completely occlude the sphincter. Angulation of the rectum alone provides sufficient resistance to reduce stool leakage. Mean biological ARA values for healthy, nulliparous patients were measured at 104.5±10.3° at rest and 84.5±14.2° during squeeze [9]. These values were in agreement with the ARA's observed for the reduction in leakage in this investigation. This highlights the potential to develop new technologies for FI which do not rely solely on occlusion of the anal canal to maintain continence but also include modulation of ARA. Too much of either mechanism would result in OD. It is hypothesised that in the future a combined and modulated strategy would allow a reduction in occlusive pressures and thereby help to mitigate against the issues of soft tissue erosion and device migration that have previously plagued implantable technology for FI.

Scope of the Simulation and Clinical Feedback: On reflection of this discussion, it should be questioned whether the simulation has clinical relevance and whether it is

suitable for clinical development of FI devices as set out from the initial objectives. The successful fabrication of a 1st iteration of the simulation demonstrated similar values of faecal leakage, IR pressure and pelvic floor kinematics to the biological system for corresponding ARAs and sphincter occlusion pressures. This suggests plausibility for the simulation to be used as a development tool for clinically viable FI technologies. However it would require the refinement of a number of aspects described above. It is clear that a number of challenges need to be addressed before the physical simulation could be used for the development of clinically viable FI devices. Most of which are associated with the comprehensibility of the simulation (material properties, model constraints and the control of variables which govern the simulation).

A number of clinicians had input in defining the clinical requirements of the simulation. Clinicians were also sought to give feedback on the clinical relevance of the simulation in its current form, following the development documented in this thesis. Two clinicians (one colorectal surgeon and one associate clinical professor) paid a visit to the laboratory and were given a demonstration of the simulation in operation before being asked the question: "does the simulation have any clinical use in its current form and (if any) what are they?". The following applications for the simulation were expressed:

1. Pre-clinical evaluation of surgical devices for the treatment of FI
2. To improve patient understanding of certain colorectal disorders (e.g. anismus) and treatment techniques (e.g. physiotherapy)
3. Findings from the simulation could be used to inform treatment pathways in the application of personalised medicine

6.2. Conclusions

This investigation has developed a physical simulation of the human defecation system. It is evident that the behaviour of the simulation is informative and comparable to the human system.

The original objectives of the thesis detailed in Chapter 1 (Section 1.1.2.) were successfully achieved:

1. A review of publications on topics surrounding the fundamentals of FI revealed a clear need for new/improved technology. While a number of computational simulations were identified in literature, these were lacking in modelling complexities required for the understanding of biomechanics of the human defecation system. In general there was a dearth of literature on computational studies, and none on physical studies which modelled continence mechanisms. To aid the development of a physical simulation, important biomechanics associated with continence were identified and attributed to key components; the anatomy and properties of which were obtained where possible. Through discussion with clinicians, the clinical needs around a physical simulation were identified. Important influential continence mechanisms were identified and attributed to key biological components (Pelvis, rectum, PR muscle, sphincter complex and adipose fat) to be included in the simulation. Finally, measurements of important biomechanical parameters (ARA, pelvic floor descent, anal pressures) were obtained from literature and through clinicians, to inform the design and configuration of the simulation.
2. Biomimetic materials were reviewed which identified silicone as a suitable material for the fabrication of reusable tissue phantoms. A vacuum casting technique was developed and used effectively to reproduce the intricate details characteristic of biological tissues in the fabrication of the rectum, PR muscle, anal sphincter and adipose tissue components.
3. Implementation of control hardware allowed the modulation of PR force to augment the ARA and delivery of stool to the rectum at a controlled rate and volume. Implementation of sensing hardware permitted the observation of the ARA and measurement of the IR pressure, PR force and stool leakage.

4. A thorough component-level validation showed that the simulation components replicated biomechanics of the human system. The tissue properties of IAS and EAS could not be obtained from publications, therefore uniaxial tensile tests were carried out, which combined with literature provided loading data on each biological component modelled in the simulation. A similar tensile test method was then conducted on 3 grades of silicone and consequently the properties of silicone and biological tissues were successfully matched. Rheological analysis on smectite clay suspensions and comparison with rheological data of human faeces identified clay-moisture concentrations which represented low viscosity faeces. Other simulation parameters which showed similarities with the human system included the anal canal DI, pelvic floor descent and rectal morphology.
5. An experimental investigation was successfully carried out which revealed correlations between a number of variables on continence and biomechanics of the system. Smaller ARAs and increased anal canal occlusion pressure were shown to reduce faecal leakage and lead to increased IR pressures, generally with more pronounced effects observed for a higher compliance rectums.

The simulation has shown that to effectively reduce faecal leakage, both anorectal angulation and sphincter occlusion pressure should be enhanced. Furthermore, it shows that to retain semisolid material in the rectum it is not necessary to completely occlude the sphincter. This finding gives notions toward FI technologies which target a combination of continence mechanisms and modulate intermittent pressures applied to soft tissues. Through demonstrating its capabilities of investigating continence mechanisms and analysing existing devices, the simulation has shown that it meets the research questions defined in Section 3.1. The simulation has direct clinical relevance in aiding pre-clinical evaluation of technologies to treat FI, improving patient understanding of colorectal disorders and treatment modalities and in informing treatment pathways in the application of personalised medicine.

6.3. Future Work

Future work and further refinements will increase the fidelity and scope of the physical simulation, as a means to develop new technologies for the treatment of FI.

6.3.1. Silicone Characterisation and Material Selection

For the purposes of this research, a simplified model was used to characterise the material properties of human tissue using a linear relationship. Future work would look to characterise the non-linear properties of human tissue, and replicate these with an appropriate material. Capturing the full behaviour of biological tissues with the phantom models would allow the simulation to replicate the biological system more accurately when subject to dynamic forces and pressures.

6.3.2. Simulating Abnormalities

There is a large scope for the simulation to be used to model abnormalities and diseased states, for an understanding of the unique effects on the biomechanics of the system. By making use of the modular design of the simulation, biomechanical modifications can be applied to replicate an array of common abnormalities. The compliance and geometry of the soft components is variable. Therefore rectoceles could be simulated by the rectum model by modifying its design. Similarly, the intrinsic properties of the PR muscle could be tailored to have a greater elasticity for the representation of weaker pelvic floor tone, and the sphincter component can be modified to include areas which represent scar tissue or muscle atrophy.

6.3.3. Physiological Modifications

Demonstrated in Figure 6.1 are several proposed physiological modifications to the simulation, as identified through consultation with clinicians.

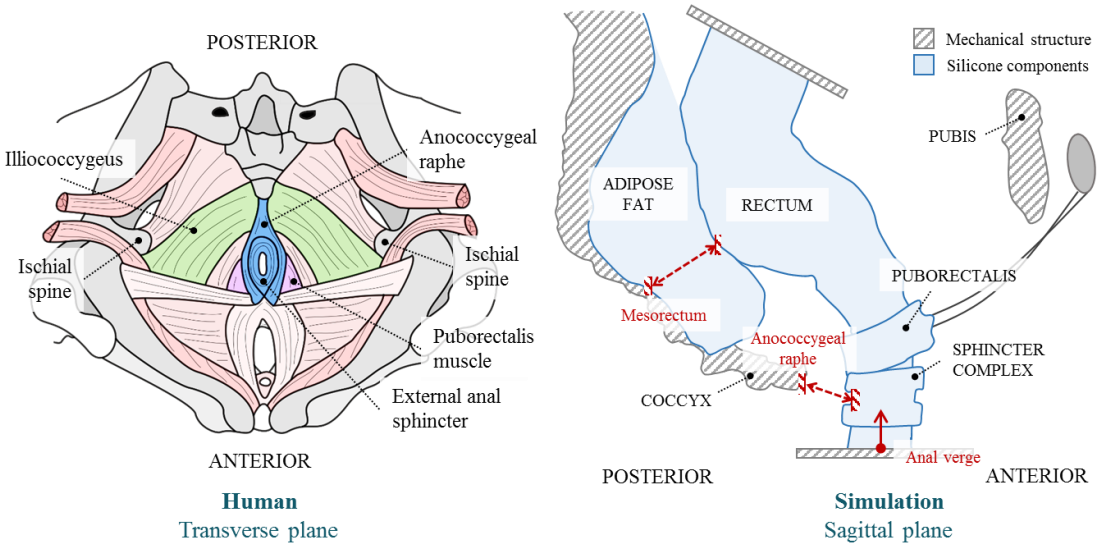

Figure 6.1 Demonstration of biological modifications showing *left*; transverse view of the female human pelvic configuration and *right*; sagittal view of the simulation.

Three main modifications were identified which detail tweaks to geometry and methods of constraints applied to the existing soft components:

1. The anal verge should be moved closer to the PR muscle, thereby shortening the anal canal so that its length is encompassed by the sphincter and PR muscle components, producing a high-pressure zone distributed along the length of the canal without the additional friction forces resulting from the excess canal.
2. The length of the posterior rectum is constrained by the mesorectum, which prevents movement of the entire component to the anterior upon PR contraction, enhancing the effect of PR contraction on anorectal angulation.
3. The anal sphincter complex (external anal sphincter) is constrained to the anococcygeal raphe which connects to the coccyx at the posterior of the pelvic cavity, and also constrained by pelvic muscles (in particular the illeococcygeus muscle, shown in *green* in Figure 6.1) which are attached to

the ischial spines. These additional fixations would result in pressure along the anterior of the anal canal from the anal sphincters when the PR contracts.

Mechanisms 2 and 3 act to increase occlusion in the anorectum and anal canal during PR muscle contraction, and suggest that the influence of the PR muscle in the maintenance of continence is more substantial than given credit in this thesis.

6.3.4. Investigation of Additional Variables

Use of an active sphincter component would facilitate investigation of the effects of dynamic sphincter pressures during simulated scenarios. 'Active' properties can be built into the sphincter muscles through techniques employed by a previous study [132].

Stool consistency plays an important role in the flow regime established through the system. Thicker consistency homogeneous stools and heterogeneous stool would allow the effects of different types of stool identified by the Bristol stool form scale to be investigated on biomechanics of the defecation system. Formulation of heterogeneous stool can be achieved by addition of a fibre-reinforcement such as grated carrot [148].

As discussed earlier in this chapter, while the PR muscle model is provided with active properties through modulation of both its position and force, the biomechanical operation of the PR muscle has not truly been replicated. For simplicity, the position of the PR muscle has been controlled. In practice, however, the muscle produces a constant force when contracted, until it relaxes or the muscle becomes fatigued. Seen as the force applied to the rectum by the PR is recorded in real-time during experimental analysis, a control loop could easily be incorporated into the control program to adjust the position of the PR muscle to maintain a constant force.

It is thought that abdominal pressure plays an important role in normal defecation [182], by including this in the simulation, its effects on the system could be empirically assessed. Inclusion of abdominal pressure is achievable by submerging the simulation in a fluid, or embedding the soft phantom models in an elastomeric gel, similar to a method used previously [135]. Embedding the phantom models and control systems in a fluid presents clear challenges in terms of fluid retention and avoiding fluid damage to components. However if these challenges were overcome, abdominal pressure could be modulated through variation to the fluids static head, or

by creating instantaneous pressure spikes through impact with the fluid container (characteristic of a cough or sneeze).

References

1. Regadas, F.S.P., et al., *Anal canal anatomy showed by three-dimensional anorectal ultrasonography.* Surgical endoscopy, 2007. **21**(12): p. 2207-2211.
2. Liu, J., et al., *Functional correlates of anal canal anatomy: puborectalis muscle and anal canal pressure.* The American journal of gastroenterology, 2006. **101**(5): p. 1092-1097.
3. Gold, D., et al., *Intraobserver and interobserver agreement in anal endosonography.* British journal of surgery, 1999. **86**(3): p. 371-375.
4. Kalantar, J.S., S. Howell, and N.J. Talley, *Prevalence of faecal incontinence and associated risk factors.* Med J Aust, 2002. **176**(2): p. 54-7.
5. Lam, L., *Prevalence of faecal incontinence: obstetric and constipation risk factors: a population based study.* Colorectal Dis., 1999. **1**: p. 197-203.
6. Saga, S., et al., *Prevalence and correlates of fecal incontinence among nursing home residents: a population-based cross-sectional study.* BMC geriatrics, 2013. **13**(1): p. 1.
7. Snell, R.S., *Clinical anatomy for medical students*. 1995: Little, Brown Medical Division.
8. Williams, P., et al., *Splanchnology.* Gray's Anatomy, 36th edn. Churchill Livingstone, London, 1980. **1318**.
9. Piloni, V., et al., *Measurement of the anorectal angle by defecography for the diagnosis of fecal incontinence.* International journal of colorectal disease, 1999. **14**(2): p. 131-135.
10. Read, N., D. Bartolo, and M. Read, *Differences in anal function in patients with incontinence to solids and in patients with incontinence to liquids.* British journal of surgery, 1984. **71**(1): p. 39-42.
11. Parks, A., *Royal Society of Medicine, Section of Proctology; Meeting 27 November 1974. President's Address. Anorectal incontinence.* Proceedings of the Royal Society of Medicine, 1975. **68**(11): p. 681.
12. Yoshioka, K. and M. Keighley, *Critical assessment of the quality of continence after postanal repair for faecal incontinence.* British journal of surgery, 1989. **76**(10): p. 1054-1057.
13. Christiansen, J. and M. Lorentzen, *Implantation of artificial sphincter for anal incontinence.* The Lancet, 1987. **330**(8553): p. 244-245.
14. Dubrovsky, B. and D. Filipini, *Neurobiological aspects of the pelvic floor muscles involved in defecation.* Neuroscience & Biobehavioral Reviews, 1990. **14**(2): p. 157-168.
15. Parks, A., N. Porter, and J. Hardcastle, *The syndrome of the descending perineum.* Proceedings of the Royal society of Medicine, 1966. **59**(6): p. 477.
16. Ma, S., S.-Y. Leu, and R.-H. Fang, *Reconstruction of Anorectal Angle After Abdominoperineal Resection of Rectum and Anus-An Animal Model.* Annals of plastic surgery, 1989. **23**(6): p. 519-522.
17. Arnold Wald, M.D., Paul Hyman, M.D., Diane Darrell, A.P.R.N., William E. Whitehead, Ph.D. *Bowel Control Problems (Fecal Incontinence)*. 2013 18th November 2016]; Available from: https://www.niddk.nih.gov/health-information/health-topics/digestive-diseases/fecal-incontinence/Pages/facts.aspx.

18. Felt-Bersma, R.J., et al., *Rectal compliance as a routine measurement.* Diseases of the colon & rectum, 2000. **43**(12): p. 1732-1738.
19. Suzuki, H., et al., *Anorectal pressure and rectal compliance after low anterior resection.* British Journal of Surgery, 1980. **67**(9): p. 655-657.
20. Macmillan, A.K., et al., *The prevalence of fecal incontinence in community-dwelling adults: a systematic review of the literature.* Diseases of the colon & rectum, 2004. **47**(9): p. 1341-1349.
21. Burton, J.H. and B.G. Staehle, *Inflatable artificial sphincter*. 1987, Google Patents.
22. NURSE, D.E. and A. Mundy, *One hundred artificial sphincters.* British journal of urology, 1988. **61**(4): p. 318-325.
23. Sofia, C., et al., *Experiences with an artificial sphincter to establish anal continence in dogs.* The American Surgeon, 1988. **54**(6): p. 390-394.
24. Satava, R.M. and G.E. King, *An artificial anal sphincter. Phase 2: implantable sphincter with a perineal colostomy.* Journal of Surgical Research, 1989. **46**(3): p. 207-211.
25. Christiansen, J. and M. Lorentzen, *Implantation of artificial sphincter for anal incontinence.* Diseases of the colon & rectum, 1989. **32**(5): p. 432-436.
26. Christiansen, J. and B. Sparsø, *Treatment of anal incontinence by an implantable prosthetic anal sphincter.* Annals of surgery, 1992. **215**(4): p. 383.
27. Christiansen, J., *Advances in the surgical management of anal incontinence.* Baillière's clinical gastroenterology, 1992. **6**(1): p. 43-57.
28. Wong, W.D., et al., *The safety and efficacy of the artificial bowel sphincter for fecal incontinence.* Diseases of the colon & rectum, 2002. **45**(9): p. 1139-1153.
29. Congilosi, S., et al., *The artificial bowel sphincter: long-term experience at a single institution.* Dis Colon Rectum, 2002. **45**: p. A26.
30. Read, N., et al., *Use of anorectal manometry during rectal infusion of saline to investigate sphincter function in incontinent patients.* Gastroenterology, 1983. **85**(1): p. 105-113.
31. Broens, P., et al., *Combined radiologic and manometric study of rectal filling sensation.* Diseases of the colon & rectum, 2002. **45**(8): p. 1016-1022.
32. Ito, T., et al., *Videomanometry of the pelvic organs: a comparison of the normal lower urinary and gastrointestinal tracts.* International journal of urology, 2006. **13**(1): p. 29-35.
33. Lees, A., M. Stern, and M. Swash, *Anal sphincter dysfunction in Parkinson's disease.* Arch Neurol, 1989. **46**: p. 1061-1064.
34. Sørensen, M., et al., *Anorectal dysfunction in patients with urologic disturbance due to multiple sclerosis.* Diseases of the colon & rectum, 1991. **34**(2): p. 136-139.
35. Iscoe, S., *Control of abdominal muscles.* Progress in neurobiology, 1998. **56**(4): p. 433-506.
36. Sakakibara, R., et al., *Bladder and bowel dysfunction in Parkinson's disease.* Journal of neural transmission, 2008. **115**(3): p. 443-460.
37. Krogh, K., et al., *Neurogenic bowel dysfunction score.* Spinal cord, 2005. **44**(10): p. 625-631.

38. NHS. *Treating bowel incontinence*. 2013 [cited 2014 29th October]; Available from: http://www.nhs.uk/conditions/incontinence-bowel/pages/treatment.aspx.
39. Rao, S.S., *Pathophysiology of adult fecal incontinence.* Gastroenterology, 2004. **126**: p. S14-S22.
40. NHS. *Causes of bowel incontinence*. 2013 [cited 2014 6th November]; Available from: http://www.nhs.uk/Conditions/Incontinence-bowel/Pages/Causes.aspx.
41. Coggrave, M., Ash, D., Adcock, C. *Guidelines for Management of Neurogenic Bowel Dysfunction in Individuals with Central Neurological Conditions*. 2012 [cited 2014 7th November]; Available from: http://www.spinal.co.uk/userfiles/pdf/Publications/CV653N_Neurogenic_Guidelines_Sept_2012_web_no_crops.pdf.
42. Chia, Y.-W., et al., *Prevalence of bowel dysfunction in patients with multiple sclerosis and bladder dysfunction.* Journal of neurology, 1995. **242**(2): p. 105-108.
43. Enck, P., et al., *Epidemiology of faecal incontinence in selected patient groups.* International journal of colorectal disease, 1991. **6**(3): p. 143-146.
44. Nelson, R., et al., *Community-based prevalence of anal incontinence.* Jama, 1995. **274**(7): p. 559-561.
45. Thomas, T.M., et al., *The prevalence of faecal and double incontinence.* Journal of Public Health, 1984. **6**(3): p. 216-220.
46. Talley, N.J., et al., *Prevalence of gastrointestinal symptoms in the elderly: a population-based study.* Gastroenterology, 1992. **102**(3): p. 895-901.
47. CAMPBELL, A.J., J. Reinken, and L. McCosh, *Incontinence in the elderly: prevalence and prognosis.* Age and Ageing, 1985. **14**(2): p. 65-70.
48. Peet, S., C. Castleden, and C. McGrother, *Prevalence of urinary and faecal incontinence in hospitals and residential and nursing homes for older people.* BMJ: British Medical Journal, 1995. **311**(7012): p. 1063.
49. Rieger, N. and D. Wattchow, *The effect of vaginal delivery on anal function.* Australian and New Zealand journal of surgery, 1999. **69**(3): p. 172-177.
50. Landefeld, C.S., et al., *National Institutes of Health state-of-the-science conference statement: prevention of fecal and urinary incontinence in adults.* Annals of Internal Medicine, 2008. **148**(6): p. 449-458.
51. Emmanuel, A., et al., *Consensus review of best practice of transanal irrigation in adults.* Spinal cord, 2013. **51**(10): p. 732-738.
52. Rao, S.S. and A.C.o.G.P.P. Committee, *Diagnosis and management of fecal incontinence.* The American journal of gastroenterology, 2004. **99**(8): p. 1585-1604.
53. Stillie, A., et al., *Rectal filling at planning does not predict stability of the prostate gland during a course of radical radiotherapy if patients with large rectal filling are re-imaged.* Clinical Oncology, 2009. **21**(10): p. 760-767.
54. Dall, F., et al., *Biomechanical wall properties of the human rectum. A study with impedance planimetry.* Gut, 1993. **34**(11): p. 1581-1586.
55. Classen, M., G.N. Tytgat, and C.J. Lightdale, *Gastroenterological endoscopy*. 2002: Thieme.
56. Kuijpers, H., *Colorectal PhysiologyFecal Incontinence*. 1994: Taylor & Francis.

57. Gray, H., C.M. Goss, and D.M. Alvarado, *Anatomy of the human body*. 1973: Lea & Febiger Philadelphia.
58. Khaikin, M. and S.D. Wexner, *Treatment strategies in obstructed defecation and fecal incontinence.* World journal of gastroenterology: WJG, 2006. **12**(20): p. 3168.
59. Hjartardóttir, S., et al., *The female pelvic floor: a dome-not a basin.* Acta obstetricia et gynecologica Scandinavica, 1997. **76**(6): p. 567-571.
60. Davila, G.W., G.M. Ghoniem, and S.D. Wexner, *Pelvic floor dysfunction*. 2006: Springer.
61. Bartolo, D., A. Roe, and N.M. Mortensen, *The relationship between perineal descent and denervation of the puborectalis in continent patients.* International journal of colorectal disease, 1986. **1**(2): p. 91-95.
62. Bharucha, A.E., *Pelvic floor: anatomy and function.* Neurogastroenterology & Motility, 2006. **18**(7): p. 507-519.
63. Percy, J., et al., *Electrophysiological study of motor nerve supply of pelvic floor.* The Lancet, 1981. **317**(8210): p. 16-17.
64. Frenckner, B. and C. Euler, *Influence of pudendal block on the function of the anal sphincters.* Gut, 1975. **16**(6): p. 482-489.
65. Penninckx, F. and R. Kerremans, *Internal sphincter-saving in imperforate anus with or without fistula.* International journal of colorectal disease, 1986. **1**(1): p. 28-32.
66. Schrøder, H. and E. Reske-Nielsen, *Fiber types in the striated urethral and anal sphincters.* Acta neuropathologica, 1983. **60**(3-4): p. 278-282.
67. Hussain, S., *Imaging of the anal sphincter complex*. 1996: Erasmus MC: University Medical Center Rotterdam.
68. Li, D. and M. Guo, *Morphology of the levator ani muscle.* Diseases of the colon & rectum, 2007. **50**(11): p. 1831-1839.
69. Duthie, H., *Progress report. Anal continence.* Gut, 1971. **12**(10): p. 844-852.
70. Marzio, L., et al., *Relationship between anal canal diameter and pressure evaluated simultaneously by endosonography and manometry in normal human subjects.* International journal of colorectal disease, 1998. **13**(1): p. 21-26.
71. Lestar, B., F. Penninckx, and R. Kerremans, *The composition of anal basal pressure.* International journal of colorectal disease, 1989. **4**(2): p. 118-122.
72. Miller, R., D. Bartolo, and F. Cervero, *Anorectal sampling: a comparison of normal and incontinent patients.* British journal of surgery, 1988. **75**(1): p. 44-47.
73. Raizada, V., et al., *Functional morphology of anal sphincter complex unveiled by high definition anal manometery and three dimensional ultrasound imaging.* Neurogastroenterology & Motility, 2011. **23**(11): p. 1013-e460.
74. Scharli, A.F. and W.B. Kiesewetter, *Imperforate anus: Anorectosigmoid pressure studies as a quantitative evaluation of postoperative continence.* Journal of pediatric surgery, 1969. **4**(6): p. 694-704.
75. Choi, J.S., et al., *Intraobserver and interobserver measurements of the anorectal angle and perineal descent in defecography.* Diseases of the colon & rectum, 2000. **43**(8): p. 1121-1126.
76. Kim, A.Y., *How to interpret a functional or motility test-defecography.* Journal of neurogastroenterology and motility, 2011. **17**(4): p. 416.

77. Mahieu, P., J. Pringot, and P. Bodart, *Defecography: I. Description of a new procedure and results in normal patients.* Gastrointestinal radiology, 1984. **9**(1): p. 247-251.
78. Felt-Bersma, R., et al., *Defecography in patients with anorectal disorders.* Diseases of the Colon & Rectum, 1990. **33**(4): p. 277-284.
79. Shorvon, P., et al., *Defecography in normal volunteers: results and implications.* Gut, 1989. **30**(12): p. 1737-1749.
80. Barkel, D.C., et al., *Scintigraphic assessment of the anorectal angle in health and after ileal pouch-anal anastomosis.* Annals of surgery, 1988. **208**(1): p. 42.
81. Madoff, R., et al., *Rectal compliance: a critical reappraisal.* International journal of colorectal disease, 1990. **5**(1): p. 37-40.
82. Sørensen, M., T. Tetzschner, and J. Christiansen, *Physiological variation in rectal compliance.* British journal of surgery, 1992. **79**(10): p. 1106-1108.
83. Rao, G., et al., *Incremental elastic modulus–a challenge to compliance.* International journal of colorectal disease, 1997. **12**(1): p. 33-36.
84. Rubod, C., et al., *Biomechanical properties of human pelvic organs.* Urology, 2012. **79**(4): p. 968. e17-968. e22.
85. Christensen, M.B., K. Oberg, and J.C. Wolchok, *Tensile properties of the rectal and sigmoid colon: a comparative analysis of human and porcine tissue.* SpringerPlus, 2015. **4**(1): p. 1-10.
86. Qiao, Y., et al., *Measurement of mechanical properties of rectal wall.* Journal of Materials Science: Materials in Medicine, 2005. **16**(2): p. 183-188.
87. Alkhouli, N., et al., *The mechanical properties of human adipose tissues and their relationships to the structure and composition of the extracellular matrix.* American Journal of Physiology-Endocrinology and Metabolism, 2013. **305**(12): p. E1427-E1435.
88. *Transanal irrigation: a proven approach to bowel dysfunction.* Gastrointestinal Nursing, 2014. **12**(Sup2): p. S3-S3.
89. Malone, P., P. Ransley, and E. Kiely, *Preliminary report: the antegrade continence enema.* The Lancet, 1990. **336**(8725): p. 1217-1218.
90. Squire, R., et al., *The clinical application of the Malone antegrade colonic enema.* Journal of pediatric surgery, 1993. **28**(8): p. 1012-1015.
91. Krogh, K. and S. Laurberg, *Malone antegrade continence enema for faecal incontinence and constipation in adults.* British journal of surgery, 1998. **85**(7): p. 974-977.
92. Gerharz MD, E.W., et al., *The value of the MACE (Malone antegrade colonic enema) procedure in adult patients.* Journal of the American College of Surgeons, 1997. **185**(6): p. 544-547.
93. Teichman, J.M., et al., *Long-term results for Malone antegrade continence enema for adults with neurogenic bowel disease.* Urology, 2003. **61**(3): p. 502-506.
94. Burcharth, F., et al., *The colostomy plug: a new disposable device for a continent colostomy.* The Lancet, 1986. **328**(8515): p. 1062-1063.
95. Christiansen, J. and K. Roed-Petersen, *Clinical assessment of the anal continence plug.* Diseases of the colon & rectum, 1993. **36**(8): p. 740-742.

96. Mortensen, N. and M.S. Humphreys, *The anal continence plug: a disposable device for patients with anorectal incontinence.* The Lancet, 1991. **338**(8762): p. 295-297.
97. Norton, C. and M. Kamm, *Anal plug for faecal incontinence.* Colorectal Disease, 2001. **3**(5): p. 323-327.
98. Oom, D.M., M.P. Gosselink, and W.R. Schouten, *Anterior sphincteroplasty for fecal incontinence: a single center experience in the era of sacral neuromodulation.* Diseases of the Colon & Rectum, 2009. **52**(10): p. 1681-1687.
99. ASERNIP-S, *Interventional procedure overview of Stimulated Graciloplasty*. 2005.
100. Bartolo, D., et al., *The role of partial denervation of the puborectalis in idiopathic faecal incontinence.* British journal of surgery, 1983. **70**(11): p. 664-667.
101. Mahieu, P., J. Pringot, and P. Bodart, *Defecography: II. Contribution to the diagnosis of defecation disorders.* Gastrointestinal radiology, 1984. **9**(1): p. 253-261.
102. NICE, *Sacral nerve stimulation for faecal incontinence*. 2004.
103. Light, J., *Long-term Clinical Results using the Artificial Urinary Sphincter around Bowel.* British journal of urology, 1989. **64**(1): p. 56-60.
104. Gallas, S., et al., *Constipation in 44 patients implanted with an artificial bowel sphincter.* International journal of colorectal disease, 2009. **24**(8): p. 969-974.
105. Gregorcyk, S.G., *The Current Status of the Acticon® Neosphincter.* Clinics in colon and rectal surgery, 2005. **18**(1): p. 32.
106. Hajivassiliou, C., K. Carter, and I. Finlay, *Anorectal angle enhances faecal continence.* British journal of surgery, 1996. **83**(1): p. 53-56.
107. Torax® Medical, I. *The FENIX® Continence Restoration System*. 2014 [cited 2014 3rd October]; Available from: http://www.toraxmedical.co.uk/fenix/.
108. Doll, A., et al., *A high performance bidirectional micropump for a novel artificial sphincter system.* Sensors and Actuators A: Physical, 2006. **130**: p. 445-453.
109. Finlay, I., W. Richardson, and C. Hajivassiliou, *Outcome after implantation of a novel prosthetic anal sphincter in humans.* British Journal of Surgery, 2004. **91**(11): p. 1485-1492.
110. Nishi, K., et al., *Development of an implantable artificial anal sphincter using a shape memory alloy.* Journal of pediatric surgery, 2004. **39**(1): p. 69-72.
111. ASERNIP-S, *Interventional procedure overview of Artificial anal sphincter*. 2002.
112. Devesa, J.M., et al., *Artificial anal sphincter.* Diseases of the colon & rectum, 2002. **45**(9): p. 1154-1163.
113. Doll, A.F., et al., *A novel artificial sphincter prosthesis driven by a four-membrane silicon micropump.* Sensors and Actuators A: Physical, 2007. **139**(1): p. 203-209.
114. Carter, K.B., I.G. Finlay, and W. Richardson, *Prosthetic anal sphincter*. 1997, Google Patents.
115. Hajivassiliou, C. and I. Finlay, *Effect of a novel prosthetic anal neosphincter on human colonic blood flow.* British journal of surgery, 1998. **85**(12): p. 1703-1707.

116. Kakubari, Y., et al., *Temperature control of SMA artificial anal sphincter.* Magnetics, IEEE Transactions on, 2003. **39**(5): p. 3384-3386.
117. Slaughter, M.S. and T.J. Myers, *Transcutaneous energy transmission for mechanical circulatory support systems: history, current status, and future prospects.* Journal of cardiac surgery, 2010. **25**(4): p. 484-489.
118. Schuder, J., H. Stephenson, and J. Townsend, *High-level electromagnetic energy transfer through a closed chest wall.* Inst. Radio Engrs. Int Conv. Record, 1961. **9**: p. 119.
119. Zan, P., G. Yan, and H. Liu, *Analysis of electromagnetic compatibility in biological tissue for a novel artificial anal sphincter.* IET Science, Measurement & Technology, 2009. **3**(1): p. 22-26.
120. Shah, H.N. and G.H. Badlani, *Mesh complications in female pelvic floor reconstructive surgery and their management: a systematic review.* Indian journal of urology: IJU: journal of the Urological Society of India, 2012. **28**(2): p. 129.
121. Rosenblatt, P., et al., *A Preliminary Evaluation of the TOPAS System for the Treatment of Fecal Incontinence in Women.* Female pelvic medicine & reconstructive surgery, 2014. **20**(3): p. 155-162.
122. Chanda, A., et al., *Computational Modeling of the Female Pelvic Support Structures and Organs to Understand the Mechanism of Pelvic Organ Prolapse: A Review.* Applied Mechanics Reviews, 2015. **67**(4): p. 040801.
123. Brandão, S., et al., *Biomechanical study on the bladder neck and urethral positions: simulation of impairment of the pelvic ligaments.* Journal of biomechanics, 2015. **48**(2): p. 217-223.
124. d'Aulignac, D., et al., *A shell finite element model of the pelvic floor muscles.* Computer Methods in Biomechanics and Biomedical Engineering, 2005. **8**(5): p. 339-347.
125. Gielen, A., P. Bovendeerd, and J. Janssen, *A finite element formulation of muscle contraction*, in *DIANA Computational Mechanics '94*. 1994, Springer. p. 139-148.
126. Kojic, M., S. Mijailovic, and N. Zdravkovic, *Modelling of muscle behaviour by the finite element method using Hill's three-element model.* International journal for numerical methods in engineering, 1998. **43**(5): p. 941-953.
127. Martins, J., et al., *A numerical model of passive and active behavior of skeletal muscles.* Computer methods in applied mechanics and engineering, 1998. **151**(3): p. 419-433.
128. Oomens, C., et al., *Finite element modelling of contracting skeletal muscle.* Philosophical Transactions of the Royal Society of London B: Biological Sciences, 2003. **358**(1437): p. 1453-1460.
129. Brandão, F.S.Q.d.S., et al., *Modeling the contraction of the pelvic floor muscles.* Computer methods in biomechanics and biomedical engineering, 2016. **19**(4): p. 347-356.
130. Peng, Y., et al., *Tu1782 Computational Modeling and Simulation of Fecal Incontinence-The Effect of Stool Consistency on Leakage.* Gastroenterology, 2016. **150**(4): p. S944.
131. Bartolo, D., R. Miller, and N. Mortensen, *Sphincteric mechanism of anorectal continence during Valsalva manoeuvres.* Coloproctology, 1987. **9**: p. 103-7.

132. Maréchal, L., et al. *Modelling of anal sphincter tone based on pneumatic and cable-driven mechanisms*. in *World Haptics Conference (WHC), 2017 IEEE*. 2017. IEEE.
133. Kenngott, H., et al., *OpenHELP (Heidelberg laparoscopy phantom): development of an open-source surgical evaluation and training tool.* Surgical endoscopy, 2015: p. 1-10.
134. Cieslicki, K. and D. Ciesla, *Investigations of flow and pressure distributions in physical model of the circle of Willis.* Journal of biomechanics, 2005. **38**(11): p. 2302-2310.
135. Ikeda, S., et al. *In vitro patient-tailored anatomical model of cerebral artery for evaluating medical robots and systems for intravascular neurosurgery*. in *Intelligent Robots and Systems, 2005.(IROS 2005). 2005 IEEE/RSJ International Conference on*. 2005. IEEE.
136. Lim, W., et al., *Pulsatile flow studies of a porcine bioprosthetic aortic valve in vitro: PIV measurements and shear-induced blood damage.* Journal of biomechanics, 2001. **34**(11): p. 1417-1427.
137. Martins, J., et al., *Finite element studies of the deformation of the pelvic floor.* Annals of the New York Academy of Sciences, 2007. **1101**(1): p. 316-334.
138. Zhang, Y., et al., *Advanced finite element mesh model of female SUI research during physical and daily activities.* Stud. Health Technol. Inf, 2009. **142**(1): p. 447-452.
139. Bhattarai, A., et al., *A 3D Finite Element model of the female pelvic floor for the reconstruction of urinary incontinence.* Rev. Urol, 2014. **16**(5): p. S2-S10.
140. Janda, Š., F.C. Van Der Helm, and S.B. de Blok, *Measuring morphological parameters of the pelvic floor for finite element modelling purposes.* Journal of biomechanics, 2003. **36**(6): p. 749-757.
141. Silva, M., et al., *Biomechanical properties of the pelvic floor muscles of continent and incontinent women using an inverse finite element analysis.* Computer Methods in Biomechanics and Biomedical Engineering, 2017. **20**(8): p. 842-852.
142. Woolley, S., et al., *Shear rheological properties of fresh human faeces with different moisture content.* Water SA, 2014. **40**(2): p. 273-276.
143. Lestár, B., F.M. Penninckx, and R.P. Kerremans, *Defecometry.* Diseases of the Colon & Rectum, 1989. **32**(3): p. 197-201.
144. Carrington, E., et al., *Traditional measures of normal anal sphincter function using high-resolution anorectal manometry (HRAM) in 115 healthy volunteers.* Neurogastroenterology & Motility, 2014. **26**(5): p. 625-635.
145. Gourcerol, G., et al., *Do endoflip assessments of anal sphincter distensibility provide more information on patients with fecal incontinence than high-resolution anal manometry?* Neurogastroenterology & Motility, 2016. **28**(3): p. 399-409.
146. Akhtar, R., et al., *Characterizing the elastic properties of tissues.* Materials Today, 2011. **14**(3): p. 96-105.
147. Boutouyrie, P., et al., *Aortic stiffness is an independent predictor of primary coronary events in hypertensive patients: a longitudinal study.* Hypertension, 2002. **39**(1): p. 10-15.

148. Johnson, K.T., et al., *Development of a cathartic-free colorectal cancer screening test using virtual colonoscopy: a feasibility study.* American Journal of Roentgenology, 2007. **188**(1): p. W29-W36.
149. Holzapfel, G.A., *Biomechanics of soft tissue.* The handbook of materials behavior models, 2001. **3**: p. 1049-1063.
150. Holzapfel, G.A. *Similarities between soft biological tissues and rubberlike materials*. in *CONSTITUTIVE MODELS FOR RUBBER-PROCEEDINGS*-. 2005. Balkema.
151. Kohli, S., et al., *Ethnic-specific differences in abdominal subcutaneous adipose tissue compartments.* Obesity, 2010. **18**(11): p. 2177-2183.
152. Gershon, B., D. Cohn, and G. Marom, *Utilization of composite laminate theory in the design of synthetic soft tissues for biomedical prostheses.* Biomaterials, 1990. **11**(8): p. 548-552.
153. Hungr, N., et al., *A realistic deformable prostate phantom for multimodal imaging and needle-insertion procedures.* Medical physics, 2012. **39**(4): p. 2031-2041.
154. Eklund, A., A. Bergh, and O. Lindahl, *A catheter tactile sensor for measuring hardness of soft tissue: measurement in a silicone model and in anin vitro human prostate model.* Medical & biological engineering & computing, 1999. **37**(5): p. 618-624.
155. Wang, Y., et al., *Silicone-Based Tissue-Mimicking Phantom for Needle Insertion Simulation.* Journal of Medical Devices, 2014. **8**(2): p. 021001.
156. Pogue, B.W. and M.S. Patterson, *Review of tissue simulating phantoms for optical spectroscopy, imaging and dosimetry.* Journal of biomedical optics, 2006. **11**(4): p. 041102-041102-16.
157. Zell, K., et al., *Acoustical properties of selected tissue phantom materials for ultrasound imaging.* Physics in Medicine & Biology, 2007. **52**(20): p. N475.
158. Dehghan, E., et al., *Needle-tissue interaction modeling using ultrasound-based motion estimation: Phantom study.* Computer Aided Surgery, 2008. **13**(5): p. 265-280.
159. Yu, Y., et al. *Robot-assisted prostate brachytherapy*. in *International Conference on Medical Image Computing and Computer-Assisted Intervention*. 2006. Springer.
160. Nuttelman, C.R., et al., *Attachment of fibronectin to poly (vinyl alcohol) hydrogels promotes NIH3T3 cell adhesion, proliferation, and migration.* Journal of biomedical materials research, 2001. **57**(2): p. 217-223.
161. Chu, K.C. and B.K. Rutt, *Polyvinyl alcohol cryogel: an ideal phantom material for MR studies of arterial flow and elasticity.* Magnetic Resonance in Medicine, 1997. **37**(2): p. 314-319.
162. Chanthasopeephan, T., J.P. Desai, and A.C. Lau, *Modeling soft-tissue deformation prior to cutting for surgical simulation: finite element analysis and study of cutting parameters.* Biomedical Engineering, IEEE Transactions on, 2007. **54**(3): p. 349-359.
163. Lee, K.Y. and D.J. Mooney, *Hydrogels for tissue engineering.* Chemical reviews, 2001. **101**(7): p. 1869-1880.
164. Ottensmeyer, M.P. and J.K. Salisbury. *In vivo data acquisition instrument for solid organ mechanical property measurement*. in *International Conference*

on Medical Image Computing and Computer-Assisted Intervention. 2001. Springer.

165. Kerdok, A.E., et al., *Truth cube: Establishing physical standards for soft tissue simulation.* Medical Image Analysis, 2003. **7**(3): p. 283-291.
166. DiMaio, S.P. and S.E. Salcudean, *Needle insertion modeling and simulation.* IEEE Transactions on robotics and automation, 2003. **19**(5): p. 864-875.
167. Meghezi, S., et al., *Effects of a pseudophysiological environment on the elastic and viscoelastic properties of collagen gels.* International journal of biomaterials, 2012. **2012**.
168. Omidi, E., et al., *Characterization and assessment of hyperelastic and elastic properties of decellularized human adipose tissues.* Journal of biomechanics, 2014. **47**(15): p. 3657-3663.
169. *TCIA Collections*. [cited 2018 25th April]; Available from: http://www.cancerimagingarchive.net/.
170. Ackerman, M.J., *The visible human project.* Proceedings of the IEEE, 1998. **86**(3): p. 504-511.
171. W. Paul Segars, P.D. *Medical Imaging Simulation using Computational Phantoms*. 2015 [cited 2015 12th July]; Available from: https://olv.duke.edu/xcat.
172. 3Dircadb. *3D image reconstruction for comparison of algorithm database*. June 2013; Available from: http://www.ircad.fr/softwares/3Dircadb/3Dircadb.php?lng=en.
173. ZAVALA, M.A.L., N. Funamizu, and T. Takakuwa, *Characterization of feces for describing the aerobic biodegradation of feces.* Doboku Gakkai Ronbunshu, 2002. **2002**(720): p. 99-105.
174. *Using the Power Law Model to Quantify Shear Thinning Behavior on a Rotational Rheometer*. 2015 Jan 9th, 2015 [cited 2018 20th Feb]; Available from: https://www.azom.com/article.aspx?ArticleID=11624.
175. Li, Y., et al., *Normal values and pressure morphology for three-dimensional high-resolution anorectal manometry of asymptomatic adults: a study in 110 subjects.* International journal of colorectal disease, 2013. **28**(8): p. 1161-1168.
176. Alqudah, M., et al., *Evaluation of anal sphincter resistance and distensibility in healthy controls using EndoFLIP©.* Neurogastroenterology & Motility, 2012. **24**(12).
177. Thapar, R.B., et al., *MR defecography for obstructed defecation syndrome.* The Indian journal of radiology & imaging, 2015. **25**(1): p. 25.
178. Bartolo, D., et al., *Differences in anal sphincter function and clinical presentation in patients with pelvic floor descent.* Gastroenterology, 1983. **85**(1): p. 68-75.
179. Sakakibara, R., et al., *Influence of body position on defecation in humans.* LUTS: Lower Urinary Tract Symptoms, 2010. **2**(1): p. 16-21.
180. Stokes, W.E., et al., *A biomechanical model of the human defecatory system to investigate mechanisms of continence.* Proceedings of the Institution of Mechanical Engineers, Part H: Journal of Engineering in Medicine, 2018: p. 0954411918756453.

181. Stokes, W.E., et al. *A physical simulation to investigate the effect of anorectal angle on continence*. in *Biomedical Engineering (BioMed), 2017 13th IASTED International Conference on*. 2017. IEEE.
182. Bannister, J., C. Gibbons, and N. Read, *Preservation of faecal continence during rises in intra-abdominal pressure: is there a role for the flap valve?* Gut, 1987. **28**(10): p. 1242-1245.

Glossary

Anterior	Located at the front
Autonomic	Not subject to voluntary control
Cloaca	Terminal end of the hindgut before division into rectum, bladder and genital organs in an embryo
Colon	Section of the large intestine from its origin to the rectum
Faeces	Solid or liquid waste discharged from the intestine
Flatus	Gaseous waste discharged from the intestine
Inferior	Located away from the head
Innervate	To supply an organ or body part with nerves
Peritoneum	The secreted membrane lining walls of the abdominal and pelvic cavities
Posterior	Located at the rear
Somatic	Affecting the body as distinguished from a body part, the mind or the environment
Stenosis	Abnormal narrowing of a passage in the body
Stool	Solid or liquid excretory product evacuated from the bowel
Striated	Series of linear ridges, furrows or marks
Superior	Located towards the head
Vascular	Characterised by blood vessels
Viscera	The internal organs contained within the abdominal cavity

Acronyms

AAS	Artificial anal sphincter
ARA	Anorectal angle
CT	Computerised tomography
DI	Distensibility index
FI	Faecal incontinence
GI	Gastrointestinal
IR	Intra-rectal
MRI	Magnetic resonance imaging
OD	Obstructed defecation
PR	Puborectalis
QoL	Quality of life

Appendix I: Publications

I. *A physical simulation to investigate the effect of anorectal angle on continence* Biomedical Engineering (BioMed), 2017 13th IASTED International Conference on Incontinence

A PHYSICAL SIMULATION TO INVESTIGATE THE EFFECT OF ANORECTAL ANGLE ON CONTINENCE

William E. Stokes, David G. Jayne, Ali Alazmani, Peter R. Culmer
University of Leeds
Woodhouse Lane, Leeds/UK
mn10ws@leeds.ac.uk, d.g.jayne@leeds.ac.uk, a.alazmani@leeds.ac.uk, p.r.culmer@leeds.ac.uk

ABSTRACT
This paper investigates the effect of the anorectal angle on continence using a physical model of the anatomical system. A method to fabricate, measure and control a physical model for the simulation of human faecal continence is presented. A model rectum and associated soft tissues, based on geometry from an anonymised CT dataset, was fabricated from silicone and showed behavioural realism to ex vivo tissue. Simulated stool matter with similar rheological properties to human faeces was developed. Instrumentation and control hardware are used to regulate injection of simulated stool into the system, define the anorectal angle and monitor stool flow rate, intra-rectal pressure and puborectalis force. A study was then conducted in which simulated stool was introduced to the system for anorectal angles between 80° and 100°. Results obtained from the study give insight into the effect of the anorectal angle on continence. Stool leakage was reduced as the angle became more acute. Conversely, intra-rectal pressure increased. These data demonstrate that the anorectal angle is fundamental in maintaining continence. This work is valuable in helping improve our understanding of the physical behaviour of the faecal system. It has particular relevance facilitating improved technologies to treat or manage severe faecal incontinence.

KEY WORDS
Faecal incontinence, anorectal angle, rectum model

1. Introduction

Faecal Incontinence (FI) is the inability to carry out controlled defecation and leads to the involuntary passing of bowel content, including flatus, mucus and liquid and solid faeces. The overall prevalence of FI in adults is estimated between 11 and 15% and increases with age, with approximately 33% of people living in retirement homes (or similar institutions) affected [1]. Stigma and social taboo are associated with FI, leading to its underreporting [2].

1.1 Anatomy and Physiology of Continence

The rectum is a hollow muscular tube, typically 13cm in length when non-distended [3], composed of a continuous layer of longitudinal muscle that interlaces with the underlying circular muscle. The anus is a muscular tube 2.5-4cm in length [4]. At rest, it forms an angle of approximately 104.5° [5] with the axis of the rectum. During voluntary squeeze the angle becomes more acute, whereas during defecation, the angle becomes more obtuse, Figure 1.

Continence relies on the coordinated function of the nervous systems, gastrointestinal (GI) tract, and anal sphincter and pelvic floor musculature [6-10]. The sphincter complex (internal and external sphincters) applies pressure over the length of the anal canal creating occlusion, while the puborectalis (PR) and levator muscles produce occlusion in the upper anal canal. The PR also creates angulation between the anal canal and the rectum, termed the anorectal angle (ARA). The presence of an acute ARA has been considered important in maintaining continence [11, 12]. Dysfunction of only one of these components can result in severe FI, with common

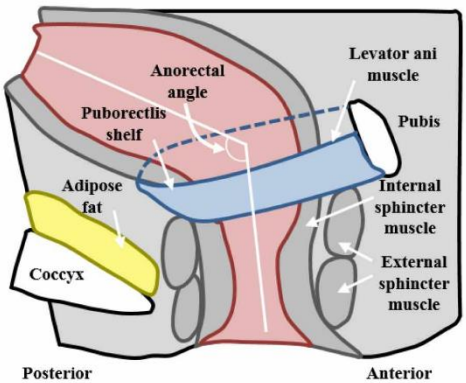

Figure 1 *Anatomy of the anorectum, components which are modelled include the rectum (red), puborectalis muscle (blue) and Adipose fat (yellow)*

causes including diarrhoea, obstetric trauma, spinal cord injury and rectal prolapse [13]. Faecal incontinence (FI) is a condition with profound consequences for individuals, their family/friends, and the wider healthcare system [14].

Efforts to improve the technology to treat FI have taken inspiration from those applied for urinary incontinence. These techniques involve using an inflatable cuff to occlude the urethra [15, 16]. Efforts to use a similar approach to treat FI by occluding the sphincter [17, 18] have been plagued with complications including local ischaemia due to the occlusive pressures necessary to maintain continence [9, 19-21].

Alternative strategies to sphincter augmentation have also been explored. Notably, *in vitro* studies have shown that increasing ARA reduces the occlusion pressure required to hold back solids and semi-solids [22, 23]. Similarly, another study reported increased retention of semisolid material when increasing ARA in an ex vivo porcine rectum, but no effect for water [23]. The question of whether the ARA or sphincter occlusion pressure is a greater contributor to continence remains unanswered, despite previous studies comparing the two [24, 25]. It is evident that modulating ARA is a key feature in maintaining continence and provides a complementary strategy to sphincter augmentation. There are currently no clinically available devices that exploit these features.

Currently only a small number of surgical treatments are available for patients with severe FI and these focus on augmentation of the anal sphincter. Two treatments currently on the market include the passive FENIX [26] system and the active Acticon Neosphincter™ [27], for which studies have shown success rates (for people with a functioning device) of 65%, at a mean follow up of 26.5 months [28]. An alternative strategy is the post-anal repair operation for idiopathic FI, designed to correct an overly obtuse ARA [7] by reducing the angulation [29, 30].

The paucity of commercially available, clinically viable, systems to treat FI reflect the difficulty of designing to meet the multi-faceted challenges surrounding this complex condition. A key failure mode in existing systems occurs when device-tissue interaction causes tissue erosion, resulting in device migration or rejection [31, 32].

There is a clear clinical need to develop improved devices to treat FI, and recent research reveals promising opportunities to exploit ARA modulation. To further advance this work requires an in-depth biomechanical understanding of continence mechanisms and models to capture their complex behaviour. This would allow detailed investigation into the complex device-tissue interactions which occur in the biological system and provide test environments to speed development prior to pre-clinical and human trials.

Little work exists in this area; previous work has focussed on computational models. Finite element models of the pelvic floor have been developed in attempts to understand its function in the urinary and faecal continence mechanisms. One model has been developed to investigate the effect of stool consistency on continence [33]. While another looks at the effect of damaged ligaments on stress urinary continence [34]. Computational models have also been developed to characterise the global behaviour of the pelvic floor muscles [35-39]. However, there are large quantitative differences between the models and parameters used.

Whilst computational studies have been developed, a physical model provides opportunities to further understand the biomechanics of FI to help develop and optimise new systems for treatment. In particular, physical models can readily simulate the complex physical properties of faecal matter and the physical interactions between this and different tissues. Furthermore, they provide a convenient means to evaluate new treatment concepts. Accordingly, our research concerns the development of a physical model to investigate the effect of ARA on continence for the future development and evaluation of novel FI technologies.

This paper presents a compliant soft model of the human rectum, integrated with an *in-vitro* simulation, consisting of physical models and computational measurement and control, which provides a stable platform for repeatable testing. We demonstrate the capabilities of this model in a study which investigates the effect of changing ARA on continence. Results from the study are then discussed to evaluate the performance of the model and its implications for future treatments of FI.

2. Materials and Methods

This section details the development of our faecal system model and the testing regime used to investigate the effect of varying ARA on continence.

2.1 Model Overview

Our approach in developing a physical model of the faecal system is to combine soft silicone representations of key parts of the anatomy, computerised control and instrumentation to objectively monitor and regulate

physiologically relevant parameters and a stool simulant to obtain a realistic flow regime in the system.

The full biological continence mechanism is complex and consists of the coordinated function of the nervous systems, GI tract, and anal sphincter and pelvic floor musculature. Our current model is focussed on investigating the effect of varying ARA and accordingly we have simplified the system to facilitate fabrication and detailed analysis of this function.

The rectum, adipose fat and PR muscle components are simulated by cast, 1:1 scale, silicone models, anatomically positioned within a housing linking these elements to control and instrumentation, as shown in Figure 2. The system is driven through a stool injection mechanism (detailed in section 2.4) while the ARA is regulated through an active PR muscle as part of the continence mechanism. By varying the pressure exerted by the PR muscle on the rectum, the ARA can be controlled and its effects on faecal leakage are observed during influx of simulated stool. The anal canal is represented within the rectum geometry with no occlusion from the anal sphincter.

2.2 Soft Tissue Modelling

For accurate biomechanical representation of the soft tissues in the model, their geometry and mechanical properties were recreated using a silicone casting process and informed by data in the literature.

The rectum represents the most complex component in the system. The open source 3D-IRCADb model [40], Figure 3a, provides full 3D geometry of the rectum with appropriate levels of detail to enable fabrication. The dataset consists of segmented CT data from a 44 year old male patient with focal nodular hyperplasia of the liver, but no condition relating to FI. This model showed close agreement with other published works on the size and shape of the human rectum. However, it should be noted that this component could be interchanged with alternate geometries if required (e.g. to represent different anatomy).

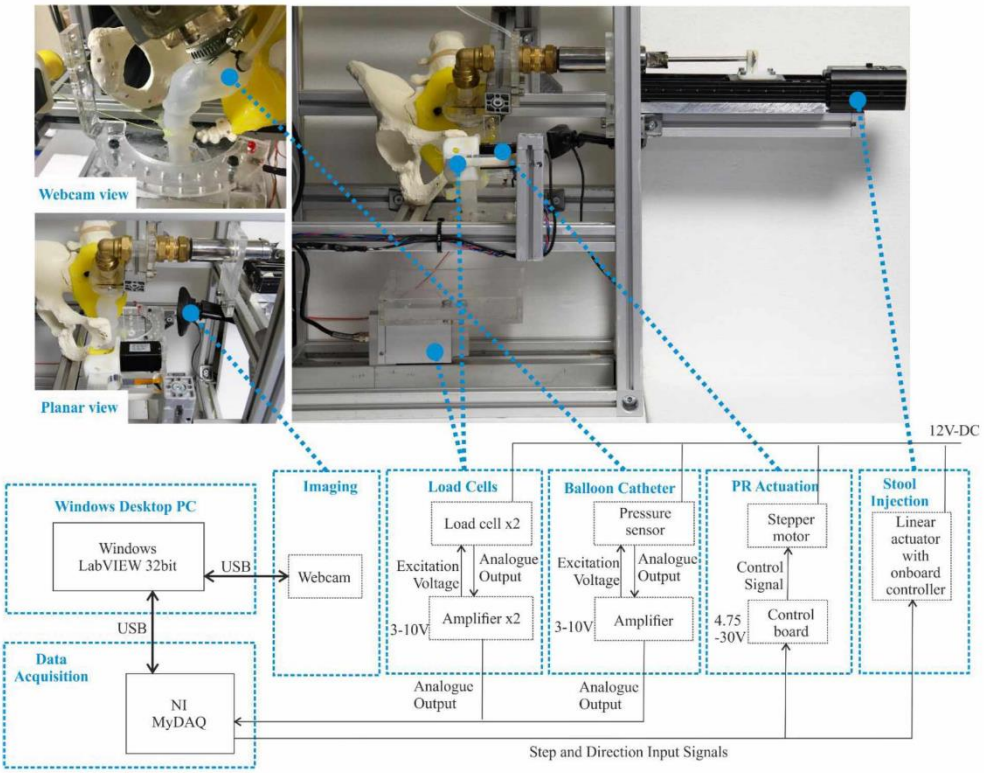

Figure 2 *A schematic overview of the faecal system simulation*

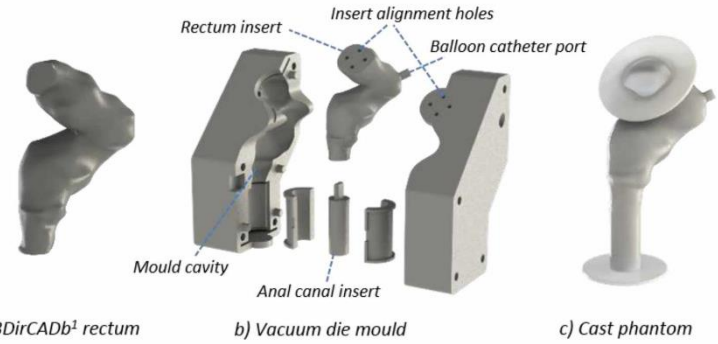

Figure 3 *Fabrication process for the rectum phantom model detailing a) the segmented 3D-IRCADb dataset geometry b) the 3D printed vacuum injection mould and c) cast phantom rectum phantom*

The 3D-IRCADb rectum model was imported into a 3D CAD package (SolidWorks™, Dassault Systèmes). The addition of flanges enabled the mechanical fixation of the soft model into the faecal simulation. A 3D CAD model of the mould, Figure 3b, was then constructed using the modified rectum geometry. The mould consisted of two halves with an insert. Fixation points allowed the rectum insert to be correctly aligned within the mould cavity such that a uniform wall thickness was achieved. The addition of a material reservoir and inlet ducts enabled fabrication of the rectum by vacuum casting. The mould was positioned in a vacuum chamber with pre-mixed, de-gassed silicone in the silicone reservoir. Air in the mould cavity is displaced by silicone as it escapes through holes between silicone trough and mould cavity. Once cured, the model could be de-cast.

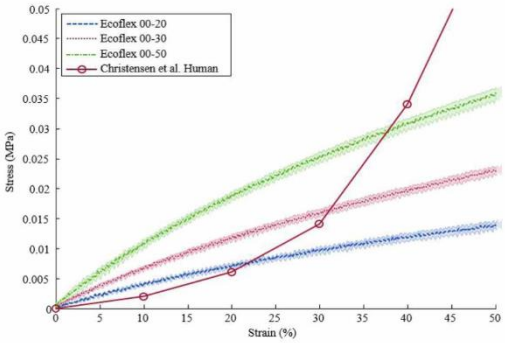

Figure 4 *Stress strain curves comparing different grades of silicone (with ±1STD shaded errors) to human rectum tissue [41]*

For mechanically realistic silicone models, linear force-displacement tests were carried out on 3 different grades of silicone for comparison to the loading curves for the biological tissues. Due to the non-linear mechanical behaviour exhibited by soft tissues like the rectum, an approximation was made, treating them as isotropic and matching their stress-strain profile across a normal physiological strain regime shown in Figure 4. The same methodology was applied to model the PR muscle and adipose fat components. Properties of the PR component were matched to tensile data of longitudinal external anal sphincter muscle tissue and the adipose fat component to properties of human adipose tissue [42]. The grades of silicone chosen to model each component are detailed in Table 1. Moulds for adipose tissue and PR were made using laser cut sections of laminar acrylic sheet glued together to form the 3D moulds. The posterior of the PR muscle was lined with an inextensible mesh to prevent longitudinal extension while maintaining a soft interface with the rectum.

Pelvic constituent	**Model material**
Rectum	Ecoflex 00-30 [6]
Adipose fat	1:1 wt% Ecoflex 00-20:SlackerTM [6]
PR	Inextensible mesh & Ecoflex 00-50 [6]

Table 1 *Test rig components and material details*

2.3 Modelling faeces

Tests to determine the physical properties of faeces have shown that they vary considerably in viscosity, hardness and consistency. Magnesium Aluminum Silicate NF Type IA (Vanderbilt Company) was used, as a pharmaceutical

grade smectite clay it is also used as simulated stool for nuclear medicine proctographic studies. It forms a homogenous substance with physical properties of density and viscosity comparable to those reported for soft faeces [43].

The shear rheological properties of fresh human faeces have been analysed. The method here adapts that presented by Woolley et al. [43] for analysing the effect of shear rate on dynamic viscosity of VEEGUM solutions.

Simulated homogeneous stool solutions were made by adding a predetermined wt% of VEEGUM R magnesium silicate powder to distilled water. The samples were dispersed using a chemical homogeniser for 2 minutes before being transferred immediately to the rheometer. Following homogenisation, samples were transferred to the rheometer vessel in preparation for testing. Experiments were performed repetitively (5 cycles) at 25°C on the same sample to determine the repeatability of flow curves and to establish if any breakdown or reconstruction had occurred during tests. Shear rate-apparent viscosity flow curves were produced for stool simulated samples of various moisture contents. Interpolated viscosity was plotted against moisture content (at a shear rate of $1s^{-1}$) and a power-law relationship enabled determination of the viscosity of stool simulant tested in the faecal simulation.

The measured moisture contents of human faeces range from 58.5% to 88.7% by mass [43], with apparent viscosities at $1s^{-1}$ ranging between 52.8 and 3306.3 Pa.s based on a power law relationship. In this study a stool simulant was selected at 90.5% water content, producing an apparent viscosity of 47.065 (Pa.s), within the bounds of high moisture content semisolid faecal samples.

2.4 Control and Data Acquisition

The faecal simulation was instrumented with a range of hardware detailed in Table 2. Sensing hardware was used to sample the PR muscle force, IR pressures and mass leakage. These data were recorded at a sample rate of 100HZ to monitor these variables over time as stool simulant was injected into the system.

Augmentation of the ARA was driven using a stepper motor and spool assembly, controlled by a host PC. The PR muscle is connected to the spool through an inextensible nylon cord and tightened against the anorectum through rotation of the spool, causing augmentation of the ARA. The stepper motor was mounted to a load cell allowing the forces acting on the anorectum by the PR to be measured. Stool simulant was introduced to the system by controlled injection using a lead-screw linear actuator which drove a syringe containing the stool simulant. Stool leakage from the anal canal is collected in a tray mounted to a second load cell such that mass, and mass flow rate, can be measured.

Testing variable	**Hardware**	**Manufacturer and model**
Anorectal angle	Stepper motor	RS Pro, 535-0366
Intra-rectal pressure	Balloon catheter	Medi Plus, 2309
	Pressure transducer	Utah Medical, Deltran® 6199
PR muscle force	Load cell	RS. 1004
Mass leakage	Load cell	RDP, RLS005kg

Table 2 *Control and sensing hardware*

LabVIEW™ (National Instruments) was used as a programming platform for the data acquisition, control and data logging described above.

2.5 Experimental Protocol: Effect of ARA on Continence

A test protocol was defined to investigate the effect of ARA on continence using the model system. In each test the system was configured and a fixed volume of stool simulant was injected into the rectum model at a constant flow rate. PR muscles forces were configured to produce a range of ARA values. Intra-rectal (IR) pressure, PR force and stool mass leakage values were recorded throughout.

The following protocol was followed for each test with the faecal system simulator.

1. Initialise System
Prime rectum with stool simulant using a rigid rectum housing until leakage from the anal canal occurs (to fill rectum without inducing strain)
2. Configure ARA position
Adjust PR until the desired ARA is achieved
3. Run Test
Initiate webcam recording and inject metered volume of stool simulate into the rectum at desired rate

4. End test
Wait until steady state (stool mass) is achieved, stop recording and save acquired data

During the tests, 59ml of stool simulate was delivered to the system at a constant flow of 9.26ml/s, a typical flow rate for stool being passed during defecation [44]. The tests were performed at room temperature (25°C). Stool simulant was prepared using the same technique as during rheology tests. Images of the rectum were analysed using ImageJ™ (National Institutes of Health) to measure the augmented ARA, varying PR force iteratively until it was correct within 0.5°. Measured outputs in each test were stool mass passed, PR muscle force and IR pressure. Tests for ARA effects were carried out at angles of 80°, 90°, and 100° with the previously described stool simulant. 5 repeats were carried out for each test. Each test was recorded using a high definition universal serial bus webcam (C920 HD Pro, Logitech).

3. Results

The full test protocol was successfully completed. Figure 5 shows images of each experimental configuration (obtained from the webcam) and the variation in ARA obtained by tensioning the model PR muscle.

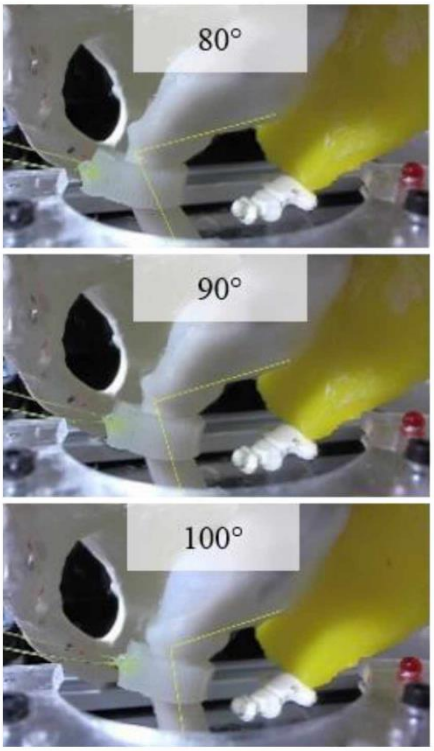

Figure 5 *View of the model rectum for the range of ARA values used in the experimental study*

The faecal mass, PR force- and IR pressure data recorded are displayed in Figure 6. These data demonstrate an effect of ARA on the resultant faecal leakage, evident in the reduction of total faecal mass passed increasing from 0.0139 kg at 80° to 0.0301 kg at 100°. The associated IR pressures show a similar increase during the initial phase of stool injection but diverge as the process approaches steady state, with higher pressures observed for lower values of ARA.

4. Discussion

Although rectal filling starts at t=0s, leakage of mass from the system doesn't occur until a period of around two seconds have passed. This delay is due to rectal filling whilst holdback pressures are great enough to overcome pressures produced by elastic energy stored in rectal walls. Fluctuation of the mass flow curve is apparent for all ARA values tested, with the phase of the fluctuation appearing larger at more acute ARA values and lower flow rates. These are formed as the semisolid exits the system in fluid globules, characteristic of viscous fluids

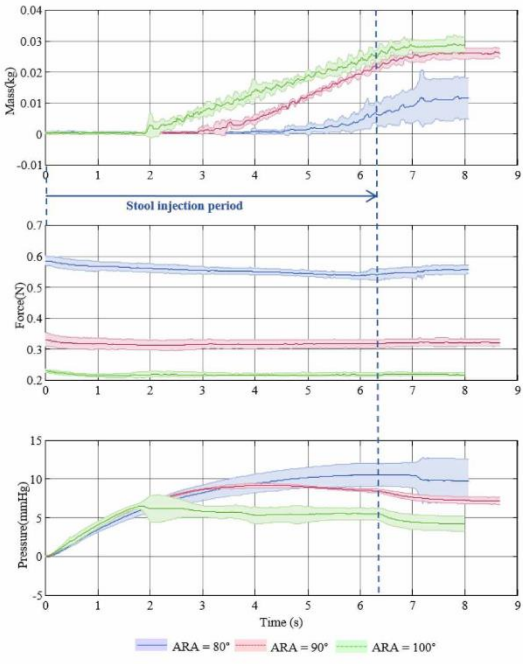

Figure 6 *Faecal mass passed, PR force and IR pressure versus time for different ARA values. Each plot shows mean (N=5) in solid with 1 STD as shaded region.*

with low surface tension under shear.

If the hold back pressure produced by PR muscle forces is sufficient, in relation to the simulated IR pressures, faecal leakage is reduced. Upon varying the ARA, a notable difference in leakage was observed between an ARA of 80° and 90°, increasing from 0.0139 to 0.0273kg. This demonstrates that as the ARA becomes more acute, a greater amount of stool is contained within the rectum during a controlled influx of stool. It would also appear that if a threshold ARA is exceeded, the amount of leakage is drastically improved. Whereas at more obtuse ARA values, small changes in angle have little effect on leakage.

This study demonstrates that to improve retention of semisolid material in the model rectum, it is not necessary to completely close the sphincter. Angulation of the rectum alone provides sufficient resistance to reduce stool leakage. Mean biological ARA values for healthy, nulliparous patients are measured at 104.5±10.3° at rest and 84.5±14.2° during squeeze [5]. These values are in agreement with the ARA's observed for the reduction in leakage in this study.

Due to the high variability and complexity of biological systems, the faecal system model has some limitations. The non-linear, anisotropic behaviour typically found in human soft tissue have been approximated with an isotropic silicone model. Furthermore, complex surface interactions which occur between the between the rectum, pelvic floor, bladder and other surrounding tissues have been neglected. Lastly, the current model uses a passive model, the active musculature in the rectum and sphincter have been neglected, most significantly the intrinsic contraction of the rectum and anal sphincter complex have not been included. Despite these simplifications it is evident that the behaviour of the model is informative and in agreement with that found in human subjects. Further refinements to this model will help increase its fidelity. In particular, continence relies upon the effects of ARA being augmented with anal sphincter contraction and these aspects will form the basis of future enhancements to the model, with active sphincter contraction and anisotropic material properties for the soft tissues.

4. Conclusion

The physical model has given an insight into the biomechanics of the human faecal system and the effect of the ARA on continence. As stool simulant is fed into the rectum, the volume expands as elastic potential energy is stored in the rectal walls. When the contraction of the rectum leads to IR pressures which are sufficient to overcome holdback pressures incurred by PR muscle forces, leakage from the anal canal occurs. As pressures reach an equilibrium, stool flows steadily from the anal canal. When the influx of stool into the rectum ceases, leakage continues at a reduced rate until the holdback pressure is sufficient to contain any remaining faeces in the rectum.

This work has shown that increasing the ARA increases continence. The study provides rational that augmenting the ARA could help relieve symptoms of chronic leakage associated with more severe cases of FI. Future work will consider the inclusion of an active anal sphincter system to explore their combined effects on continence.

References

1. Stoker, J., S. Halligan, and C.I. Bartram, *Pelvic Floor Imaging 1.* Radiology, 2001. **218**(3): p. 621-641.
2. Saga, S., et al., *Prevalence and correlates of fecal incontinence among nursing home residents: a population-based cross-sectional study.* BMC geriatrics, 2013. **13**(1): p. 1.
3. Snell, R.S., *Clinical anatomy for medical students.* 1995: Little, Brown Medical Division.
4. Williams, P., et al., *Splanchnology.* Gray's Anatomy, 36th edn. Churchill Livingstone, London, 1980. **1318**.
5. Piloni, V., et al., *Measurement of the anorectal angle by defecography for the diagnosis of fecal incontinence.* International journal of colorectal disease, 1999. **14**(2): p. 131-135.
6. Read, N., D. Bartolo, and M. Read, *Differences in anal function in patients with incontinence to solids and in patients with incontinence to liquids.* British journal of surgery, 1984. **71**(1): p. 39-42.
7. Parks, A., *Royal Society of Medicine, Section of Proctology; Meeting 27 November 1974. President's Address. Anorectal incontinence.* Proceedings of the Royal Society of Medicine, 1975. **68**(11): p. 681.
8. Yoshioka, K. and M. Keighley, *Critical assessment of the quality of continence after postanal repair for faecal incontinence.* British journal of surgery, 1989. **76**(10): p. 1054-1057.
9. Christiansen, J. and M. Lorentzen, *Implantation of artificial sphincter for anal incontinence.* The Lancet, 1987. **330**(8553): p. 244-245.
10. Dubrovsky, B. and D. Filipini, *Neurobiological aspects of the pelvic floor muscles involved in defecation.* Neuroscience & Biobehavioral Reviews, 1990. **14**(2): p. 157-168.
11. Parks, A., N. Porter, and J. Hardcastle, *The syndrome of the descending perineum.* Proceedings of the Royal society of Medicine, 1966. **59**(6): p. 477.
12. Ma, S., S.-Y. Leu, and R.-H. Fang, *Reconstruction of Anorectal Angle After Abdominoperineal Resection of Rectum and Anus-An Animal Model.* Annals of plastic surgery, 1989. **23**(6): p. 519-522.
13. Arnold Wald, M.D., Paul Hyman, M.D., Diane Darrell, A.P.R.N., William E. Whitehead, Ph.D. *Bowel Control Problems (Fecal Incontinence).* 2013 18th November 2016]; Available from:

https://www.niddk.nih.gov/health-information/health-topics/digestive-diseases/fecal-incontinence/Pages/facts.aspx.
14. Macmillan, A.K., et al., *The prevalence of fecal incontinence in community-dwelling adults: a systematic review of the literature.* Diseases of the colon & rectum, 2004. **47**(9): p. 1341-1349.
15. Burton, J.H. and B.G. Staehle, *Inflatable artificial sphincter*. 1987, Google Patents.
16. NURSE, D.E. and A. Mundy, *One hundred artificial sphincters.* British journal of urology, 1988. **61**(4): p. 318-325.
17. Sofia, C., et al., *Experiences with an artificial sphincter to establish anal continence in dogs.* The American Surgeon, 1988. **54**(6): p. 390-394.
18. Satava, R.M. and G.E. King, *An artificial anal sphincter. Phase 2: implantable sphincter with a perineal colostomy.* Journal of Surgical Research, 1989. **46**(3): p. 207-211.
19. Christiansen, J. and M. Lorentzen, *Implantation of artificial sphincter for anal incontinence.* Diseases of the colon & rectum, 1989. **32**(5): p. 432-436.
20. Christiansen, J. and B. Sparsø, *Treatment of anal incontinence by an implantable prosthetic anal sphincter.* Annals of surgery, 1992. **215**(4): p. 383.
21. Christiansen, J., *Advances in the surgical management of anal incontinence.* Baillière's clinical gastroenterology, 1992. **6**(1): p. 43-57.
22. Hajivassiliou, C. and I. Finlay, *Effect of a novel prosthetic anal neosphincter on human colonic blood flow.* British journal of surgery, 1998. **85**(12): p. 1703-1707.
23. Hajivassiliou, C., K. Carter, and I. Finlay, *Anorectal angle enhances faecal continence.* British journal of surgery, 1996. **83**(1): p. 53-56.
24. Shorvon, P., et al., *Defecography in normal volunteers: results and implications.* Gut, 1989. **30**(12): p. 1737-1749.
25. Bartolo, D., R. Miller, and N. Mortensen, *Sphincteric mechanism of anorectal continence during Valsalva manoeuvres.* Coloproctology, 1987. **9**: p. 103-7.
26. Torax® Medical, I. *The FENIX® Continence Restoration System*. 2014 [cited 2014 3rd October]; Available from: http://www.toraxmedical.co.uk/fenix/.
27. Gregorcyk, S.G., *The Current Status of the Acticon® Neosphincter.* Clinics in colon and rectal surgery, 2005. **18**(1): p. 32.
28. Devesa, J.M., et al., *Artificial anal sphincter.* Diseases of the colon & rectum, 2002. **45**(9): p. 1154-1163.
29. Bartolo, D., et al., *The role of partial denervation of the puborectalis in idiopathic faecal incontinence.* British journal of surgery, 1983. **70**(11): p. 664-667.
30. Mahieu, P., J. Pringot, and P. Bodart, *Defecography: II. Contribution to the diagnosis of defecation disorders.* Gastrointestinal radiology, 1984. **9**(1): p. 253-261.
31. Wong, W.D., et al., *The safety and efficacy of the artificial bowel sphincter for fecal incontinence.* Diseases of the colon & rectum, 2002. **45**(9): p. 1139-1153.
32. Congilosi, S., et al., *The artificial bowel sphincter: long-term experience at a single institution.* Dis Colon Rectum, 2002. **45**: p. A26.
33. Chanda, A., et al., *Computational Modeling of the Female Pelvic Support Structures and Organs to Understand the Mechanism of Pelvic Organ Prolapse: A Review.* Applied Mechanics Reviews, 2015. **67**(4): p. 040801.
34. Brandão, S., et al., *Biomechanical study on the bladder neck and urethral positions: simulation of impairment of the pelvic ligaments.* Journal of biomechanics, 2015. **48**(2): p. 217-223.
35. d'Aulignac, D., et al., *A shell finite element model of the pelvic floor muscles.* Computer Methods in Biomechanics and Biomedical Engineering, 2005. **8**(5): p. 339-347.
36. Gielen, A., P. Bovendeerd, and J. Janssen, *A finite element formulation of muscle contraction*, in *DIANA Computational Mechanics '94*. 1994, Springer. p. 139-148.
37. Kojic, M., S. Mijailovic, and N. Zdravkovic, *Modelling of muscle behaviour by the finite element method using Hill's three-element model.* International journal for numerical methods in engineering, 1998. **43**(5): p. 941-953.
38. Martins, J., et al., *A numerical model of passive and active behavior of skeletal muscles.* Computer methods in applied mechanics and engineering, 1998. **151**(3): p. 419-433.
39. Oomens, C., et al., *Finite element modelling of contracting skeletal muscle.* Philosophical Transactions of the Royal Society of London B: Biological Sciences, 2003. **358**(1437): p. 1453-1460.
40. 3Dircadb. *3D image reconstruction for comparison of algorithm database*. June 2013; Available from: http://www.ircad.fr/softwares/3Dircadb/3Dircadb.php?lng=en.
41. Christensen, M.B., K. Oberg, and J.C. Wolchok, *Tensile properties of the rectal and sigmoid colon: a comparative analysis of human and porcine tissue.* SpringerPlus, 2015. **4**(1): p. 1-10.
42. Alkhouli, N., et al., *The mechanical properties of human adipose tissues and their relationships to the structure and composition of the extracellular matrix.* American Journal of Physiology-Endocrinology and Metabolism, 2013. **305**(12): p. E1427-E1435.
43. Woolley, S., et al., *Shear rheological properties of fresh human faeces with different moisture content.* Water SA, 2014. **40**(2): p. 273-276.
44. Lestár, B., F.M. Penninckx, and R.P. Kerremans, *Defecometry.* Diseases of the Colon & Rectum, 1989. **32**(3): p. 197-201.

II. *A biomechanical model of the human defecatory system to investigate mechanisms of continence.* Proceedings of the Institution of Mechanical Engineers, Part H: Journal of Engineering in Medicine, 2018

A BIOMECHANICAL MODEL OF THE HUMAN DEFECATORY SYSTEM TO INVESTIGATE MECHANISMS OF CONTINENCE

William E. Stokes[1], David G. Jayne[2], Ali Alazmani[1], Peter R. Culmer[1]

1. University of Leeds, Woodhouse Lane, Leeds/UK

2. St James's University Hospital, Beckett St, Leeds/UK

mn10ws@leeds.ac.uk, d.g.jayne@leeds.ac.uk, a.alazmani@leeds.ac.uk, p.r.culmer@leeds.ac.uk

Abstract

Introduction: This paper presents a method to fabricate, measure and control a physical simulation of the human defecatory system to investigate individual and combined effects of anorectal angle and sphincter pressure on continence. To illustrate the capabilities and clinical relevance of the work the influence of a passive-assistive artificial anal sphincter (FENIX^{TM}) is evaluated.

Methods: A model rectum and associated soft tissues, based on geometry from an anonymised CT dataset, was fabricated from silicone and showed behavioural realism to the biological system and *ex-vivo* tissue. Simulated stool matter with similar rheological properties to human faeces was developed. Instrumentation and control hardware were used to regulate injection of simulated stool into the system, automate balloon catheter movement through the anal canal, define the anorectal angle and monitor stool flow rate, intra-rectal pressure, anal canal pressure and puborectalis force. Studies were conducted to examine the response of anorectal angles at 80°, 90° and 100° with simulated stool. Tests were then repeated with the inclusion of a FENIX device.

Results: Stool leakage was reduced as the anorectal angle became more acute. Conversely, intra-rectal pressure increased. Overall inclusion of the FENIX reduced faecal leakage, while combined effects of the FENIX and an acute anorectal angle showed the greatest resistance to faecal leakage. These data demonstrate that the anorectal angle and sphincter pressure are fundamental in maintaining continence. Furthermore it demonstrates that use of the FENIX can increase resistance to faecal leakage and reduce anorectal angles required to maintain continence.

Conclusions: Physical simulation of the defecatory system is an insightful tool to better understand, in a quantitative manner, the effects of the anorectal angle and sphincter pressure on continence. This work is valuable in helping improve our understanding of the physical behaviour of the continence mechanism and facilitating improved technologies to treat severe faecal incontinence.

KEY WORDS

Faecal incontinence, fecal, physiological model, incontinence device

1. Introduction

Faecal Incontinence (FI) is the inability to carry out controlled defecation and leads to the involuntary passing of bowel content, including flatus, mucus and liquid and solid faeces. Stigma and social taboo are associated with FI, leading to its underreporting (1). Despite this the known prevalence of FI in adults is high, estimated at 11-15% and increasing with age, where approximately 33% of people living in retirement homes (or similar institutions) are affected (2). Overall, FI is a condition with profound consequences for individuals, their family/friends, and the wider healthcare system (3). Unfortunately, treatment options for FI are limited and there is a consequent need to develop new understanding and technology to help address this deficit.

1.1 Anatomy and Physiology of Continence

Continence relies on the coordinated function of the nervous system, gastrointestinal tract, and anal sphincter and pelvic floor musculature (4-8). Figure 1 shows key parts of the anatomy associated with continence. The rectum, which stores faecal matter prior to defecation, is a hollow muscular tube approximately 13cm in length and composed of a continuous layer of longitudinal muscle that interlaces with the underlying circular muscle (9). The distal end of the rectum joins to the anal canal, a muscular tube 2.5-4cm in length which ends at the anus (10).

The anal sphincter complex (internal and external sphincters) applies pressure over the length of the anal canal, enabling it to be occluded. The puborectalis (PR) and levator muscles are anchored at the pubis and loop around the bottom of the rectum. They act to support this structure and can also occlude the top of the anal canal. The PR also acts to mediate the angulation between the anal canal and the rectum, termed the anorectal angle (ARA). The presence of an acute ARA has been considered important in maintaining continence (11, 12). At rest, the anal canal forms an angle of approximately 105° (13) with the axis of the rectum. During voluntary hold the ARA becomes more acute, whereas during defecation, the angle

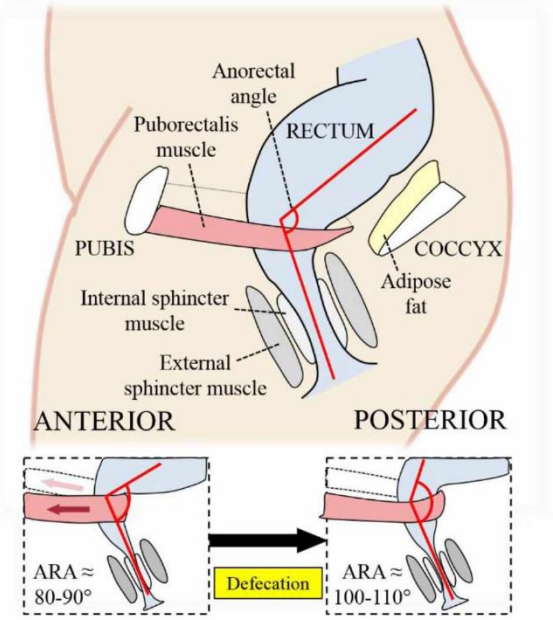

Figure 1 *A schematic showing key components of the physiology of the defecatory system and their action.*

becomes more obtuse.

During defecation, evacuation of faecal matter is promoted by minimising resistance to its passage while applying motive pressures. Relaxation of the anal sphincters minimises occlusion of the anal canal while relaxation of the PR enables the ARA to straighten so the bend is less acute. In conjunction abdominal pressures are elevated and the rectal wall muscle contract to force faeces through the rectum and anal canal until it is expelled at the anus. Dysfunction of any one of these components can result in FI, with common causes including diarrhoea, obstetric trauma, spinal cord injury and rectal prolapse (14).

1.2 Clinical Treatment of FI

Treatment to address FI is a complex process, a reflection of the multifaceted, interlinked causative factors and the wide array of physiological mechanisms used to maintain continence. Conservative methods such as dietary modifications, lifestyle alteration, constipating drugs, suppositories and biofeedback therapies (15) are effective at treating mild cases of FI. As symptoms become more severe, treatment modalities move toward surgical intervention.

Sacral nerve modulation and sphincteroplasty are the commonest surgical modalities for the treatment of FI, but their efficacy deteriorates in the longer term. There is therefore a need for treatments with more durable benefit. For worse cases of FI, efforts have been made to use technology developed for urinary incontinence in which an implantable, manually inflatable cuff is used to occlude the urethra (16, 17). Unfortunately, using a similar approach to treat FI by occluding the sphincter (18, 19) has been plagued with complications including local ischaemia due to the occlusive pressures necessary to maintain continence (7, 20-22). Currently only a small number of implantable devices are available to treat patients with severe FI and these focus on augmentation of the anal sphincter. Two treatments currently on the market include the passive FENIX^{TM} (Torax Medical, Minnesota) (23) system and the active Acticon Neosphincter^{TM} (24), for which studies have shown success rates (for people with a functioning device) of 65%, at a mean follow up of 26.5 months (25). A previous, but less often used, strategy is the post-anal repair operation for idiopathic FI, designed to correct an overly obtuse ARA (5) by reducing the angulation (26, 27). More recently, the TOPAS posterior sling is designed to restore anorectal angulation, although in practice it has not shown to be particularly effective, with an improvement seen in 16.1% of patients at a mean follow up of 24.9 months (28).

The paucity of commercially available, clinically viable systems to treat FI reflects the difficulty of designing medical technologies to meet the multi-faceted challenges surrounding this complex condition. A key failure mode in many attempts at new technology has been when device-tissue interaction causes tissue erosion, resulting in device migration or rejection (29, 30). Alternative strategies to sphincter augmentation have also been explored. Notably, *in-vitro* studies have shown that increasing ARA reduces the occlusion pressure required to hold back solids and semi-solids (31, 32). Similarly, another study reported increased retention of semisolid material when

increasing ARA in an *ex-vivo* porcine rectum, but no effect for water (32). The question of whether the ARA or sphincter occlusion pressure is a greater contributor to continence remains inconclusive, despite previous comparative studies (33, 34). However, it is evident that modulating ARA is a key feature in maintaining continence and that this provides a complementary strategy to sphincter augmentation. Unfortunately, there are currently no clinically available devices that exploit these features.

1.3 Modelling FI

There is a clear clinical need to develop improved technology to treat FI, and a promising opportunity to exploit mechanisms around ARA modulation. To further advance this work requires an in-depth biomechanical understanding of the associated physiological continence mechanisms and the effect of rectal disorders to capture their complex behavior and interaction.

There is a dearth of research in this area. Existing work is dominated by the use of computational models to simulate aspects of the pelvic floor system. Finite element models of the pelvic floor have been developed in attempts to understand its function in the urinary and faecal continence mechanisms. One model has been developed to investigate the effect of stool consistency on continence (35), whilst another looks at the effect of damaged ligaments on stress urinary continence (36). Computational models have also been developed to characterise the global behaviour of the pelvic floor muscles (37-41). However, there are large quantitative differences between the models and parameters used (42).

Whilst computational studies have been developed, a physical model provides opportunities to further understand the biomechanics of FI to help develop and optimise new systems for treatment. In particular, physical models can readily simulate the complex physical properties of faecal matter and the physical interactions between faecal matter and different tissues. Furthermore, they provide a convenient means to evaluate new treatment concepts. Accordingly, our research concerns the development of a physical model to investigate the effect of ARA on continence for the future development and evaluation of novel FI technologies.

This paper presents a biomechanical model of the human defecation system with an exploratory study to illustrate its capabilities and relevance. Section 2 details the approach and constituent physical models of the anatomy combined with computational measurement and control. An exploratory study using this model is defined in Section 3 which aims to firstly investigate the effects of rectal compliance and changing ARA on continence and secondly explores the clinical relevance of the work by evaluating the influence of a passive-assistive artificial anal sphincter (FENIX). Results from the study are then reported in Section 4 and discussed in Section 5, with particular consideration of their relevance to inform future treatment options for FI.

2. Model Development

Our approach in developing a physical model of the faecal system is to combine soft silicone representations of key parts of the anatomy, computerised control and instrumentation to objectively monitor and regulate physiologically relevant parameters and a stool simulant to obtain a realistic flow regimen in the system.

2.1 Anatomical Representation

The full biological continence mechanism is complex and consists of the coordinated

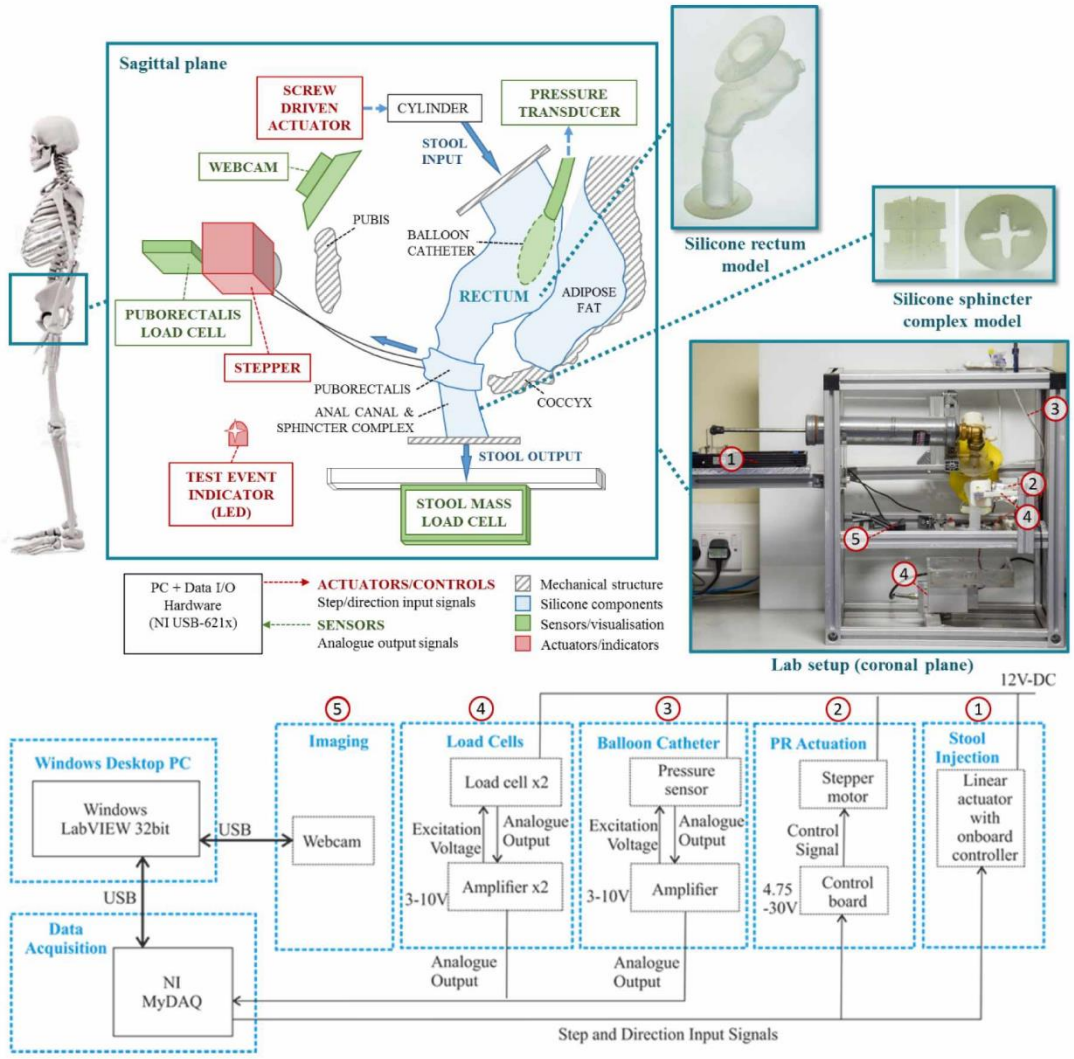

Figure 2 *Key components of the defecation model*

function of the nervous systems, gastrointestinal tract, and anal sphincter and pelvic floor musculature. Our current model is focused on investigating the effects of varying ARA and sphincter pressure, and accordingly we have simplified the system to facilitate fabrication and detailed analysis of these parts of the anatomy.
The model has been based on data for a 50th percentile adult male, although the methods and principles would extend to other percentiles, ages or gender. The rectum, adipose fat and PR muscle components are simulated by cast, 1:1 scale, silicone models, anatomically positioned within a housing linking these elements to control and instrumentation, as shown in Figure 2. The system is driven through a stool injection mechanism (detailed in section 2.4) while the ARA is regulated through an active PR muscle as part of the continence mechanism. By varying the pressure exerted by the PR muscle on the rectum, the ARA can be controlled and its effects on faecal leakage are observed during influx of simulated stool. The anal canal is represented within the rectum geometry with passive occlusion from an anal sphincter cuff. The anal sphincter occludes the anal canal by producing mucosal folds in the wall of the rectum phantom. This allows for expansion without elastic deformation of the rectal wall, to observe effects of sphincter pressure on the system.

2.2 Modelling Soft Tissues

A biomechanical representation of the soft tissue components in the model was achieved using a silicone casting process in which their geometry and mechanical properties were approximated.

Rectum Model

The rectum represents the most complex component in the model. The 3D geometry, shown in Figure 3a, was obtained from the open source 3D-IRCADb database (43) which contains a wide-range of high-fidelity anatomical structures, segmented from medical imaging by clinical experts, in 3D form. The particular dataset used here consists of segmented CT data from a 44 year old male patient with focal nodular hyperplasia of the

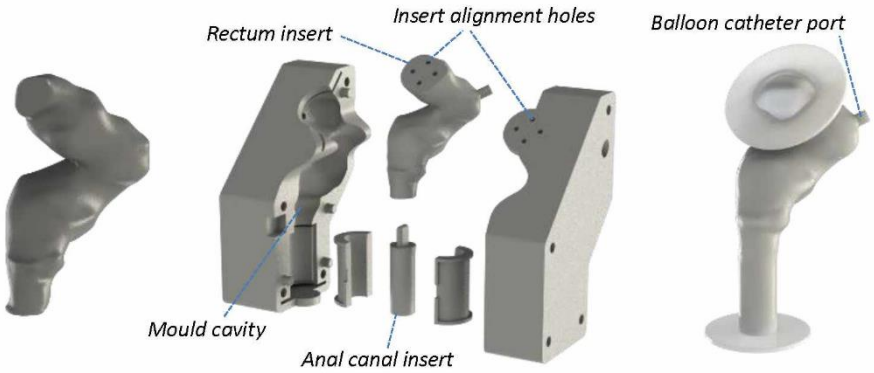

Figure 3 *Fabrication process of the rectum model with a) the segmented geometry b) the 3D printed vacuum injection mould and c) a cast rectum model in silicone*

liver, but no condition relating to FI. This model showed close agreement with other published works (9, 44) on the size and shape of the human rectum. However, it should be noted that this component could be interchanged with alternate geometries if required (e.g. to represent different anatomy).
To fabricate the rectum as a hollow silicone shell a custom mould was required. Firstly, the 3D geometry was imported into a CAD package (SolidWorks^{TM}, Dassault Systèmes) and modified to add flanges for mechanical fixation and interfacing with adjoining components. A 3D mould, Figure 3b, was then constructed using the modified rectum geometry. The mould consisted of two halves with an insert. Fixation points allowed the rectum insert to be correctly aligned within the mould cavity such that a uniform wall thickness was achieved. Lastly, a material reservoir and inlet ducts were added to the mould to enable fabrication by vacuum casting. With pre-mixed, de-gassed silicone in the material reservoir the mould was positioned in a vacuum chamber for 4 hours. When a vacuum is applied, air in the mould cavity is displaced with silicone where it cures, and the rectum model is de-cast (Figure 3c).

Soft tissues like the rectum exhibit highly non-linear mechanical behaviour which would be challenging to fully represent using a homogenous silicone material. However, based on the assumption that these tissues are operating within normal physiological conditions we found a good approximation could be achieved using commercial grades of silicone. To select this we compared the stress-strain response of passive human rectum tissue (45) within this limited strain regime [0-35%] to a range of commercially available silicone elastomers. Since the rectum is 'active' and modulates its contraction upon defecation we selected three variants of silicone whose compliance represent the rectum during contraction in healthy and diseased states (Dragon Skin 10A, 20A & 30A, Smooth-On Inc., Easton, USA).

Anal Canal and Sphincter Complex

The anal canal and sphincter complex are located at the distal end of the rectum (shown in Figure 2) and are modelled as a passive assembly, Figure 4, consisting of an inner silicone tube (the anal canal) and an outer constraint layer used to represent the combined occlusive action of the sphincter complex. The anal canal was modelled in a distended

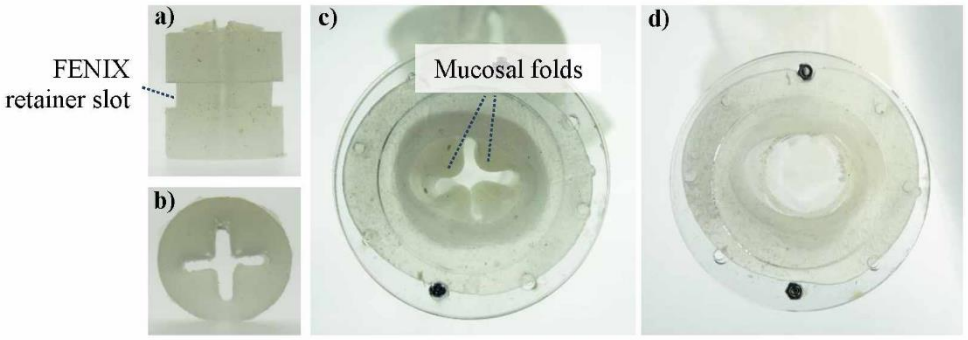

Figure 4 *The model sphincter showing a) side view; b) top view; c) simulated mucosal folds along the anal canal and d) the anal canal with the sphincter distended*

state (as during defecation) which is then constrained by the passive sphincter element to produce an occluded cross-section with features representing mucosal folds. The dimensions of these features were obtained from anatomical studies (46) and the 3D-IRCADb database (43) discussed above. A 1mm × 3mm retaining groove was added to the outer wall of the sphincter to locate the FENIX device and prevent the device moving longitudinally along the canal during use.

The anal canal and sphincter complex were fabricated from silicone elastomer (Ecoflex 00-30, Smooth-On Inc., Easton, USA), selected experimentally such that the resultant distensibility of the anal canal approximated that of a healthy adult in a rest state. A clinical anal manometry system (the EndoFLIP®, Crospon LTD (47)) was used to develop and validate this aspect, using the Distensibility index (DI) measure[1] (48, 49). The DI of the modelled anal canal complex was calculated at 4.18, in line with the ranges reported for healthy adults (DI=0.3-10.4, N=40) and those with FI (DI=0.7-12.1, N=34) (48).

Puborectalis Muscle

The puborectalis is part of the sheet-like *'levator ani'* musculature which forms a key part of the pelvic floor, anchored about the pelvis. It is the primary component of the levator ani associated with modulation of the ARA and therefore this model focuses solely on the PR, representing this structure as a simplified 'band' which wraps around the base of the rectum from anchor points at the pubis (40-42).

The key geometry of the PR in this model is its contact area at the rectum which was approximated from anatomical studies (46, 50) and defined as 18mm in width. The length of the PR is varied through an actuation mechanism described in the next section. The band was fabricated using a fine inextensible mesh (fiberglass mesh) embedded within a soft silicone elastomer (Ecoflex 00-50, Smooth-On, Inc.) to provide a soft interface between PR and rectum.

Connective and Supportive Structures

A range of elements were made to hold and support the functional parts of the defecation model (the rectum, anal canal and sphincter complex). An adult male pelvis model (Male Pelvis Skeleton, 3B Scientific, Hamburg, Germany) was used to house all the components and provide visual anatomical reference points for later analysis. Adipose fat was modelled using a soft silicone (Ecoflex 00-20, Smooth-On Inc., Easton, USA) to approximate the mechanical properties in healthy adults (51). The most distal part of the anal canal and the proximal end of the rectum were fixed relative to the pelvis using the soft silicone flanges and an adjustable aluminum framework (Rexroth, Bosch), positioned such that the combined rectum structure assumed a resting anatomical position (see Figure 1).

2.3 Modelling Faeces

[1] DI is defined as the cross sectional area at the narrowest point of the canal divided by catheter bag pressure at 50 ml inflation volume

Tests to determine the physical properties of faeces have shown that they vary considerably in viscosity, hardness and consistency. A pharmaceutical grade smectite clay, (VEEGUM R, Magnesium Aluminum Silicate NF Type IA, Vanderbilt Company), was selected as the stool medium for the simulation. It forms a homogenous solution with water that can be adjusted to obtain similar physical properties of density and viscosity comparable to those reported for soft faeces (52). This material is also used as simulated stool for nuclear medicine proctographic studies, enabling future comparative studies.
The formulation of the stool solution was determined through experimental analysis of its rheological properties. A range of samples were made by adding measured amounts of magnesium silicate powder to distilled water to produce 7, 8 and 9wt% magnesium silicate suspensions. Samples were dispersed using a chemical homogeniser for 2 minutes before being transferred immediately to the rheometer. Following homogenisation, samples were transferred immediately to a rheometer vessel to obtain shear rate-apparent viscosity flow curves for varying clay moisture contents. Interpolated viscosity was then plotted against moisture content (at a shear rate of $1s^{-1}$). The measured moisture contents of human faeces range from 58.5% to 88.7% by mass, with apparent viscosities at $1s^{-1}$ ranging between 52.8 and 3306.3 Pa.s based on a power law relationship. In this study the clay formulation was selected at 90.5% water content, producing an apparent viscosity of 47.065 Pa.s similar to high moisture-content semisolid faecal samples (52).

2.4 Measurement and Control

Instrumentation and control systems were integrated into the model to quantitatively measure key aspects of the model and to provide repeatable automation of the defecation process, as shown in Figure 2.
A central PC was used to coordinate the measurement and control components using a commercially available data interface (NI USB-621x, National Instruments Ltd.) in conjunction with a custom control program on the LabVIEW™ platform (National Instruments). The control program is used to define the operating configuration of the defecation model (e.g. parameters such as stool injection rate), to initiate experiments and to record subsequent data streams with reference to a hardware-timed clock.
Modulation of the ARA was driven using a stepper motor (RS Pro, 535-0366) and spool assembly, controlled by a host PC. The simulated PR muscle is connected to the spool through an inextensible nylon cord and tightened against the anorectum through rotation of the spool. The stepper motor was mounted to a load cell (RS, Model 1004) connected to an amplifier (DR7DC, RDP UK Ltd.) allowing the forces acting on the anorectum by the PR to be measured.
Stool simulant was introduced to the system by controlled injection using a lead-screw linear actuator (SMC, PSAA-60 W) which drove a 500ml syringe containing the stool simulant. Stool leakage from the anal canal is collected in a tray mounted to a second load cell (RDP, RLS005kg) connected to an amplifier (RDP, DR7DC) such that mass, and mass flow rate, can be determined.
A balloon catheter (Medi Plus, 2309) was located within the rectum and fed to a pressure transducer (Utah Medical, Deltran® 6199) connected to an amplifier (RDP, DR7DC) to obtain dynamic measures of pressure inside the rectum during simulated defecation.

A high definition universal serial bus webcam (C920 HD Pro, Logitech) was mounted on the model's supportive framework to provide a sagittal plane video-stream of the rectum at 30 Hz throughout each experiment. The video stream was used to monitor ARA (as shown in Figure 5) and was recorded by the control program for post-hoc analysis.

3. Experimental Methods

A study was defined to investigate the effects of ARA, rectum compliance and sphincter augmentation (using a FENIX device) on continence using the defecation model. This was achieved using an experimental matrix in which the controlled experimental variables were ARA (80°, 90° and 100°), rectum compliance (material was 10A, 20A or 30A DragonSkin) and sphincter state (baseline, with FENIX fitted). The FENIX was fitted for the extremes of the ARA values tested. A series of tests were defined to evaluate each permutation of these experimental parameters across 10 repeats. The control program was used to measure and record Intra-rectal (IR) pressure, PR force and stool mass leakage at 100Hz and the webcam stream at 30Hz.

All experiments were performed at room temperature (25°C). During the tests, 100ml of stool simulate was delivered to the system at a constant flow of 9.26 ml/s, a typical flow rate for stool being passed during defecation (53). Stool simulant was prepared using the same technique as during rheology tests.

The desired ARA was achieved by varying the PR length (through the control program) then analysing the webcam image of the rectum using ImageJ™ (National Institutes of Health) to measure the augmented ARA, as shown in Figure 5. This process was iterated until ARA was obtained within a tolerance of 0.5°. Subsequent repeats at this ARA used the same PR configuration to help ensure consistency.

The FENIX was fitted and configured as specified in the clinical guidance provided with the device. A supplied sizing tool was used to measure the sphincter circumference and thus determine the appropriate length of the device. It was then applied around the recess in the sphincter complex, as shown in Figure 5.

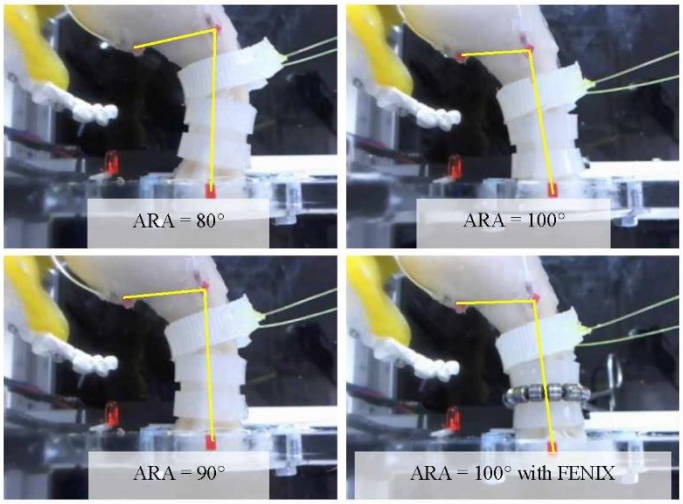

Figure 5 *View of the model rectum for the range of ARA values and sphincter configurations used in the experimental study*

The following protocol was followed for each experiment:

1. Initialise System: Prime the rectum with stool simulant, using a rigid rectum covering shell to prevent distention, until leakage from the anal canal occurs (thus filling the rectum without inducing wall strain).

2. Configure Experiment: Adjust the PR muscle length. Apply the FENIX is fitted if required

3. Initiate Recording: The control program is used to begin recording all sensor and webcam data to a time-stamped datafile.

4. Run Test: The syringe driver is started to inject a pre-metered volume of stool simulant into the rectum at a controlled rate

5. End test: 10 seconds after the system reaches steady state (with respect to stool mass) all data recording is stopped and saved to disk)

4. Results

The full study procedure was successfully completed for each specified experimental configuration. Figure 6 shows typical data obtained from the system for faecal mass passed and IR pressure during simulated defecation, in this case without the presence of sphincter augmentation.

From each experimental dataset, metrics for peak mass, pressure change and time at leakage were calculated, summarised in Table 1 and illustrated in Figure 6. These data demonstrate an effect of ARA on the resultant faecal leakage, evident in the reduction of total faecal mass passed decreasing from 0.0597 kg at 100° to 0.0109 kg at 80°. The associated IR pressures show a similar increase during the initial phase of stool injection

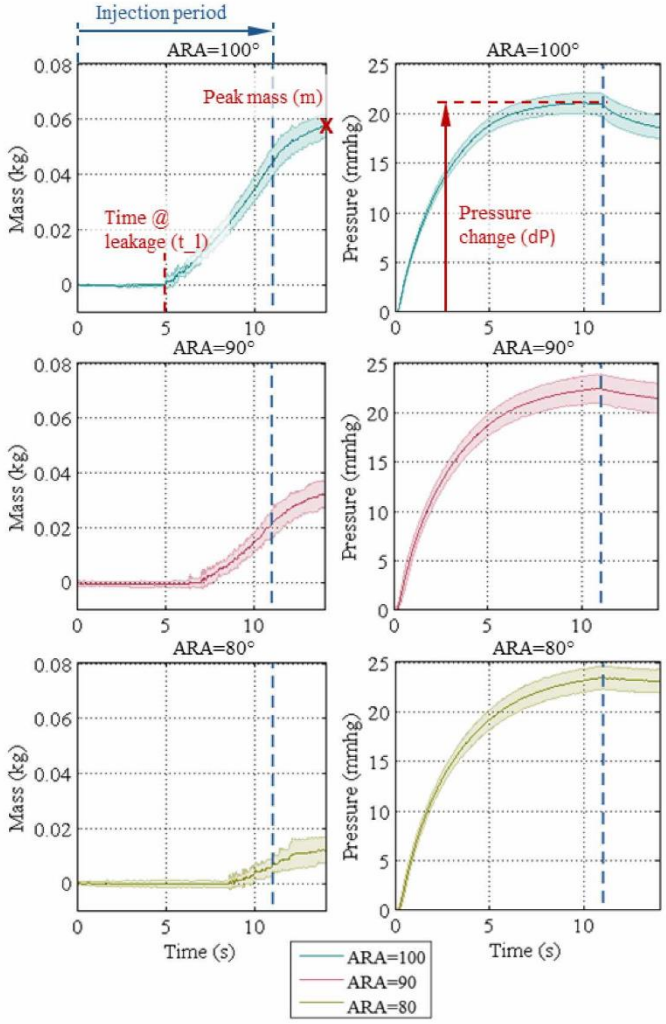

Figure 6 ***Left;*** *Faecal mass passed and* ***Right;*** *IR pressure versus time for different ARA configurations. Each plot shows mean (N=10) in solid with 1 STD as shaded region.*

but diverge as the process approaches steady state, with higher pressures observed for lower values of ARA.
The metrics shown in Figure 7 reveal how the effects of rectal compliance and sphincter augmentation (through the FENIX device) couple with changing ARA.

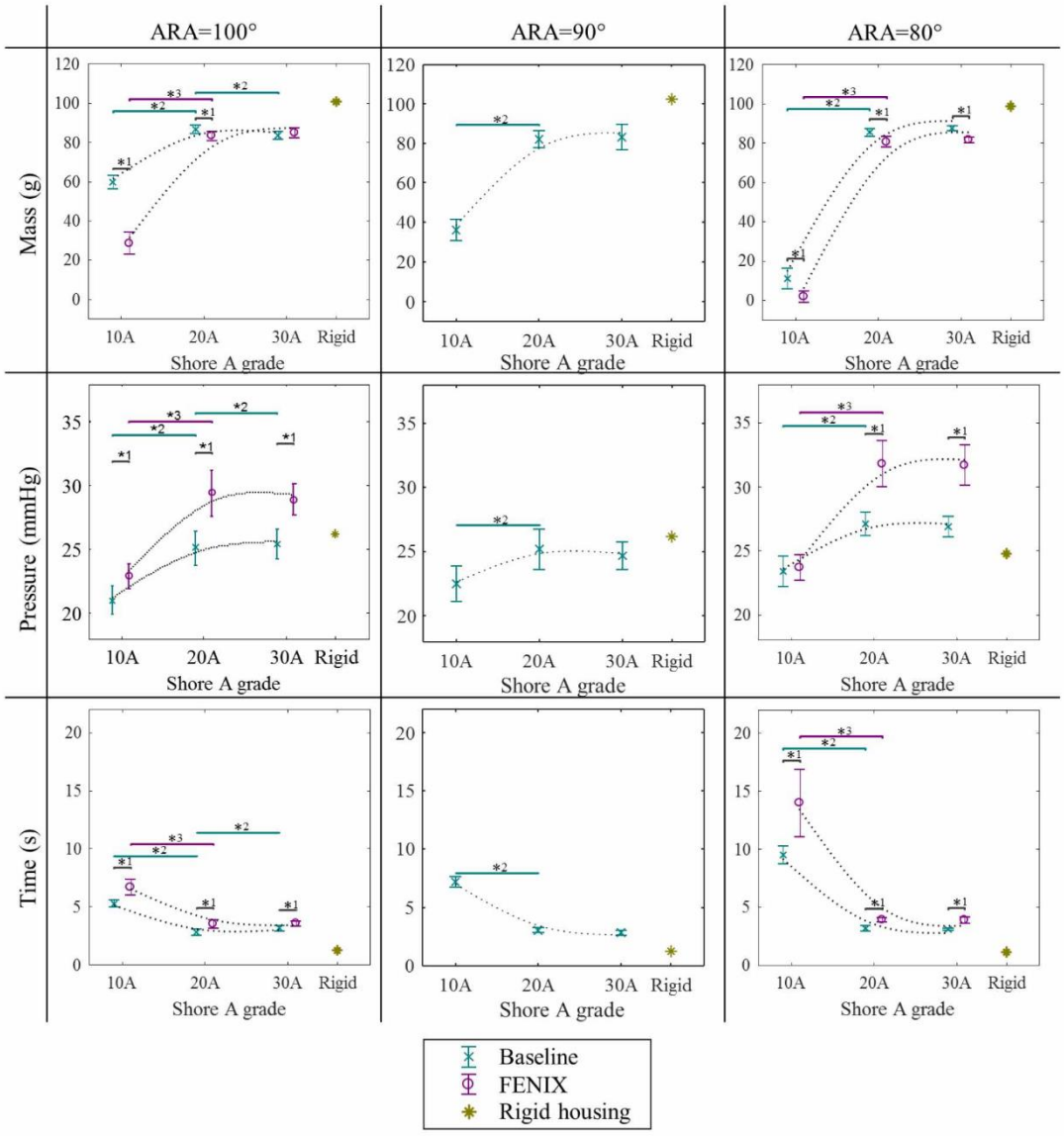

Figure 7 *Effects of rectal compliance on faecal mass passed* ***(top)****, IR pressure change* ***(middle)*** *and leakage time* ***(bottom)****. Each plot shows mean (N=10) with 1STD error bars. Statistical significance (P<0.05) is shown between configurations of sphincter state (*1), compliance without the FENIX (*2) and compliance with the FENIX (*3)*

Effect of sphincter occlusion on faecal leakage is most pronounced and significant ($p<0.05$) when rectum has a high compliance (10A) and the ARA is obtuse. As shown by

ARA	Compliance	Sphincter config.	m (g)	Sig.	dP (mmHg)	Sig.	t_l (s)	Sig.
100°	10A	Baseline	59.7±3.6	P<0.01	21.0±1.1	P<0.01	5.25±0.29	P<0.01
		FENIX	28.5±5.6		22.9±1.0		6.67±0.70	
	20A	Baseline	86.6±2.2	P<0.05	25.1±1.3	P<0.01	2.79±0.27	P<0.01
		FENIX	83.2±2.2		29.4±1.8		3.50±0.36	
	30A	Baseline	83.4±2.0		25.4±1.2	P<0.01	3.14±0.24	P<0.01
		FENIX	84.7±2.6		28.9±1.2		3.53±0.22	
90°	10A	Baseline	36.3±5.4		22.5±1.4		7.19±0.46	
	20A		82.1±4.4		25.2±1.6		3.04±0.23	
	30A		83.2±6.3		24.7±1.1		2.83±0.22	
80°	10A **(n=9)**	Baseline	10.9±5.2	P<0.01	23.4±1.2		9.49±0.79	P<0.01
		FENIX	1.8±2.9		23.7±1.0		13.96±2.9 **(n=8)**	
	20A	Baseline	85.5±2.0	P<0.01	27.1±0.9	P<0.01	3.17±0.23	P<0.01
		FENIX	80.6±2.8		31.8±1.8		3.91±0.20	
	30A	Baseline	87.4±1.3	P<0.01	26.9±0.8	P<0.01	3.05±0.09	P<0.01
		FENIX	81.5±1.4		31.7±1.6		3.87±0.26	

Table 1 *Mean vales ± 1SE (n=10) for stool injection tests, reporting peak mass (m), pressure change (dP) and time at leakage (t_l) for ARAs of 80° and 100°, significance is reported between the different sphincter states for each ARA*

a reduction of total faecal mass passed from 0.597 kg without the FENIX to 0.0285 kg with the FENIX, with good statistical significance ($p<0.001$). Effect of sphincter occlusion on faecal leakage is least pronounced and insignificant ($p>0.05$) for low rectal compliance (30A) and when the ARA is obtuse. Rectal compliance has a significant effect on faecal leakage for the range of ARA's observed between 10A and 20A. However little variation is observed between total mass passed at rectal compliances of 20A and 30A.

Effect of sphincter occlusion on IR pressure change is least pronounced and least significant for high rectal compliances (10A) and acute ARA's. Effect of the FENIX compared with baseline sphincter occlusion on IR pressure change is small but significant for high rectal compliance (10A) and obtuse ARA's. Effect of sphincter occlusion on IR pressure change is most pronounced and significant for lower rectal compliances (20A & 30A), with little effect apparent from the ARA at these compliances. Tests with a rectal compliance of 20A revealed no significant difference in the total faecal mass passed with and without the FENIX.

The effect of sphincter occlusion on time at faecal leakage is most pronounced and significant for high rectal compliance (10A) and acute ARA's. The effect of sphincter occlusion on time at faecal leakage is less pronounced for a rectal compliance of 20A, but highly significant ($P<0.0005$) for both ARA's. The effect of sphincter occlusion on time at faecal leakage is least pronounced and least significant for low rectal compliances (30A), particularly for obtuse ARA's.

5. Discussion

The results obtained from this study reveal the complex dynamics of the defecation process and the interplay between the mechanisms involved. A particular benefit of this model is the ability to control and time the processes involved, revealing the temporal characteristics of defecation. Once simulated stool starts to be introduced into the system (t=0s) there is a notable time lag before leakage of feacal matter which tends to occur after approximately two seconds have passed. This delay is due to rectal filling whilst holdback pressures are great enough to overcome pressures produced by elastic energy stored in the rectal walls. Consequently this delay varies as a function of rectal compliance, with longer delays observed from more compliant rectum models (which overcome the holdback pressure more slowly as they fill with stool simulant). This has a clinical analogue in those patients with low rectal muscle tone (and so compliance) who find it difficult to generate sufficient driving pressure to defecate.

The effect of the PR modulating the ARA is notable in this study. Upon varying the ARA, a notable difference in leakage was observed between an ARA of 80° and 100°, increasing from 0.0109 to 0.0597 kg. This demonstrates that as the ARA becomes more acute, a greater amount of stool is contained within the rectum during a controlled influx of stool. It would also appear that if a threshold ARA is exceeded, the amount of leakage is drastically reduced, whereas at more obtuse ARA values, small changes in angle have little effect on leakage. This signifies that more acute ARAs produce an elevation in the apparent hold back pressure, and that if this is sufficient in relation to induced IR pressures, faecal leakage will be reduced. Fluctuation of the mass flow rate is apparent for all ARA values tested, with the phase of the fluctuation appearing larger at more acute ARA values and lower flow rates. These are formed as the semisolid exits the system in fluid globules, characteristic of viscous fluids with low surface tension under shear.

In the simulation, augmentation of the sphincter complex using the FENIX device exhibits a similar effect to making the ARA more acute. Additional pressure applied to the anal canal by the FENIX causes a restriction to flow and thus greater retention of faecal matter in the rectum, with consequent increases in IR pressures. The FENIX was particularly effective when used with more compliant rectum models (10A), where a significant difference ($p<0.01$) was observed in peak masses passed from 0.0597 to 0.0285 kg and generated IR pressures of 21.0 and 22.9 mmHg respectively. However, the effect diminishes as variations were observed for less compliant rectum models (20A, 30A) although effects were still significant ($p<0.05$). This demonstrates that while sphincter augmentation can be effective at reducing faecal leakage it does not have universal application.

To defecate effectively requires a reduction in occlusive pressure at the sphincter and achieving a less acute ARA (i.e. straightening the rectum-canal configuration), as observed during proctographic studies (33). These traits are reflected in this study, particularly evident in tests using a low compliance rectum (30A), and an obtuse ARA (100°) for which case there is no statistical significance (p.0.05) for faecal mass passed at baseline (0.0834 kg) and with FENIX (0.0847 kg).

This study demonstrates that to effectively reduce faecal leakage, both anorectal angulation and occlusion pressure at the sphincter should be enhanced. Furthermore, it shows that to retain semisolid material in the rectum, it is not necessary to completely occlude the sphincter. Angulation of the rectum alone provides sufficient resistance to reduce stool leakage. Mean biological ARA values for healthy, nulliparous patients are measured at 104.5±10.3° at rest and 84.5±14.2° during squeeze (13). These values are in agreement with the ARA's observed for the reduction in leakage in this study. This highlights the potential to develop new technologies for FI which do not rely solely on occlusion of the anal canal to maintain continence but also include modulation of ARA. Too much of either mechanism would result in obstructed defecation. A combined and modulated strategy would allow a reduction in occlusive pressures and thereby help to mitigate against the issues of soft tissue erosion and device migration that have previously plagued implantable technology for FI.

To the best of our knowledge there are no other studies reported in literature on the use of physical simulations to understand mechanisms associated with continence, or for the modelling of FI disorders. While computational studies have been developed to model ligament damage on continence (36) and to provide an understanding of the biomechanics of the pelvic floor (37), fundamental mechanisms of continence have not been addressed, such as the ARA and sphincter pressures. This is probably due to the complexities of such modelling parameters. In contrast, use of a physical model allows complex interactions to be modelled with relative modelling ease, and establishes a basis around which refinements can be made in terms of biomechanical properties and physiology. Due to the high variability and complexity of biological systems, the faecal system model has some limitations. The non-linear, anisotropic behaviour typically found in human soft tissue have been approximated with an isotropic silicone model. Furthermore, complex surface interactions which occur between the between the rectum, pelvic floor, bladder and other surrounding tissues have been neglected. The anal canal closure mechanism is complex due to its interaction with adjoining tissue bodies, of particular relevance here is that contraction of the PR effects forces which act to occlude the anal canal, in conjunction with the EAS, due to connectivity of neighboring tissues. These features are only partially approximated in the current model. Lastly, the current model uses a passive model, the active musculature in the rectum and sphincter have been neglected, most significantly the intrinsic contraction of the rectum and anal sphincter complex have not been included. Despite these simplifications it is evident that the behaviour of the model is informative and in agreement with that found in human subjects. Further refinements to this model will help increase its fidelity. In particular, continence relies upon the effects of ARA being augmented with anal sphincter contraction when IR pressures are elevated, and these aspects will form the basis of future enhancements to the model, with the inclusion of intra-abdominal pressures and anisotropic material properties for the soft tissues, and inclusion of tissues adjoining the sphincter, PR muscle and rectum to the pelvis.

6. Conclusion

The physical model has given an insight into the biomechanics of the human faecal system and the combined effects of the ARA and sphincter pressure on continence. As stool simulant is fed into the rectum, the volume expands as elastic potential energy is stored in the rectal walls. When the contraction of the rectum leads to IR pressures which are sufficient to overcome holdback pressures incurred by PR muscle forces, leakage from the anal canal occurs. As pressures reach an equilibrium, stool flows steadily from the anal canal. When the influx of stool into the rectum ceases, leakage continues at a reduced rate until the holdback pressure is sufficient to contain any remaining faeces in the rectum.

This work has shown that, in this simulation, decreasing the ARA increases continence, and augmenting sphincter function improves continence. The study provides rationale that modulation of the ARA could help relieve symptoms of chronic leakage associated with more severe cases of FI, complementing occlusion of the anal canal by existing technology like the FENIX. Future work will increase the fidelity and scope of the physical simulation, as a means to develop new technologies for the treatment of FI.

Acknowledgements

This research has been financially supported by the IMPRESS Network.

This research would not have been possible without the continued support of the IMPRESS Network and the NIHR Healthcare Technology Co-operative, through the arrangement of regular networking events among clinicians, patients and engineers through which clinical needs were identified.

References

1. Saga S, Vinsnes AG, Mørkved S, Norton C, Seim A. Prevalence and correlates of fecal incontinence among nursing home residents: a population-based cross-sectional study. BMC geriatrics. 2013;13(1):1.
2. Stoker J, Halligan S, Bartram CI. Pelvic Floor Imaging 1. Radiology. 2001;218(3):621-41.
3. Macmillan AK, Merrie AE, Marshall RJ, Parry BR. The prevalence of fecal incontinence in community-dwelling adults: a systematic review of the literature. Diseases of the colon & rectum. 2004;47(9):1341-9.
4. Read N, Bartolo D, Read M. Differences in anal function in patients with incontinence to solids and in patients with incontinence to liquids. British journal of surgery. 1984;71(1):39-42.
5. Parks A. Royal Society of Medicine, Section of Proctology; Meeting 27 November 1974. President's Address. Anorectal incontinence. Proceedings of the Royal Society of Medicine. 1975;68(11):681.
6. Yoshioka K, Keighley M. Critical assessment of the quality of continence after postanal repair for faecal incontinence. British journal of surgery. 1989;76(10):1054-7.
7. Christiansen J, Lorentzen M. Implantation of artificial sphincter for anal incontinence. The Lancet. 1987;330(8553):244-5.
8. Dubrovsky B, Filipini D. Neurobiological aspects of the pelvic floor muscles involved in defecation. Neuroscience & Biobehavioral Reviews. 1990;14(2):157-68.
9. Snell RS. Clinical anatomy for medical students: Little, Brown Medical Division; 1995.
10. Williams P, Warwick R, Dyson M, Bannister L. Splanchnology. Gray's Anatomy, 36th edn Churchill Livingstone, London. 1980;1318.

11. Parks A, Porter N, Hardcastle J. The syndrome of the descending perineum. Proceedings of the Royal society of Medicine. 1966;59(6):477.
12. Ma S, Leu S-Y, Fang R-H. Reconstruction of Anorectal Angle After Abdominoperineal Resection of Rectum and Anus-An Animal Model. Annals of plastic surgery. 1989;23(6):519-22.
13. Piloni V, Fioravanti P, Spazzafumo L, Rossi B. Measurement of the anorectal angle by defecography for the diagnosis of fecal incontinence. International journal of colorectal disease. 1999;14(2):131-5.
14. Arnold Wald MD, Paul Hyman, M.D., Diane Darrell, A.P.R.N., William E. Whitehead, Ph.D. Bowel Control Problems (Fecal Incontinence) 2013 [Available from: https://www.niddk.nih.gov/health-information/health-topics/digestive-diseases/fecal-incontinence/Pages/facts.aspx.
15. Emmanuel A, Krogh K, Bazzocchi G, Leroi A, Bremers A, Leder D, et al. Consensus review of best practice of transanal irrigation in adults. Spinal cord. 2013;51(10):732-8.
16. Burton JH, Staehle BG. Inflatable artificial sphincter. Google Patents; 1987.
17. NURSE DE, Mundy A. One hundred artificial sphincters. British journal of urology. 1988;61(4):318-25.
18. Sofia C, Rush Jr B, Koziol J, Rocko J, Seebode J. Experiences with an artificial sphincter to establish anal continence in dogs. The American Surgeon. 1988;54(6):390-4.
19. Satava RM, King GE. An artificial anal sphincter. Phase 2: implantable sphincter with a perineal colostomy. Journal of Surgical Research. 1989;46(3):207-11.
20. Christiansen J, Lorentzen M. Implantation of artificial sphincter for anal incontinence. Diseases of the colon & rectum. 1989;32(5):432-6.
21. Christiansen J, Sparsø B. Treatment of anal incontinence by an implantable prosthetic anal sphincter. Annals of surgery. 1992;215(4):383.
22. Christiansen J. Advances in the surgical management of anal incontinence. Baillière's clinical gastroenterology. 1992;6(1):43-57.
23. Torax® Medical I. The FENIX® Continence Restoration System 2014 [Available from: http://www.toraxmedical.co.uk/fenix/.
24. Gregorcyk SG. The Current Status of the Acticon® Neosphincter. Clinics in colon and rectal surgery. 2005;18(1):32.
25. Devesa JM, Rey A, Hervas PL, Halawa KS, Larrañaga I, Svidler L, et al. Artificial anal sphincter. Diseases of the colon & rectum. 2002;45(9):1154-63.
26. Bartolo D, Jarratt J, Read M, Donnelly T, Read N. The role of partial denervation of the puborectalis in idiopathic faecal incontinence. British journal of surgery. 1983;70(11):664-7.
27. Mahieu P, Pringot J, Bodart P. Defecography: II. Contribution to the diagnosis of defecation disorders. Gastrointestinal radiology. 1984;9(1):253-61.
28. Mellgren A, Zutshi M, Lucente VR, Culligan P, Fenner DE, Group TS. A posterior anal sling for fecal incontinence: results of a 152-patient prospective multicenter study. American journal of obstetrics and gynecology. 2016;214(3):349. e1-. e8.
29. Wong WD, Congliosi SM, Spencer MP, Corman ML, Tan P, Opelka FG, et al. The safety and efficacy of the artificial bowel sphincter for fecal incontinence. Diseases of the colon & rectum. 2002;45(9):1139-53.
30. Congilosi S, Spencer M, Madoff R, Jensen L, Wong W, Rothenberger D. The artificial bowel sphincter: long-term experience at a single institution. Dis Colon Rectum. 2002;45:A26.
31. Hajivassiliou C, Finlay I. Effect of a novel prosthetic anal neosphincter on human colonic blood flow. British journal of surgery. 1998;85(12):1703-7.
32. Hajivassiliou C, Carter K, Finlay I. Anorectal angle enhances faecal continence. British journal of surgery. 1996;83(1):53-6.
33. Shorvon P, McHugh S, Diamant N, Somers S, Stevenson G. Defecography in normal volunteers: results and implications. Gut. 1989;30(12):1737-49.
34. Bartolo D, Miller R, Mortensen N. Sphincteric mechanism of anorectal continence during Valsalva manoeuvres. Coloproctology. 1987;9:103-7.
35. Chanda A, Unnikrishnan V, Roy S, Richter HE. Computational Modeling of the Female Pelvic Support Structures and Organs to Understand the Mechanism of Pelvic Organ Prolapse: A Review. Applied Mechanics Reviews. 2015;67(4):040801.

36. Brandão S, Parente M, Mascarenhas T, da Silva ARG, Ramos I, Jorge RN. Biomechanical study on the bladder neck and urethral positions: simulation of impairment of the pelvic ligaments. Journal of biomechanics. 2015;48(2):217-23.
37. d'Aulignac D, Martins J, Pires E, Mascarenhas T, Jorge RN. A shell finite element model of the pelvic floor muscles. Computer Methods in Biomechanics and Biomedical Engineering. 2005;8(5):339-47.
38. Martins J, Pato M, Pires E, Jorge RN, Parente M, Mascarenhas T. Finite element studies of the deformation of the pelvic floor. Annals of the New York Academy of Sciences. 2007;1101(1):316-34.
39. Zhang Y, Sweet RM, Metzger GJ, Burke D, Erdman AG, Timm GW. Advanced finite element mesh model of female SUI research during physical and daily activities. Stud Health Technol Inf. 2009;142(1):447-52.
40. Bhattarai A, Frotscher R, Sora M-C, Staat M. A 3D Finite Element model of the female pelvic floor for the reconstruction of urinary incontinence. Rev Urol. 2014;16(5):S2-S10.
41. Janda Š, Van Der Helm FC, de Blok SB. Measuring morphological parameters of the pelvic floor for finite element modelling purposes. Journal of biomechanics. 2003;36(6):749-57.
42. Silva M, Brandão S, Parente M, Mascarenhas T, Natal Jorge R. Biomechanical properties of the pelvic floor muscles of continent and incontinent women using an inverse finite element analysis. Computer Methods in Biomechanics and Biomedical Engineering. 2017;20(8):842-52.
43. 3Dircadb. 3D image reconstruction for comparison of algorithm database June 2013 [Available from: http://www.ircad.fr/softwares/3Dircadb/3Dircadb.php?lng=en.
44. Dall F, Jørgensen C, Houe D, Gregersen H, Djurhuus J. Biomechanical wall properties of the human rectum. A study with impedance planimetry. Gut. 1993;34(11):1581-6.
45. Christensen MB, Oberg K, Wolchok JC. Tensile properties of the rectal and sigmoid colon: a comparative analysis of human and porcine tissue. SpringerPlus. 2015;4(1):1-10.
46. Liu J, Guaderrama N, Nager CW, Pretorius DH, Master S, Mittal RK. Functional correlates of anal canal anatomy: puborectalis muscle and anal canal pressure. The American journal of gastroenterology. 2006;101(5):1092-7.
47. Sørensen G, Liao D, Lundby L, Fynne L, Buntzen S, Gregersen H, et al. Distensibility of the anal canal in patients with idiopathic fecal incontinence: a study with the functional lumen imaging probe. Neurogastroenterology & Motility. 2014;26(2):255-63.
48. Gourcerol G, Granier S, Bridoux V, Menard J, Ducrotté P, Leroi A. Do endoflip assessments of anal sphincter distensibility provide more information on patients with fecal incontinence than high-resolution anal manometry? Neurogastroenterology & Motility. 2016;28(3):399-409.
49. Alqudah M, Gregersen H, Drewes A, McMahon B. Evaluation of anal sphincter resistance and distensibility in healthy controls using EndoFLIP©. Neurogastroenterology & Motility. 2012;24(12).
50. Li D, Guo M. Morphology of the levator ani muscle. Diseases of the colon & rectum. 2007;50(11):1831-9.
51. Alkhouli N, Mansfield J, Green E, Bell J, Knight B, Liversedge N, et al. The mechanical properties of human adipose tissues and their relationships to the structure and composition of the extracellular matrix. American Journal of Physiology-Endocrinology and Metabolism. 2013;305(12):E1427-E35.
52. Woolley S, Cottingham R, Pocock J, Buckley C. Shear rheological properties of fresh human faeces with different moisture content. Water SA. 2014;40(2):273-6.
53. Lestár B, Penninckx FM, Kerremans RP. Defecometry. Diseases of the Colon & Rectum. 1989;32(3):197-201.

Appendix II: Clinical Meetings

I. IMPRESS Meetings

Date & time: 29/09/2014, 10:00-16:30

Location: St James University Teaching Hospital, Leeds

A meeting among clinicians, patients and engineers to present clinical needs associated with faecal incontinence.

Bowel – Faecal Incontinence

FI is a sign or symptom, not a diagnosis. It affects 1%-10% of adults and incidences increase with age.

- Patients undergo an examination, if their symptoms cannot be diagnosed, an investigation is carried out
- Investigations consist of colonic imaging, anorectal manometry and endoanal ultrasound and reveal physiological defects in patients:
    - Sphincter defect
    - Physiological function
        - Urge incontinence
        - Co-existent pudendal neuropathy
        - Passive incontinence
- The symptoms are classified into four categories which are treated using different methods
    - Loose Stools and Irritable Bowel Syndrome (IBS)
    - Passive incontinence
    - Sphincter failure (accounts for about 5% of all cases)

Sphincter Failure

- Specialist evaluation is important to determine if a surgically correctable cause is present
- Obstetric injuries and prolapse are most likely to benefit from surgery
- Conservative management can be effective for less serious cases
    - Dietary modification
    - Bulking and constipating agents
    - Rectal enemas

    - Irrigation techniques
    - Biofeedback therapy
- Surgical Intervention is required for severe FI
    - Anterior sphincteroplasty
    - Sacral Nerve Modulation
        - Posterior Tibial Nerve Stimulation
    - Graciloplasty
    - Artificial Bowel Sphincter

Interventional Treatment

Anterior Sphincteroplasty:

- Short-term results
    - 70% improved continence at 2 years follow-up
- Long-term results
    - Deteriorate with age
    - 50% improved continence at 5 years follow-up
    - Worse with large sphincter defect; multiple defects; atrophy; pudendal neuropathy

Sacral Nerve Modulation:

- Test Stimulation (2 weeks)
    - S3 stimulation
    - 50% improvement
- Permanent Implant

Complex 2nd Line Surgery:

Patients who fail the therapeutic strategies outlined above need to be considered for more complex surgery and therefore need to be assessed in a unit with experience of these.

- Stimulated gracilis neo-sphincter
- Artificial bowel sphincter

Artificial Bowel Sphincter:

- Inflatable Artificial Anal Sphincter

A fluid filled cuff is placed around the anal canal, mimicking the natural function of the sphincter muscle. When the fluid is displaced from the cuff, via a patient controlled pump, defecation can take place.

- Magnetic Anal Sphincter Augmentation:

The FENIX® Continence Restoration System is a new medical device to treat faecal incontinence. It consists of a ring of magnetic beads which is placed inside the body, around the outside of the anal sphincter in a surgical operation. It assists the muscles that normally stop you passing stools when you don't want to. It usually keeps them closed, but is designed to open to let stools pass when the person wants to open their bowels. Early studies on a few patients suggest that this device works but more studies are needed.

Stoma:

- Often considered treatment of last resort
- Quality of life often better than with FI

II. Clinical Interview with David Jayne

Date & time: 18/12/2014, 14:00-15:00

Location: St James University Teaching Hospital, Leeds

Present: A. Neville, M. Bryant, W. Stokes, S. King

David Jayne was visited at St. James' University Hospital and an hour was spent discussing the clinical needs in colorectal surgery and faecal incontinence.

Background

Research has been carried out into the development of an artificial anal sphincter, both active (Acticon Neosphincter) and passive (FENIX) devices have been researched and implanted while the graciloplasty procedure has also been practised. Studies into these methods have been limited or have revealed major limitations to their success. Due to the research already implemented in these areas, it is of the opinion that an entirely new approach to continence restoration is required.

Pelvic Floor and Puborectalis Reinforcement or Augmentation

In almost all cases of FI, an underlying problem is a lack of support from the pelvic floor. In conjunction, patients with weak pelvic floors tend to have poor Puborectalis function, both of which are crucial for maintaining continence. The diagram in figure 1 shows the Puborectalis muscle and its influence on the anorectum.

History

A number of operations were developed in the 20th century to provide a treatment solution to patients whose anal sphincter was intact but weak. One unique procedure is known as the Parks postanal repair, devised in 1975 the procedure used sutures to restore the anorectal angle. Despite a good success being observed in some patients, other procedures failed due to the limited properties of materials available, inadequate modification to the anorectal angle and poor patient cooperation with post-operative care [1].

Opportunities for Future Work

[1] Mayo Foundation for Medical Education and Research, *Treating patients with pelvic floor dysfunction*. 2014. [Date accessed: 19th December 2014]. Available from: http://www.mayoclinic.org/medical-professionals/clinical-updates/general-medical/treating-patients-with-pelvic-floor-dysfunction

There is scope for development of a medical device which modifies the Puborectalis or pelvic floor function. These procedures would be appropriate for a large proportion of patients who experience FI and have the ability to 'push' but may not be suitable for the minority with the most extreme cases.

The opportunity to obtain an electric stimulator was discussed; this could be used to investigate its effects on piezoelectric materials, which may give an indication of how it would augment human muscle.

Puborectalis

1. Use of a more suitable artificial material and fixation method (than Parks postanal procedure [2]) to tighten the Puborectalis muscle against the anorectal junction
2. Puborectalis muscle fixation to the pubic bone – potential for suitable fixation of a suture or sling
3. Reinforcement of the whole muscle or just a section
4. Passive material would require 'pushing' from the patient, active material could be actuated to relax during defecation

Pelvic Floor

1. Electric mesh which could stimulate the pelvic floor to restore tone
2. Potential for stimulation of innervation to the pelvic floor (similar to SNS)

[2] Parks, A. (1975). "Royal Society of Medicine, Section of Proctology; Meeting 27 November 1974. President's Address. Anorectal incontinence." Proceedings of the Royal Society of Medicine **68**(11): 681.

III. Clinical Interview with Damian Tolan

Date & time: 01/10/2015, 14:30-15:30

Location: St James University Teaching Hospital, Leeds

Present: P. Culmer, W. Stokes, S. King

Damian Tolan was visited at St. James' University Hospital and an hour was spent discussing the clinical needs in radiology and faecal incontinence.

Impaired pelvic floor function, effect on FI and treatment

Discussions were based around a test rig for the development of a puborectalis assistive FI device in relation to the normal biological system. In addition, the patient criteria for such a device were considered.

Background

- In patients whom experiences a lot of rectal descent, the pelvic floor is generally very poor
- Pelvic floor tone usually weakens with age however various factors can also cause a weak pelvic floor (e.g. collagen degenerative disorder etc.)
- Pelvic floor meshes generally fail due to the material not being flexible and compliant

Overview of imaging methods

There was discussion as to how closely the medium used to simulate faecal matter should mimic normal faeces.

- For dynamic MRI, an ultrasound jelly is used as the imaging medium
    - Dynamic MRI used for prolapse etc.
    - Jelly is dissimilar to faeces but allows imaging of rectal descent etc.
- For CT imaging, barium contrast is used
    - Damian uses non-viscous mixture of Ready Brek and injects using a syringe

Biomechanical study on intra-rectal pressure

Understanding the intra-rectal pressure under various conditions (rest/squeeze/strain) is crucial for the development of an active and adaptive device.

Upon defecation, intrinsic contraction of the rectum increases pressure, in addition to abdominal pressure.

To simulate this system in *vitro*, the rectal pressure and pelvic floor morphology upon defecation should be investigated:

- Carry out a series of tests which measure this pressure
    - In females via a pressure probe in the vagina (trans-vaginal pressure measurement)
- Pelvic floor morphology should be observed
    - Take measurements as they void
        - Strain and relaxed

Appendix III: Experimental Investigation – Mass, Force and Pressure Plots

This section presents plots of mass leakage, PR force and IR pressure. Using rectums fabricated from 3 different grades of silicone, tests were conducted with two ARA configurations (80° and 100°), and 3 sphincter configurations (without a device, with the FENIX & with the FENIX Plus). Metrics were calculated from this data to characterise the physical simulation and compare it to the human system.

1. Dragon Skin 10A

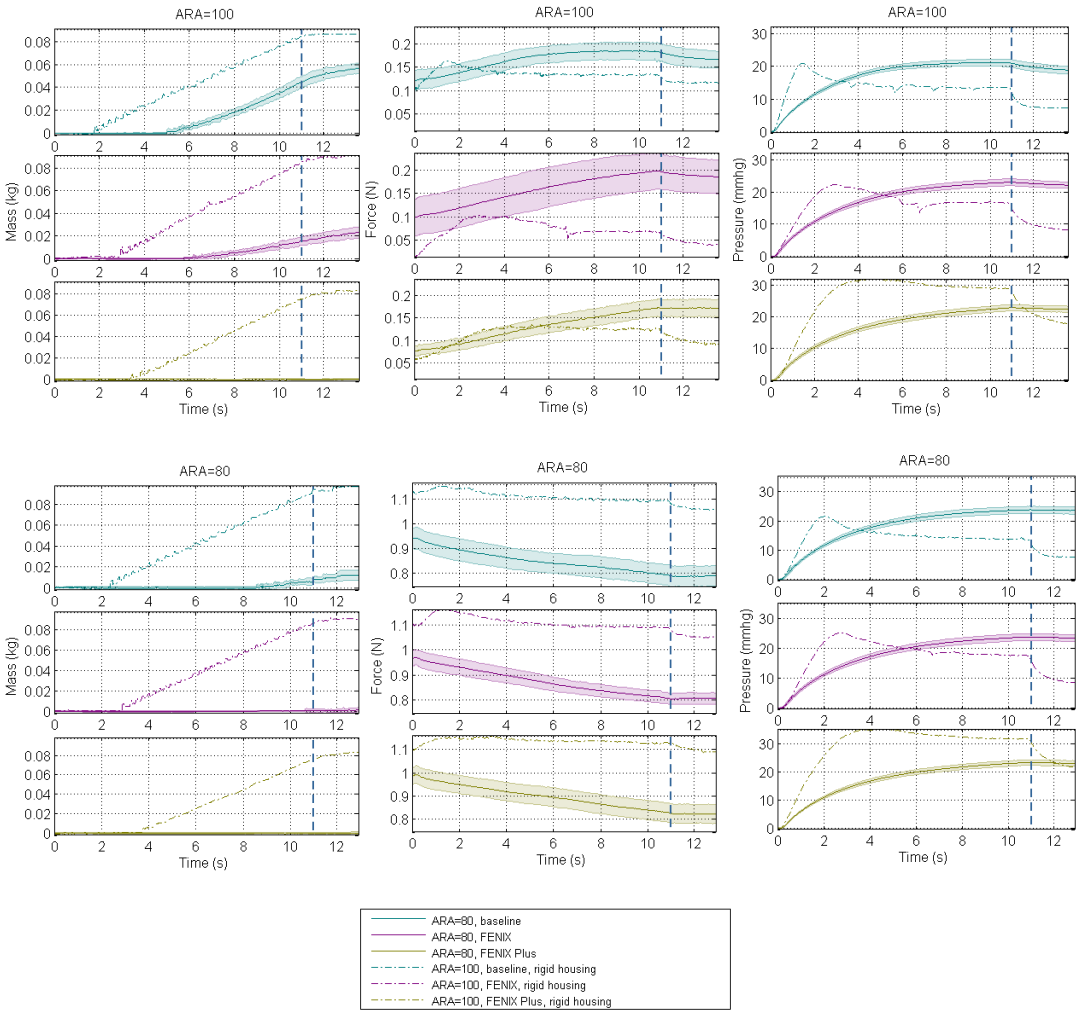

Figure 0.1 Plots of mass leakage, PR force and IR pressure, recorded during tests conducted with a rectum fabricated from Dragon Skin 10A.

2. Dragon Skin 20A

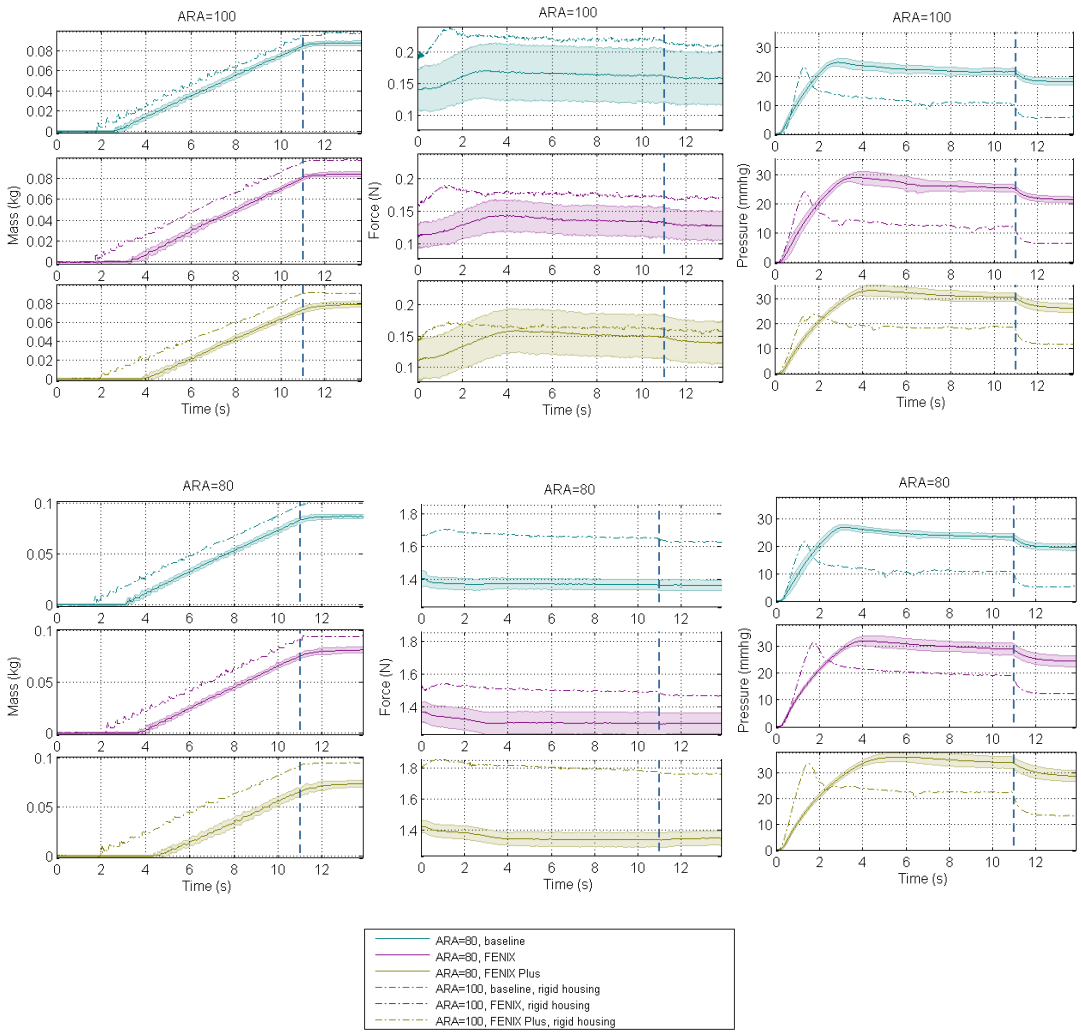

Figure 0.2 Plots of mass leakage, PR force and IR pressure, recorded during tests conducted with a rectum fabricated from Dragon Skin 20A.

3. Dragon Skin 30A

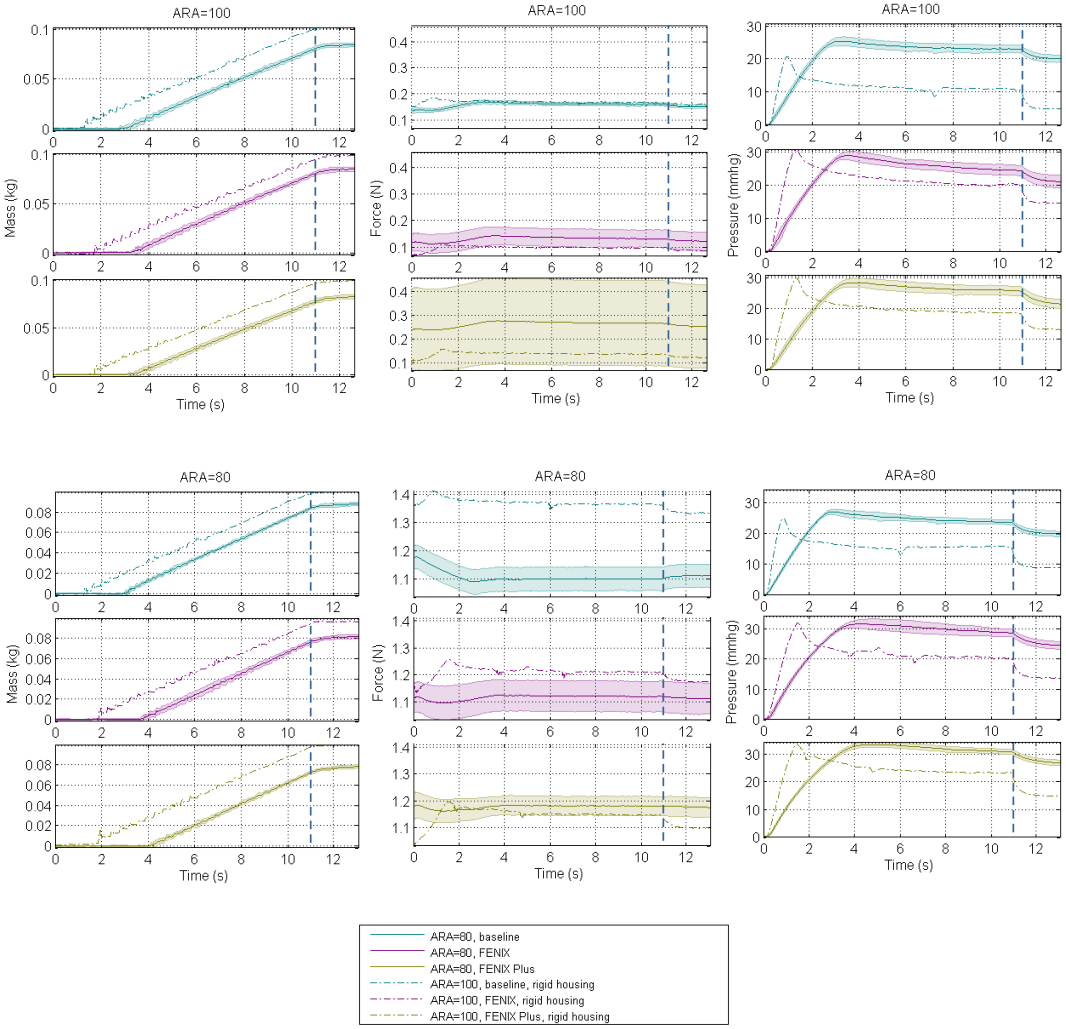

Figure 0.3 Plots of mass leakage, PR force and IR pressure, recorded during tests conducted with a rectum fabricated from Dragon Skin 30A.

Tests were also carried out using the same 3 grades of silicone, but with the ARA configured to 90°. These tests were conducted with the sphincter configured without a device:

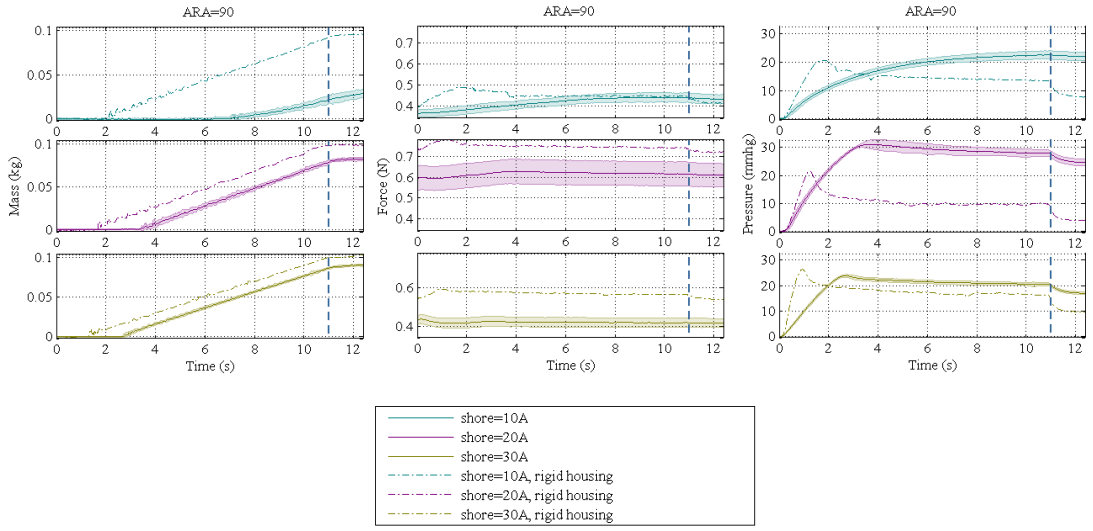

Figure 0.4 Plots of mass leakage, PR force and IR pressure, recorded during tests conducted with the ARA configured to 90°.

Appendix IV: Experimental Investigation – Raw Data

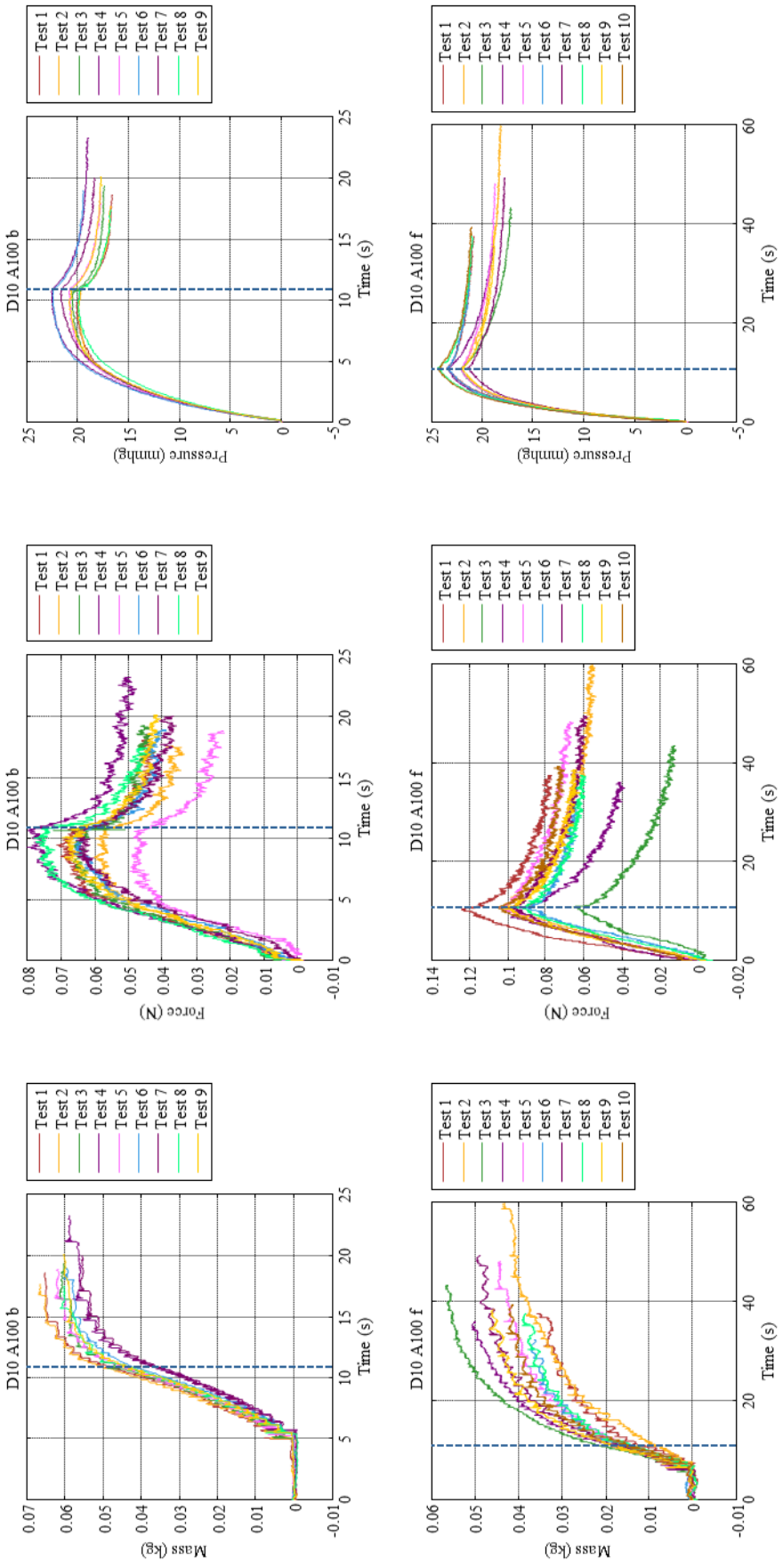

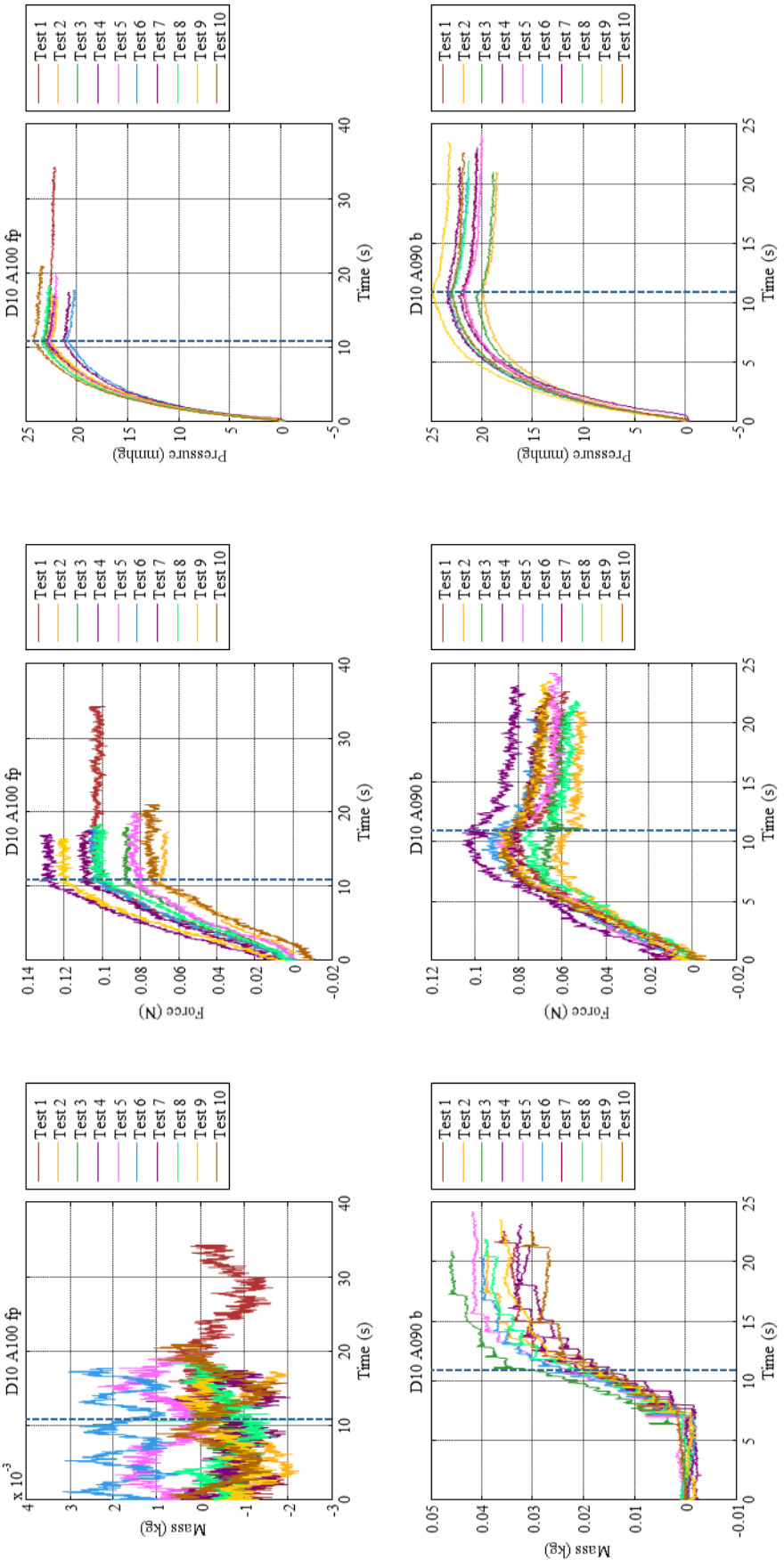
D10 A100 fp
D10 A090 b
Pressure (mmhg)
Force (N)
Mass (kg)
x 10^-3
Time (s)
Test 1
Test 2
Test 3
Test 4
Test 5
Test 6
Test 7
Test 8
Test 9
Test 10

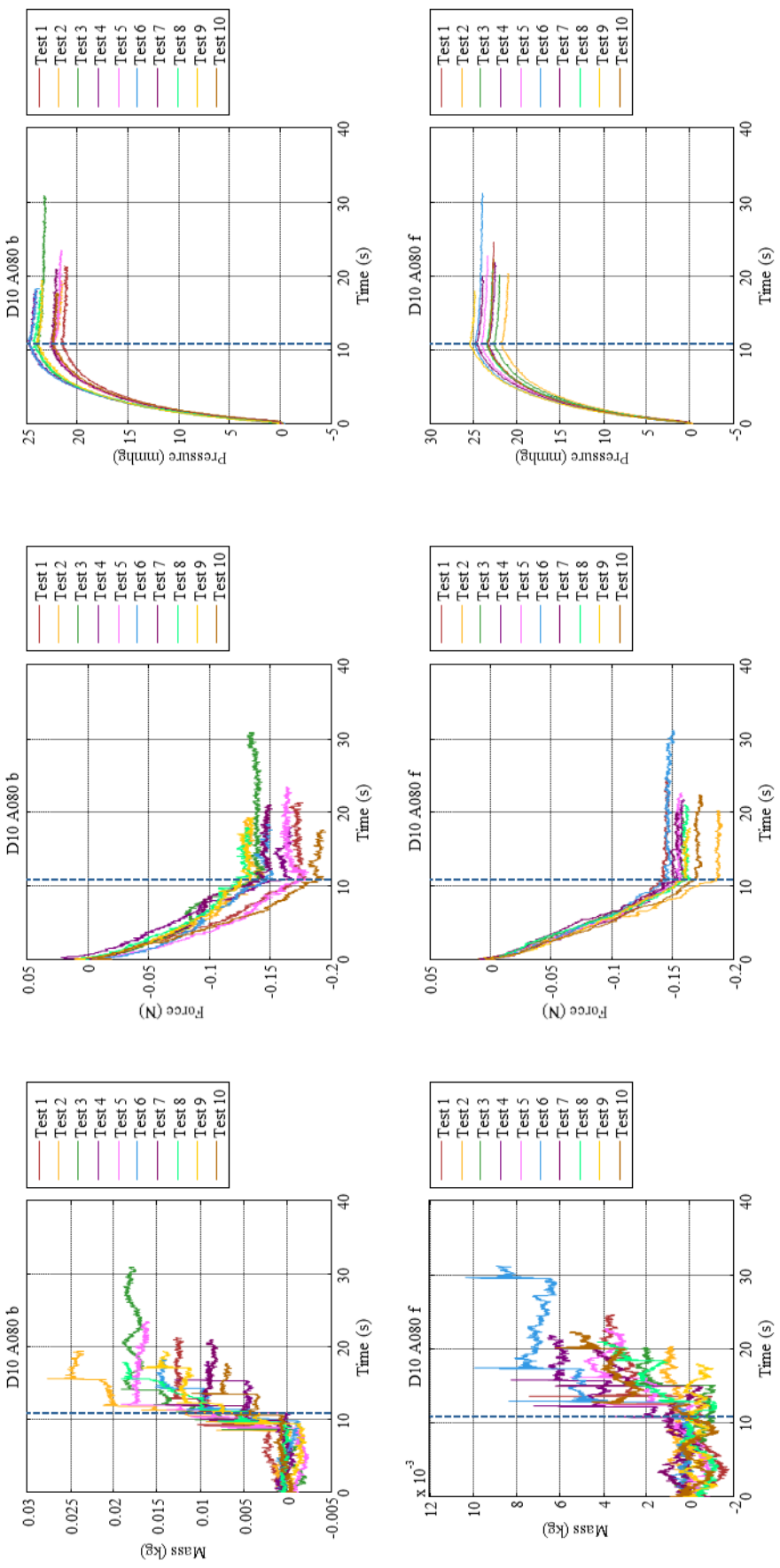
D10 A080 b
D10 A080 f
Time (s)
Pressure (mmhg)
Force (N)
Mass (kg)
x 10^-3
Test 1
Test 2
Test 3
Test 4
Test 5
Test 6
Test 7
Test 8
Test 9
Test 10

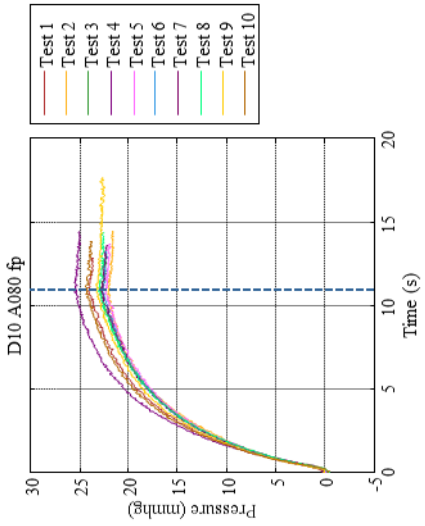
Test 1
Test 2
Test 3
Test 4
Test 5
Test 6
Test 7
Test 8
Test 9
Test 10
D10 A080 fp
Pressure (mmhg)
Time (s)

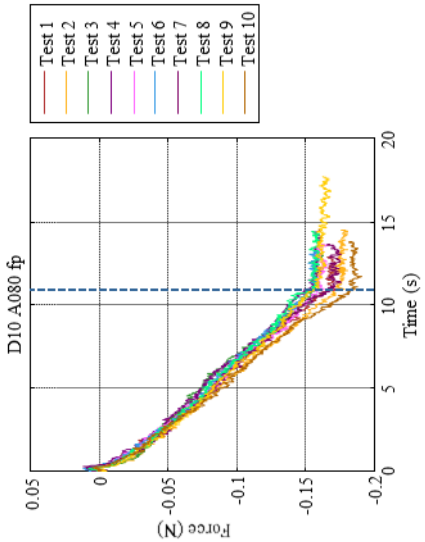
Test 1
Test 2
Test 3
Test 4
Test 5
Test 6
Test 7
Test 8
Test 9
Test 10
D10 A080 fp
Force (N)
Time (s)

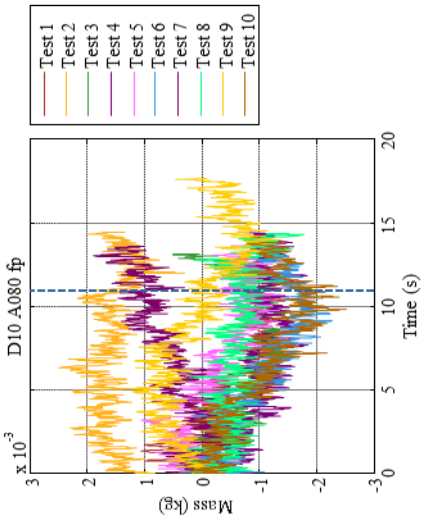
Test 1
Test 2
Test 3
Test 4
Test 5
Test 6
Test 7
Test 8
Test 9
Test 10
D10 A080 fp
x 10-3
Mass (kg)
Time (s)

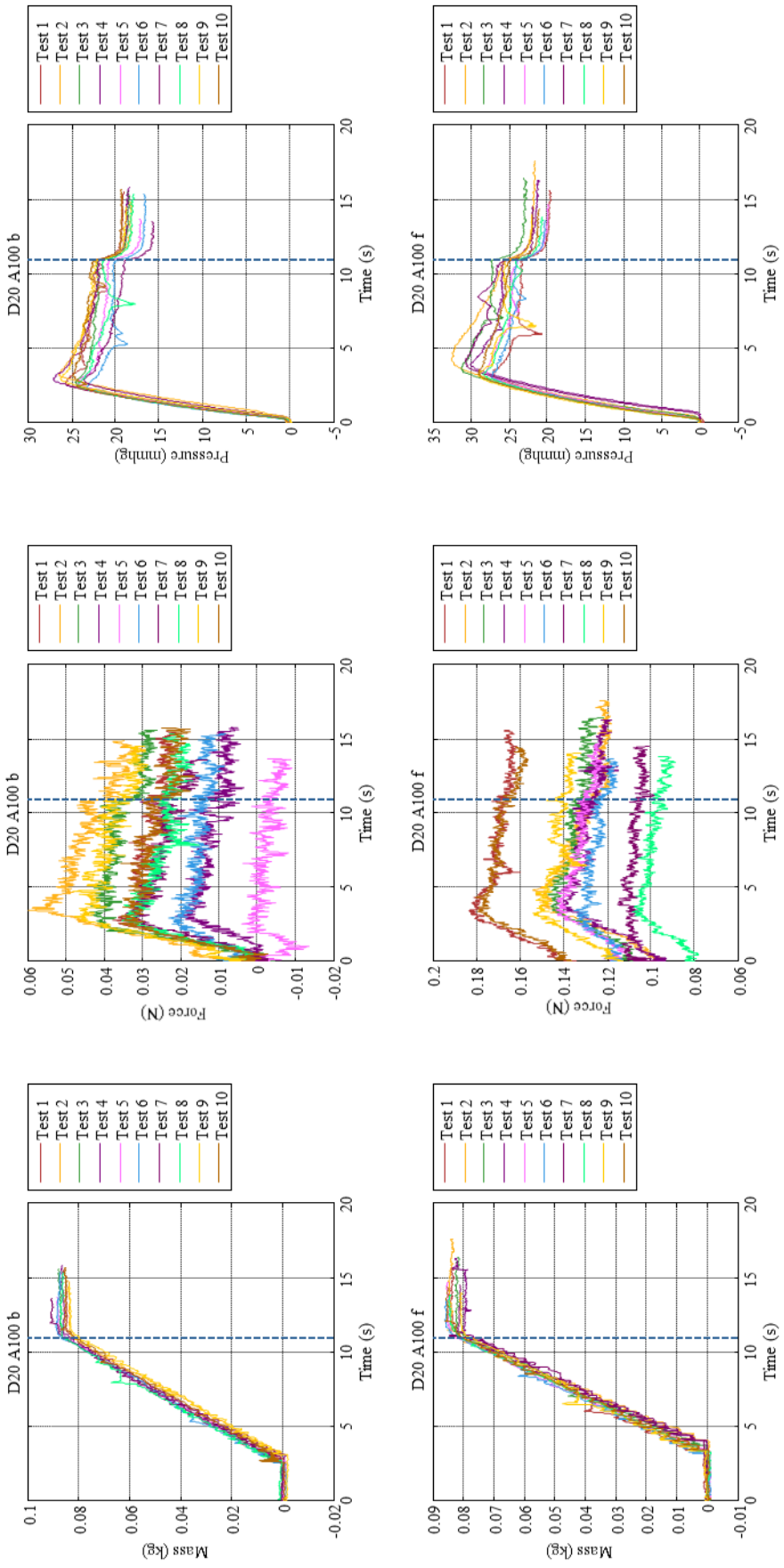
D20 A100 b
D20 A100 f
Time (s)
Pressure (mmhg)
Force (N)
Mass (kg)
Test 1
Test 2
Test 3
Test 4
Test 5
Test 6
Test 7
Test 8
Test 9
Test 10

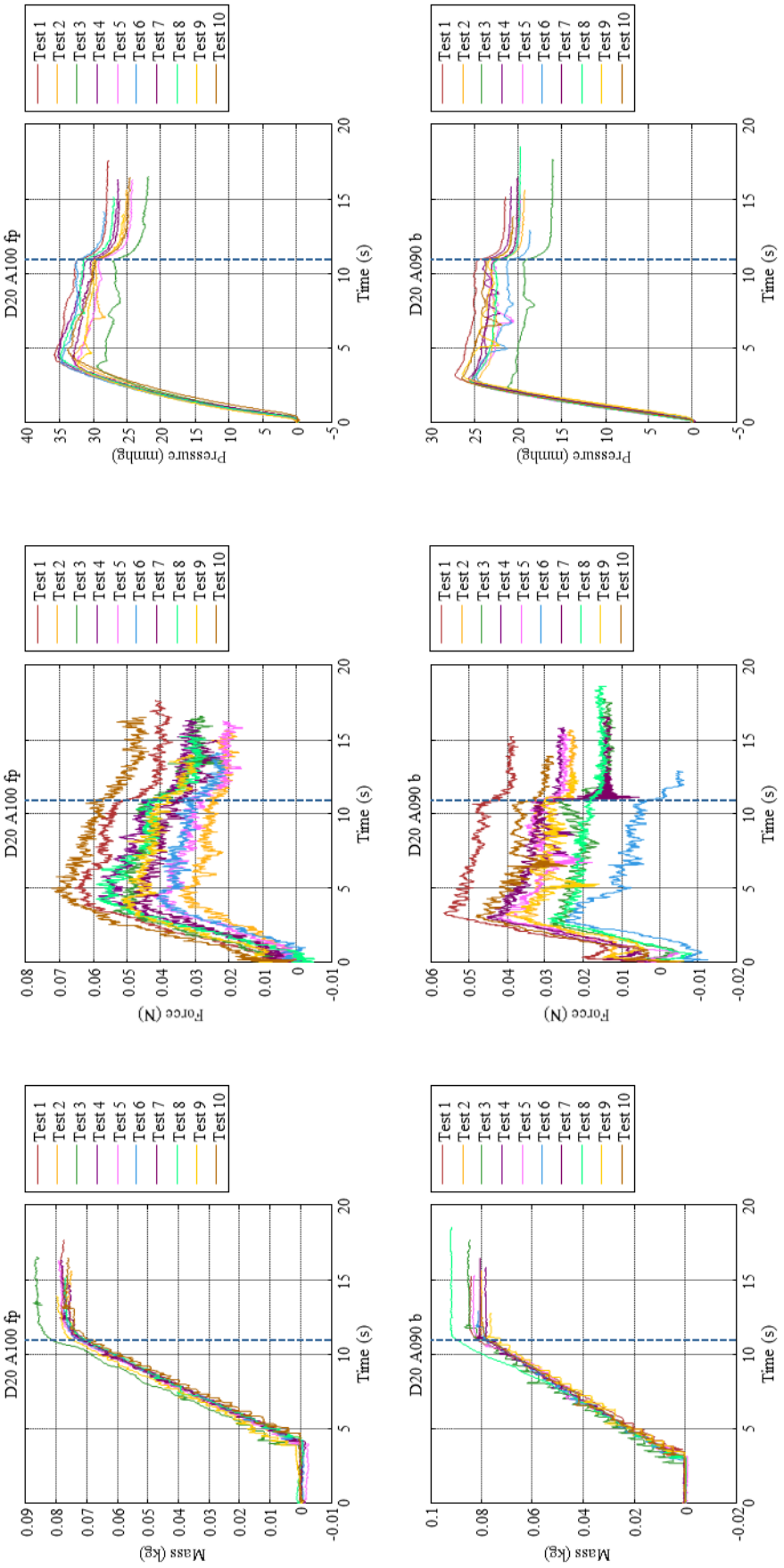
D20 A100 fp
D20 A090 b
Time (s)
Pressure (mmhg)
Force (N)
Mass (kg)
Test 1
Test 2
Test 3
Test 4
Test 5
Test 6
Test 7
Test 8
Test 9
Test 10

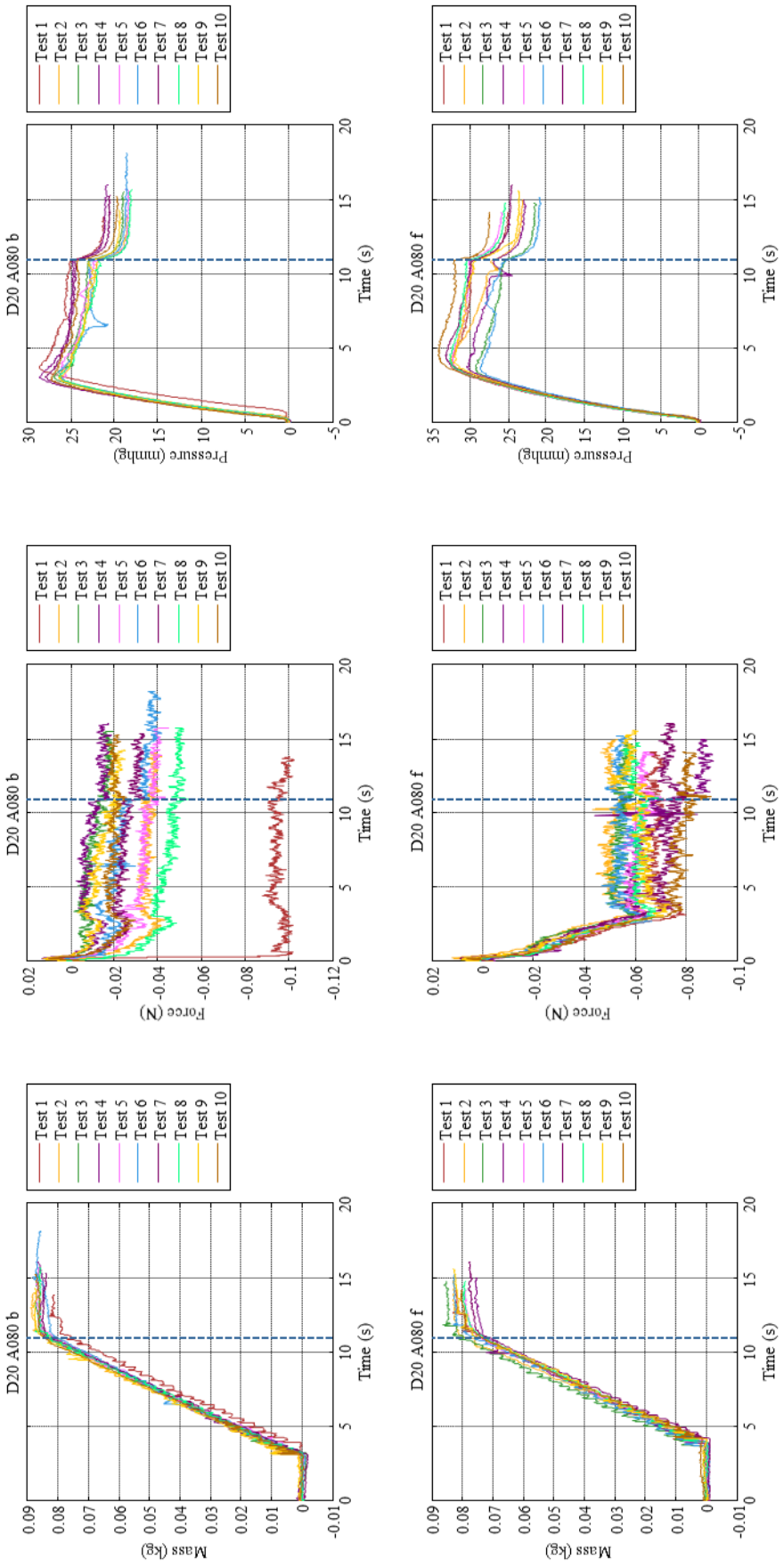
D20 A080 b
D20 A080 f
Time (s)
Pressure (mmhg)
Force (N)
Mass (kg)
Test 1
Test 2
Test 3
Test 4
Test 5
Test 6
Test 7
Test 8
Test 9
Test 10

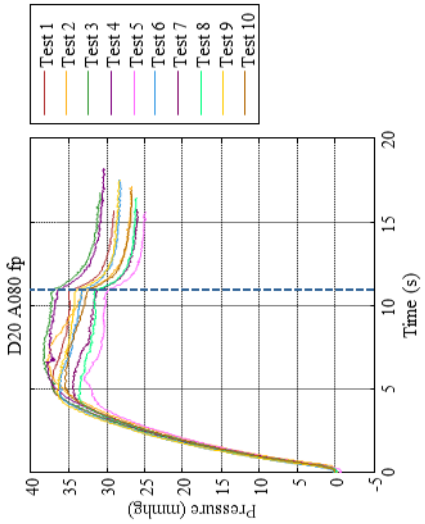
Test 1
Test 2
Test 3
Test 4
Test 5
Test 6
Test 7
Test 8
Test 9
Test 10
D20 A080 fp
Pressure (mmhg)
Time (s)

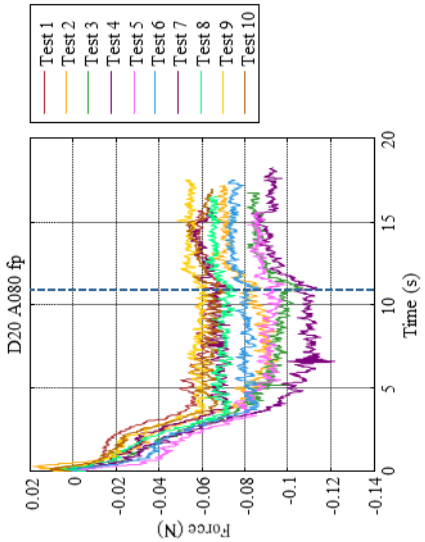
Test 1
Test 2
Test 3
Test 4
Test 5
Test 6
Test 7
Test 8
Test 9
Test 10
D20 A080 fp
Force (N)
Time (s)

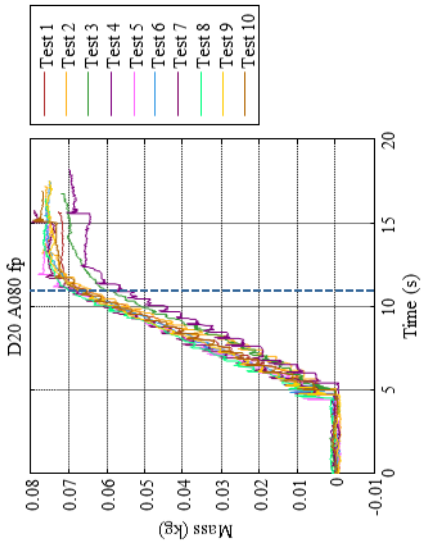
Test 1
Test 2
Test 3
Test 4
Test 5
Test 6
Test 7
Test 8
Test 9
Test 10
D20 A080 fp
Mass (kg)
Time (s)

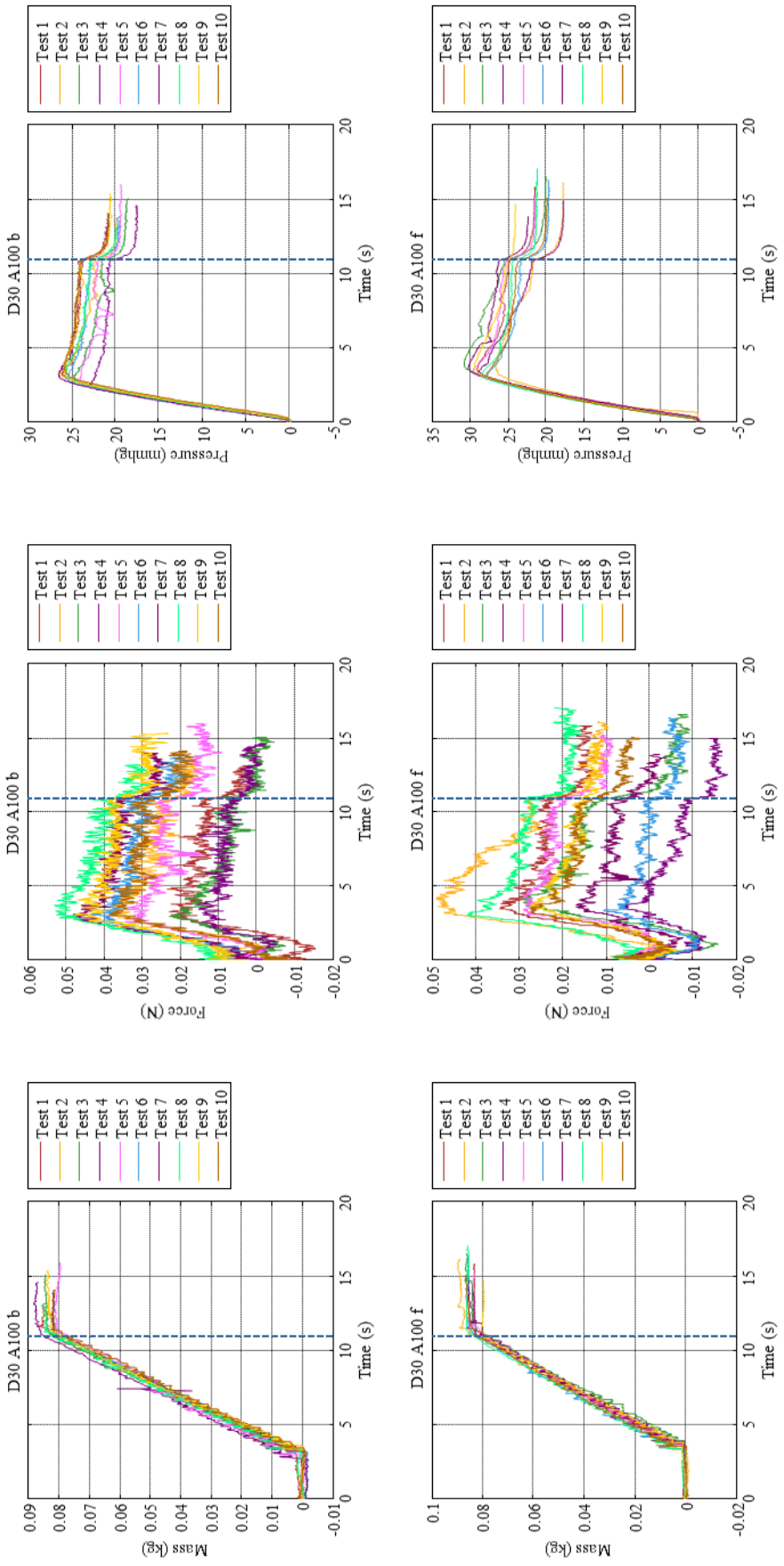
D30 A100 b
D30 A100 f
Time (s)
Pressure (mmhg)
Force (N)
Mass (kg)
Test 1
Test 2
Test 3
Test 4
Test 5
Test 6
Test 7
Test 8
Test 9
Test 10

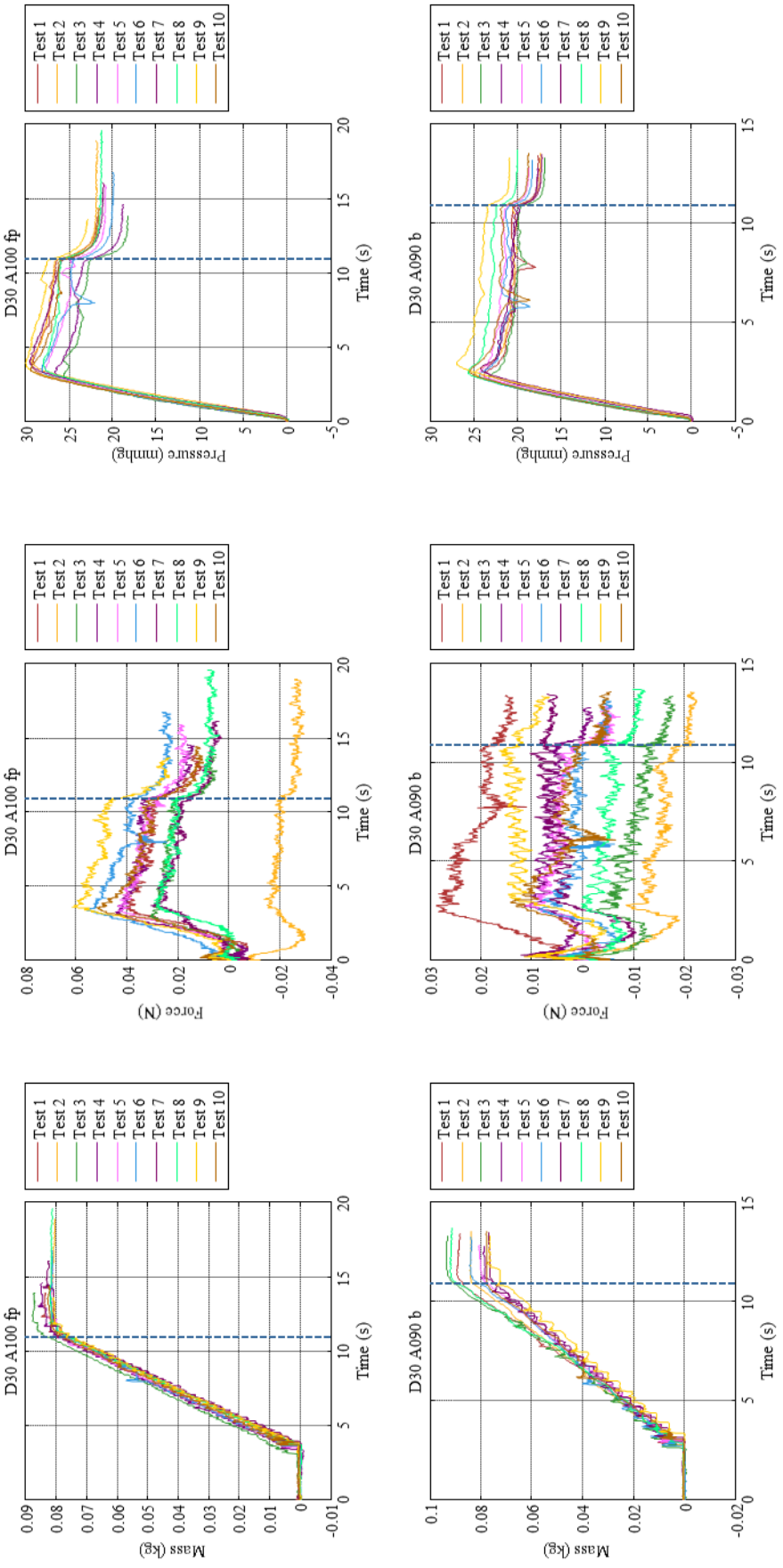
D30 A100 fp
D30 A090 b
Pressure (mmhg)
Force (N)
Mass (kg)
Time (s)
Test 1
Test 2
Test 3
Test 4
Test 5
Test 6
Test 7
Test 8
Test 9
Test 10

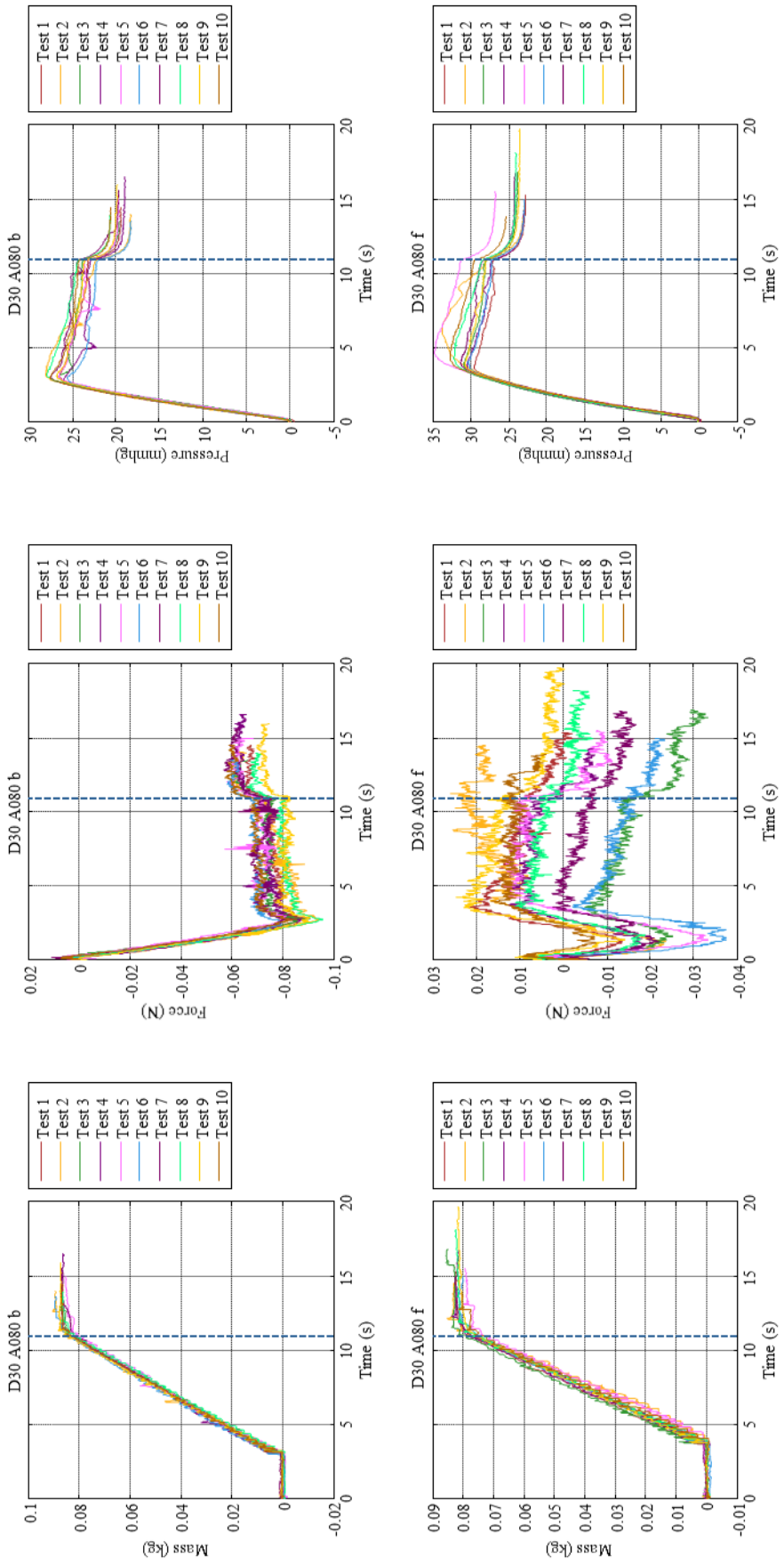
D30 A080 b
D30 A080 f
Time (s)
Pressure (mmhg)
Force (N)
Mass (kg)
Test 1
Test 2
Test 3
Test 4
Test 5
Test 6
Test 7
Test 8
Test 9
Test 10

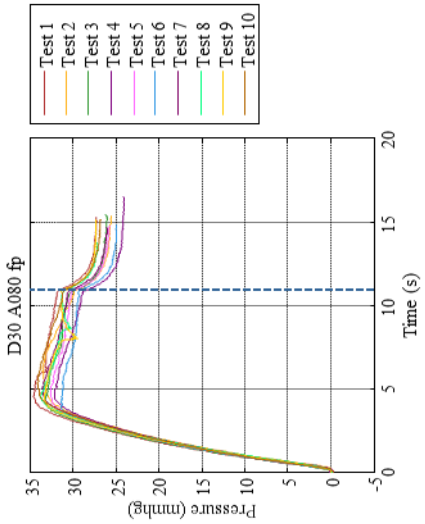
Test 1
Test 2
Test 3
Test 4
Test 5
Test 6
Test 7
Test 8
Test 9
Test 10
D30 A080 fp
Pressure (mmhg)
Time (s)

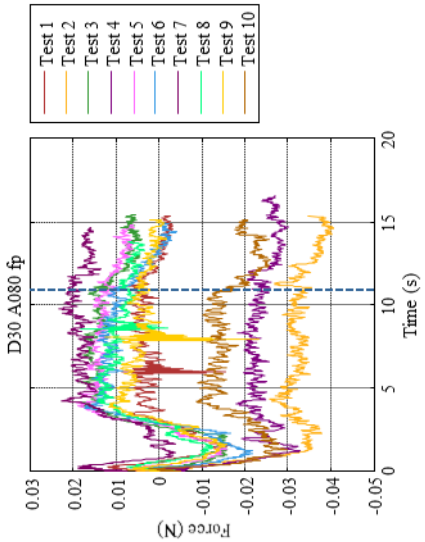
Test 1
Test 2
Test 3
Test 4
Test 5
Test 6
Test 7
Test 8
Test 9
Test 10
D30 A080 fp
Force (N)
Time (s)

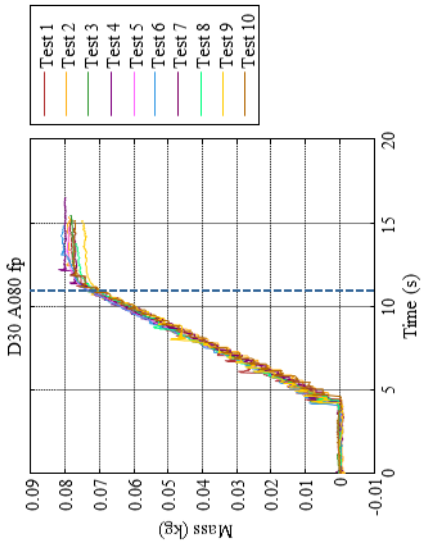
Test 1
Test 2
Test 3
Test 4
Test 5
Test 6
Test 7
Test 8
Test 9
Test 10
D30 A080 fp
Mass (kg)
Time (s)